Functional Characterization of Spastin and its Role in Hereditary Spastic Paraplegia

Thesis

UNRESTRICTED

FUNCTIONAL CHARACTERIZATION OF SPASTIN AND ITS ROLE IN HEREDITARY SPASTIC PARAPLEGIA

Alessia Errico
M.Phil.

Telethon Institute of Genetic and Medicine (TIGEM)

A thesis submitted for the degree of Doctor of Philosophy by research
April 2004

DATE OF SUBMISSION 19 APRIL 2004
DATE OF AWARD 17 JUNE 2004

To my family, to Marco and particularly to my grandparents:

Nonna Giovanna, Nonno Orlando,
Nonna Maria and Nonno Gianni

I know they are proud of me.

ACKNOWLEDGEMENTS

I would like to thank my supervisor Elena Rugarli for giving me the opportunity to work in her laboratory and for her assistance, support and encouragement. I'm very thankful to her for her trust and for letting me free to follow my ideas. These thanks extend to Paul Freemont, my second supervisor, for his interest in my work and for his help throughout my PhD and in the preparation of this thesis.

I gratefully acknowledge Ellis Jaffray and Prof. Ron T. Hay from University of St Andrews for doing the SUMO-1 conjugation *in vitro* assays experiments and for providing us some reagents.

I acknowledge Dr. Shuail Islam and Dr. Lawrence Kelly at ICRF for helping me in the generation of the structural model.

I would like to thanks Prof. Giannino Del Sal for providing us some reagents, for being always very kind to me, for his esteem, suggestions and helpful discussion.

Many thanks to all the people I met at the TIGEM institute, but particularly to Francesca, Caterina, Giuseppe, Bianca, Gilda, Pia, Anna, Ciro, Silvana, Stefano e Maria Teresa for friendship, support and many interesting discussions (scientific and non-scientific) and for making my permanence at TIGEM very pleasant and fruitful. I would like to thank Dr. Alex Reymond and Germana Meroni for teaching me the two hybrid technique and Pietro for helping me with the Real Time PCR. I'm very grateful to all the researchers at TIGEM for their esteem and for supporting me during my permanence at TIGEM.

A special thank-you to Graciana, Pia and Caterina for their support especially in the last period, for encouraging me and helping me in finding a future position. Additional thanks to Graciana and Marinella for listening and having something comforting to say when I was depressed.

No thanks can be enough to all the people in the lab, especially to Marinella, Fatima, Pamela and Gennaro for their help and their support.

Finally, I'm deeply grateful to my family and to Marco for their love and their constant support throughout this period.

ABSTRACT

Hereditary spastic paraplegia (HSP) is a neurodegenerative disease characterized by the spasticity of the lower limbs due to degeneration of the corticospinal tracts. The gene responsible for the most frequent form of autosomal dominant HSP encodes spastin, an ATPase belonging to the AAA family.

Studies with specific antibodies indicate that spastin has both a nuclear and cytosolic localization. In human fibroblasts spastin localizes to the PML bodies, but is also present on the centrosome. In HeLa and Cos7 cells, during mitosis, spastin is enriched in regions rich in microtubules, like the spindle poles and the midbody. Furthermore, in an immortalized motoneuronal cell line, spastin is detected in the growth cone of the axons. By overexpressing wild-type or ATPase-defective spastin, we show that spastin interacts dynamically with microtubules. This association is mediated by the N-terminal region of the protein and regulated through its ATPase activity. The overexpression of wild-type spastin promotes microtubule disassembly; leading to the hypothesis that spastin may play a role in microtubule dynamics.

We identify Spastin nuclear and centrosomal interactors, reflecting the complex subcellular localization of the protein. We demonstrate that Spastin interacts with Daxx, a transcriptional regulator, and that the overexpression of Daxx causes an increase of spastin transcript, suggesting that Spastin may play a role in regulation of transcription. We show that spastin is sumoylated, although the function of this modification is unclear. Moreover, Spastin interacts with a centrosomal protein,

Na14, and we postulate that this protein may represent the anchor for spastin to bind centrosomes and microtubules.

All these data suggest that spastin has a complex role in the cell and may contribute in different ways to the integrity of corticospinal axons. Spastin localization to the neurites and its dynamic association with microtubules let us hypothesise that a defect in axonal transport may underlie HSP.

TABLE OF CONTENTS

LIST OF FIGURES

CHAPTER 1.

CHAPTER 3.

CHAPTER 4.

CHAPTER 5.

CHAPTER 6.

CHAPTER 7.

LIST OF TABLES

ABBREVIATIONS

A	Absorbance
aa	amino acid
AAA	ATPase associated with a variety of cellular activity
Ab	Antibody
AMCA	7-Amino-4-methylcoumarin-3-acetic acid
APS	2,2'-azino-bis(3-ethylbenz-thiazoline)-6-sulphonic acid
ATP	adenosine triphosphate
bp	basepair
°C	degrees Celsius
CMV	Cytomegalovirus
Da	Dalton
DAPI	4',6-diamidine-2-phenylindole, Hydrochloride
DMEM	Dulbecco's modified Eagle's medium
dNTP	deoxyribonucleotide triphosphate
DNA	deoxyribonucleic acid
cDNA	complementary DNA
DTT	Dithiothreitol
E. Coli	*Escherichia Coli*
ECL	Enhanced chemiluminescence
EDTA	ethylenediaminetetraacetic acid
ELISA	enzyme-linked immuno-sorbent assay
FBS	foetal bovine serum
FITC	Fluorescein isothiocyanate
g (rcf)	relative centrifugal force
g	grams
µg	micrograms
mg	milligrams
GAPDH	Glyceraldehyde-3-phosphate dehydrogenase
GFP	green fluorescent protein
GST	glutathione S-transferase
GTP	guanosine triphosphate
HA	hemagglutinin
HCl	Hydrochloridric acid
HEPES	N-(2-Hydroxyethyl)-piperazine-N'-2-ethanesulfonic acid
6HIS	6-histidine

HRP	horseradish peroxidase
Ig	immunoglobulin
IF	immunofluorescence
IP	immunoprecipitate
IPTG	isopropyl β-D-thiogalactoside
Kb	kilobase
kDa	kilodalton
l	litre
µl	microlitre(s)
ml	millilitre(s)
LB	Luria Broth
M	molar
µM	micromolar
mM	millimolar
mA	milli Ampère
mw	molecular weight
NLS	nuclear localisation signal
nm	nanometer
NP-40	Nonidet P-40
OD	optical density
PAGE	polyacrylamide gel electrophoresis
PBS	phosphate buffered saline
PCR	polymerase chain reaction
PIPES	1,4 Piperazin-bis-(ethansulfonsaeure)
PMSF	phenylmethylsulphonyl fluoride
PVDF	Polyvinylidene difluoride
RNA	ribonucleic acid
mRNA	messenger RNA
RNase	ribonuclease
rpm	revolutions per minute
SAE	SUMO-1 activating enzyme
SDS	sodium dodecyl sulphate
SP	Spastin
SUMO-1	Small ubiquitin-like modifier
TBS	Tris buffer saline
Tris	2-amino-2-(hydroxymethyl)propane-1,3-diol
TRITC	Tetramethylrhodamine isothiocyanate
UBC9	SUMO-1 conjugating enzyme
UV	ultraviolet
w	weigth

WB	Western blot
V	volt
v	volume
X-gal	5-bromo-4-chloro-3-indolyl-β-D-galactosidase

CHAPTER 1: INTRODUCTION

1.1 Neurons

Neurons are the main signalling cells of the nervous system. To transmit signals, neurons stop dividing early in development and then generate long cellular processes. Every neuron consists of a cell body, containing the nucleus, with a number of long processes radiating outward from it. A typical vertebrate neuron extends one axon and many dendrites. Axons are long processes that are specialised in transmitting information, while dendrites are shorter processes specialised to receive and process information. The neuron grows in size and moves during development, sends out branches, transport substances and organelles within these branches, and make synapses with other cells. Therefore, there are demanding requirements for maintaining a complicated structure that has to be extremely flexible. These requirements are absolved by the neuronal cytoskeleton, which contain three main filamentous structures: microtubules, neurofilaments and actin microfilaments.

1.1.1 Microtubules

Microtubules play a key role in developing and maintaining the neuron's processes. Microtubules are highly dynamic structures, made of α- and β- tubulin dimers, and arranged head to tail into protofilaments that assemble to form hollow tubes (usually constituted of 13 protofilaments) (Downing and Nogales, 1998). The microtubule array within cells is capable of rapid rearrangements that depend on the

ability to exchange subunits between the soluble and polymer pools (Soltys and Borisy, 1985). They switch stochastically between growing and shrinking phases and this dynamic behaviour is essential for fundamental processes such as cell division and differentiation. Thus, microtubules are polar structures with a rapidly growing end (*plus end*) and an opposite slow-growing end (*minus end*) prone to lose subunits if not stabilised. The ability to regulate the equilibrium between polymerization and depolymerization of the microtubule plus end is known as "dynamic instability". The energy required for this process comes from GTP hydrolysis (Heald and Nogales, 2002). GTP binds to β-tubulin subunit of the heterodimeric tubulin, and is hydrolysed to GDP when a tubulin molecule adds to the end of a microtubule. When a microtubule grows rapidly, tubulin molecules add to a polymer end faster than GTP hydrolysis occurs, this results in the formation of a GTP cap on one end of the polymer. Since tubulin molecules carrying GTP have higher affinity for other tubulin molecules than tubulin-GDP, the GTP cap will favour microtubule growing. When the GTP is hydrolysed to GDP, for example because of a decrease in the microtubule polymerisation rate, the polymer will start to shrink, leading to a progressive disruption of the microtubule and eventually its disassembly to form "free" tubulin dimers.

The primary site of microtubules nucleation in animal cells is the centrosome (or microtubule organizing center). The new microtubules grow out from the centrosome and elongate towards the cell periphery with their minus end anchored at the centrosome and their plus end in the cytoplasm. In living cells where the microtubules minus end are anchored at the centrosome, microtubules are thought to exchange subunits by polymerisation and depolymerization at their plus end, via the

dynamic instability mechanism. But additional pathways exist by which microtubule dynamics can be affected: i.e. "treadmilling" and "severing." Treadmilling involves the addition of subunits to the plus end of a MT and loss of subunits from the opposite (minus) end, always coupled to GTP hydrolysis. Treadmilling seems to be more common for actin filaments, but it has been observed also for microtubules and it allows free microtubules to move towards the cell periphery (Keating et al., 1997).

Alternatively, microtubules can be broken or severed along their length by microtubules severing activities. For example, Katanin is a protein involved in microtubule severing (McNally and Vale, 1993). This process seems to be very important for the production of non-centrosomal microtubules and for spindle pole formation (McNally et al., 2000; Odde et al., 1999). Cells can modify the dynamic instability of their microtubules for different purpose, during the M phase of the cell cycle for example, microtubules turnover is very high, so that chromosomes can capture growing microtubules and a mitotic spindle can rapidly be formed. On the contrary, when a cell is differentiating, microtubules need to be stabilised. The ability to stabilise microtubules in a particular configuration provides an important mechanism for a cell to organise its cytoplasm.

A neuron is a postmitotic cell and, unlike an interphase cell, does not display the typical radial array of microtubules emanating from the centrosome. Few microtubules are attached to the centrosome while most of them are free in the cytoplasm, where they tend to form bundles that funnel from the cell body into axons and dendrites. Microtubules are important as structural support of the neuron, but they also act as railways for the transport of various materials along the length of neuronal processes. It is believed that the neuronal microtubules array is established

by mechanisms similar to those that an interphase cell utilizes for organizing the mitotic spindle. Neurons have a soluble pool of γ-tubulin and a pool associated to the centrosome, but no γ-tubulin signal was ever detected in axons or dendrites (Baas and Joshi, 1992). Since γ-tubulin is required for the nucleation of microtubules in all the cell types, it has been proposed that also in neurons microtubules are nucleated at the centrosome, released and then actively transported to the developing axons and dendrites (Baas, 1999). To support this hypothesis, experiments with functional blocking antibody to katanin, a microtubule severing AAA protein which is also involved in release of microtubules from centrosomes in mitotic cells, inhibits the release of microtubules from the centrosome and severely compromises process outgrowth (Ahmad et al., 1999b). Microtubules in axons are uniformly oriented with their plus ends distal to the cell body, while in dendrites they have both orientations (Baas, 1998).

1.1.2 Neurofilaments

Neurofilaments constitute the set of intermediate filaments of a neuron. Three main kind of neurofilaments have been identified, corresponding to polypeptides with molecular mass of 70 kDa (NFM-70), 160kDa (NFM-160) and 200 kDa (NFM-200). Neurofilaments are composed of fibers that twist around each other to produce coils of increasing thickness. The thinnest unit is a heterodimer composed of two α-helical chains oriented in parallel and intertwined in a coiled-coil rod. Unlike microtubules, neurofilaments are very stable in their basic structure; nonetheless they are involved in the continual remodelling of nerve processes. They are phosphorylated at the C-terminal portion and they represent the primary cytoskeletal

component of a nerve cell. Neurofilaments are present in both axons and dendrites, but they are much more numerous and more phosphorylated in axons. Phosphorylation regulates NF-NF interactions and also interactions between neurofilaments and other cytoskeletal protein, so to provide the cytoskeletal lattice that supports the mature axon (Grant et al., 1995; Pant et al., 2000). Abnormal accumulation and disorganization of neurofilaments is a hallmark of a collection of motor neuron diseases including familial and sporadic amyotrophic lateral sclerosis (ALS), infantile spinal muscular atrophy, and hereditary sensory motor neuropathy (Xu et al., 1993).

1.1.3 Actin microfilaments

Actin microfilaments are polar polymers of globular actin monomers wound into a double stranded helix. Unlike microtubules and neurofilaments, actin filaments are short. They are concentrated at the cell's periphery, where they interact with numerous actin-binding proteins. The resulting matrix plays a very important role in the dynamic function of the cell's periphery, such as the motility of the growth cones during development. Actin microfilaments also undergo cycles of polymerization and depolymerization. In addition to their role as cytoskeleton constituents, microtubules and actin filaments are important for intracellular transport; in fact they act as tracks along which other organelles and proteins are driven by molecular motors.

1.2 Axonal Transport: an example of cellular trafficking

Transport vesicles allow communication within the cell between the various membrane-bound organelles and the plasma membrane. The plasma membrane is a dynamic structure that separates the cytoplasm from the extracellular environment by regulating the entry and exit of small and large molecules. Uptake of nutrients and all communications among cells and between cells and their environment occurs through this interface. Essential small molecules, such as amino acids, sugars and ions, can traverse the plasma membrane through the action of integral membrane protein pumps or channels. Macromolecules must be carried into the cell in membrane-bound vesicles derived by the invagination of the plasma membrane in a process termed endocytosis. The macromolecules, once internalised, are delivered to lysosomes where they are digested and the resulting metabolites are then delivered from lysosomes to the cytosol.

The internal membrane system provides also a mean to deliver newly synthesised proteins and carbohydrates to the exterior. These molecules travelling along the biosynthetic-secretory pathway (figure 1) pass through various compartments, where they can be modified by the cell, stored until needed and then delivered to a specific cell-surface domain by a process called "exocytosis". Generally, a protein is synthesised on the ribosome and then is transported through the biosynthetic-secretory pathway till the final destination is reached. Proteins can move from one compartment to another in three different ways: by gated transport, by transmembrane transport and by vesicular transport. The signals that drive the transport of a protein across the cell and eventually its localisation in a specific compartment are contained in the primary structure of the protein itself. The protein

trafficking between the cytosol and the nucleus is an example of gated transport; it occurs through the nuclear pore complexes, which function as a selective gate that can actively transport specific macromolecules. In transmembrane transport, membrane bound protein translocators directly transport specific proteins across a membrane. Proteins must be unfolded in order to pass through the membrane. When proteins are instead transferred from a compartment to another inside the cell, as from the ER to the Golgi apparatus, this transport occurs through vesicle (vesicular transport). All the compartments of this biosynthetic-secretory pathway are constantly in communication with each other by means, at least in part, of numerous transport vesicles which bud off from one compartment membrane and fuse to another. Cellular trafficking is a well organised process; the biosynthetic-secretory pathway leads out from the endoplasmic reticulum (ER) toward the Golgi apparatus and cell surface, while the endocytic pathway leads from the plasma membrane towards endosomes and lysosomes. Each transport vesicle that buds from a specific compartment must take up only specific proteins and fuse only with the appropriate target membrane.

1.2.1 Endocytosis

Endocytosis occurs by multiple mechanisms that can be grouped into two broad categories, "phagocytosis" (the uptake of large particles) and "pinocytosis" (the uptake of fluid and solutes) (Conner and Schmid, 2003). These diverse endocytic pathways control all aspects of intercellular communication and of entry into the cell. Furthermore, they play a crucial role in development, immune response,

neurotransmission, intercellular communication, signal transduction, and cellular and organismal homeostasis (Conner and Schmid, 2003).

Phagocytosis is restricted to specialized mammalian cells (macrophages, monocytes and neutrophils) that function to clear large pathogens such as bacteria or yeast, or large debris such as the remnants of dead cells (Aderem and Underhill, 1999); for example it is crucial for clearing apoptotic cells (Fadok and Chimini, 2001). It is an active and highly regulated process involving specific cell-surface receptors and signalling cascades mediated by Rho-family GTPases (Hall and Nobes, 2000). Both for phagocytosis and pinocytosis the molecule to be internalised and its receptor determine the specific pathway through which it can enter into the cell.

1.2.2 Multiple pathways for pinocytosis

Pinocytosis, instead, occurs in all cells essentially by four mechanisms: macropinocytosis, clathrin-mediated endocytosis (CME), caveolae-mediated endocytosis, and clathrin- and caveolae-independent endocytosis (Conner and Schmid, 2003).

Macropinocytosis accompanies the membrane ruffling that is induced in many cell types upon stimulation by growth factors or other signals. It involves the Rho-family GTPases signalling cascade, which trigger the actin-driven formation of membrane protrusions (Chimini and Chavrier, 2000). Little is known about the nature of this fusion process, which is highly regulated and fulfils diverse functions.

Another mechanism of pinocytosis is the Caveolae-mediated endocytosis; caveolae are flask-shaped invaginations of the plasma membrane, which are

proposed to mediate the extensive transcellular transport (Anderson, 1998; Conner and Schmid, 2003).

Clathrin-mediated endocytosis (CME) occurs constitutively in all mammalian cells, and carries out the continuous uptake of essential nutrients. CME is crucial for intercellular communication during tissue and organ development (Seto et al., 2002), and throughout the life of the organism, as it modulates signal transduction by controlling the levels of surface signalling receptors. CME is also involved in cell and serum homeostasis by regulating the internalization of membrane pumps that control the transport of small molecules and ions across the plasma membrane. The clathrin-mediated endocytosis of calcium channels in neurons helps to control the strength of synaptic transmission (Beattie et al., 2000) and is required for efficient recycling of synaptic vesicle membrane proteins after neurotransmission (De Camilli and Takei, 1996). CME involves the concentration of high-affinity transmembrane receptors and their bound ligands into 'coated pits' on the plasma membrane. The main assembly unit of those vesicles is clathrin. Once these clathrin vesicles, CCVs (clathrin-coated vesicles), are formed, they carry receptor–ligand complexes into the cell.

A part from those described till now, other kind of vesicles exists. They are referred to as "rafts" and can diffuse freely on the cell surface (Tang and Edidin, 2001). Their unique lipid composition provides a physical basis for specific sorting of membrane proteins and/or glycolipids based on their transmembrane regions (Anderson and Jacobson, 2002; Tang and Edidin, 2001). These small rafts can be captured by, and internalized within any endocytic vesicle and this process is known as clathrin- and caveolin-independent endocytosis (Lamaze et al., 2001). The

mechanisms that control caveolae- and clathrin-independent endocytosis are not clear. It is likely that each of the pathways described fulfil unique functions in the cell and varies mechanistically not only in how the vesicles are formed, but in terms of which cargo molecules they transport, to what intracellular destination their cargo is delivered, and how their entry is regulated. Through these different pathways pinocytosis can be highly regulated and modulated depending on signal transduction, development and modulation of the cell's responses upon interactions with its environment.

1.2.3 Axonal transport

The process of axonal transport represents a particular example of the general cellular trafficking. The axon lacks protein synthesis machinery, and thus all the proteins required in the axon and synaptic terminal must be transported down the axon after they are synthesized in the cell body. Most proteins are conveyed in membranous organelles or protein complexes. In this sense, organelle transport in the axon is fundamentally important for neuronal morphogenesis and functioning.

Because of the length of their axons and their highly polarized architecture, neurons are highly dependent on an intricate system of transport designed to ensure correct targeted delivery of cell components (Almenar-Queralt and Goldstein, 2001). Fast and slow axonal transport occurs along microtubules. Slow axonal transport, by which many cytoskeletal proteins move, is thought to occur only in the anterograde direction (i.e., towards the plus end of the microtubule). Fast anterograde transport, powered by kinesin motor proteins, is used for the transport of vesicles, membranes, and membranous organelles such as mitochondria. Fast retrograde transport (i.e.,

towards the minus end of the microtubule) is powered by dynein motor proteins and delivers endosomes, other organelles, and neurotrophic signals back to the cell bodies (Apodaca, 2001). Kinesin and dynein are molecules that have a globular domain at one end, followed by a rod. The globular domain serves as 'motor domain' that slides against the tracks using energy from ATP hydrolysis. The motor domains of kinesins and dyneins have ATP-binding and microtubule-binding sites. They repeat cycles of attachment, sliding and dissociation on the microtubules in an ATP-dependent manner, and move along the microtubules (Hirokawa, 1998). The cargoes of kinesines (KIFs) include various membranous organelles, mitochondria, lysosomes, endocytic vesicles, tubulin oligomers, intermediate filament proteins, mRNA complexes and other macromolecular complexes. Some KIFs transport different kinds of cargoes depending on cell type. For example, KIF3 motors transport membrane vesicles in the axon, but macromolecular complexes in cilia. In addition, some cargoes are transported by multiple KIFs; for example, mitochondria are transported by both KIF5 and KIF1Bα (Hirokawa and Takemura, 2003).

1.3 Axonal degeneration

Axon degeneration appears to be an auto-destructive process that can be triggered by diverse insults. In many neurodegenerative diseases, the degeneration of the axon is responsible for the clinical progression of the disorder and for the patient's disability more than the neuronal death. There are several ways for axonal degeneration to occur, we can distinguish between pathological and physiological axonal degeneration. A typical example of pathological axonal degeneration is the

Wallerian degeneration (Raff et al., 2002; Waller, 1850). This can occur both in the peripheral nervous system and in the central nervous system when a trauma locally injures axon. So the axon is cut and the part of the axon which is separated from the cell body rapidly undergoes wallerian degeneration, disassembling in a characteristic and orderly way. Basically the endoplasmic reticulum breaks down, the neurofilaments are degraded, the mitochondria swell and the axon breaks up into fragments that are phagocytosed (Griffin et al., 1996). As a consequence, the neuronal cell body frequently undergoes apoptosis. Wallerian degeneration has been considered for a long time as a passive process, with axon degenerating through loss of proteins synthesized in the cell body or activation of Ca^{2+} dependent proteases (George et al., 1995). The discovery of a spontaneous mutation in mice called *Wallerian degeneration slow* (Wld^S) suggests instead that the degeneration could be an active process (Lunn et al., 1989). In these mice, apparently normal, wallerian degeneration, both in the peripheral nervous system and in the central nervous system, is greatly slowed. The Wld^S mutation has been mapped to the distal end of mouse chromosome 4 (Lyon et al., 1993) where there is an 85 Kb tandem triplication that results in the production of an abnormal fusion protein (Coleman et al., 1998). The fusion protein contains the N-terminal 70 amino acids of the ubiquitination factor E4B and the entire coding region of the nicotinamide mononucleotide adenyl transferase (NMAT) (Conforti et al., 2000). This let hypothesize that the ubiquitin-proteasome pathway is involved in determining the Wld^S phenotype (Coleman and Perry, 2002). Another kind of axonal degeneration which is more important for neurodegenerative diseases is known as dying back process. The axon of an unhealthy neuron degenerates, progressively in time, starting from the distal part of

the axon and sometimes with preservation of the cell body (as in HSP) (Cavanagh, 1964; Schaumburg et al., 1974). This is the most common pathology presents in peripheral nerve diseases due to toxic, metabolic and infectious insult and seems to be also a feature of central nervous system neurodegenerative diseases, including motor neuron disease (Azzouz et al., 1997), Alzheimer and Parkinson disease (Iseki et al., 2001). The dying back process is very interesting and the mechanisms by which it occurs are not known. A crucial point is to understand how can a neuron eliminate part of itself (the distal portion of the axon), leaving the rest intact. The dying-back-type neuropathies (Cifuentes-Diaz et al., 2002; Saigoh et al., 1999), are traditionally considered distinct from Wallerian degeneration, although there is no evidence that their mechanisms are unrelated.

Axonal degeneration may also occur during normal development. Many projection neurons in the brain initially extend axonal branches to inappropriate regions of the CNS; these branches are later lost by a process called branch elimination (O'Leary and Koester, 1993). It is not clear whether axonal branch elimination in vertebrate development occurs by degeneration or by retraction, but still the interesting question is how a neuron avoid to extend the self destruction program to the rest of the axon and to the cell body.

The molecular mechanisms of axon degeneration are poorly understood. One of the pathways that have been implicated in axonal degeneration is the Ubiquitin-proteasome pathway.

Mutations in ubiquitin proteasome pathway proteins affect neuronal degeneration, including axon degeneration. Beyond the involvement of the ubiquitin-proteasome pathway in the Wld^S mice phenotype, mutations in other proteins of the

ubiquitin-proteasome pathway can affect axonal degeneration. In fact, in the gracile axonal dystrophy (*gad*) mouse, axons progressively die back from the first few weeks of life (Mukoyama et al., 1989), owing to an in-frame deletion in the gene encoding Uch-L1 (Saigoh et al., 1999), an ubiquitin C-terminal hydrolase that is abundant in all neuronal compartments (Kent and Clarke, 1991). Uch-L1 releases and stabilizes monomeric ubiquitin, thus promoting protein turnover, which is essential for maintaining axons. The importance of the ubiquitin-proteasome pathway in chronic neurodegeneration has also been highlighted by a mutation in the gene encoding the ubiquitin-E3 ligase parkin that causes recessive juvenile parkinsonism (Shimura et al., 2000). Intracellular accumulation of insoluble aggregates of ubiquitinated protein, either in the cell body or in dystrophic neurites, is a hallmark of chronic neurodegenerative disease (Lowe et al., 1993). Deposition of such ubiquitinated proteins and their failure to be degraded by the proteasome could disrupt the normal physiology of the neuron, in particular could impair axonal transport. Alternatively, the formation of protein aggregates could be a protective mechanism to decrease levels of soluble toxic proteins, and ubiquitination might be a step towards their degradation (Layfield et al., 2003).

Interestingly, several line of evidence suggests that axons and synapses degenerate by active and regulated mechanisms that are molecularly distinct from apoptosis (Coleman and Perry, 2002). The *pmn/pmn* mutant mouse develop a motor neuropathy in which motor neuronal axon degenerate in a dying back pattern and the neurons dye by apoptosis (Schmalbruch et al., 1991). When those mice have been crossed with transgenic mice expressing the human bcl-2 gene in many of their neurons (Dubois-Dauphin et al., 1994), the death of the motor neuron cell body was

prevented, as expected by the anti-apoptotic activity of Bcl-2, but there was no effect on the axonal degeneration and on the pathological phenotype of the mice (Sagot et al., 1995). It seems like the axonal degeneration of the motor neuron and not the death of the cell body that causes the clinical feature of the disease and lead to the mice death.

1.4 Impairment of axonal transport and diseases

Proteins synthetic machineries are absent in nerve axons, therefore, most proteins that are vital for the maintenance and function in the axon and synaptic regions need to be transported down the axon. Many proteins, such as those of the kinesin and dynein superfamilies (Hirokawa, 1998), mediate axonal transport. Therefore it is not surprisingly that mutations in those genes results in axonal loss. In addition, mutations, not in the motor itself, but in the proteins associated with the motor proteins can also causes diseases. It was recently shown that a mutation of KIF1Bβ is the cause of Charcot–Marie–Tooth disease (CMT) type 2A (Zhao et al., 2001a). KIF1Bβ is a plus-end-directed motor that transports synaptic vesicle precursors in the axon from the cell body to the synapse. *kif1b*$^{-/-}$ mice show defects in both sensory- and motor-nerve functions. A detailed analysis shows that both the number of synapses and the density of synaptic vesicles at the synapse are reduced, which is consistent with a defect in the transport of synaptic vesicle precursors (Tanaka and Hirokawa, 2002; Zhao et al., 2001a). All affected individuals of CMT2A have a heterozygous point mutation, Gln98Leu, which occurs in the ATP-binding site of the motor region of KIF1Bβ and causes significant reduction in

ATPase and *in vitro* motor activities. Furthermore, the transport of amyloid precursor protein (APP) by KIF5 might contribute to the pathogenesis of Alzheimer's disease. It is known that APP plays a major role in the development of Alzheimer's disease, and that cleavage of APP mediated by β-secretase or γ-secretase produces pathogenic amyloid. Cleavage by γ-secretase is carried out by an enzyme complex that contains presenilins. APP appears to be one of the cargoes transported in the axon by KIF5 conventional kinesin, which interacts with APP through the light chain (Kamal et al., 2000). In addition, APP has been shown to be transported in vesicles containing presenilin-1 and β-secretase, and it has been suggested that the processing of APP to amyloid-β by secretases could occur in axonal membrane compartments transported by KIF5 (Kamal et al., 2001).

Recent evidences suggest that also polyglutamine proteins (polyQ) can disrupt axonal transport leading to axonal degeneration (Feany and La Spada, 2003). The polyQ disorders include several neurodegenerative diseases and one of the best studied of this group is Huntington disease. Expansion of glutamine repeats within the coding region of a protein confers a toxic gain of function that disrupts essential cellular processes and leads to loss of affected neurons. In general, theories on the pathogenesis of polyQ toxicity have not focused on abnormality in axonal transport but on several other cellular targets, such as impaired proteasomal degradation (Ross, 2002). But recently, it has been shown that normal levels of huntingtin are required for proper axonal transport in drosophila and that expression of expanded polyQ proteins disrupts axonal transport in larval neurons (Gunawardena et al., 2003). Moreover, polyQ proteins have been involved in the inhibition of fast axonal transport in the squid giant axon system (Szebenyi et al., 2003). These results suggest

that the polyQ disorders can be included in that group of neurodegenerative disease linked to abnormalities of axonal transport.

The importance of axonal transport for maintaining motor neuron viability has been also highlighted by the finding that mutations in dynactin, a multiproteic complex associated with dynein and required for axonal transport, have been described in patients with a motor neuron disease (Puls et al., 2003). Moreover in mice, disruption of dynactin function (by overexpression of dynamitin, a subunit of the dynactin complex) produces motor neuron degeneration (LaMonte et al., 2002).

Mutations in the kinesin KIF5 have been found in a neurodegenerative disease, hereditary spastic paraplegia (HSP) (Reid et al., 2002), leading to the hypothesis that a defect in axonal transport could be the cause for the axonal degeneration phenotype which characterizes this disease.

Thus, although we are far from understand the pathogenic mechanism of Alzheimer's disease, HSP and other chronic neurodegenerative diseases, axonal-transport deficiency could play an important role in pathogenesis.

1.5 Hereditary Spastic Paraplegia

The genetic information is carried in the linear sequence of nucleotide in DNA (deoxyribonucleic acid). More precisely, it is organised in structural units, named genes. Each gene contains a particular set of instructions, usually coding for a particular protein. Many, if not most, diseases have their roots in our genes. In fact, many diseases are thought to arise from mutated genes. A mutation can be defined as a permanent change in the DNA. Mutations that affect the germ cells are transmitted

to the progeny and can give rise to inherited diseases. When a gene is mutated, this will result in the transcription and translation of an abnormal protein product; some protein changes are insignificant but some other are disabling and therefore disease causing.

Hereditary spastic paraplegia (HSP) (also known as familial spastic paraparesis and Strumpell-Lorrain syndrome) is a mendelian disorder characterised primarily by progressive weakness, spasticity and loss of the vibratory sense in the lower limbs (Fink, 1997; Harding, 1983). These disorders are classified according to their symptoms and to the mode of inheritance; they are divided into pure and complicated forms depending on whether spasticity occurs in isolation or with additional features such as mental retardation, ataxia, cortical atrophy, optic neuropathy, deafness and ichthyosis. The age of onset symptoms, rate of symptom progression and the extent of disability are extremely variable both within and between the different HSP forms. There are few forms arising in childhood, and most cases between 20 and 40 years of age. Usually the later the onset of the disease, the faster is the progression of its course. Although HSP is an invalidating disease, it never causes shortening of the life-span of patients.

1.5.1 Neuropathology

The major neuropathological feature of HSP is axonal degeneration that is maximal in the terminal portions of the longest motor and sensory axons of the central nervous system (CNS), i.e. the crossed and uncrossed corticospinal tracts projecting to the legs, the fasciculus gracilis fibers and to a lesser extent the

spinocerebellar fibers (Fig.2) (Behan et al., 1988; Behan and Maia, 1974; Harding, 1993; Schwarz and Liu, 1956).

Axons of the corticospinal tracts arise from pyramidal neurons in layer V of the motor cortex and project through the internal capsule to reach the ventral surface of medulla where they form two elongated swellings, the pyramids. These axons cross the midline at the junction between the bulb and the spinal cord and descend in the contralateral funiculus of the spinal cord. The crossed corticospinal tract conveys voluntary motor impulses to the secondary motor neurons located in the ventral horns of the spinal cord. The fasciculus gracilis is composed of central branches of axons of pseudounipolar neurons located in dorsal root ganglia and ascend in the most medial part of the dorsal funiculus. These axons transmit deep sensory information from the lower extremities to secondary sensory neurons in the nucleus gracilis. The corticospinal axons are exceptionally long, in some cases over 1 metre, with axonal volumes that can be up to one thousand times of the cell bodies. Corticospinal tract neurons therefore provide an excellent example of the difficulties encountered in diverse cellular processes, such as trafficking, transport and energy metabolism (Reid, 2003).

Interestingly, a specific pattern of degeneration is seen in HSP, during which the cell bodies remain largely intact while the degeneration is principally limited to the axon and may be considered as a dying-back axonopathy, beginning distally and proceeding towards the cell body (Schwarz and Liu, 1956). In contrast to other neurodegenerative diseases, such as amyotrophic lateral sclerosis (ALS), which is characterised by degeneration of functionally and physically related motor system elements (including pyramidal neurons, corticospinal tracts, spinal motor neurons

and skeletal muscle), axonal degeneration in HSP involves different classes of neurons. The common feature shared by these degenerating axons is their length. In fact, these are the longest axons in the CNS.

1.5.2 Genetics

All mendelian disorders are the result of expressed mutations in single genes. The patterns of inheritance of single Genes mutations typically depend on two factors. First, the chromosomal location of the gene mutated, which may be autosomal (located on an autosome) or X-linked (located on the X chromosome); second, whether the phenotype is dominant (expressed only when one chromosome of a pair carries the mutated allele) or recessive (expressed when both chromosome of a pair carry the mutated allele).

HSP is extremely heterogeneous from a genetic point of view. So far, 21 different loci have been mapped and more will be identified. HSP can be transmitted as an X-linked (SPG1, SPG2, SPG16), autosomal dominant (SPG3A, SPG4, SPG6, SPG8, SPG9, SPG10, SPG12, SPG17, SPG19) or autosomal recessive trait (SPG5A, SPG7, SPG11, SPG14, SPG15, SPG20, SPG21). Despite the large number of loci mapped for the various form of HSP (table1) and the identification of 11 genes to date, the pathogenetic basis underling most forms of HSP remains unclear, but the identification and characterisation of the causative genes suggest that a common mechanism could underlie several forms of HSP (Crosby and Proukakis, 2002). Although the disease is genetically heterogeneous, approximately 70% of all pure HSP are inherited as dominant traits, the 20-30% as recessive tracts and only rare cases are reported as X-linked.

1.5.3 The X-Linked HSP Genes

Two X-linked genes, L1 cell adhesion molecule (SPG1, *L1CAM*) and proteolipid protein (SPG2, *PLP1*), were identified as responsible, when mutated, for a complicated HSP phenotype. PLP1 mutations may additionally lead to pure HSP (Jouet et al., 1994; Saugier-Veber et al., 1994).

SPG1: L1CAM

In this form of HSP, spastic paraplegia begins in the first two decades of life with slow progression of symptoms. Although this form may manifest as pure HSP, it is more often observed in association with a complex disorder, referred to as "MASA syndrome" (mental retardation, adducted thumbs, spasticity and aphasia) or "CRASH syndrome" (corpus callosum hypoplasia, mental retardation, adducted thumbs, spastic paraplegia, and hydrocephalus) (Fransen et al., 1995). The *L1CAM* gene encodes a transmembrane glycoprotein with extracellular immunoglobulin and fibronectin type III repeats, which mediates cell adhesion, neurite outgrowth and axon pathfinding. L1CAM is expressed throughout the nervous system on populations of developing and differentiated neurons, as well as in Schwann cells in the peripheral nervous system. Several studies indicated that this molecule is required for normal development of the corticospinal tract (Casari and Rugarli, 2001), and recent data suggest a function for L1CAM in potentiation of neuronal migration (Thelen et al., 2002).

SPG2:PLP1

SPG2 maps to Xq22 and results from mutations in the proteolipid protein, PLP, one of the major protein components of myelin in the central nervous system (CNS). PLP is a four-helix spanning membrane protein that stabilizes the structure of the

CNS myelin, by forming the intraperiod line. *PLP1* is mutated in complicated and, rarely, in pure forms of HSP. Mutations in *PLP1* are also responsible for Pelizaeus-Merzbacher disease (PMD) (Saugier-Veber et al., 1994), which is characterized by hypomyelination of the CNS with a reduced number of mature oligodendrocytes.

Knockout mice lacking completely PLP1 have normal CNS function; they assemble compact myelin sheaths and subsequently develop widespread axonal swelling and degeneration (Griffiths et al., 1998). Consequently, a lack of PLP1 protein does not cause the dysmyelination seen in PMD, and the axonal defect is explained by a deficiency in oligodendroglial function. This together with the accumulation of membranous dense bodies and mitochondria suggests that axonal transport is impaired in HSP due to PLP1 mutations (Griffiths et al., 1998).

1.5.4 SPG7and SPG13: The Mitochondrial Story

The mitochondria are membrane-bound organelles that convert energy to forms that can be used to drive cellular reaction. They are localised to the regions of the cell where ATP consumption is high and are dispersed according to changes in local energy requirements (Wagner et al., 2003). A mitochondrion is bounded by two highly specialised membranes that play a crucial role in its biological function. Together they create two separate mitochondrial compartments: an internal matrix space and a narrower intermembrane space. The outer membrane contains many copies of transport proteins, the porins, which forms large aqueous channel through the lipid bilayer. Therefore this membrane is permeable to all molecules of 5000 daltons or less. Other proteins present in this membrane include enzymes involved in lipid synthesis and enzymes that convert lipid substrates. The major working part of

the mitochondrion is the matrix space and the inner membrane that surrounds it. The inner membrane is highly specialised, it is folded into numerous cristae and contains several proteins which are involved into three types of function: 1) proteins that carry out the oxidation reactions of the respiratory chain; 2) an enzymatic complex, the ATP synthase, which produces ATP in the matrix; and 3) proteins that regulate the transport of metabolites into and out of the matrix. The matrix contains, instead, a high variety of enzymes involved in the pyruvate and fatty acid oxidations and in the citric acid cycle; furthermore the matrix contains the mitochondrial genome and several enzymes necessary for the expression of the mitochondrial genes.

SPG7: paraplegin

Mutations in *SPG7* gene are responsible for both complicated and pure forms of autosomal recessive HSP (Casari et al., 1998). Paraplegin, the protein product of the SPG7 gene, is a mitochondrial metalloprotease with strong homology to the yeast mitochondrial ATPases Yta10p and Yta12p. Like its yeast homologues, Paraplegin has an N-terminal mitochondrial leader sequence and two transmembrane domains that anchor the protein to the inner mitochondrial membrane. Paraplegin contains two functional domains: an AAA (ATPases associated with diverse cellular activities) domain common to the AAA proteins (Patel and Latterich, 1998), a group of molecules possessing a range of functions that include protein degradation, trafficking and organelle biogenesis, and a proteolytic domain with a consensus metal binding site.

The yeast Yta10p and Yta12p form a high molecular weight complex, the *m*-AAA, which is embedded in the inner mitochondrial membrane and exposes proteolytic sites to the mitochondrial matrix (Langer et al., 2001). The *m*-AAA

complex guarantees the protein quality control system for inner membrane proteins and is required for the maintenance of the functional membrane embedded protein complexes (Guelin et al., 1994; Paul and Tzagoloff, 1995; Tauer et al., 1994). It ensures the removal of misfolded or not-assembled proteins and performs crucial steps in mitochondrial biogenesis. Yeast cells lacking the *m*-AAA proteolytic complex exhibit deficiencies in the expression of mitochondrially-encoded polypeptides and in the post-translational assembly of the ATP-synthase and of the respiratory chain complexes (Guelin et al., 1994; Tauer et al., 1994; Tzagoloff et al., 1994). Recent studies showed that paraplegin form a high molecular weight complex very similar to the one described in yeast (Atorino et al., 2003). This complex complements the respiratory deficiency of yeast cells lacking the *m*-AAA complex, indicating that the *m*-AAA protease is functionally conserved across species and that the paraplegin complex has the same proteolytic activity of the yeast counterpart. Furthermore, very recent data of electron microscopy studies in mice lacking paraplegin reveal that, long before degeneration, the axons are filled with abnormal mitochondria. Subsequently, axons swell because of accumulation of membranous organelles and neurofilaments. These findings suggest that a mitochondrial-based mechanism underlies this form of the disorder and that the mitochondrial dysfunction may lead to axonal degeneration by impairing axonal transport (Ferreirinha et al., 2004).

SPG13: Hsp60

Further support to the role of mitochondria in HSP pathogenesis came from the identification of a missense mutation (V72I) in the mitochondrial chaperonin, heat shock protein 60 (Hsp60), (SPG13) in a French family with an autosomal

dominant form of HSP (Hansen et al., 2002). Hsp60 proteins belong to a conserved subgroup of chaperone proteins, which promote protein folding in the mitochondrial matrix, in cooperation with the co-chaperonin Hsp10. A complementation assay was performed using wild-type Hsp60 or Hsp60/V72I, together with Hsp10, in bacteria (*E. coli*) where the homologous *groES groEL* chaperonin genes have been deleted. Only the *wt* HSP60, but not the mutant Hsp60/V72I, was able to support the growth of the defective bacteria, showing that the V72I mutant is functionally inactive. So far, there are no clues on how mutations in hsp60 cause HSP, although a mitochondrial defect can be hypothesised.

The reason why the loss of ubiquitous mitochondrial proteins, such as Paraplegin and hsp60, causes the specific degeneration of a subset of axons is still unknown. This will be a central issue for all the genes involved in the different forms of HSP. The most accepted hypothesis is that primary motor neurons are more susceptible to a defect in mitochondrial functions. These neurons in fact have very long axons and they depend, for their survival and function, on efficient transport of organelles, molecular cargoes and synaptic vesicle along the axons. This process requires energy and this is supplied from the mitochondria, which are also transported along the axon. It is possible that mitochondria located very distal from the cell body have to endure for longer time and could be much less efficient in adapting to inefficient protein quality control mechanisms (Ferreirinha et al., 2004).

1.5.5 Genes involved in cellular trafficking

A second group of genes involved in HSP appear to play a role, direct or not, in cellular trafficking. Their identification supports the hypothesis that any defect of

normal trafficking processes and therefore of the axonal transport, may lead to axonal degeneration. The long axons composing the corticospinal tracts and the fasciculus gracilis would be preferential pathological target for this defect.

Kinesin Mutation Found in HSP

The best example of the pathogenic role of impaired axonal transport in HSP comes from the fact that recently, a mutation in a kinesin heavy chain gene, *KIF5A,* has been identified in one family with autosomal dominant form of HSP (SPG10) (Reid et al., 2002). KIF5A, a specific neuronal kinesin, is part of a heterotetrameric complex that constitutes the kinesin motor for transporting cargoes along microtubules in an anterograde direction in axon (from the cell body to the distal end of the axons) (Goldstein, 2001; Goldstein and Yang, 2000; Xia et al., 1998). The mutation identified in this family occurs in an invariant asparagine residue (N256S) located within the motor domain of the molecule, which has been previously identified as crucial to motor function in biochemical studies of kinesin proteins. Studies of a yeast mutant with a substitution in the corresponding amino acid position (N650K) suggest that the human mutation may result in a dominant-negative version of the neuronal kinase-I motor (Hoyt et al., 1993). Moreover, loss-of-function mutations in kinesin heavy chain related genes of various species, such as yeast and Drosophila, cause movement defects that are reminiscent of those observed in human spastic paraplegia (Reid et al., 2002). When the kinesin heavy chain is mutated in this invariant asparagine, this prevents the stimulation of the motor ATPase by microtubule binding. Thus, kinesin mutation studies clearly support a role for defective microtubule-mediated trafficking in causing axonal degeneration.

Atlastin (SPG3A) and the Dynamins

Additional support for defective trafficking as the basis for some forms of HSP is provided by the identification of four different missense mutations in atlastin (SPG3A) that result in dominantly inherited early-onset HSP. The SPG3A gene encodes a product, atlastin, possessing structural homology with members of the dynamin family of large GTPases, particularly guanylate binding protein-1. It is widely expressed, but it is most abundant in brain and spinal cord (Muglia et al., 2002; Zhao et al., 2001b). Mutations in atlastin gene account for approximately 10% of AD-HSP (Reid, unpublished data). Dynamins play essential roles in a wide variety of vesicle trafficking events, i.e. during the formation of clathrin-coated vesicles from the plasma membrane, receptor-mediated endocytosis and endosome trafficking to the trans-Golgi network (Jones and Wessling-Resnick, 1998; Nicoziani et al., 2000). This is important for the action of neurotrophic factors and during neurotransmission (McNiven et al., 2000). Dynamins are essential for the rapid and efficient recycling of synaptic vesicles, a crucial process for neurotransmission and the maintenance of synaptic membrane morphology. In addition, dynamins have been implicated in the maintenance and distribution of mitochondria (Pitts et al., 1999) and have been found to associate with cytoskeletal elements, including actin and microtubules (Ochoa et al., 2000).

The homology with Dynamins let to postulate many possibilities by which atlastin mutations can cause axonal degeneration in HSP. Defective synaptic vesicles and impaired neurotransmission, as well as impaired activation of selective neurotrophic factors or impaired mitochondria distribution could be one of the pathogenetic mechanisms underlying HSP due to SPG3A mutations (Fink, 2003).

SPG20, SPG21: Spartin, Maspardin and Endosomal Trafficking

The Troyer syndrome (TRS) is an autosomal recessive complicated form of HSP associated with dysarthria and distal amyotrophy, present at high frequency in the Amish population of the United States (Cross and McKusick, 1967). *SPG20* is the gene mutated in Troyer syndrome and it encodes for a novel protein named Spartin (Patel et al., 2002). Spartin contains three novel domains, two of which are located in the C-terminal portion and for which no functional data are available. The N-terminal portion contains a recently described ESP domain, so named because it was identified in three molecules: End13/Vps4, SNX15 (sorting nexin 15), and PalB (Phillips et al., 2001). This domain is also referred to as MIT domain (microtubule interacting and endosomal trafficking molecules) (Crosby and Proukakis, 2002). The N-terminal portion of the MIT domain has similarity to the tetratricopeptide repeat homology consensus sequence (Phillips et al., 2001), which mediates protein-protein interactions (Blatch and Lassle, 1999). The MIT domain is present in many other molecules (fig.3). For example, the sorting nexins (SNX) are a family of cytoplasmic and membrane-associated proteins that are involved in various aspect of endocytosis and protein trafficking. Endocytic pathways function to internalize extracellular components. After internalisation by clathrin-coated vesicles, cargo proteins are delivered to early endosomes and then they are sorted for delivery to one of these destinations: to the cell surface via the recycling endosomes; to the lysosomes via the late endosomes or to the Trans Golgi network (TGN) (Worby and Dixon, 2002). Different sorting nexin function in one of these specific pathways. Sorting nexin 15 (SNX15) is a recently discovered SNX that is thought to play a crucial role in trafficking through the endocytic pathway (Barr et al., 2000; Phillips et al., 2001). In

particular SNX15 affects the internalisation of the transferrin receptor and of the platelet-derived growth factor (PDGF) and is important for the protein trafficking process that involves the endocytic pathway and the TGN, and in particular for the localisation of furin to the TGN. Furin is predominantly localised to the TGN, but cycles continuously from the TGN to the plasma membrane, and returns to the TGN through sorting/recycling or late endosome (Ghosh et al., 1998; Worby and Dixon, 2002), #1998)(Mallet and Maxfield, 1999).

In addition, the MIT domain has been also identified in yeast vacuolar protein sorting factor (Vps4p), in its mammalian orthologues VPS4 and SKD1, and in spastin (commonly mutated in AD-HSP), which are all closely related ATPases (Babst et al., 1997; Beyer, 1997; Hazan et al., 1999; Yoshimori et al., 2000). Yeast Vps4p is an essential component of the intracellular protein transport machinery, being required for the efficient transport of newly synthesized carboxy-peptidase Y from the Golgi network to the vacuole, the yeast counterpart of the animal lysosome (Babst et al., 1998).

Like SNX15, Vps4p primary sequence lacks a clear membrane-binding region. Nevertheless it contains a putative coiled-coil motif (Scheuring et al., 2001) corresponding to the terminal portion of the MIT domain. Deletion of the region including this coiled-coil motif abolishes the membrane association, thus demonstrating that the MIT domain is implicated in the binding to endosomal membranes (Babst et al., 1998). SKD1, a mouse orthologue of VPS4 (Scheuring et al., 2001), is also involved in this process and is believed to associate transiently with membranes. Recent data suggest that SKD1 is required for the formation of autolysosomes in the late stages of the autophagic pathway (Nara et al., 2002).

Finally, the MIT domain is also contained within the recently identified human protein RPK118, which was found to colocalize with early endosomes (Hayashi et al., 2002).

Recently, the SPG21 gene has been identified as the gene mutated in Mast syndrome (Simpson et al., 2003). Mast syndrome is a complicated form of HSP in which progressive spastic paraplegia is associated with dementia and other CNS abnormalities (Cross and McKusick, 1967). The SPG21 protein product, named Maspardin, localises both to the cytosol and to vesicles of the endosomal/trans-Golgi network (Zhang et al., 2002). On those bases maspardin is believed to be involved in the sorting and/or trafficking of molecules and would therefore represent another HSP gene involved in cellular trafficking.

1.6 SPG4 and its protein product: SPASTIN

The most common form of AD-HSP, 40% of AD cases, is linked to the SPG4 locus on chromosome 2p21-p22 (Hazan et al., 1994; Hentati et al., 1994). This gene consists of 17 exons and encodes a 616 amino acid protein, ubiquitously expressed, of unknown function, named Spastin.

Spastin is expressed at a very low level; therefore the expression pattern of human and murine spastin has been detected by PCR on normalised cDNA collections. The murine spg4 transcripts are ubiquitously expressed in adult tissues and from embryonic day (E) 7 to E17. The human SPG4 is ubiquitously express in adult and fetal human tissues, with a slightly higher expression in fetal brain (Hazan et al., 1999). Human spastin is 96% identical to its mouse orthologue, this high level

of identity together with the low level of polymorphism throughout the coding region of spastin gene suggest a low level of tolerance for amino acids substitutions (Svenson et al., 2001).

Analysis of Spastin primary structure underlines the presence in the N-terminal region of a NLS, between amino acids 7 and 11, (Hazan et al., 1999) and of a MIT domain. The carboxy-terminal portion of the protein is characterized by the presence of an AAA cassette (aa 342-599), where the three characteristic ATPase domains are recognisable, the walker domain A and B (Walker et al., 1982) located respectively between amino acid positions 382-389 and 437-442 and the AAA minimal consensus located between 480-498 (Hazan et al., 1999). Notably, the MIT domain present within the endosomal trafficking molecules was also detected in the N-terminus of Spartin. Since the MIT domain lies within the N-terminal portion of spastin and spartin, and no other domains in this region have been discovered, it seems possible that the MIT provides the structural framework in which a common pathogenetic mechanism of HSP can be found. However, the domain is also present within molecules not involved in HSP, i.e. the Vps4p orthologues, as well as within SNX15 and RPK118, which are involved in endosome modulation (Crosby and Proukakis, 2002). Recently, Charvin *et al* reported the existence of a spastin splice variant lacking the exon 4. The two isoforms are both present in human and mouse tissue with a tissue specific variability of the isoform ratio, and so far none of the mutations found in HSP-SPG4 patients map to the exon 4. Moreover, consistently with the NLS presence, Spastin seems to be a nuclear protein, abundant in neural tissues (Charvin et al., 2003).

1.6.1 Spastin mutations

The spectrum of SPG4 mutations in AD-HSP includes missense, nonsense and splice site mutations, as well as insertions and deletions (table 2). Notably, all the missense mutations found in SPG4 patients fall into the AAA domain, with the exception of the S44L substitution that appears to be disease causing only in the homozygous state, underlying the functional significance of this domain (Fonknechten et al., 2000; Hentati et al., 2000; Ki et al., 2002; Lindsey et al., 2000; Namekawa et al., 2002; Proukakis et al., 2003; Proukakis et al., 2002; White et al., 2000; Yabe et al., 2002). The other mutations are scattered along the coding region of the gene (with the exception of the exons 1,4,6 and 17) and lead to premature termination codons, and mRNA instability suggesting that haploinsufficiency is the molecular cause of the disease (Burger et al., 2000). There is no correlation phenotype-genotype, and the phenotype of the missense mutations is the same of the loss of function mutations.

It has also been reported a late onset dementia in association with one patient with pure HSP due to a missense mutation (A1395G) in SPG4 gene. Two other affected family members were reported to have had late onset memory loss, and a younger affected individual of the same family showed signs of memory disturbance and learning difficulties (White et al., 2000). Autopsy of the patient with dementia confirmed changes in the spinal cord typical of HSP and also demonstrated specific cortical pathology. Corticospinal tract pathology showed myelin pallor and loss of axons in the lateral and ventral corticospinal tracts. In relation to dementia seen in this patient, there were some interesting findings. The substantia nigra, in fact, showed frequent Lewy bodies formation. There was neuronal depletion in the

hippocampus and the surviving neurons showed frequent neurofibrillary tangles that were immunoreactive for tau, but no senile plaque formation was reported in any region of the brain (White et al., 2000). These pathological findings are not typical of known tauopathies (Dickson, 1998; Spillantini and Goedert, 1998) and confirm that HSP linked to chromosome 2 can be associated with dementia, although the role of spastin in generating this phenotype is unknown (White et al., 2000).

Moreover mRNA expression studies on RNA extracted from lymphocytes from patients permit to identify a leaky mutation (splice-site mutation); that is, the mutant allele produced both mutant (skipped exon) and wild-type (full length) transcripts. This finding suggests that relatively small differences (less than 50%) in the level of wild-type spastin expression can have significant functional consequences (Svenson et al., 2001).

1.7 AAA proteins

AAA proteins are ATPase enzyme associated with diverse cellular activities, they are found in eukaryotes, prokaryotes and archeabacteria, underlining their ancient origin and the important role played, virtually, in all life forms. The unifying feature of the AAA superfamily is a conserved ATPase domain, of about 220 amino acid, referred to as AAA module or AAA cassette (Confalonieri and Duguet, 1995; Patel and Latterich, 1998). The classical AAA proteins are easily recognised, in fact, by their strong sequence conservation in the AAA domain (~ 30% identity). Furthermore, a broader AAA^+ superfamily, embracing the classical AAA family, has been proposed on the basis of more accurate sequence alignments and structural

information (Neuwald et al., 1999). In fact, although their sequences are more divergent compared with the classical AAA proteins, clamp loading subunits for DNA polymerase (Guenther et al., 1997), the Clp/Hsp100 family of ATPase (Bochtler et al., 2000), and the microtubule-based motor dynein (Neuwald et al., 1999) all contain an AAA structural fold (Vale, 2000).

The members of the originally defined "AAA family" contain a specific motif, named SRH (by Second Region of Homology) or AAA minimum consensus, in addition to the Walker motif A and B, present in all the AAA^+ proteins. In general, the domain architecture of the AAA proteins consists of a non ATPase N-terminal domain, mainly involved in substrate recognition, followed by one or two AAA domains, named D1 and D2. When two AAA modules are present on a polypeptide, they can both be conserved or just one of them, but usually only one module (D1 or D2) has an high enzymatic activity, while the other as a more structural role (Whiteheart, 1994). All the wide range of functions absolved by the different members of the AAA family requires a chemo-mechanical converter, the AAA module, which drives its energy from ATP hydrolysis. The "motor" module is attached to other domains that act usually by interacting directly or through adaptors with substrates.

In figure 4 are represented the different localisation and the different processes in which some of the AAA proteins are involved. The members of the AAA ATPase family play important roles in numerous cellular activities including proteolysis, protein folding, membrane trafficking, cytoskeleton regulation, organelle biogenesis, DNA replication, and intracellular motility. Some of them are involved in recognizing specific proteins and prepare them for degradation. In eukaryotes, the

regulatory particle of the 26S proteasome contains six distinct AAA proteins (Walz et al., 1998). They form an oligomeric structure that sits on the top of the proteolytic channel. It seems that the AAA enzymes are used to unfold target proteins so that they can enter the protease cavity (Weber-Ban et al., 1999). Other AAA-ATPases involved in the unfolding and degradation of misfolded proteins is the member of the *m*-AAA complex in mitochondria. For these proteins the same chaperone activity, that unfolds proteins for degradation, can also assist proteins in folding to their active conformation.

Another subgroup of AAA proteins is involved in disassembling stable protein-protein complexes using the energy derived from the ATP hydrolysis. The best example of this category is the N-ethylmaleimide sensitive factor (NSF), which dissociates a complex of SNAREs (soluble NSF attachment protein (SNAP) receptors). The SNARE complex facilitates the fusion in vesicle trafficking pathways by bringing two membranes together and NSF is involved in the recycling of these complexes for other membrane fusion events. For this purpose NSF needs another protein, □SNAP, which functions as a bridge between NSF and the SNARE complex. The precise mechanism of this process is not known, but it's believed that an ATP-driven conformational change in NSF is relayed to □SNAP and as a consequence to SNARE. Another AAA protein highly homologous to NSF, p97, seems to be involved in membrane fusion events. p97 is one of the most abundant cytosolic proteins and it is involved in different cellular processes depending on the co-factor to which is complexed. In mammals, p97 and its cofactor p47, participate in postmitotic fusion processes which reconstitute the endoplasmic reticulum and the Golgi apparatus (Acharya et al., 1995; Latterich et al., 1995; Rabouille et al., 1995).

p47 is an adaptor which targets certain substrates to p97. Additional adaptor proteins for p97 have been identified. A heterodimeric complex of Ufd1 and Npl4 competes with p47 for binding to p97 (Meyer et al., 2000). Ufd1 is involved in ubiquitin-dependent processes and Npl4 is involved in nuclear targeting, suggesting that p97 is involved in other processes, different from membrane fusions, and in particular it could be involved in ubiquitin dependent nuclear events. Recent data show that RNA interference of p97 in *Drosophila* S2 and human HeLa cells caused significant accumulation of high-molecular-weight conjugates of ubiquitin, an indication of inhibited ubiquitin-proteasome system (UPS) These results lead Wojcik et al. to postulate that p97 plays an important general role in mediating the function of the UPS, probably by interacting with potential proteasome substrates before they are degraded by the proteasome (Wojcik et al., 2004).

Furthermore, the AAA-ATPase Cdc48/p97 and its adapters Ufd1-Npl4 also regulate spindle disassembly by modulating microtubule dynamics and bundling at the end of mitosis (Cao et al., 2003). Genetic analyses of Cdc48, the yeast homolog of p97, reveal that Cdc48 is also required for disassembly of mitotic spindles after execution of the mitotic exit pathway. Moreover, Cdc48/p97-Ufd1-Npl4 directly binds to spindle assembly factors and regulates their interaction with microtubules at the end of mitosis. Therefore, Cdc48/p97-Ufd1-Npl4 is proposed to be an essential chaperone that regulates transformation of the microtubule structure as cells re-enter interphase (Cao et al., 2003). Another potential adaptor protein is the DNA unwiding factor (DUF), suggesting that p97 could be implicated also in DNA replication (Yamada et al., 2000). Therefore, p97 represents an example of how a single AAA

protein can use the energy derived from ATP hydrolysis to assist different cellular processes.

Because AAA proteins functions in so many different cellular processes, it has been very difficult to define a common mechanism of action. However, the structural and sequence conservation of the AAA module throughout three phylogenetic kingdoms strengthen the hypothesis that some similarity in their function exist.

Recent structural and enzymatic studies are providing new data on the properties of the conserved AAA domain.

1.7.1 Structure and mechanism of AAA ATPase

So far two structures of AAA domains have been determined the D2 domain of NSF (Lenzen et al., 1998; Yu et al., 1998) and the D1 domain of p97 (Zhang et al., 2000). The two structure showed high level of similarity, although only the D1 domain of p97 is a catalytically active and conform to the AAA consensus (Lupas and Martin, 2002). The AAA module is formed by two subdomains, an N-terminal subdomain which has a α/β fold and a nucleotide binding pocket and a smaller C-terminal α-helical subdomain (Fig.5). The N-terminal subdomain has a RecA like fold and consists of a five stranded parallel βsheet (strand order β5-β1-β4-β3-β2) flanked on one side by two and on the other side by three α-helices. The highly conserved residues of the Walker A motif form a loop (The P-loop) connecting strand β1 to helix α2, while the Walker B motif is in strand β3 and the ensuing loop (Ogura and Wilkinson, 2001). The C-subdomain, instead, is variable in size and structurally less conserved than the N-subdomain, although it has preferentially a α-helical composition. Even if the nucleotide binding pocket is in the N domain,

positively charged residues from the C-subdomain contribute significantly to the ATP binding. Therefore, ATP binding or hydrolysis might be associated with movement in both the N and C subdomains of the AAA module (Ogura and Wilkinson, 2001). AAA proteins usually function as oligomers, and in most cases they form hexameric ring. VPS4 (Babst et al., 1998) and p60 Katanin (Hartman and Vale, 1999) are AAA proteins with a single ATPase cassette. They exist in equilibrium between monomers and oligomers, in particular for katanin the oligomeric state was confirmed to be a hexameric ring (Hartman and Vale, 1999). For these proteins the oligomerization process is promoted by the presence of non-hydrolysable ATP analogue and by substrate binding. In the case of p97 or NSF, where two AAA modules are present, both AAA modules generate hexameric rings. As already mentioned, in this case one AAA cassette is the main hydrolytic domain and the other, which binds ATP, but hydrolyses it very slowly, has a structural role in hexamer stability (Whiteheart, 1994).

Atomic structures have been solved also for members of the more general AAA^+ superfamily, for one of the clamp loading subunit (δ') (Guenther et al., 1997) and for HsIU (Bochtler et al., 2000), a member of the Clp/Hsp100 protease family. It is evident that the structural folds of these distantly related AAA proteins can be quite well superimposed to the p97/NSF data, indicating that all AAA domains will probably share this basic core structure. This core is composed by an N-terminal α/βsubdomain that contains the ATP pocket and a C-terminal four-helix bundles subdomain that lies on the top of the nucleotide pocket (Vale, 2000). The crystal structure of AAA domain in the hexameric ring (Bochtler et al., 2000; Lenzen et al., 1998; Yu et al., 1998) showed that in the hexamer the nucleotide is located near the

interface between subunits and the active sites contain important residues from the adjacent subunit. This finding can provide an explanation of the fact that oligomerization of some AAA proteins, such as Katanin (Hartman and Vale, 1999), VPS4 (Babst et al., 1998) and NSF (Nagiec et al., 1995), accelerate ATP turnover. Moreover the nucleotide state of the AAA protein, whether it is ATP or ADP bound, affects the affinity for the substrate. In fact, most AAA proteins bind their substrates tightly in the ATP-bound state. Basically, this structural information suggests that ATP binding induces structural rearrangements which increase interactions between adjacent AAA domains as well as between the AAA protein and its target (Vale, 2000). This brings the AAA complex in a "tense state". In turn, the tight interactions between subunits stimulate the ATPase reaction. Once the ATP has been hydrolysed to ADP, the complex pass to a relaxed state in which the interaction between the subunits and with the substrate are weaken. This conformational change between the ATP and the ADP-bound state supply the energy and the mechanical force necessary for the AAA protein function.

1.7.2 AAA proteins and disease

Since the AAA proteins are involved in so many fundamental processes, it is understandable how mutations in gene encoding for AAA ATPases can correlate with human diseases. The first identified human diseases related to AAA protein, were peroxisome disorders such as Zellweger syndrome and neonatal adrenoleukodystrophy. Peroxisome biogenesis requires many proteins (peroxins); in particular two of these proteins, Pex1p and Pex6p, are members of the AAA family.

Approximately 65% of peroxisome disorders are due to mutations in the PEX1 gene (Reuber et al., 1997).

Mutations in the Torsin A, an AAA+ protein, cause a movement disorder, known as early onset (torsin) dystonia, which is characterised by twisting muscle contractures (Ozelius et al., 1997).

Dyneins are minus-end-directed microtubule motors. They can be divided into two classes, cytoplasmic and axonemal. Cytoplasmic dyneins are expressed in most eukaryotic cells and are important for vesicle trafficking and cell division. Axonemal dyneins generate sliding forces between adjacent axonemal microtubule doublets and produce the beating of cilia or undulating movement of flagella. Dynein motor mutations are also associated with several human diseases. For example defects in the axonemal dynein cause primary ciliary dyskinesia (Omran et al., 2000). Also connected to dynein dysfunctions is a brain developmental disorder, lissencephaly. Lissencephaly is a developmental disease of the brain (Vallee et al., 2001; Wynshaw-Boris and Gambello, 2001). It is characterized by disorganization of the cortical regions resulting from defects in neuronal migration. It has been shown that a significant part of the disease is caused by mutations in the gene encoding LIS1, but how LIS1 causes a neuronal migration defect is not clear (Reiner et al., 1993) (Cardoso et al., 2002). Recently, it was shown that LIS1 interacts with cytoplasmic dynein (Smith et al., 2000; Tai et al., 2002) and that their interaction is evolutionarily conserved. This interaction (of LIS1 and cytoplasmic dynein) might cause neuronal migration defects either by affecting cell division, which is crucial for deciding the final destination of a cortical neuron, or by affecting the extension of leading processes.

As discussed previously, two AAA proteins are involved in different forms of hereditary spastic paraplegia: Paraplegin (Casari et al., 1998) and Spastin (Hazan et al., 1999).

So far, not many disease related to AAA proteins defect are known, but given the crucial role of AAA proteins, it is likely that more AAA genes will be associated with human diseases in the future.

1.8 Spastin and AAA proteins

As described above, Spastin is the protein mutated in the most common autosomal dominant form of HSP and it belongs to the AAA family.

Based on sequence homology and on phylogenetic studies, the AAA proteins can be divided in subgroups that are related not only in structure but also in cellular function. In particular, Spastin belongs to the subfamily-7 of AAA proteins, also called the "meiotic group" (Fig.6) or "cytoskeleton interaction protein" group because of its member's function (Beyer, 1997; Swaffield and Purugganan, 1997). The best characterized proteins of this group are p60 katanin and Vps4/SKD1.

The murine SKD1 and its yeast homolog Vps4p are ATPase involved in regulation of the morphology of endosomes and in endosomal trafficking (Bishop, 2000; Yoshimori et al., 2000).

Katanin is a microtubule-stimulated ATPase, requires ATP hydrolysis to severe microtubules (McNally and Vale, 1993), and is proposed to be involved in mitosis (Vale, 1991), neuronal differentiation (Ahmad et al., 1999a) and flagellar physiology (Lohret et al., 1999). Katanin is a heterodimer consisting of an AAA-ATPase subunit

(p60) and an accessory subunit (p80) (Hartman et al., 1998; McNally and Vale, 1993). The p60 subunit is composed of an N-terminal domain that binds microtubules (Hartman and Vale, 1999) and a C-terminal domain sharing homology with the AAA proteins (Hartman et al., 1998). The p80 subunit is composed of an N-terminal WD40 repeat domain and a C-terminal domain required for dimerization with the catalytic p60 subunit. The WD40 domain of p80 is required to target katanin to the spindle pole, possibly through interactions with other spindle pole proteins (Hartman et al., 1998; McNally, 2000). By structural studies in presence of a non-hydrolysable ATP analogue, it has been possible to draw a model in which microtubules act as a scaffold upon which katanin oligomerizes after it has exchanged ADP for ATP. Once a complete katanin ring (hexamer of katanin dimer) is assembled on microtubules, the ATPase activity of katanin is stimulated. Successively to ATP hydrolysis and phosphate release, katanin oligomers undergo a conformational change that creates a pushing force on the underlying tubulin subunits, leading to a destabilisation and a consequent dissociation of tubulin-tubulin contacts (severing) (fig.7)(McNally, 2000; Quarmby, 2000).

For other AAA proteins, such as Vps4, a similar mechanism can be adopted, where ATP binding, together with enzyme-substrate binding, may allow the formation of a transient, closed ring conformation. Vps4 exists as a homodimer in the ADP bound state, whereas, when ADP/ATP exchange occurs, Vsp4 dimers assemble into a decameric complex. The oligomeric structure is susceptible to ATP hydrolysis, which drives cycles of association and dissociation of the Vps4 dimers/decamers and at the same time regulates the association with the substrate, the endosomes (Babst et al., 1998).

As for the other proteins of the Sb7 family, Mei-1 from *C. elegans* has a high degree of similarity to katanin p60. It forms a heterodimeric complex with mei-2, and mei-1/mei-2 complex shows microtubule severing activity and is required for meiotic spindle pole organization in *C.elegans* (Dow and Mains, 1998; Srayko et al., 2000).

Sap1 from *S. cervisiae* associates with the transcriptional activator Sin1p and is required for mitotic chromosome segregation (Liberzon et al., 1996). A very recent identified gene of this subfamily is the mouse Fidgetin-1, which seems to be involved in embryonic development (Cox et al., 2000).

1.9 Aims of the project

Hereditary spastic paraplegia is a very heterogeneous disease. Many genes are involved and each of them seems to play a different role. Almost all the proteins mutated in the different forms of HSP are ubiquitously expressed, thus an important point is to understand how a defect in a ubiquitous protein give rise to an extremely specific cellular phenotype. Moreover, it's also interesting how proteins involved in so many different pathways and processes can all lead, when mutated, to the specific degeneration of the longest axons in human body.

Spastin has been identified only recently (Hazan et al., 1999) and nothing is known about its biological role. In this context, the aim of this work has been to get insight on spastin biological function. A first step has been to investigate spastin subcellular localisation, by looking at the exogenous and at the endogenous protein. Therefore, spastin cDNA has been introduced in several tagged eukaryotic expression vectors and exogenous protein localization has been analysed by immunofluorescence after the transfection of spastin plasmid into the cell. On the other hand, several spastin specific antibodies have been produced in the lab and the endogenous subcellular localisation of spastin was analysed by immunofluorescence studies with the different antibodies on different cell lines. In a second step, two hybrid screening techniques has been used to identify spastin putative interactors and to try to insert spastin in a specific cellular process. Thus, this thesis represents a preliminary work in understanding spastin biological function by elucidating its subcellular localization and its biological partners. Moreover, comparison of spastin function with the role exerted by other genes involved in the different forms of HSP

will provide more information in understanding whether there is a common pathogenetic mechanism underlying hereditary spastic paraplegias and which role spastin is playing in generating the disease.

Symbol/Locus	Cytogenetic Location	Inheritance	Protein	HSP Syndrome(s)
L1CAM(SPG1)	Xq28	X-linked	L1CAM	Complicated
PLP1 (SPG2)	Xq28	X-linked	PLP1	Complicated (rarely pure)
SPG3A	14q11-q21	Autosomal dominant	Atlastin	Pure
SPG4	2p22	Autosomal dominant	Spastin	Mainly pure
SPG5A	8q	Autosomal recessive		Pure
SPG6	15q11.1	Autosomal dominant	NIPA1	Pure
SPG7	16q24.3	Autosomal recessive	Paraplegin	Pure and complicated
SPG8	8q23-q24	Autosomal dominant		Pure
SPG9	10q23.3-q24.2	Autosomal dominant		Complicated
SPG10	12q13	Autosomal dominant	KIF5A	Pure
SPG11	15q13-q15	Autosomal recessive		Pure
SPG12	19q13	Autosomal dominant		Pure
SPG13	2q24-q34	Autosomal dominant	HSP60	Pure
SPG14	3q27-q28	Autosomal recessive		Complicated
SPG15	14q22-q24	Autosomal recessive		Complicated
SPG16	Xq11.2	X-linked		Complicated
SPG17 (Silver syndrome)	11q12-q14	Autosomal dominant	BSCL2 (seipin)	Complicated
SPG19	9q33-q34	Autosomal dominant		Pure
SPG20 (Troyer syndrome)	13q12.3	Autosomal recessive	Spartin	Complicated
SPG21	15q22.31	Autosomal recessive	Maspardin	Complicated

Table 1. Summary of the Known HSP Loci and Genes (Crosby and Proukakis, 2002).

Location	Mutation	Amino acid change	References
Missense			
Exon 1	C256T	S44L	(Lindsey et al., 2000)
Exon 6	T1031A	I344K	(Ki et al., 2002)
Exon 7	C1164A	Q347K	(Yabe et al., 2002)
Exon 7	C1210G	S362C	(Fonknechten et al., 2000)
Exon 8	G1233A	G370R	(Fonknechten et al., 2000)
Exon 8	T1267G	F381C	(Fonknechten et al., 2000)
Exon 8	T1283G	N386K	(Fonknechten et al., 2000)
Exon 8	A1282G	N386S	(Orlacchio et al., 2004)
Exon 8	A1288G	K388R	(Fonknechten et al., 2000)
Exon 9	T1336C	F404S	(Hentati et al., 2000)
Exon 10	A1395G	R424G	(Lindsey et al., 2000)
Exon 10	C1401G	L426V	(Fonknechten et al., 2000)
Exon 11	G1468A	C448Y	(Fonknechten et al., 2000)
Exon 11	G1504T	R460L	(Fonknechten et al., 2000)
Exon 12	C1579T	T486I	(Namekawa et al., 2001)
Exon 13	C1620T	R499C	(Fonknechten et al., 2000)
Exon 13	G1633T	R504L	(Proukakis et al., 2003)
Exon 13	G1659C	E512D	(Patrono et al., 2002)
Exon 13	G1704A	G526D	(Hentati et al., 2000)
Exon 14	T1726C	L534P	(Molon et al., 2003)
Exon 15	G1788A	D555N	(Fonknechten et al., 2000)
Exon 15	C1792T	A556V	(Fonknechten et al., 2000)
Exon 15	C1809G	R562G	(Svenson et al., 2001)
Exon 17	G1875C	D584H	(Lindsey et al., 2000)
Nonsense			
Exon 1	G459T	E112STOP	(Hentati et al., 2000)
Exon 1	G465T	E114STOP	(Svenson et al.,

			2001)
Exon 3	C702T	Q193STOP	(Fonknechten et al., 2000)
Exon 5	C859G	S245STOP	(Lindsey et al., 2000)
Exon 5	A873T	K229STOP	(Fonknechten et al., 2000)
Exon 5	C907A	S261STOP	(Fonknechten et al., 2000)
Exon 5	C932G	Y269STOP	(Fonknechten et al., 2000)
Exon 9	C1195T	R399STOP	(Hentati et al., 2000)
Exon 10	C1416T	R431STOP	(Fonknechten et al., 2000)
Exon 15	C1809T	R562STOP	(Fonknechten et al., 2000)
Frameshift			
Exon 1	190-208dup19		(Proukakis et al., 2003)
Exon 1	411delG		(Lindsey et al., 2000)
Exon 2	578-579insA		(Fonknechten et al., 2000)
Exon 4	710insA		(Hentati et al., 2000)
Exon 5	852del11		(Fonknechten et al., 2000)
Exon 5	882-883insA		(Fonknechten et al., 2000)
Exon 5	906delT		(Fonknechten et al., 2000)
Exon 8	1259-1260delGT		(Proukakis et al., 2003)
Exon 9	1299delG		(Fonknechten et al., 2000)
Exon 9	1340del5		(Fonknechten et al., 2000)
Exon 10	1406delT		(Lindsey et al., 2000)
Exon 10	1442delT		(Molon et al., 2003)
Exon 11	1486insA		(Svenson et al., 2001)
Exon 11	1520delT		(Fonknechten et al., 2000)
Exon 12	1574delGG		(Fonknechten et al., 2000)
Exon 13	1634del22		(Fonknechten et al., 2000)
Exon 14	1684-1685insTT		(Fonknechten et al., 2000)
Exon 14	1685del4		(Fonknechten et al.,

			2000)
Exon 14	1702-1705delGAAG		(Proukakis et al., 2003)
Exon 16	1845delG		(Proukakis et al., 2003)
Splicing			
Intron 4	808-2A>G		(Fonknechten et al., 2000)
Intron 6	1129+2T>G		(Fonknechten et al., 2000)
Intron 6	1130-1G>T		(Proukakis et al., 2003)
Intron 7	1223+1G>T		(Fonknechten et al., 2000)
Intron 8	1298+1G>A		(Lindsey et al., 2000)
Intron 8	1299+1G>A		(Fonknechten et al., 2000)
Intron 9	1370+1G>T		(Yabe et al., 2002)
Intron 11	1538+5G>A		(Fonknechten et al., 2000)
Intron 11	1538+3del4		(Fonknechten et al., 2000)
Intron 11	1538+3A>C		(Lindsey et al., 2000)
Intron 11	1538+3-6del(AAGT)		(Lindsey et al., 2000)
Intron 12	1618+2T>A		(Lindsey et al., 2000)
Intron 13	1661+1G>T		(Fonknechten et al., 2000)
Intron 13	1661+2T>C		(Lindsey et al., 2000)
Intron 13	1662-2A>T		(Fonknechten et al., 2000)
Intron 14	1742-1G>T		(Yabe et al., 2002)
Intron 15	1812+1G>A		(Fonknechten et al., 2000)
Intron 15	1812+2T>G		(Lindsey et al., 2000)
Intron 15	1813-2A>G		(Fonknechten et al., 2000)
Intron 16	1853+1G>A		(Fonknechten et al., 2000)
Intron 16	1853+2T>A		(Proukakis et al., 2003)
Intron 16	1853+2T>C		(Lindsey et al., 2000)

Table 2. Mutations found in patients with HSP linked to the SPG4 locus.

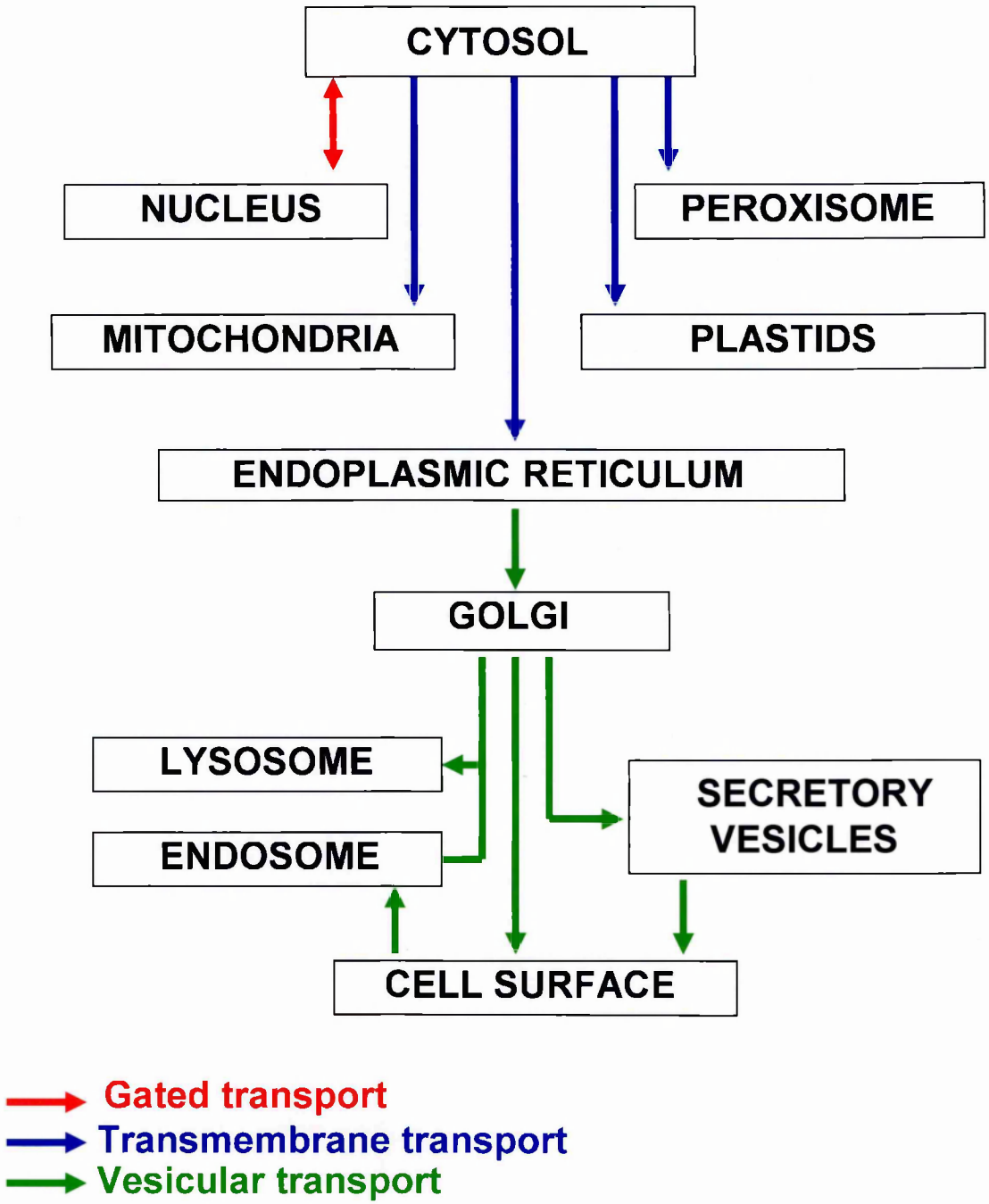

Figure 1. Map of protein trafficking.

Protein can move from one compartment to another by gated transport (red), transmembrane transport (blue) or vesicular transport.

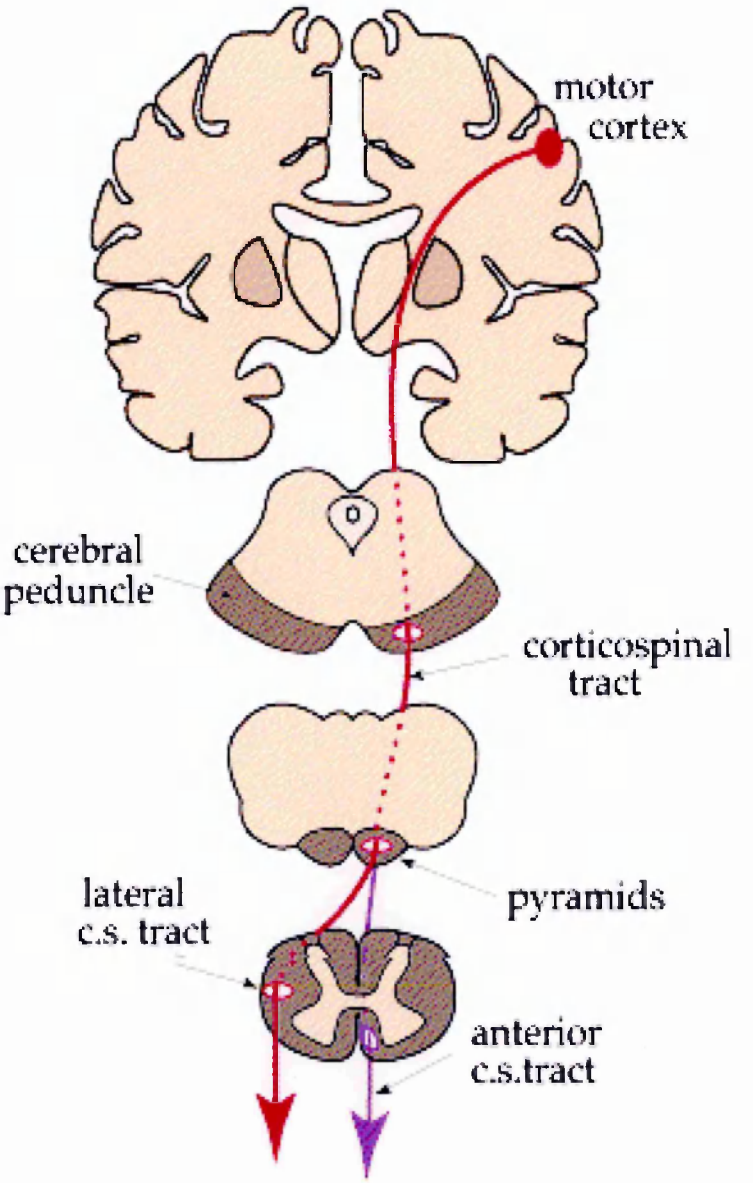

Figure 2. Corticospinal tract.

The pathway that drives a deliberate movement can be divided into: descending connection between neurons in the motor cortex and cells in the anterior and posterior horns of the spinal cord (corticospinal tract) and the lower motor neuron in the anterior horn connect to the skeletal muscle.

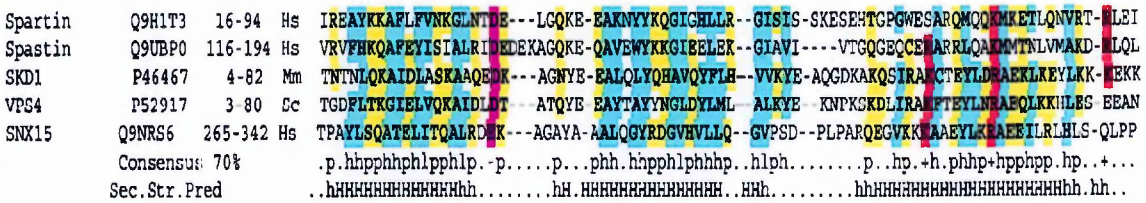

Figure 3. Multiple sequence alignment of selected members of the MIT domain containing proteins.

Sequences are indicated using their database accession number followed by the starting and the ending residues of the domain and by the species. The consensus present in 70% of the sequences is given below the alignment; residues and colours are as follows: h (hydrophobic, *blue*), l (aliphatic, *blue*), K (lysine), p (polar, *yellow*), and R (arginine). Plus signs (+) indicate conserved, positively charged residues (lysine and arginine), which are in red in the alignment; minus signs (-) indicate conserved negatively charged residues, which are indicated in pink. The secondary structure prediction ("Sec.Str.Pred.") at the bottom of the alignment is derived from the alignment (H = helix predicted with expected average accuracy >82%; h = helix predicted with expected average accuracy <82%). Abbreviations: Hs, *Homo sapiens;* Mm, *Mus musculus;* and Sc, *Saccharomyces cerevisiae* (Ciccarelli et al., 2003).

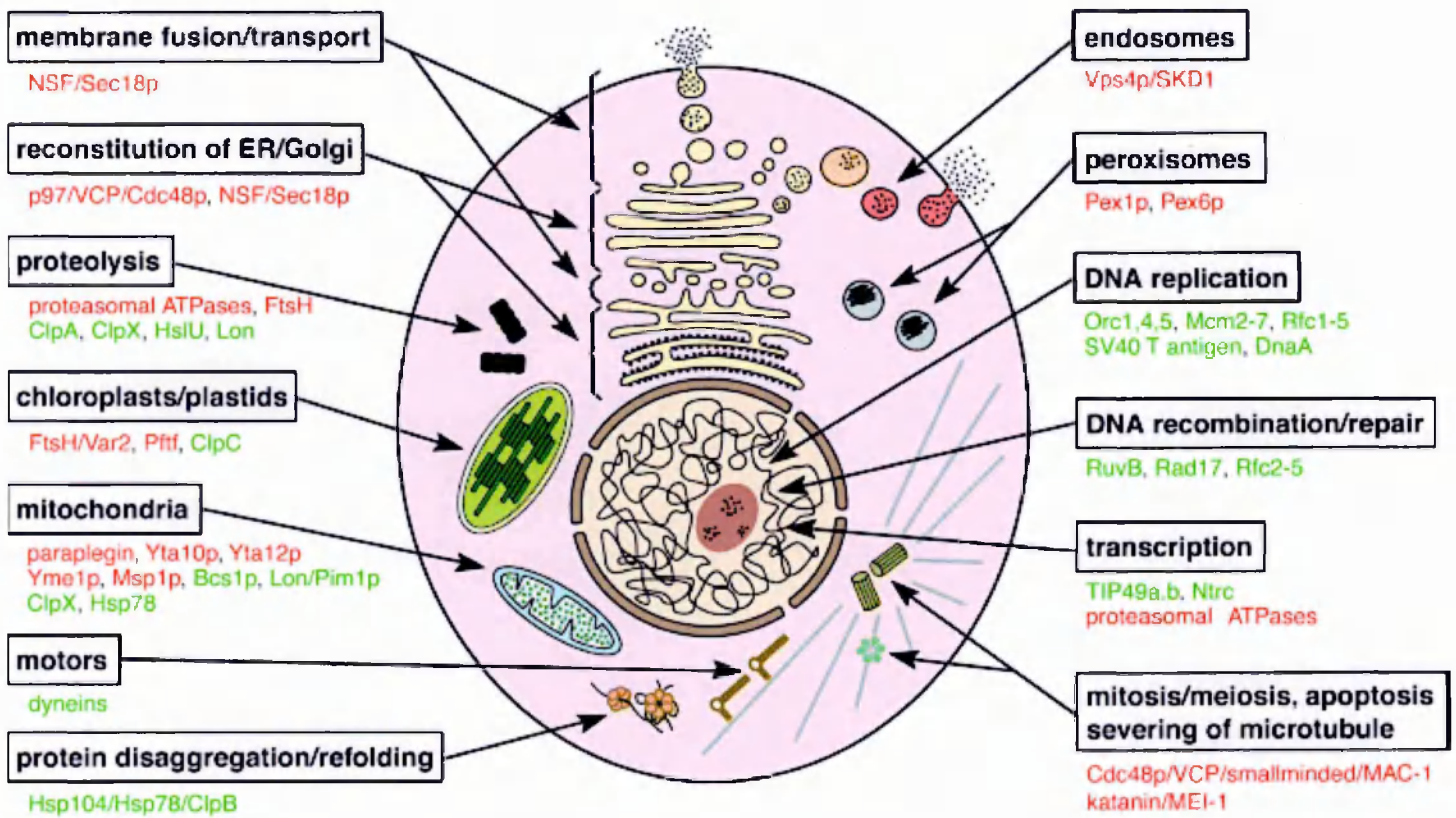

Figure 4. The diverse cellular functions of AAA+ proteins.

Schematic diagram of a hypothetical eukaryotic cell with representative organelles and macromolecular assemblies. The subcellular localization of AAA+ proteins and the processes in which they participate are indicated. Prokaryotic members are also included. AAA members are in red and other AAA+ members in green (Ogura et al., 2001).

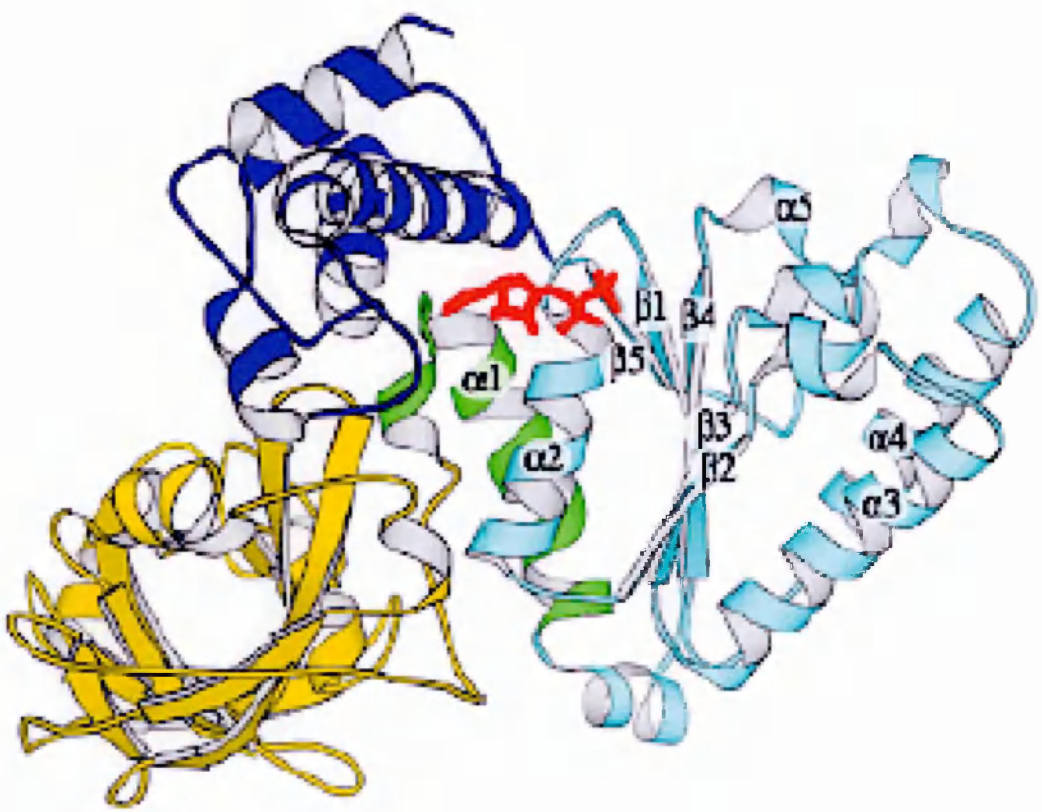

Figure 5. AAA structure.

Structure of p97-D1 AAA domain. The N and C terminal domains of the AAA module are coloured cyan and blue, respectively, with the sequence at the N-terminus of the N-domain coloured in green. The additional N-domain of p97 is coloured in yellow. Adenine nucleotides are shown in red (Ogura and Wilkinson, 2001).

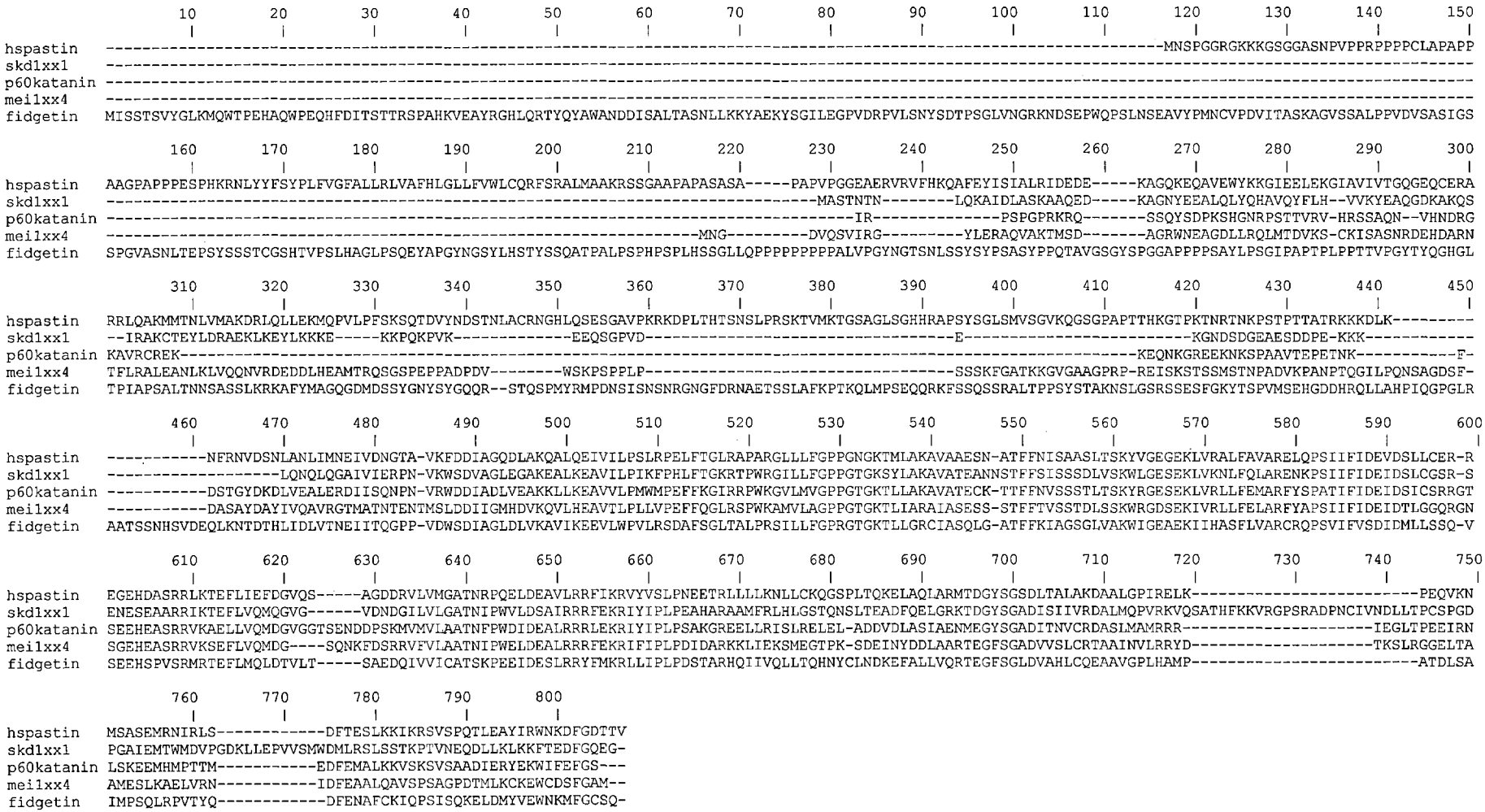

Figure 6. Sequence alignment of the different member of the subfamily 7 or meiotic group of the AAA superfamily.
Multiple alignment was done with Clustal W at the PBIL (http://npsa-pbil.ibcp.fr/cgi-bin/npsa_automat.pl?page=npsa_clustalw.html). Identical amino acids are in pink, strongly similar amino acids are in green and weakly similar residues are in blu.

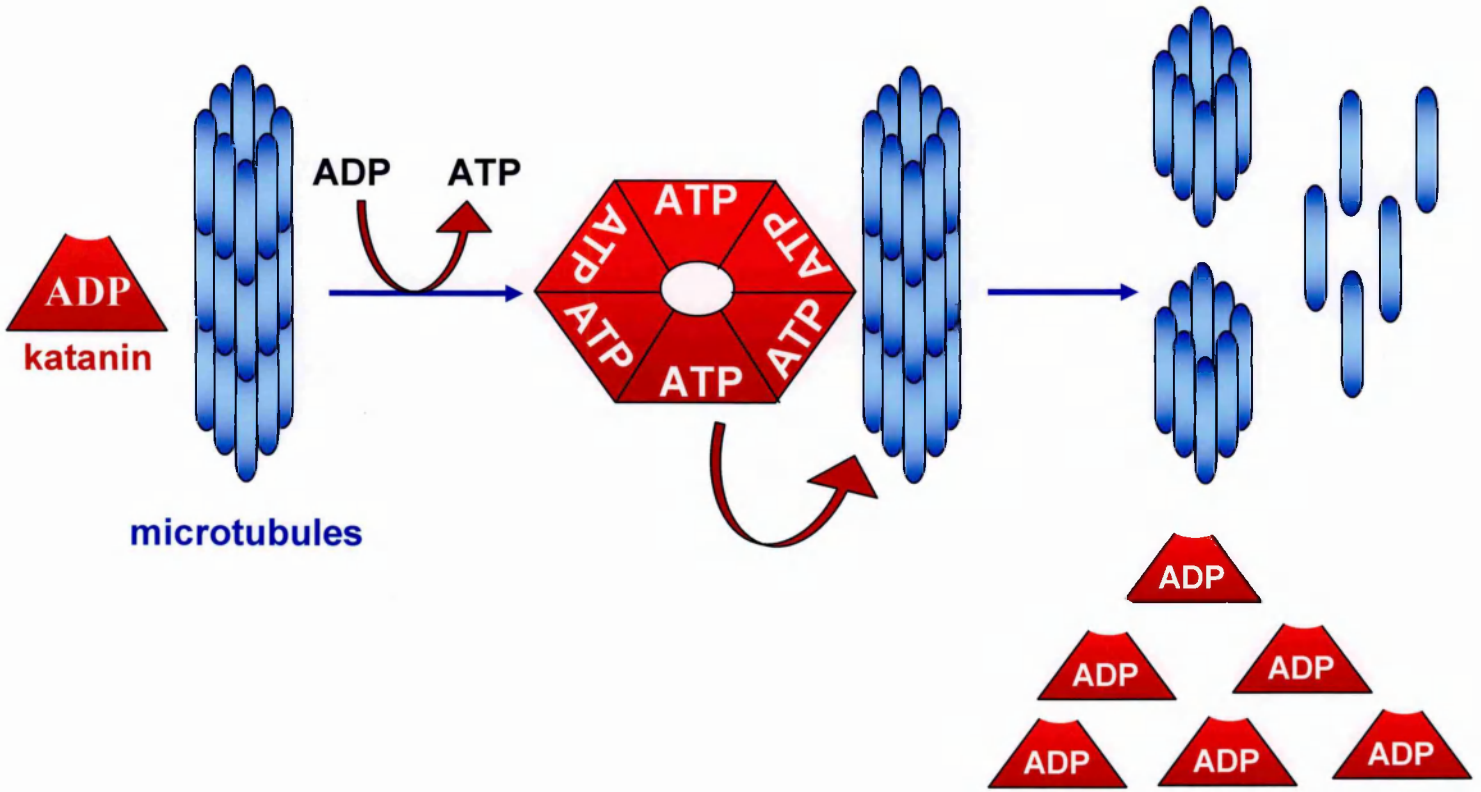

Figure 7. Model for katanin severing activity.

Microtubules act as a scaffold upon which katanin oligomerizes after it has exchanged ADP for ATP. Once a complete katanin ring is assembled on microtubules, the ATPase activity of katanin is stimulated. Successively to ATP hydrolysis and phosphate release, katanin oligomers undergo a conformational change that creates a pushing force on the underlying tubulin subunits, leading to a destabilisation and a consequent dissociation of tubulin-tubulin contacts, with the recycling of katanin subunit.

CHAPTER 2: MATERIALS AND METHODS

2.1 Generation of spastin constructs for expression studies

2.1.1 Constructs for expression studies

To clone the full-length or partial Spastin cDNA into sveral expression vectors (appendix B), conventional Polymerase Chain Reaction (PCR) was performed with appropriate primers that incorporated convenient restriction enzyme sites. HeLa cDNA was used as template and specific primers designed on available sequence (Hazan et al., 1999).

For the PCR, *Pfu Turbo* Polymerase (Stratagene) was used as follows:

5 µl 10x *Pfuturbo* buffer

0.4 mM of each dNTP

125 ng forward primer

125 ng reverse primer

1 µl *Pfuturbo* Polymerase

50 ng DNA template

dH_2O to 50 µl

For the amplification of Spastin cDNA, PCR reactions were usually performed with the following cycling parameters:

1 cycle: 5 min at 95°C

30 cycles: 30 sec at 95°C

30 sec at the primer annealing temperature

2 min at 72°C (or 1 min per each Kb of DNA to amplify)

1 cycle: 10 min at 72°C

The resulting PCR product was analysed by agarose gel electrophoresis, and extracted from the gel using Quiaquick columns (Quiagen), according to the manufacturer's protocol. The purified DNA was then digested with the appropriate restriction enzymes and the resulting fragments were subcloned in frame into the following eukaryotic vectors (previously digested): pMT21-myc (blant/SalI) (primers SP1/SP2, see appendix A), pcDNA3-HA (EcorI/XhoI) (primers SP1/SP3) and pcDNA3-myc-GFP (EcorV/XhoI) (primers SP1/SP3) and in pcDNA3 (BamHI/NotI) (primers SP4/SP5).

The vectors (3 µg) were digested using the same restriction enzymes of the respective inserts, the DNA were analysed and purified from agarose gel (eluted in 30 µl) and the ligations were set up as follows:

2 µl 10x ligation buffer

2 µl vector DNA

5-10 µl insert DNA

1 µl T4 DNA Ligase (New England Biolabs)

dH_2O to 20 µl

Ligation was carried out at 2 hrs at room temperature. The whole reaction was used for transformation of chemical competent DH5α *E. coli* cells. The resulting clones were analysed by restriction digest and sequencing.

In the resulting constructs, the myc and GFP tags are positioned C-terminal to the spastin coding region, while the HA-tag is N-terminal to it.

The spastin$^{\Delta\text{-AAA}}$ construct (corresponding to the nonsense mutation C932G, Y269STOP) was generated by PCR amplification with specific primers (primers SP1/SP6), using Pfu Turbo polymerase, and subcloned into the pMT21-myc vector (blant/SalI). The spastin$^{\Delta\text{-N}}$ construct, lacking the first 241 amino acids of spastin, was generated by digesting the spastin-myc construct with EcorI/SpeI, followed by KlenowI (Biolabs) treatment at room temperature for 10 min and self-ligation. The ATG is reconstituted after self-ligation. In each case the integrity of the clones was determined by direct sequencing.

2.1.2 Constructs for yeast two hybrid screening

The constructs pAR202-LexA-Spastin (primers SP4/SP5) and pAR202-LexA-spastin$^{\Delta\text{-AAA}}$ (primers SP4/SP7) for the two hybrid screening were prepared by PCR amplification with specific primers (as described above) and subcloned into the pAR202 vector (BamHI/NotI). The pAR202-LexA- spastin$^{\Delta\text{-N}}$ construct was prepared by digesting the pAR202-LexA-Spastin construct with EcorI/SpeI, followed by KelnowI treatment at room temperature for 10 min and self-ligation. The integrity of the clones was determined by direct sequencing.

2.1.3 Constructs for antibodies production

Two different constructs were used for the production of specific spastin antibodies. A construct that has been previously prepared in the lab and corresponded to a portion of spastin between amino acids 1 and 120 fused with its 5' to a 6His tag (6HisSP). A different portion of spastin, corresponding to amino acids 80-354, was obtained by PCR amplification (primers SP8/SP9) with Pfu Turbo polymerase and subcloned into a pGEX-3X vector (BamHI/EcorI), where the protein product results fused with its N-terminus to the GST protein (GST-SP)

2.1.4 Generation of a chimera NLS (sv40)-Spastin

The SV40 Large T antigen NLS was fused to the N-terminus of Spastin (Kruyt et al., 1997) by using the oligonucleotides NLS-Up (5'-GATCCATGCCGCCGAAGAAAAAGAGAAAGGTGGAG-3') and NLS-Dw (5'-AATTCTCCACCTTTCTCTTTTTCTTCGGCGGCATG). The oligonucleotides have been designed with the restriction sites post-digestion. 5 µg of both oligonucleotides were incubated in a final volume of 20 µl in TrisHCl 200mM pH 7.4/$MgCl_2$ 20 mM/ NaCl 500mM for 5 min at the melting temperature of the oligonucleotides (100 °C). The samples were then cooled in a water bath to 30°C and then kept on ice. The resulting fragment was directly used for the ligation reaction in $pCDNA_3$-spastin (BamHI/EcoRI). As control spastin was also fused to mNLS-Up and mNLS-Dw, which are identical to NLS-Up and -Dw except for the substitution of the underlined nucleotides for C or G respectively, to harbour a hybrid spastin protein with an inactivated Large T NLS.

2.1.5 Cloning of spastin Δex4

pRSET-Δex4 was from Elena Pegoraro. This plasmid was used as template for amplifying Δex4 cDNA by PCR (primers SP1/SP2) and subcloned it into the pMT21-myc vector.

2.1.6 Constructs for mapping the MTs interacting region

Deletion constructs of spastin were prepared by PCR using specific primers. Δ50 (primers SP10/SP2), Δ100 (primers SP11/SP2), Δ190 (primers SP12/SP2) (constructs lacking 50, 100 190 amino acids from the N terminus of spastin) were subcloned into the pMT21-myc vector (EcoRI/ SalI). These constructs were then subjected to site direct mutagenesis to produce for each of them the K388R mutation.

A construct lacking the MIT (340-600bp) domain was prepared in a two-step cloning strategy. pMT21-Spastin-myc plasmid was digested EcoRI/XbaI. The digestion generated two fragment of different size: a small insert of about 600bp and the remaining linearized plasmid. These fragments were separated on a 1% agarose gel and the band corresponding to the linearized plasmid was purified from gel as described above. Using specific primers (SP1/SP13) a portion of 340bp (from 1 to 340 bp) was amplified by PCR and digested EcoRI/XbaI. The plasmid and the PCR product digested have been used for a ligation reaction, and then transformation into DH5□ competent cells.

Furthermore Δ50 (primers SP15/SP5), Δ100 (primers SP16/SP5), Δ190 (primers SP17/SP5), were also subcloned into the pAR202 vector (BamHI/NotI) and used in interaction mating assay.

2.2 Restriction enzyme digestion of DNA

DNA was digested in a final volume of 20 µl at 37°C for 1 h. All the restriction enzymes were from New England Biolabs, and digestions were performed in appropriate buffers, supplied by the manufacturer with the enzyme. All digestions were analysed by agarose gel electrophoresis.

2.3 Agarose gel electrophoresis

Agarose gels (1 % w/v in TAE; 40 mM Tris-acetate pH 7.5, 2 mM EDTA) were prepared and supplemented with ethidium bromide (ca. 1 µg/ml). The percentage of the agarose in gels was determined depending on the size of the DNA fragments to be resolved. Gels were generally run at 120 V in 1x TAE buffer, and DNA was visualised on a UV transilluminator.

2.4 DNA sequence analysis

For DNA sequence analysis, plasmids or PCR were processed by the DNA sequencing core at TIGEM.

2.5 Isolation of DNA from agarose gels

Following agarose gel electrophoresis, DNA gel slices were excised under UV light. DNA was extracted from these gel slices using Quiaquick columns (Quiagen)

following the gel extraction protocol supplied by the manufacturer. Purified DNA was eluted from the columns using 30-50 µl deionized water.

2.6 Quantification of plasmidic DNA

DNA concentration was determined for 1:100 dilutions of stocks according to the following formula:

Absorbance of one A_{260} unit indicates a DNA concentration of approximately 50 µg/ml.

2.7 Transformation of *E. coli* with plasmidic DNA

Transformation of chemical competent cells was generally used for the transformation of *E. coli* DH5□ with plasmid DNA. *E. coli* DH5α cells were prepared for transformation as follows: Cells were grown to mid-log phase (A_{600} = 0.6) in Luria Broth (LB; 1 % bactotryptone, 1 % NaCl and 0.5 % Bacto-yeast extract) at 37°C with shaking. Cells were collected by centrifugation at 1200 rpm at 4°C, resuspended into 30ml (for each 100 ml of culture) of RF1 and kept on ice for 90 min. This suspension was then centrifuged at 1200 rpm for 15 min, the resulting pellet was resuspended in 4ml (for each 100 ml of culture) of ice cold RF2 and kept on ice for 30 min. At this point cells were aliquoted and stored at –80°C. For each transformation, DNA was added to 50 ml of competent cells and incubated on ice for 30 min, then cells were subjected to heat shock treatment at 42°C for 2 min an successively incubated on ice for 10 min. Cells were recovered in 1ml of LB and incubated at 37°C for 1 h, before

plating on LB-agar containing appropriate antibiotics and incubation at 37°C overnight.

Solutions:

RF1 (V=250ml)

1.86g KCl

2.47g $MnCl_2$ $4H_2O$

0.74g CH_3COOK

0.367g $CaCl_2 2 H_2O$

37.5mls Glycerol

pH=5.8 (with CH_3COOH)

RF2 (V=250ml)

0.52g MOPS

0.187g KCl

2.75g $CaCl_2 2 H_2O$

37.5mls Glycerol

pH=7 (with HCl)

2.8 Isolation of plasmid DNA from *E. coli*

Large-scale ('midi-preps') plasmid DNA preparations were carried out using the Quiagen MIDI prep kits according to the manufacturers instructions (Quiagen), while plasmid mini-preps were carried out using the Quiagen MINI prep kits. Both procedures are based on the alkaline lysis method (Sambrook J et al., 1989), but use a support column to purify isolated plasmid DNA. Purified DNA was always checked by enzymatic digestion with appropriate enzymes.

2.9 In vitro site directed mutagenesis

To introduce the point mutations, S44L, S362C, G370R, F831C, N386K, K388R, L426V, C448Y, R460L, R499C and A556V into both the spastin-myc and/or spastin-mycGFP constructs, *in vitro* mutagenesis was performed using the Quickchange site directed mutagenesis kit (Stratagene, La Jolla, CA), according to the manufacturer instructions. The point mutations of the lysine K340R, K462R, K565R were also introduced in the pCDNA$_3$-Spastin construct. Both single and multiple lysine mutants were produced and tested in the *in vitro* SUMO-conjugation assay. The presence of the point mutation was then confirmed by DNA sequencing. The following primers were used:

S44L, 5'-GCCCCTCCGCCCGAGTTGCCGCATAAGCGGAAC-3'

S362C, 5'-GTTATTCTTCCTTGTCTGAGGCCTGAG-3'

G370R, 5'-CCTGAGTTGTTCACAAGGCTTAGAGCTCCTG-3'

F381C, 5'-GGCTGTTACTCTGTGGTCCACCTGG-3'

N386K, 5'-GTCCACCTGGGAAGGGGAAGACAATGC-3'

N386S, 5'-GTCCACCTGGGACTGGGAAGACAATGC-3'

K388R, 5'-CTGGGAATGGGAGGACAATGCTGGC-3'

L426V, 5'-GAAATTGGTGAGGGCTGTTTTTGCTGTGGCTCG-3'

C448Y, 5'-GTTGATAGCCTTTTGTATGAAAGAAGAGAAGGG-3'

R460L, 5'-GCACGATGCTAGTAGACTCCTAAAAACTGAATTTC-3'

R499C, 5'-GGCTGTTCTCAGGTGTTTCATCAAACG-3'

A556V, 5'-GCTTTGGCAAAAGATGTAGCACTGGGTCCTATC-3'

K340R, 5'- AATGGAACAGCTGTTAGATTTGATGATATAGCT-3'

K462R, 5'- GCTAGTAGACGCCTAAGAAGTGAATTTCTAATAG-3'

K565R, 5'- CCTATCCGAGAACTAAGACCAGAACAGGTGAAG-3'

2.10 Expression and purification of spastin fusion protein

6his-SP (6his-Spastin 1-122) construct was expressed in *Escherichia Coli* strain M15. Protein expression was induced with 2mM IPTG over night at 25°C and then purified under denaturing condition.

This cloning, protein production and purification were carried out previously in the lab.

GST-SP (GST-spastin 87-354) construct was expressed in *Escherichia Coli* strain B834. 100 mls LB medium containing the appropriate antibiotic were inoculated overnight at 37°C with vigorous shaking, the morning after the culture was diluted 1:10 (to 1l) and grown at 37°C until their OD_{600} was 0.6. Before induction, 1 ml of bacterial culture was removed as control. After induction with 2 mM IPTG, cells were grown for 3 hours at 25°C. Bacterial samples (1ml of uninduced and 1 ml of induced bacteria) were centrifuged to pellet cells, which were then resuspended in 100 µl of boiling mix (see SDS-PAGE methods). Samples were fractionated by SDS-PAGE and the protein gel was stained with Blue-Comassie (0.1 % Coomassie Blue, 40 % Methanol, 10 % glacial acetic acid in dH_2O) for 15 min and destained in (40 % Methanol, 10 % glacial acetic acid in dH_2O). If the fusion protein was induced, all the bacteria culture was centrifuged to pellet the cells. Cells were processed for native lysis and resuspended in (PBS/500mM NaCl/1mM DTT/1mM protease inhibitor cocktail) and sonicated (6x30sec). The resulting

bacterial suspension was supplemented with Triton-X-100 to a final concentration of 1% (v/v) and centrifuged at 14000 rpm for 30 min in a JA-14 Beckman rotor. Supernatant was collected, transferred to new tubes and centrifuged at 20000 rpm for 2hrs in a JA-20 Beckmann rotor. The lysates obtained was supplemented with 1ml of GST-Agarose beads suspension (50% w/v) and incubated over night at 4°C under stirring. This suspension was then put on a 1ml polypropylene Quiagen column and F/T was collected. Beads were washed with 10 times bed volumes of (PBS/500mM NaCl/1mM DTT) and fusion protein was eluted in 50mM TrisHCl pH 8.5/ 500mM NaCl/1mM DTT/ 10mM Glutathione (1ml fractions). 5 µl of each fraction were checked by SDS/PAGE analysis and those containing the fusion protein were unified. Purified fusion proteins were used for the production of specific rabbit polyclonal and monoclonal antibodies.

2.11 Quantification of protein

Protein concentrations were determined using Bradford's method (Bradford, 1976). Protein samples were mixed with Bradford's reagent (Biorad) and the absorbance at 595 nm was measured on a spectrophotometer. Protein absorbances were converted to mg/ml concentrations using a standard curve constructed by measuring the absorbances of a range of bovine serum albumin (BSA) concentrations.

2.12 Affinity purification of spastin polyclonal antibodies (SP-R74, SP-50 and SP-51)

Primary antibodies to spastin were raised in rabbit (SP-R74 at Primm, Italy; SP-50 and SP-51 at Biogenes, Germany) and were antigen affinity purified. NHS Hi-Trap™ affinity columns were used for the purification of the antibodies from the crude rabbit serum. The columns were washed with 10 volumes of coupling buffer (200mM $NaHCO_3$/ 500mM NaCl pH 7.8). All the antigens were dialysed in coupling buffer. Following this, the appropriate ligand was bound to the column by recirculation of 5mg of recombinant protein (GSTSP or 6HisSP) over the column for 2 hrs at RT. In order to deactivate any excess groups that have not coupled ligand and to wash out not-bound ligand, the columns were washed in buffer A (500mM NaCl/ 500mM Ethanolamine, pH 8.3) and buffer B (100mM CH_3COONa/ pH 4.0). After columns preparation, a 1:10 dilution (in PBS) of rabbit serum was recirculated over the column over night at 4°C. Then, the column were washed with 20 volumes of 10mM Tris/ 500mM NaCl/ pH 7.5 and eluted with 100mM Glycine pH 2.25. 500 µl fractions were collected in 50µl of 1M Tris pH 8.0 in order to neutralise the acidic eluate and preserve antibodies activity. The antibodies so purified were then dialysed in PBS and stored at 4°C.

In the case of SP-50 and SP-51, the sera were first passed through a GST-agarose beads column to discard the portion of antibodies raised against the GST moiety. The flow through from this step was then used for the affinity purification.

2.13 Cell culture and antibodies

Monkey kidney Cos-7 and HeLa cells were maintained in exponential growth in Dulbecco's modified Eagle's medium (DMEM, Highclone) containing 10% fetal bovine serum (Highclone). Immortalised motoneuronal cells NSC-34 (kindly provided by Angelo Poletti, Milan) were cultured in DMEM supplemented with 5% defined fetal bovine serum (Highclone). Human fibroblasts were cultured in a-MEM (GIBCO) supplemented with 10% of defined fetal bovine serum (Highclone).

The affinity purified spastin specific antibodies produced in this work were used as follow: R74 (1:5, IF); SP-50 (1:5 IF, 1:2000 WB and 1:200 in IP); SP-51 (1:5 IF, 1:2000 WB and 1:200 in IP); M3 and M4 (1:1 IF and 1:10 WB).

Monoclonal anti-myc was produced from 9E10 hybridoma cells (Evan et al., 1985), used 1:5 for western blot (WB) and 1:1 for immunofluorescence (IF). For immunoprecipitation experiments, 500µl of 9E10 hybridoma supernatant were concentrated on 100µl of protein A beads at 4°C for 1 hr, beads were then used directly for the immunoprecipitation.

HA-tagged proteins were detected using monoclonal or polyclonal antibody (SIGMA), specific for a 9 amino acid HA peptide sequence (YPYDVPDYA) from influenza HA, both used at a dilution of 1:2000 for western blot (WB), 1:200 for immnufluorescence (IF) and 1:200 for immunoprecipitation (IP).

Anti-catalase was from SIGMA (1:200), Lysotracker and Mitotracker (Orange) were from molecular probes. The Mitotracker and the Lysotracker were used at 200nM final concentration in culture medium for 30 min at 37 °C, and then cells are fixed and processed with the normal immunofluorescence protocol. Anti α-tubulin (1:250, IF) was from Molecular probes; anti-58K protein (1:100, IF), anti-flag

(1:1000, WB and 1:100 for IP), anti β-tubulin (1:2500, WB), monoclonal anti γ-tubulin (GTU-88, 1:50, IF) and polyclonal γ-tubulin (1:1000, WB) were from SIGMA. Monoclonal anti-PML was a kind gift from Pellicci (Milan, Italy) and was used 1:5 in IF. Monoclonal anti RT97 was from Development Studies Hybridoma Bank (University of Iowa, IA)(Wood and Anderton, 1981)(1:50, IF) and monoclonal anti-NF200 was from SIGMA (1:100, IF). Goat-polyclonal anti-GST (1:1000, WB) was from Amersham. Monoclonal anti-SUMO-1 antibody was purchased from Cambridge Bioscience and use in western blotting at a ratio, respectively of 1:500. Rabbit polyclonal anti-SUMO1 was from Santa Cruz and used 1:200 in WB and 1:50 for IP.

All the secondary antibodies for immunofluorescence were from Dako (1:200); while horseradish peroxidase (HRP)-conjugated antibodies were from Amersham (1:3000). The Mouse secondary antibody AMCA-conjugated was from Jackson laboratories (1:50).

2.14 Cell transfection and immunofluorescence

All constructs were transfected using Lipofectamine (Invitrogen) or Polyfect (Quiagen) according to instructions provided by Manufacturer. Transfection to obtain a low level of expression were performed by incubating cells with DNA-lipofectamine mixture for 4 hrs and fixing cells 2 hrs later.

Cells were grown on coverslips or on multiwell chamberslides (Nunc), transfected as described and fixed for 5 min with a solution of 4% paraformaldehyde

in PBS or for 5 min in Methanol at -20°C. Then cells were permeabilized with a 10 minutes treatment in PBS/0.2% Triton X-100 and blocked (before antibody addition) by incubation in 10% pig serum/PBS for 30 min. The appropriate dilution of primary antibodies was prepared in 1% pig serum /PBS and subsequently the cells were incubated at room temperature for 2 hrs. Immobilised antibody/antigen complexes were detected using secondary antibodies at a concentration of 1:200 for 1 h. To detect nuclei, cells were stained using DNA specific stain DAPI (1µg/ml, Roche). For confocal microscopy, cells were treated with RNase A (10µg/ml at 37°C for 30 min, SERVA) and nuclei were stained with Propidium iodide (2.5 µg/ml, SIGMA).

When requested, cells were treated with 20 µM Nocodazole (SIGMA) for 2.5 hrs at 37°C. Cells were mounted with vectashield (DBA) and examined with an Axioplan microscope (Zeiss) equipped with an Axiocam CCD camera and Axiovision digital imaging software (Zeiss). Alternatively, cells were analysed with a confocal microscope (Leica). The images obtained were processed using Photoshop 5.5 software (Adobe).

2.15 Microtubule disassembly in transfected Cos-7 cells

Cells were transfected with spastin-GFP, spastin^{K388R}-GFP, or pcDNA3-GFP, fixed 24 hrs post-transfection and analyzed by double immunofluorescence using GFP fluorescence and a monoclonal antibody against α-tubulin. Three independent transfection experiments were performed for each constructs. For each experiment, 100 transfected cells were examined to evaluate the intensity of anti α-tubulin

staining. We scored a cell as having a microtubule disassembly phenotype only when a dramatic reduction in tubulin fluorescence was appreciated compared to neighbouring untransfected cells. To analyze the integrity of microtubules in cells showing a dramatic decrease in the intensity of α-tubulin staining, images were acquired with a longer time of exposure.

2.16 Subcellular fractionation and immunoprecipitation

Transfected cells were collected 48 hrs post-transfection, resuspended in buffer A (10mM Hepes pH7.9, 1.5mM $MgCl_2$, 10mM KCl, 0.5mM DTT, 0.5mM PMSF), incubated on ice for 10 min and homogenized. Samples were centrifuged at 510 x g for 10 min at 4°C; the supernatant was collected and stored as cytoplasmic fraction. The resulting pellet was resuspended in buffer B (20mM Hepes pH 7.9, 1.5mM $MgCl_2$, 0.42M NaCl, 25% Glycerol, 0.2mM EDTA, 0.5mM DTT, 0.5mM PMSF), homogenized and incubated on ice for 30 min. The sample was then centrifuged at 12900 x g for 30 min at 4°C and the supernatant was analyzed as nuclear fraction. Both nuclear and cytoplasmic fractions were concentrated by immunoprecipitation of the protein the 9E10 antibody. Samples from immunoprecipitation were fractionated on an 8% SDS/PAGE acrylamide gel, blotted on a PVDF membrane and revealed by immunoblot analysis.

2.17 Immunoprecipitation

To assess protein-protein interactions, HeLa cells were collected and lysed in PEM/DNNA buffer (Pipes 80mM pH 6.8, EGTA 1mM, $MgCl_2$ 1mM, DTT 1 mM, NaCl 150mM, NP40 1%). PEM/DNNA was supplemented with 1mM protease inhibitor cocktail (SIGMA) and 25 mM NEM (N-ethilmaleymide, SIGMA). Samples were subjected to brief sonication (3 x15 sec) to ensure full lysis and after they were incubated on ice for 10 min. Samples were then centrifuged at 10000 rpm for 5 min at 4°C to remove cellular debris. Total extracts were pre-cleared with 100 µl protein A sepharose (10% w/v in PBS, SIGMA) for 1 hr at 4°C to minimise the amount of non-specific binding during immunocomplex formation. Following incubation, non-specific complexes were removed by centrifugation, discarding the protein A beads. The precleared lysates were supplemented with the appropriate primary antibody and incubated at 4°C for 3 hrs. To isolate the immunocomplexes, samples were then supplemented with 100µl of protein A 10% and incubated for 1 hr at 4°C. Samples were then centrifuged at 5000g for 2 min and washed 4 times with PBS/0,1% Triton-X-100. Immunocomplexes were recovered by adding 30µl of disruption buffer to the protein A beads. Samples were boiled for 5 min, resolved by SDS-PAGE and analysed by Western blotting.

2.18 Microtubule-binding assay

Transfected cells were collected 48 hrs post-transfection and lysed in PEM/DNNA buffer supplemented with protease inhibitors, at 4°C for 1 hr. Lysates

were centrifuged at 610 x g for 10 min at 4°C. Cytosol was then purified by successive centrifugations at 10,000 x g for 10 min, at 21,000 x g for 20 min and at 100,000 x g for 1 hr at 4°C. Each supernatant was then supplemented with 1mM GTP (Boeringher) and 40 μM taxol (Molecular probes) and incubated at 37°C for 30 min. Corresponding samples without taxol were also prepared. Each sample was layered over a 15% sucrose cushion and centrifuged at 30,000 x g for 30 min at 30°C to sediment polymerized microtubules. The resulting supernatants were saved and pellets were resuspended in an equal volume of sample buffer 1X for electrophoresis and immunoblot analysis.

2.19 Centrosomes purification

Centrosomes were isolated from HeLa cells by discontinuous gradient ultracentrifugation according to the method of Moudjou and Bornens (Moudjou and Bornens, 1998). Cells in the exponential phase of growth were treated with 1 μg/ml cytochalasin D and 0.2 μM nocodazole for 1 hr at 37°C. Cells were trypsinized and collected by centrifugation. The resulting pellet was washed in TBS (10mM Tris-HCl pH 7.4, 150mM NaCl) and successively in 0.1X TBS/ 8% Sucrose. Cells were resuspended in 2 ml of 0.1X TBS/ 8% Sucrose, followed by the addition of 8 ml of lysis buffer (1mM Hepes pH 7.2, 0.5% NP40, 0.5mM $MgCl_2$, 0.1% β-mercaptoethanol, 1μg/ml leupeptin, 1μg/ml pepstatin, 1μg/ml aprotinin and 1mM PMSF). The suspension was gently shaken and passed more times through a 10ml serological pipette to lyse the cells. The lysates was spun at 2500g for 10 min to remove the swollen nuclei, chromatin aggregates and unlysed cells. The resulting

supernatant was supplemented with hepes buffer to a final concentration of 10 mM and with 1μg/ml DNaseI, and incubated on ice for 30 min. The mixture was gently underlaid with 1ml of 60% Sucrose solution (10mM Pipes pH 7.2, 0.1% tritonX-100, and 0.1% β-mercaptoethanol containing 60% sucrose w/v) and spun at 10000g for 30 min to sediment centrosomes on the cushion. The upper 8 ml of the supernatant was removed and the remaining part, containing the concentrated centrosomes, was vortexed and loaded onto a discontinuous sucrose gradient consisting of 70, 50 and 40% w/v solution from the bottom (500 μl 70% sucrose, 300 μl 50% sucrose and 300 μl 40 % sucrose), and spun at 120000g for 1 hr. 200 μl fractions were collected and centrosomes of each fraction were sedimented by addition of 1ml of 10mM pipes pH 7.2 and centrifugation at 20000g for 15 min at 4°C. Supernatants were removed and centrosomes were resuspended in disruption buffer and fractionated on an SDS/PAGE.

2.20 SDS/PAGE and Western Blot analysis

Protein samples were resuspended in disruption buffer (1X: 20 mM Tris/ HCl pH6.8, 2% SDS, 5% b-mercaptoethanol, 2.5% glycerol and 2.5% bromophenol blue) and denaturated at 100°C for 5 minutes before loading on a 8.5-12.5% SDS-polyacrylamide gel (acrylamide percentage appropriate for the size of proteins to be separated). Bio-Rad mini gel equipment was used in accordance with the manufactures instructions. New England Biolabs protein molecular weight markers were used as standards to establish the apparent molecular weights of proteins resolved on SDS-polyacrylamide gels. All gels were run at 150 V for an appropriate

length of time, using SDS-PAGE running buffer (25 mM Tris, 192 mM glycine, 0.1 % SDS). Separated polypeptides were stained with Comassie Blue (0.2% Comassie brilliant blue R250; 50% methanol; 10% acetic acid) for 30 minutes and then destained (20% methanol; 10% acetic acid). Alternatively, proteins were transferred to a polyvinylidene difluoride membrane (PVDF, Amersham) using a wet blotter (Biorad Systems) at 100V for 1 h in blotting buffer (25 mM Tris, 192 mM glycine, 20% Methanol).

The membranes were blocked against non-specific binding of antibodies with TBS containing 5% skimmed milk powder and 0.1% Tween 20. Successively, membranes were incubated with monoclonal or polyclonal antibodies diluted in blocking buffer for 2 hrs at room temperature. After primary antibody incubations, membranes were washed (3x 5 min) in a large excess of TBS/0.1 % Tween 20 (TBST), before incubation with the relevant horseradish peroxidase-(HRP) conjugated secondary antibody for 1 h at room temperature. Horseradish peroxidase conjugated anti-mouse IgG, anti-rabbit IgG (Amersham) and anti-goat (Jackson laboratories) were used as secondary antibodies (1:3000). Membranes were again washed (3x 5 min) in PBST, before developing using the ECL reagent system (Amersham) according to the manufacturer's protocol.

2.21 Yeast two hybrid screening

The yeast strain used for the two hybrid screening is the EGY48, which has the LEU2 reporter gene integrated. Additional DNAs are introduced into this strain by transformation.

2.21.1 Yeast transformation

The appropriate yeast strain is grown over night at 30°C. The morning after, yeasts were diluted 1:3 and grown till the absorbance at 600 nm (OD_{600}) reach 0.6. Yeast cultures are centrifuged at 2000g for 5 min. The resulting pellet is washed with 5 mls of sterile H_2O and then with 5 mls of TELiOAc (10mM Tris-HCl pH 7.5, 1mM EDTA, 100mM LiOAc pH 7.5). Cells were centrifuged at 2000g for 5 min and the yeast pellet was then resuspended into 500 µl (for a starting culture of 100mls) of TELiOAc. 50 µl of cells were used for each transformation and were supplemented with 6 µl of DMSO, 5 µl of Salmon sperm (10mg/ml) (carrier DNA), 1-2 µg of DNA to transform, 300 µl of PEG/TELiOAc (40% PEG 3500 in TELiOAc). The transformation mix was incubated at 30°C for 30 min and then heat shock was performed at 42°C for 15 min. 150 µl of this mixture was then plated on selective plates, depending on the plasmid transformed and their selectable marker genes (HIS for pAR202; URA for SH18.34, lacZ plasmid reporter; TRP for pJG4-5). Plates were then incubated at 30°C for 3 days.

2.21.2 Testing whether the bait protein activates transcription of the reporters

EGy48 yeast strain was transformed with the LacZ reporter SH18.34 (URA) and either with empty pAR202 (HIS) or with pAR202 plasmid containing the baits to test. Three different baits have been tested for transactivation of the reporters: pAR202-LexA-Spastin, pAR202-LexA-spastin$^{\Delta\text{-AAA}}$ and pAR202-LexA-spastin$^{\Delta\text{-N}}$. Yeast selection strains EGy48/SH18.34/pAr202empty, EGY48/SH18.34/ pAR202-Spastin, EGY48/SH18.34/pAr202-spastin$^{\Delta\text{-AAA}}$ and EGY48/SH18.34/pAr202-

spastin$^{\Delta N}$ were grown in liquid cultures (URA, HIS, Glucose; UH Glc) at 30°C and then several dilution in water (from 10^{-1} to 10^{-5}) of the culture were spotted onto three selective plates:

UH Gal/Raf (URA, HIS Galactose/Raffinose) (for Leu reporter)

UHL Gal/Raf (URA, HIS, LEU Galactose/Raffinose) (for Leu reporter)

UH Glc Xgal (URA, HIS, Glucose Xgal) (for LacZ reporter)

Plates were incubated at 30°C for 3 days. All the yeast strains should grow at a similar rate on the UH Gal/Raf plates. Yeasts with plasmid baits that do not transactivate the system should not grow on UHL Gal/Raf and form white colonies on UH Glc Xgal, while yeasts transformed with a transactivating bait grow on this selective plate and form blue colonies on UH Glc Xgal.

In the same way the yeast selection strains above mentioned were transformed also with the pJG4-5 empty vector, grown in liquid cultures and several dilutions were spotted on selective plates:

UHWL Glc (URA, HIS, TRP, LEU Glucose) (for Leu reporter)

UHWL Gal Raf (URA, HIS, TRP, LEU Galactose/Raffinose) (for Leu reporter)

UHW Glc Xgal (URA, HIS, TRP, Glucose Xgal) (for LacZ reporter)

UHW Gal/Raf Xgal (URA, HIS, TRP, Galactose/Raffinose Xgal) (for LacZ reporter)

Plates were incubated at 30°C for 3 days. All the yeast strains should grow on the UHWL Glc plates. Yeasts with plasmid baits that do not transactivate the system should not grow on UHWL Gal/Raf and form white colonies on UHW Glc Xgal

plates, while yeasts transformed with a transactivating bait grow on UHWL Gal/Raf and form blue colonies on UHW Gal/Raf Xgal.

pAR202-LexA-spastin$^{\Delta\text{-}AAA}$ was transactivating the system and therefore could not be used for the yeast two hybrid screening, while pAR202-LexA-Spastin and pAR202-LexA-spastin$^{\Delta\text{-}N}$ were non-transactivating baits.

2.21.3 Verifying that a full-length fusion protein is made

To verify that the full-length bait protein is made, yeast extract from yeast strain expressing the appropriate bait were prepared. The appropriate yeast selection strain is grown over night at 30°C in selective medium. The morning after yeast culture was diluted 1:3 and when OD_{600} was 0.6, 1ml of yeast culture was centrifuged at 2000g for 5 min. The yeast pellet was then resuspended in 125 µl of 80mM Sorbitol, 8mM NaCitrate pH 5, 0.8mM EDTA pH 8, 0.8mM DTT, 0.8mM KH_2PO_4, 1mM PMSF, 1mg/ml zymolase) and incubated at 30°C for 30 min. Samples were supplemented with 62,5 µl of disruption buffer (3X). Cells were then lysed by freezing on dry ice followed by boiling for 5 min prior to loading samples on SDS/PAGE. Proteins are then transferred to a PVDF filter and immunoblot analysis is performed using an anti-LexA antibody (1:2500, Clontech) to detect the fusion protein.

2.21.4 Introducing the library into the selection strain

The selection strain (EGY48/SH18.34/pAR202-Spastin or EGY48/SH18.34/pAR202- spastin$^{\Delta\text{-}N}$) was grown in liquid medium UH Glc at 30°C over night, the morning after the culture was diluted in 500mls and let grow till OD_{600} is 1.1. Cells were processed as for a normal yeast transformation, using 2.5 times the amounts of a normal transformation. So 125 µl of yeast cells were supplemented with 15 µl of DMSO, 12.5 µl of Salmon sperm, 2.5 µg Library DNA and 750 µl PEG/TELiOAc. This mixture has been incubated at 30°C for 30 min and then at 42°C for 15 min. All the reaction mixture has been plated on a 24x24 cm^2 bioessay dish (Nunc) (UHW Glc) and incubated at 30°C for 3-4 days.

When yeasts are grown, the total number of transformants is calculated, by counting the number of colonies per cm^2, and then considering the area of each bioassay dish and how many dishes have been plated (usually around 600000 total transformants). Then, yeast are collected, washed with sterile water, resuspended into a glycerol solution (65% v/v glycerol, 0.1 M $MgSO_4$, 25 mM Tris-HCl pH 7.4) and stored at -80°C. The plating efficiency is calculated by thawing an aliquot of library transformants and making serial dilution in sterile water. 100 µl of each dilution are plated on to 100mm diameter UHW Gal/Raf dish. Yeasts are incubated at 30°C for 3 days and then the number of colonies formed is counted. In this way, the plating efficiency is calculated as the colony forming unit (c.f.u.) per unit volume (1µl) of frozen cells (10^6 cfu/µl).

2.21.5 Selecting interactors

An aliquot of library transformants is thawed. A volume (µl) corresponding to 10 times the number of total transformants (10 x 600000 = 6 x 10^6 cfu) is incubated in 10-20 mls of UHW Gal/Raf liquid medium and incubated at 30°C for 4 hrs. Then, yeast are centrifuged at 2000g for 5 min and washed with sterile water. The yeast pellet is resuspended in sterile water and plated on 150mm UHWL Gal/Raf selective plates (0.5 x 10^6 c.f.u. per plate). Plates were incubated at 30°C for 2-5 days. When yeasts are grown, single colonies are picked and streaked onto UHW Glc selective plates and let at 30°C for 2-3 days. Then yeasts are replicated on four selective plates (UHWL Glc and Gal/Raf; UHW Xgal Glc and Gal/Raf) in order to check the activation of both reporters and individuate the positive interacting clones. Good candidate for interactors are those yeast which grow on UHWL Gal/Raf but not on UHWL Glc, and that forms blue colonies on UHW Xgal Gal/Raf and white colonies on UHW Xgal Glc.

DNA from positive clones was isolated, reintroduced in the appropriate yeast selection strain (EGY48/SH18.34/pAR202-Spastin or EGY48/SH18.34/pAR202-spastin$^{\Delta\text{-}N}$) via transformation and the activation of the reporter genes was reconfirmed.

2.21.6 Preparation of yeast DNA miniprep and isolation of positive interactor DNAs

A large mass of yeast is scraped from the plate and resuspended into 1ml of sterile TE (10mM Tris-HCl pH 7.5, 1mM EDTA). This suspension is centrifuged at

2000g for 5 min and yeast is resuspended in 0.5 ml of S-buffer (10mM K_2HPO_4 pH 7.2, 10mM EDTA, 50 mM 2-mercaptoethanol, 50 µg/ml zymolase) and incubated at 37°C for 30 min. Then 0.1 ml of lysis solution (25mM Tris-HCl pH 7.5, 25 mM EDTA, 2.5% SDS) was added and samples were incubated at 65°C for 30 min. This solution was supplemented with 166 µl of 3M potassium acetate and kept on ice for 10 min. Samples were centrifuged for 10 min, and the supernatant was poured in a new tube. DNA was precipitated by adding 0.8 ml of cold ethanol, incubating on ice for 10 min and centrifuging for 10 min. The pellet was washed with 70% ethanol, dried and resuspended into 40 µl of sterile water. 1-2 µl of this crude yeast DNA were used to transform a special *E.Coli* strain (KC8) of competent cells, so to isolate only the pJG4-5 plasmid. The KC8 strain of *E. Coli* contains a mutation in the TRP gene and therefore is unable to grow in the absence of tryptophan, this inability is complemented by the yeast TRP gene present on the library plasmid.

2.21.7 Screening of positive clone by PCR

Yeast colonies were resuspended in 20 µl of 0,25% SDS and vortex. Samples were centrifuged shortly and supernatant was recovered. 1µl of this supernatant was used as template in a PCR reaction to determine the length of the clones. The PCR reaction was set up as follow:

For the PCR, *AmpliTaqGold* (Applied Biosystem) was used as follows:

5 µl 10x *PCR* buffer

4 µl $MgCl_2$ 20mM

0.4 mM of each dNTP

200 ng forward primer

200 ng reverse primer

1 µl *AmpliTaqGold* Polymerase

1 µl DNA template

dH_2O to 50 µl

For the amplification of positive clones, PCR reactions were usually performed with the following cycling parameters:

1 cycle: 10 min at 94°C

30 cycles: 30 sec at 94°C

30 sec at 42°C

2 min at 72°C

1 cycle: 10 min at 72°C

PCR products were used for direct DNA sequence analysis.

2.22 Interaction mating

In this mating assay, the activation tagged proteins are expressed in the EGY48 (mating type α) that contains the LEU reporter and grown on TRP (lacking tryptophan) Glc plates; the baits are expressed in the EGY42 (mating type a), where it has been also transformed the LacZ reporter, and grown on URA/HIS Glc plates. The yeasts are streaked on selective plates. The two strains are mated by applying

them to the same replica velvet (one perpendicular to the other), replicated to a YPD (complete rich medium) plate and incubated at 30°C for 1-2 days. At the intersection of the YPD plate the diploids are formed. This plate is then replicated on the four selective plates for testing the activation of the two reporter genes.

2.23 Generation of constructs for putative spastin interactors

The coding region of Na14 cDNA was amplified by PCR using Pfu turbo polymerase (Stratagene), HeLa cDNA as template and specific primers designed on available sequence (Ramos-Morales et al., 1998). Na14 was the subcloned into pcDNA3-HA vector (primers Na14-1/Na14-2) (EcorI/XhoI) and into the pGEX3X vector (primers Na14-3/Na14-4)

CMV-Daxx was a kind gift from Prof. Gianni Del Sal (University of Trieste, Italy). Daxx open reading frame was amplified by PCR (primers daxx1/daxx2) with the Pfu Turbo polymerase and cloned into pMT21-myc vector (EcorI/SalI).

pcDNA3-6his-SUMO1 was a gift from Ron T. Hay (University of St. Andrews, SCOTLAND). SUMO1 and UBC9 cDNA in yeast vector pAR202 and pJ4-5 as well as $pcDNA_3$-HA-PML were from Germana Meroni. $pcDNA_3$-Flag-BRD7 was a kind gift from Dr. Julia Kzhyshkowska (University of Heidelberg).

2.24 Purification of GST-Na14

GST-Na14 construct was expressed in *Escherichia Coli* strain B834. Induction and purification were conducted as described in paragraph 2.10.

2.25 GST pull-down assay

Cells were collected and resuspended in lysis buffer (50mM Tris-HCl pH 7.5, 10mM MgCl2, 0.5 mM DTT, protease inhibitors), sonicated and kept on ice for 10 min. The resulting suspension was centrifuged at 14000 rpm for 10 min. The supernatant was supplemented either with GST-agarose beads or with specific GST fusion protein bound to agarose beads and incubated at 4°C for 1hrs. Samples were then centrifuged at 2000g for 4 min and beads were washed 4 times in the lysis buffer.

After the last wash, beads were resuspended in the disruption buffer, boiled for 5 min and analysed by SDS/PAGE.

2.26 Purification of 6XHIS-tagged SUMO-1- conjugates

Cells transfected with 6His-tagged SUMO-1 in a 100mm dish (Rodriguez et al., 1999; Treier et al., 1994) were lysed in 1 ml of 6 M guanidinium-HCl, 0.1 M Na_2HPO_4/NaH_2PO_4, 0.01 M Tris/HCl, pH 8.0 plus 5mM imidazole and 10 mM □-mercaptoethanol. After sonication, to reduce viscosity, the lysates were mixed with 50 µl of Ni^{2+}-NTA-agarose beads (Quiagene) prewashed with lysis buffer and incubated for 2 hours at room temperature. The beads were successively washed with the following: 6 M guanidinium-HCl, 0.1 M Na_2HPO_4/NaH_2PO_4 , 0.01 M Tris/HCl , pH 8.0, 10 mM β-mercaptoethanol; 8 M Urea, 0.1 M Na_2HPO_4/NaH_2PO_4 , 0.01 M Tris/HCl , pH 8.0, 10 mM β-mercaptoethanol; 8 M Urea, 0.1 M Na_2HPO_4/NaH_2PO_4 , 0.01 M Tris/HCl , pH 6.3, 10 mM β-mercaptoethanol (buffer A) plus 0.2% Triton X-

100; buffer A and then buffer A plus 0.1% Triton x-100. After the last wash with buffer A the beads were eluted with 200 mM imidazole in disruption buffer. The eluates were subjected to SDS-PAGE analysis and the proteins transferred to a polyvinylidene difluoride membrane (Amersham).

2.27 In vitro transcription-translation

In vitro transcription/translation was performed using 1-2 □g of plasmid DNAs and a TNT Coupled Wheat Germ Extract System (Promega) according to the instructions provided by the manufacture. ^{35}S-methionine (Amersham) was used in the reactions to generate radiolabelled proteins.

2.28 In vitro SUMO-1 conjugation assay

^{35}S-methionine labelled in vitro transcribed/translated proteins (1 µl) were incubated with 2 µl of HeLa cell fraction containing SUMO-1 E1 (SAE1/2) activity (fr II.4) (Desterro et al., 1999) in a 10 µl reaction including an ATP regenerating system (50 mM Tris pH 7.6, 5 mM $MgCl_2$, 2 mM ATP, 10mM creatine phosphate, 3.5 U/ml of creatine kinase and 0.6 U/ml of inorganic pyrophosphatase), SUMO-1 (1 mg/ml), Ubch9 (60 µg/ml). Reactions were incubated at 37^{0}C for 2 h. After terminating the reactions with SDS sample buffer containing mercaptoethanol, reaction products were fractionated by SDS-PAGE (8.5%) and the dried gels analysed by phosphoimaging (Fujix BAS 1500, MacBAS software).

The in vitro transcription translation and the SUMO-1 conjugation assay were carried out by Ellis Jaffray at the University of St Andrews (in collaboration with Prof. R.T. Hay)

2.29 RNA extraction from cells

RNA was extracted from transfected and mock cells using the RNeasy Mini Kit (Quiagen). Cells were plated on 100 mm dishes and transfected (as described above). 48hrs post transfection cells were washed with PBS and harvested in 600 □l of RLT buffer (supplemented with 0.1% β-mercaptoethanol) and homogenized using a Quiashredder spin column (Quiagen) and centrifuging for 2 min at maximum speed.

1 volume of 70% ethanol was added to the flow-through; the resulting solution was loaded on RNeasy column (Quiagen) and centrifuged at 8000g for 15 sec. The RNeasy column was then washed with 700 µl of buffer RW1 (Quiagen) and successively with 500 µl of buffer RPE (Quiagen). RNA was then eluted from the column into two successive centrifuged in a final volume of 60 µl. RNA was then checked on 1% agarose gel and quantified by measuring the absorbance at 260 nm. An absorbance of 1 unit at 260 nm corresponds to 40 µg of RNA per ml.

2.30 cDNA transcription

cDNA synthesis was performed using the SuperScript™ First-Strand Synthesis System for RT-PCR (Invitrogen). cDNA syntesis was performed using random hexamers as follow:

RNA	3 µg
Random hexamers	3 µl
10mM dNTP mix	1 µl
DEPC-treated water	to 10 µl

Each sample was incubated at 65°C for 5 min and incubated on ice for 1 min.

Then 9 µl of the following reaction mixture were added to each sample:

10X RT buffer	2 µl
25mM MgCl2	4 µl
0.1M DTT	2 µl
RNase inhibitor	1 µl

Samples were incubated at 25 °C for 2 min, and then 1 µl of Superscript™ II RT was added to each tube. Samples were then treated as follow:

42°C for 50 min

70°C for 15 min

Samples were then chilled on ice and treated with 1 µl of RNaseH at 37 °C for 20 min.

The cDNA so synthesized was used as template in real time PCR experiments.

2.31 Real Time quantitative PCR

The Spastin mRNA was measured by real-time quantitative PCR method using an ABI PRISM 7700 instrument (PE Applied Biosystems), in several cells transfected either with Daxx, or Na14 or untransfected. PCR primers were designed using the Primer Express Software (PE Applied Biosystems). After reverse transcription, a quantity of cDNA was amplified by PCR. For each sample, three distinct amplifications were carried out in parallel, in order to amplify Spastin cDNA, □-actin cDNA as control, and the GAPDH cDNA as a reference gene. The primers used for amplification are the following:

B-actin.up	5'-TCACCCACACTGTGCCCATCTACGA-3'
B-actin.dw	5'-CAGCGGAACCGCTCATTGCCAATGG-3'
GAPDH.up	5'-GAAGGTGAAGGTCGGAGTC-3'
GAPDH.dw	5'-GAAGATGGTGATGGGATTTC-3'
Spastin.up	5'-TCGAGTACATCTCCATTGCCC-3'
Spastin.dw	5'-TTCCACAGCTTGCTCCTTCTG-3'

The SYBR® Green PCR Core Reagents Kit (PE Applied Biosystems) was utilized for fluorescent detection of cDNA. For each sample, spastin and β-actin mRNA values were normalized to the mean value of GAPDH mRNA calculated from three independent determinations in the corresponding cell extract. Data were then analyzed with Microsoft Excel.

CHAPTER 3: Subcellular localization of Spastin

3.1 Exogenous spastin localizes to cytoplasmic aggregates

In order to get an insight on the biological role of spastin, we investigated its subcellular distribution by transiently transfecting different epitope-tagged spastin constructs in Cos7 cells (Fig. 8A). As a first step, Cos7 cells were transfected with the spastin-myc construct. Cells were collected 48 hrs post transfection; the cellular lysates were subjected to subcellular fractionation followed by immunoprecipitation in order to concentrate spastin. Samples were then fractionated by SDS/PAGE, transferred to a Polyvinylidene fluoride (PVDF) membrane and analysed by immunoblotting with an anti-myc antibody. A band of the expected size (68 KDa), corresponding to the spastin-myc protein, was present in the cytoplasmic fraction (Fig. 8B).

Moreover, immunofluorescence experiments on Cos-7 cells transfected with the spastin-myc construct showed that exogenous spastin localizes to discrete punctuate cytosolic structures, which display a perinuclear distribution (Fig. 9A). These structures tend to increase in size with longer period of expression and ultimately fill up the cytoplasm. We have observed the same pattern of expression in other cell types such as HeLa (Fig. 9B) and human fibroblasts (Fig.9C).

Cos7 cells were transfected with the spastin-myc-GFP construct to perform double immunofluorescence experiments, using antibodies specific to known organelles. These experiments ruled out the possibility that the cytosolic spastin

spots may correspond to known organelles, such as mitochondria (Mitotracker Orange) (Fig.9D), lysosomes (LysoTracker) (Fig.9E) or peroxisomes (anti-catalase) (Fig.9F). These data were confirmed by the transfection of different epitope-tagged spastin constructs (Fig.8A). In fact, the use of different promoters and epitopes (HA versus myc or GFP) either positioned at the N-terminus or C-terminus did not change spastin fluorescent pattern.

Finally, transfection experiments were designed in order to monitor spastin localisation in cells that are just beginning to express the construct (see methods). Under these conditions, specific spastin fluorescence labelled only one perinuclear region (Fig. 9G). This region is located near the Golgi apparatus (Fig. 9H), and corresponds to the center of microtubule asters, as assessed by double labelling with anti α-tubulin antibody (Fig. 9I). This domain of expression is close to the centrosome revealed by γ-tubulin staining (Fig. 9L, M). These data suggest that onset of spastin expression may be in the microtubule-organizing center and that, upon longer periods of expression, spastin may accumulate in cytoplasmic aggregates.

3.2 Production and characterization of spastin specific polyclonal and monoclonal antibodies

To assist with the *in vivo* studies on the function of spastin protein, polyclonal and monoclonal antibodies were produced using as antigen two different portions of the spastin protein, expressed in bacteria: a his-tagged polypeptide corresponding to amino acids 1 to 122 (His-Spastin) and a GST fusion protein corresponding to the portion of spastin between amino acids 87 to 354 (Gst-Spastin).

3.2.1 The polyclonal antibody: SP-R74

The antigen His-Spastin obtained previously in the lab, is a his-tagged protein, produced in bacteria and purified under denaturing condition. It was used for the immunization of rabbits at PRIMM (Milan, Italy). The resulting antiserum, SP-R74, was tested previously in our laboratory by immunoprecipitation and Western blot. The studies conducted precedent to this thesis reported that this antibody recognizes the transfected protein, but was unable to detect a signal corresponding to the endogenous protein in whole cell extracts. By immunoprecipitation, instead, it was possible to detect a band of the expected size. In my work, this antibody has been characterized by immunofluorescence in order to investigate the endogenous localization of spastin.

3.2.2 The polyclonal antibodies SP-50 and SP-51

To raise antisera against a different antigen, the portion of spastin, corresponding to the region between amino acid 87 and 354, was cloned into the pGEX3x vector for inducible expression of a GST-tagged spastin protein in *E. coli.* The pGEX plasmids are designed for inducible, high-level intracellular expression of genes or fragments as a fusion protein with the glutathione S-transferase (GST) domain of Schistosoma japonicum (26 kDa) (Sj26) (Smith and Johnson, 1988). The plasmid contains the *tac* Promoter (Amann et al., 1983) followed by the coding sequence of Sj26 and also contains the lacI gene which encodes the lac repressor protein. In the absence of inducer, the lac repressor binds to the *tac* Promoter, repressing expression of the GST fusion protein. Upon induction with isopropyl β-D-thiogalactoside (IPTG), derepression occurs because the lac repressor now binds IPTG, and the GST fusion protein is expressed.

The production of the fusion protein was induced by adding 2 mM IPTG to 1 litre of *E. coli* transformed with the pGEX3x-Spastin (87-354) construct. This resulted in increasing expression of the expected 60 kDa fusion protein over a period of three hours at room temperature (Fig. 10A). Cells were harvested and the GST-spastin fusion protein was purified under native condition through binding to glutathione agarose beads. The protein was eluted and the collected fractions were analysed on a SDS/PAGE (Fig. 10B). The most concentrated fractions (1, 2, 3, 4 in figure 10B) were pooled and used for the immunisation of two rabbits (Biogenes, Germany). The obtained antisera, SP-50 and SP-51, were tested by immunoprecipitation and Western blot analysis, and were successively used in immunofluorescence studies for the characterization of the subcellular localization of the endogenous spastin.

Western blot analysis

The anti-spastin SP-50/SP-51 pre- and post-immune sera were tested by Western blot analysis. SP-50 and SP-51 were first affinity purified. Sera were passed though a column of GST-agarose beads to eliminate the fraction of antibodies raised against the GST portion of the protein. Successively the antibodies were affinity purified on a NHS Hi-Trap™ column on which the GST-Spastin was previously bound (see Methods).

5 µg of GST-Spastin and GST proteins were loaded on 10% SDS/PAGE and transferred to a PVDF membrane. Western blot analysis was performed using SP-50/SP-51 pre- and post-immune sera and also antibodies against GST. The GST-Spastin protein is approximately 60 kDa in size. The antibody against the GST tag detected both the band corresponding to the GST-Spastin (Fig. 11 A,D lane1) and to

the GST alone (Fig. 11 A,D lane 2). The affinity purified anti-spastin SP-50 and SP-51 detected specifically the GST-Spastin (Fig. 11 B,E lane 1), but failed to detect the band corresponding to the GST alone (Fig. 11 B,E lane 2). The other bands detected from the antibodies (both the anti-GST and anti-Spastin) are probably due to degradation product of the fusion protein. None of the pre-immune sera recognized the recombinant GST-Spastin (Fig. 11 C,F). Therefore, we concluded that by affinity chromatography we eliminated the fraction of antibodies raised against the GST moiety from our polyclonal sera.

SP-50 and SP-51 antibodies were also used in Western blot analysis on HeLa total cell extracts, either untransfected or transiently transfected with a $pcDNA_3$-spastin (full length) construct or with a construct expressing the spastin splicing variant Δex4. We compared the results obtained using the crude sera or the affinity purified antibodies (Fig. 12). The pattern of bands recognized by the affinity purified antibodies was, more or less, the same of the crude sera. In the case of the SP-51 the upper band of about 80 kDa disappears after the affinity purification, indicating that it was a non specific band (Fig. 12). Both antibodies, SP-50 and SP-51, recognize the exogenous spastin (figure 12 A,B,C,D lane 3) and Δex4 (Fig. 12 A,B,C,D lane 2). In the lane corresponding to the HeLa cells transfected with Δex4 (Fig. 12 A,B,C,D lane 2), it is possible to reveal also a slower migrating form respect to the Δex4 band, which could also represent a post-translational modification of this splicing variant. However they failed to detect the endogenous protein when 30 μg of HeLa lysates were loaded, although affinity purified SP-51 detected a faint band of approximately the same size of transfected spastin when 100 μg of HeLa lysates were loaded (Fig. 12 A,B,C,D lane 4). The main band that both the antibodies recognize has an

apparent molecular weight of 60 kDa and is lower than both the full length and the spliced variant of spastin.

To confirm the specificity of the bands detected by SP-50 and SP-51 antibodies, cell extracts from HeLa untransfected (50 μg or 100 μg) or transfected (50 μg) with full length spastin ($pCDNA_3$-spastin) were fractionated on a 7,5% SDS/PAGE. Samples were then transferred to a PVDF membrane and probed with pre-immune sera (pre SP-50 and pre SP-51) and affinity purified antibodies (Fig. 13). Both SP-50 and SP-51 recognized the band corresponding to the transfected spastin (Fig. 13 B,C lane 2), but they did not detect the endogenous protein, even when 100 μg of lysates were loaded (Fig. 13 B,E lane 3). The ability of the antibodies to recognize the endogenous protein may therefore depend on the preparation of the lysates. The pre-SP50 and pre-SP51 did not recognize the exogenous spastin (Fig. 13 C,F lane 2) and detected few bands in the untransfected and transfected cell extracts. These bands were different from the main bands recognized by the affinity purified antibodies. The comparison between the pre-SP51 staining and the corresponding affinity purified antibody suggests that the lower band of about 50 kDa (arrow in figure 13 A,B) is already present in the pre-immune serum and therefore it is not specific. Furthermore, the specificity of the signal detected from the SP-50 and SP-51 antibodies is underlined by the disappearing of the bands after the competition with the antigen.

Immunoprecipitation analysis

The SP-50 and SP-51 antibodies were then tested for their ability to immunoprecipitate transfected spastin. HeLa cells were transiently transfected with a $pCDNA_3$-Spastin expression construct, and 48 h post-transfection,

immunoprecipitation of the whole cell extract using the SP-50 and SP-51 affinity purified antibodies was performed.

Immunoprecipitation with the affinity purified SP-50 and SP-51 antibodies resulted in detection of the 68-kDa spastin transfected protein by the SP-50 and SP-51 (Fig. 14A, arrows). Immunoprecipitation from untransfected cells using both antibodies and revealing either with SP-50 or Sp-51 (Fig. 14B, arrows) resulted in detection of a band of the same size of the transfected spastin, which should correspond to the endogenous protein. Moreover, after immunoprecipitation, the antibodies are able to detect a slower migrating form (around 90 kDa), which could represent a post-translational modification of spastin. The immunoprecipitation using the pre-immune serum gave no bands at these molecular weights. Thus, it can be concluded that both antibodies are able to specifically immunoprecipitate the transfected and the endogenous spastin.

Two additional major signals are detected following immunocomplex formation with both antibodies. The band at ~50-55 kDa represents the heavy chain of the rabbit IgG used for the immunoprecipitation, revealed with the anti-rabbit IgG used in the Western blot. The other band of ~60-62 kDa is the major band recognised also in the total cell extract. Therefore, this 60-62 kDa band seems to be a protein specifically recognized by the anti-spastin SP-50 and SP-51. Whether this is a specific signal for a different post-translational modification, a splicing variant of spastin, a cross-reacting protein, or a signal coming from a contaminant protein in the antigen preparation, is not clear at the moment. However this band is not recognized by the SP-R74 antibody (data not shown).

3.2.3 Monoclonal spastin specific antibodies

The GST-spastin fusion protein was also used for the production of monoclonal antibodies (Biogenes, Germany). Five clones with high affinity for Spastin and no affinity for GST (tested in ELISA assay from Biogenes) were obtained: M1, M2, M3, M4, M5. The supernatants from the hybridoma cultures were used in Western blot and immunofluorescence analysis. Total cell extract from HeLa untransfected or transfected with pCDNA$_3$-spastin were fractionated on a 7,5% SDS/PAGE and transferred to a PVDF membrane. Membranes were then incubated with the different monoclonal antibodies (1:10) or with the antibodies that have been pre-incubated with the antigen. Only M3 and M4 detected a signal corresponding to the transfected protein in western blot analysis (Fig.15). They also recognized a lower band which seems to be the main band detected from the SP-50 and SP-51 antibodies in total cell extract from HeLa. M3 shows a higher affinity for this lower band respect to M4. This result suggests that this band, recognized from both polyclonal and monoclonal antibodies, might be specific and represent another form of spastin.

3.3 Subcellular localization of endogenous spastin

3.3.1 Immunofluorescence experiments with SP-R74

The SP-R74 antibody was affinity purified and tested by indirect immunofluorescence on several fixed cell line (HeLa, Cos7, human and mouse

Fibroblast, NSC34). SP-R74 showed different pattern of localization depending on the cell line used.

In HeLa and Cos7 cells, the antibody showed a faint diffuse nuclear and cytosolic staining on interphase cells (Fig. 16 C, G, H). A strongest signal was instead recognized in different phases of the cell cycle, where the SP-R74 recognized the spindle poles (Fig. 16 B,D) and stained the midbody at cytokinesis (Fig. 16 C, H). These signals were not present with the preimmune serum (Fig. 16 A, F) and were competed by pre-incubation of the antibody with the antigen (Fig. 16 E, L).

Immunofluorescence analysis on human primary fibroblasts showed both a nuclear and a cytosolic localization. In particular, the SP-R74 antibody showed a peculiar cytosolic spot, which was highly reminiscent of the centrosome (Fig. 17 A,B). Indeed co-immunofluorescence experiments using a centrosomal marker, □-tubulin, confirmed the localization of endogenous spastin to the centrosome in this cell line (Fig. 17 B). The antibody revealed also an additional discrete punctuate staining in the nucleus (Fig. 17 A,B). It is known that the nucleus is organized in different subdomains such as PML bodies, Cajal bodies or polycomb bodies (Spector, 2001). As a first step to understand if this nuclear spots were belonging to any known subnuclear compartment, fibroblasts were transfected with a HA-tagged-PML construct and double immunofluorescence experiments using the anti-HA antibody and the SP-R74 antibody to recognize the endogenous spastin were performed. PML is the structural constituent of the PML bodies (or Nuclear bodies) and this co-immunofluorescence showed that the nuclear dots were indeed PML bodies (Fig. 17 C). To confirm this result we have performed a double immunofluorescence experiment using SP-R74 antibody and a monoclonal antibody recognizing the

endogenous PML. Endogenous spastin and PML were co-localizing in the PML bodies (Fig. 17 D), although it is evident that in this case there is a partial co-localization of spastin to the PML bodies. This is probably due to the fact that when PML is overexpressed; PML bodies increase in number and size, and this may cause a more efficient recruitment of a protein to these structures. Both the centrosomal and the nuclear staining were absent in immunofluorescence experiment with the preimmune serum and the specificity of the signal was demonstrated by its disappearance after the competition with the antigen (Fig. 17 A).

Because of the specific cellular phenotype of the disease, we wanted to investigate also the subcellular localization of spastin in neuronal cells. We used, therefore, the NSC34 cell line, which is an immortalised murine motoneuronal cell line. Also in these cells the antibody revealed both a nuclear and a cytosolic staining. In the nucleus, it labelled discrete nuclear domains (Fig. 19 A). More interestingly there was a specific staining in the terminal portion of the neuronal processes (Fig. 19 A), which corresponds to the growth cone as assessed from the white field image (Fig. 19 A). Double immunofluorescence experiments were performed using the anti-NF200 marker for neurofilaments or the RT97 antibody which recognizes phosphorylated epitopes on neurofilament proteins (Anderton et al., 1982), fetal tau, and also recognizes a developmentally regulated phosphorylation epitope on MAP 1B (MAP 1B is the first MAP to be expressed in neurons and plays an important role in neurite outgrowth) (Johnstone et al., 1997). The NF-200 staining is homogeneous on all the axonal length (Figure 19 B) and do not co-localize with spastin (Fig. 19B), while the RT97 antibody recognized a specific signal in the terminal part of the neuronal processes, which was co-localizing with spastin signal (Fig. 19 C). The

NSC34 are immortalized cells, therefore they undergo cell cycle. When cells were in different phases of the cell cycle, as showed by the DAPI staining (blue signal), SP-R74 antibody marked peculiar filaments that were surrounding the nucleus (Fig. 19 A,B). Spastin signal was also detected at the midbody during the cytokinesis, as confirmed by a double staining with an anti-αtubulin antibody (Figure 14). Both the nuclear and cytoplasmic staining were not detected with the pre-immune sera and were competed by the antigen (Fig. 18 A).

Thus, endogenous spastin seems to have a complicated subcellular localization, which is dependent on the cell type analyzed.

3.3.2 Immunofluorescence experiments with SP-50/51

To get more data concerning the subcellular localization of the endogenous spastin, the antibodies SP-50 and SP-51 were used in immunofluorescence experiments on different cell lines.

Immunostaining of fixed HeLa cells with the affinity purified SP-51 gave a specific staining at the midbody (Fig. 20 B,C red arrows) and it was also possible to detect a signal between cells that are going through cytokinesis, in a region where, probably, the midbody will form (Fig. 20 B,C yellow arrows). It seems that the level of spastin in HeLa cells is very low and only when the protein is concentrated in these structures, it is possible to detect a signal. The localization of spastin at the midbody was confirmed by the SP-50 staining (Fig. 20 A). These signals were not detected when the pre-immune sera were used as control (Fig. 20A).

In human fibroblasts both antibodies recognized punctuate nuclear structures (Fig. 21 A,B), which are not present in the immunofluorescence with the preimmune

sera (Fig. 21 A,B). Since the Sp-R74 antibody permits us to localize spastin in the PML bodies in these cells, we have performed double staining with a monoclonal PML antibody. In both cases (SP-50 and SP-51), we confirmed a partial co-localization between spastin and PML (Fig. 21 A,B). It was also possible to detect a centrosomal staining, but experiments with the preimmune sera revealed also the presence of a faint staining at the centrosome (data not shown).

We have also looked at the spastin localization in the motoneuronal cell line NSC34. SP-50 and SP51 showed a very diffuse staining on the cell (Fig. 22 A,B), without any enrichment in the terminal part of the neuronal processes (as seen with the SP-R74 antibody). The SP-50 detected also a nuclear spotted signal (Fig. 21 A) similar to that observed with SP-R74.

3.3.3 Immunofluorescence experiments with spastin monoclonal antibodies

Monoclonal antibodies have also been tested in immunofluorescence experiments on different cell lines (HeLa, human fibroblasts and NSC34). None of them detected a significant signal in the different cell lines, probably because they are not enough concentrated. Nonetheless, M4 stained the terminal portion of the neuronal processes in the NSC34 cells, confirming the localization revealed by the SP-R74 antibody (Fig. 22 C)

3.4 Spastin and centrosome

Immunofluorescence experiments using the SP-R74 antibody showed that spastin has both a nuclear and a centrosomal localization. Moreover the antibodies SP-50 and SP-51 detected a signal in correspondence of the midbody. During the

telophase, before cytokinesis occurs, centrosomes migrates in the region were the midbody will form (Piel et al., 2001). Because the nuclear localization has also been confirmed by the other antibodies, we investigated if spastin was indeed localizing at the centrosomes. To this end we have purified centrosomes from HeLa cells by discontinuous gradient ultracentrifugation according to the method of Moudjou and Bornens (1989). Several fractions were collected and loaded on a 10% SDS/PAGE. Western blot analysis was performed using SP-R74, β-tubulin and γ-tubulin antibodies. While the γ-tubulin, which is a centrosomal marker, is detected in the first fractions eluted from the discontinuous gradient, the β-tubulin is detected in the last fractions, showing that we have purified effectively the centrosomes (Fig.23A). The SP-R74 antibody revealed the 68kDa spastin band and also an additional band of 83 kDa (Fig.23A). Spastin is enriched in the same fractions were the γ-tubulin is present suggesting that spastin is a centrosomal protein. The 83 kDa band correspond to a cross-reacting protein.

The same experiment was performed using the SP-51 antibody to detect the spastin signal. Also in this case, the band corresponding to the endogenous spastin (figure 23B, arrow) is enriched in the centrosomal fractions, as confirmed by the γ-tubulin staining. The lower 60 kDa band described before was also present in these fractions.

These experiments indicate that spastin is also a centrosomal protein.

3.5 Spastin and PML

We have several data indicating that spastin colocalize with the PML bodies in human fibroblast. To confirm this evidence we have performed a double immunofluorescence staining on human fibroblasts using the anti-PML antibody and an additional antibody specific for spastin. This antibody was obtained from A. Molon and has been raised against the peptide (56-76) of spastin. The anti-peptidic antibody showed a punctuate staining in the nucleus. These nuclear structures colocalized with the PML bodies, as assessed by the double immunofluorescence experiment (Fig.24 A).

This confirms the nuclear localization of spastin and this localization to the PML bodies in human fibroblasts.

Since this localization to the nuclear bodies is specific for the human fibroblasts, we decided to investigate the subcellular localization of spastin in murine fibroblasts.

We used both mouse embryonic fibroblasts (mef) and primary fibroblasts from an adult mouse (P0, post natal day 0). Immunofluorescence studies on these cell lines showed that the nuclear signal revealed by the SP-R74 antibody was quite different with less numerous and larger dots in the nucleus (Fig. 24 B). To assess if this was a different localization in respect to that observed in the human fibroblasts, HA-PML was transfected into these cells. Double immunofluorescence analysis revealed that these larger nuclear domains were not co-localizing with the PML bodies (Fig. 24 B). Because the PML construct encoded for the human protein, we have also performed a double staining with SP-R74 antibody and with an antibody which recognise the murine PML (data not shown), confirming that in mouse fibroblasts spastin was localized to discrete nuclear structure different from the PML bodies.

3.6 A NLS-spastin chimera does not localize to the nucleus

The antibodies produced against different spastin antigens showed that the endogenous spastin has a complex subcellular localization which is also cell type dependent. Spastin localizes both to the nucleus and to the cytoplasm. This is in contrast with the results obtained overexpressing spastin into the cell, where the protein exhibits a predominant cytoplasmic localization. This different behaviour in terms of localization between the endogenous and exogenous spastin may have several explanations. It is possible that spastin shuttles between the cytoplasm and the nucleus, or that a post-translational modification is necessary for its nuclear localization and therefore the overexpression of the protein results in the mis-localization. It could also be that when the levels of spastin are over a threshold value, spastin become toxic for the nucleus and therefore it is released in the cytoplasm. As a first step, we investigated if we could force spastin to stay into the nucleus. We have, therefore, generated a chimeric protein where the strong nuclear localization signal (NLS) of the SV40 large T antigen has been fused at the N-terminus of spastin protein. We have generated a wild-type NLS-spastin and a mutated NLS-spastin with a mutation in the NLS sequence which abrogates the nuclear localization. These constructs were transfected in Cos7 cells and their localization was analysed by immunofluorescence. We have compared the localization of the full-length spastin myc-tagged, the full length spastin without a tag and these two chimeric proteins. Cells were analysed by confocal microscopy. As shown in figure 25, there is no difference in the localization of these different spastin constructs, they are all predominantly cytoplasmic. The fact that a strong NLS, such as the NLS of SV40, does not force spastin into the nucleus, lead us to hypothesize

that high level of spastin may be toxic for the nucleus, therefore when we overexpress this gene, we observe a cytoplasmic localization.

Summary

- ✓ Endogenous spastin shows a different localization depending on the cell type.
- ✓ Exogenous spastin has a prevalent cytosolic localization, while the endogenous spastin has both a nuclear and a cytosolic localization.
- ✓ All the antibodies tested (SP-R74, SP-50, SP51 and anti-peptidic) showed that spastin partially co-localize with the PML bodies in human fibroblasts.
- ✓ Both the SP-R74 and the monoclonal M4 antibodies showed that beyond the nuclear signal, spastin is enriched in the terminal part of the neuronal processes.
- ✓ In HeLa cells SP-R74 detected a specific signal in correspondence of the centrosome in metaphase cells and the midbody in cells that were going through cytokinesis. Also SP-50 and SP-51 antibodies stained the midbody in HeLa cells. A centrosome staining was detected in human fibroblasts by the SP-R74 antibody and the centrosomal localization of spastin was confirmed by the presence of the endogenous spastin in the fraction were □-tubulin is enriched after the purification of the centrosomes.

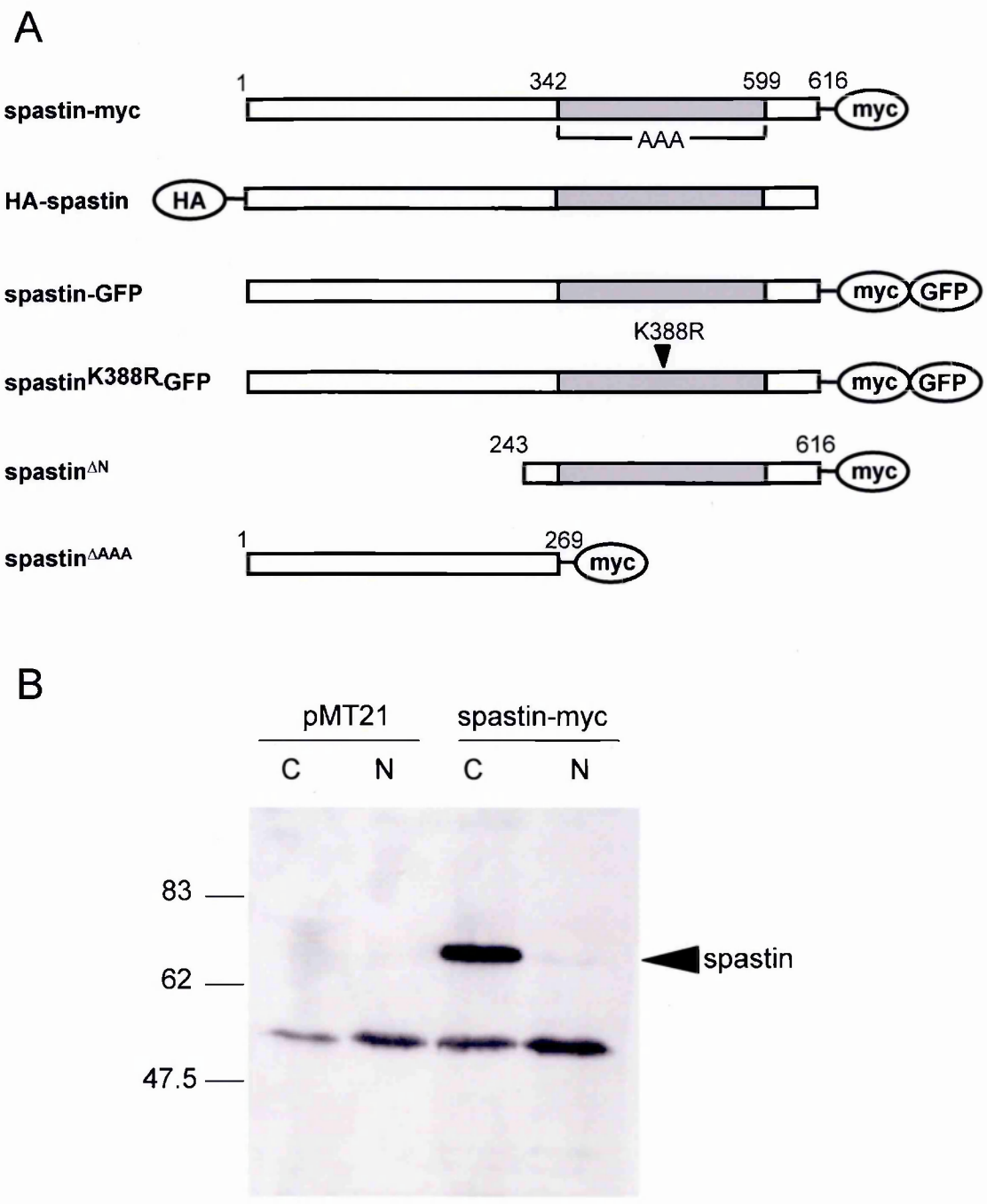

Figure 8. Spastin constructs and subcellular fractionation.

(A) Schematic representation of the spastin constructs used in this thesis. The AAA domain is indicated by the grey bar. The N- and C- terminal position of the different tags are shown. Numbers denote residues present at the beginning and at the end of the AAA domain. (B) Cos7 cells were transfected either with the pMT21-myc empty vector or with the spastin-myc constructs. 48 hours post-transfection samples were processed to make a cytoplasmic (C) and a nuclear (N) fraction. Both fractions were then concentrated by immunoprecipitation with the anti-myc antibody, subjected to electrophoresis on a 10% SDS/PAGE followed by immunoblotting with the anti-myc (9E10) antibody.

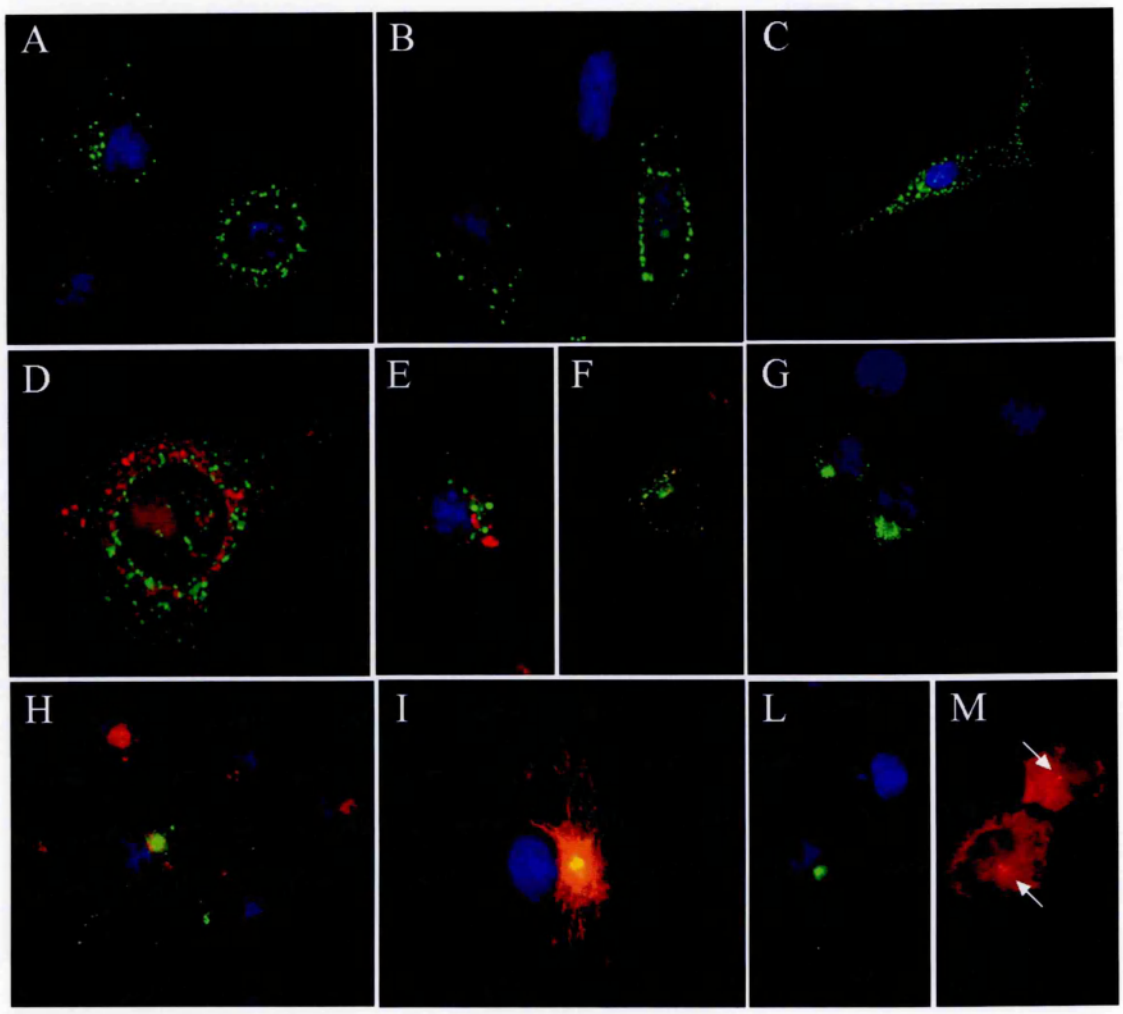

Figure 9. Subcellular localization of exogenous spastin.

Spastin-myc construct was transfected in Cos7, HeLa and human fibroblasts cells. Cells were analyzed by immunofluorescence with the anti-myc antibody 24h post-transfection. Spastin-myc shows a discrete punctuate cytoplasmic localization in Cos7 (A), HeLa (B) and human fibroblasts (C). Spastin-myc-GFP construct was transfected in Cos7 cells. Double immunofluorescence analysis using Spastin-myc-GFP (green signal) and appropriate markers (red signal), revealed that spastin cytosolic spots do not co-localize with mitochondria (D), lysosomes (E) and peroxisomes (F). When low levels of expression were achieved (see Material and Methods), spastin localizes to a discrete perinuclear area (G). Double immunofluorescence experiments using spastin-myc-GFP showed that this expression domain is in the proximity to the Golgi apparatus (H), and co-localize with the microtubule aster (I) and the centrosome (L, M). In (I) the yellow color of the merged figure indicate the co-localization of spastin with the aster of microtubule. In (M), arrows point the centrosomes. Monoclonal antibodies against 58kDa Golgi protein, α-tubulin and γ-tubulin were used to detect the Golgi apparatus, microtubules and the centrosome, respectively.

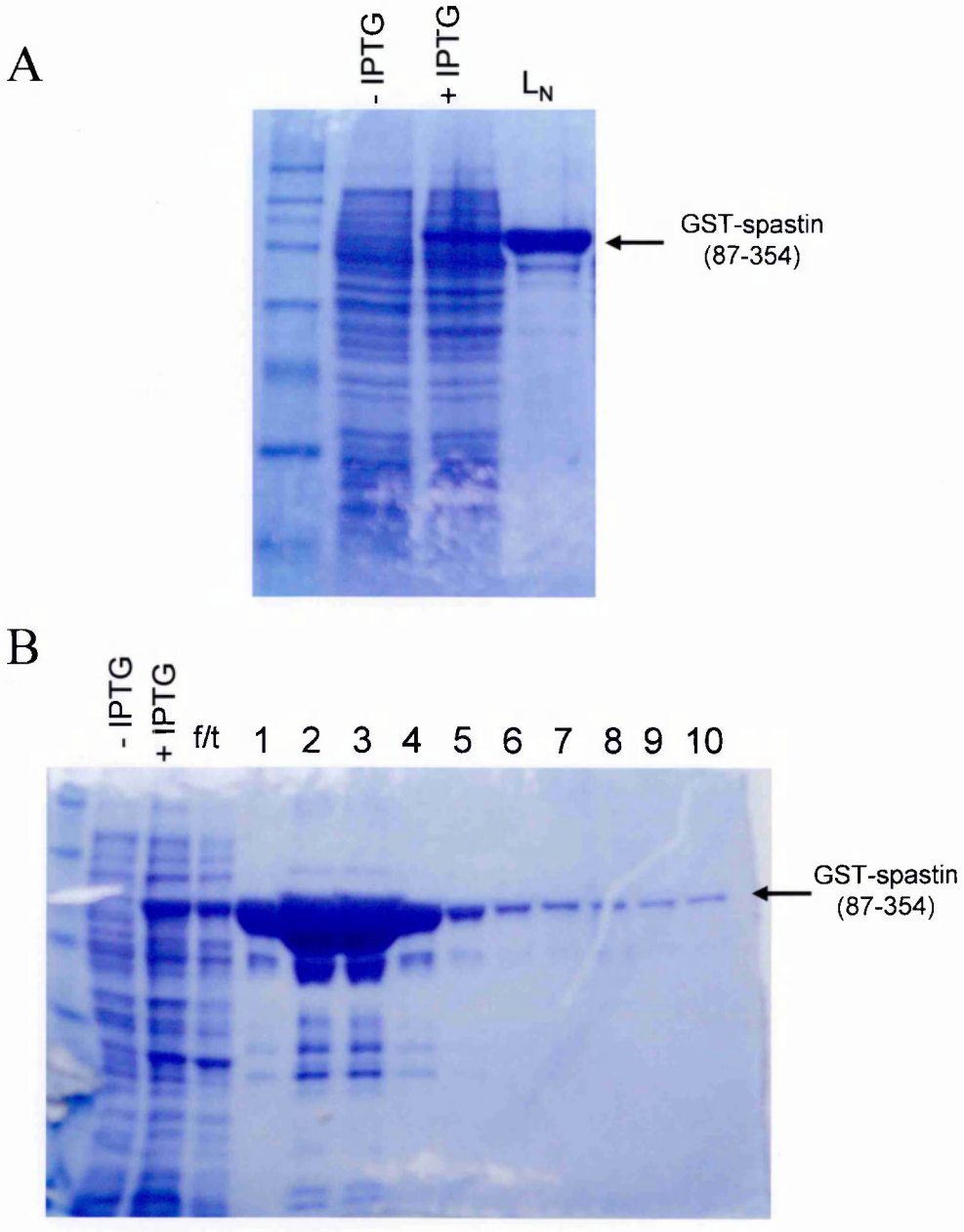

Figure 10. Production of recombinant GST-spastin.

pGEX3X-Spastin was transformed in *E. Coli* cells (strain B834). (A) The production of the recombinant protein was induced by the addition of 2mM IPTG. The recombinant protein is soluble under native condition, as assessed by the presence of the GST-spastin (87-354) in the lane of the native lysate (Ln). (B) GST-spastin was purified on GST-agarose column. The recombinant protein was bound to the GST-agarose beads; the flow through (f/t) was discarded. After washing, the recombinant protein was eluted in a glutathione buffer, 1000 µl fractions were collected and 5 µl of each fraction were tested on 10% SDS/PAGE.

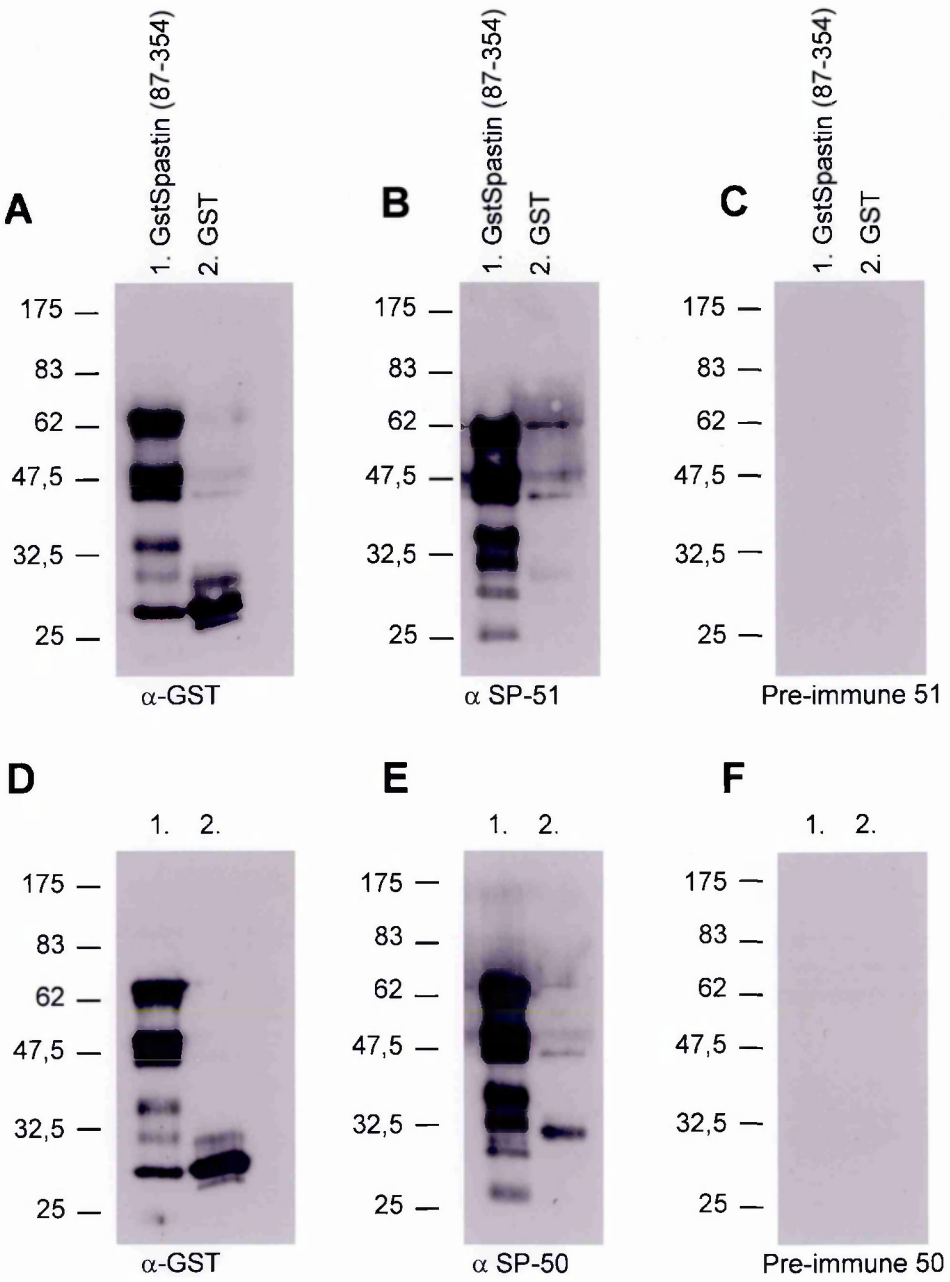

Figure 11. Affinity purified SP-50 and SP51 recognize specifically the recombinant protein.

5 µg of GST-Spastin and of GST were loaded on a 10% SDS/PAGE and transferred to a PVDF membrane for immunoblot analysis. The anti-GST antibody detects both the GST-Spastin (A, B lane1) and GST bands (A, B lane 2). The affinity purified anti-spastin SP-50 and SP-51 recognize specifically the GST-spastin (B, E lane 1), but do not recognize the GST alone (B, E lane 2). None of the preimmune sera (50, 51) detect the recombinant protein (C, F lane 1, 2).

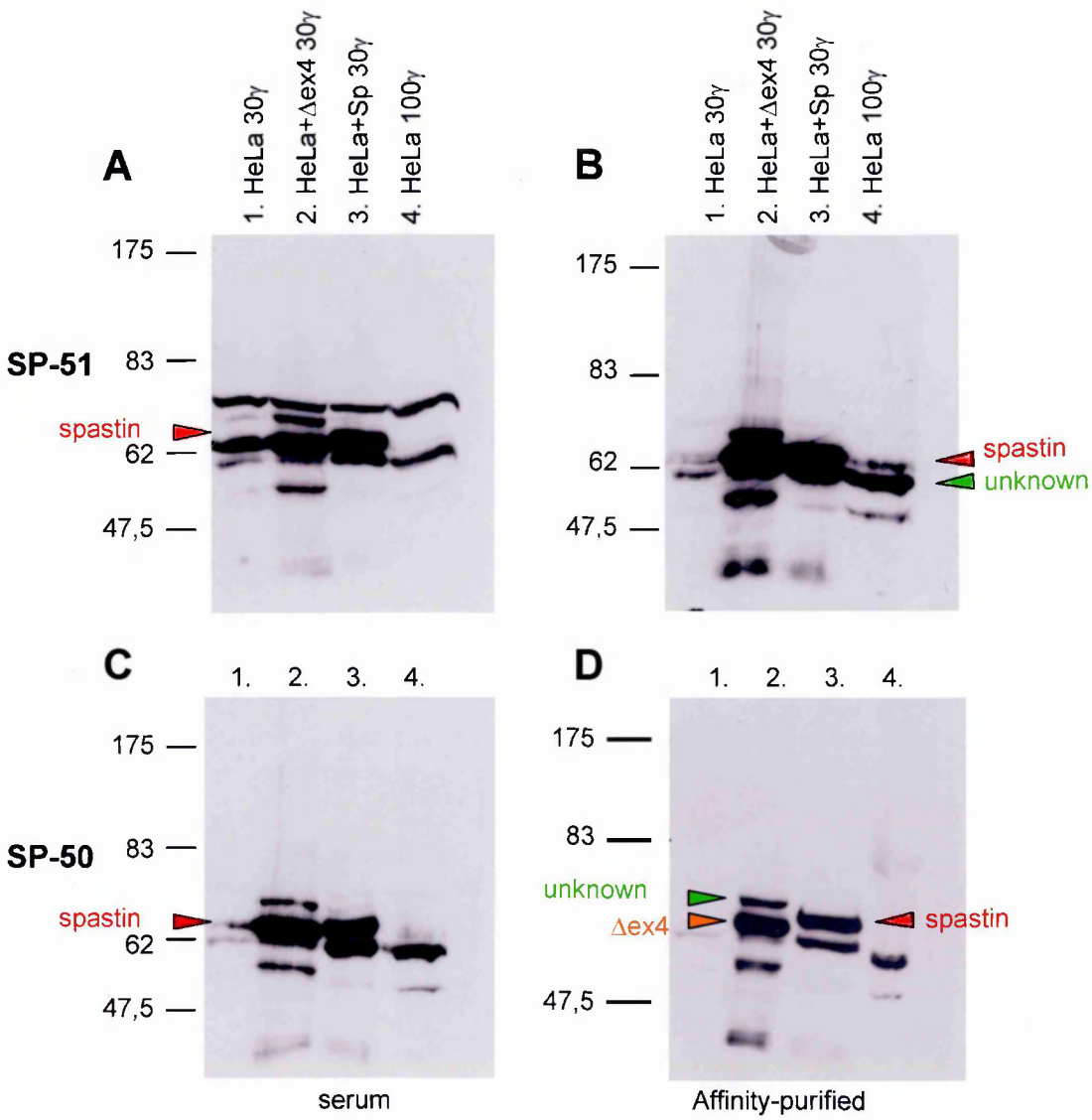

Figure 12. SP-50 and SP-51 recognize spastin in transfected cells.

Total cell extracts were prepared from HeLa untransfected or transfected with pcDNA$_3$-Spastin (full length without tag) or with pMT21-Δex4myc. 30μg of extracts from pcDNA$_3$-Spastin transfected cells, 30μg of extracts from pMT21-Dex4myc transfected cell and 30μg or 100μg of extracts from untransfected cells were fractionated on a 7.5% SDS/PAGE and transferred to a PVDF membrane. Membranes were then analyzed by immunoblot with the crude sera and the affinity purified antibodies. The results obtained with the affinity purified SP-50 (D) or SP-51 (B) were approximately the same of the crude antisera (A, C). Both, SP-50 and SP-51 recognize the exogenous spastin (A, B, C, D lane 3, red arrow) and Δex4 (A, B, C, D lane 2). The endogenous proteins was not detect when 30μg of lysate were loaded (A, B, C, D lane 1), although a faint band is recognized when 100μg of extracts are loaded (B, lane 4).

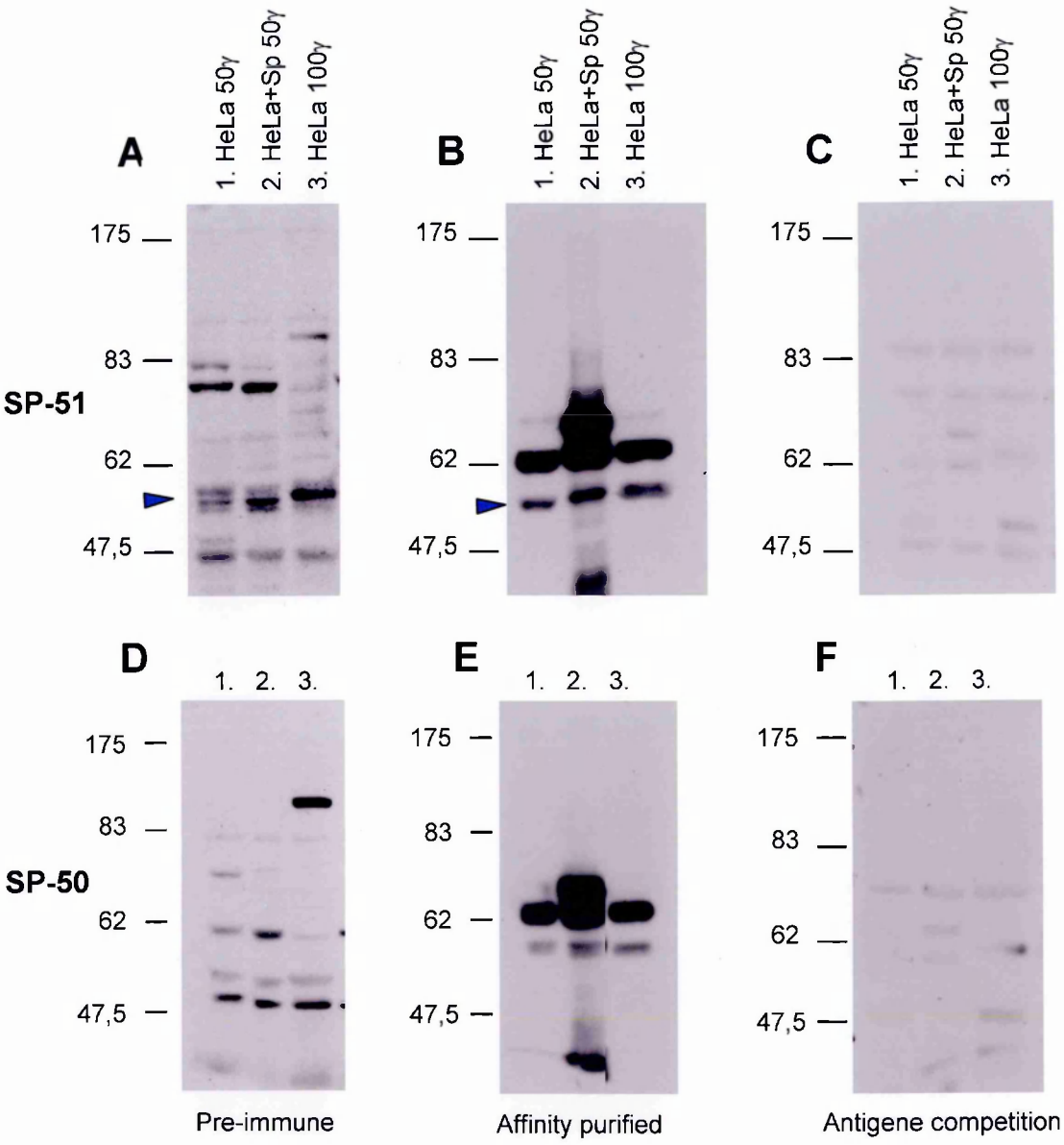

Figure 13. SP-50 and SP-51 are specific for spastin.

HeLa cells were transfected with pcDNA$_3$-Spastin.Total cell extracts were prepared from untransfected and transfected HeLa cells. 50 or 100μg (lane 1, 3) of untransfected cell extracts and 50μg (lane 2) of extracts from transfected cells were fractionated on a 7.5% SDS/PAGE. Western blot analysis was performed probing the filters with preimmune sera (A, D) and affinity purified antibodies (B, E). The specificity of the signals was evaluated after the competition with the antigen (C, F). Both SP-50 and SP-51 detected the band corresponding to the exogenous spastin (B, E lane 2), this band was not recognized by the preimmune sera (A, D lane 2) and disappeared after the antigen competition (C, F lane 2). The band of about 55 kDa (B, arrow) seems to be present also in the preimmune serum (A, arrow) and therefore is a non specific signal.

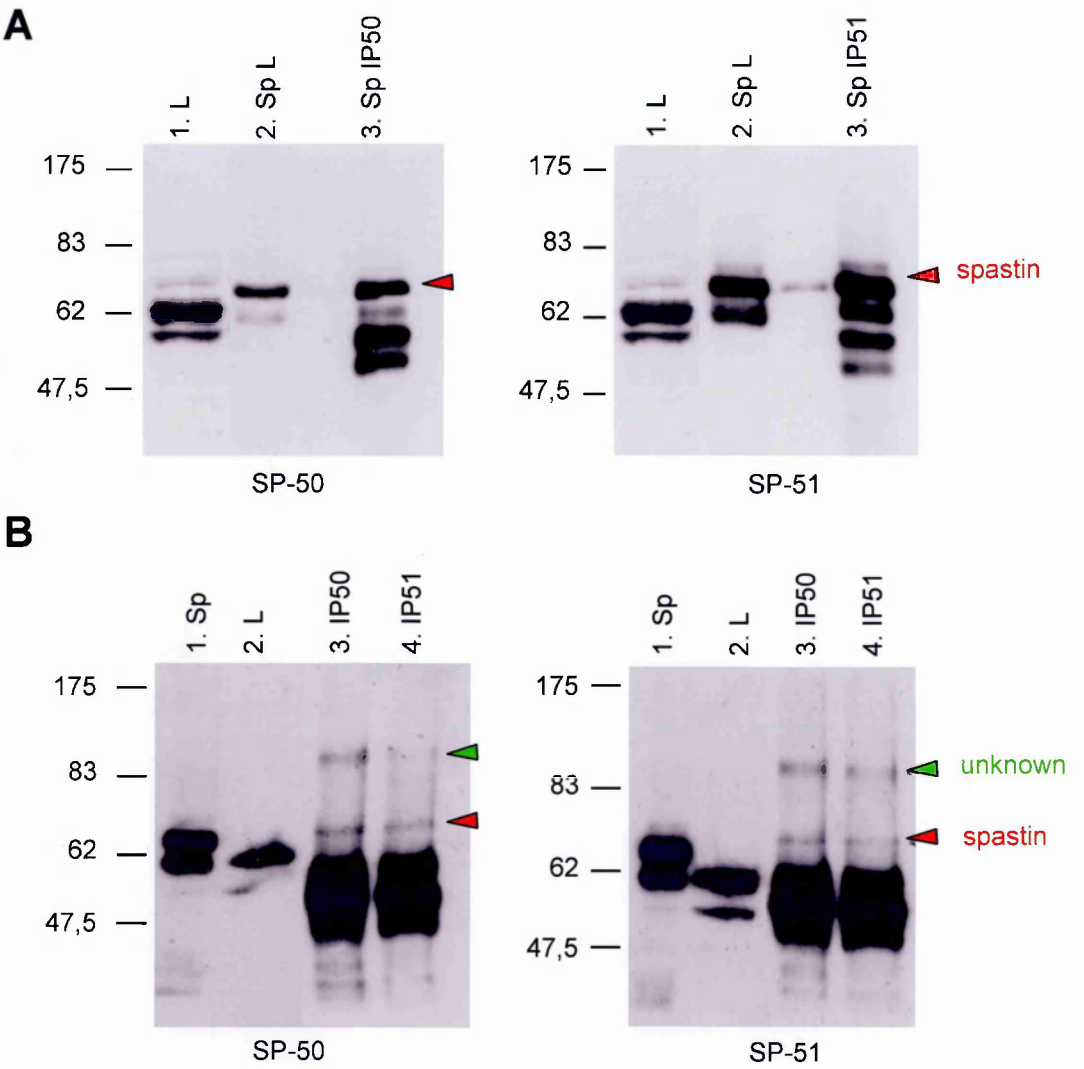

Figure 14. SP-50 and SP-51 immunoprecipitate both exogenous and endogenous spastin.

(A) HeLa cells were transfected with pcDNA$_3$-Spastin. Lysates were prepared from untransfected and transfected cells. Immunoprecipitation experiments were performed on transfected extracts using the antibodies SP-50 and SP-51 (1:100). Untransfected HeLa extracts (100μg; lane 1), extracts from transfected cells (30μg, lane 2) and immunoprecipitation samples obtained either with SP-50 or SP-51 (lanes 3,4) were loaded on a 7.5% SDS/PAGE. Immunoblot analysis, respectively with SP-50 or SP-51, showed that both antibodies were able to immunoprecipitate the transfected spastin protein (lane 3, arrows). (B) Cell extracts were prepared from HeLa cells; immunoprecipitation was carried out with the antibodies SP-50 and SP-51. HeLa cells transfected (30μg, lane 1) or not (100μg, lane 2) with spastin and immunoprecipitation samples were resolved on a 7.5% SDS/PAGE and western blot analysis was performed using the SP-50 or the SP-51 antibody. Both antibodies were able to immunoprecipitate a protein of the same size of the transfected spastin, which should correspond to the endogenous spastin (lane 3, 4 of both panels) (red arrows). A slower migrating band is also revealed with both antibodies. This band has an apparent molecular weight of 90 kDa (green arrows).

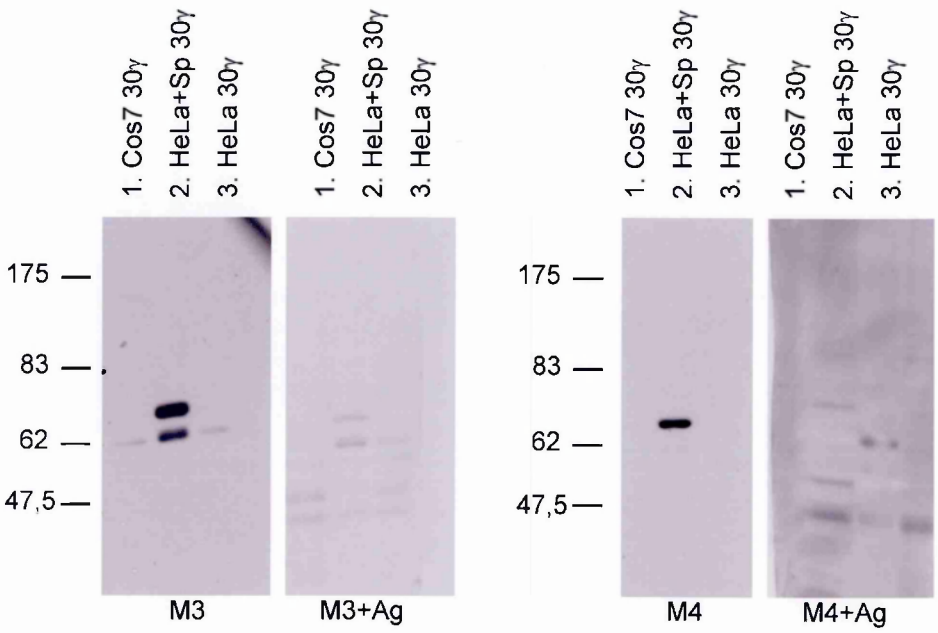

Figure 15. Monoclonal antibodies M3 and M4 recognized exogenous spastin.
HeLa cells were transfected with pcDNA$_3$-Spastin. Total extracts were prepared from untransfected (HeLa and Cos7) and transfected (HeLa + Spastin) cells. Samples were fractionated on a 7.5% SDS/PAGE, transferred to a PVDF membrane and analyzed by western blot using the M3 or M4 antibodies. Both antibodies detected the band corresponding to the transfected spastin, but failed to detect the endogenous protein. When the M3 or M4 antibodies were pre-incubated for 3 hrs at 4°C with the antigen (GST-spastin) and then used for western blot analysis, all the signals revealed by the M3 and M4 antibodies disappeared.

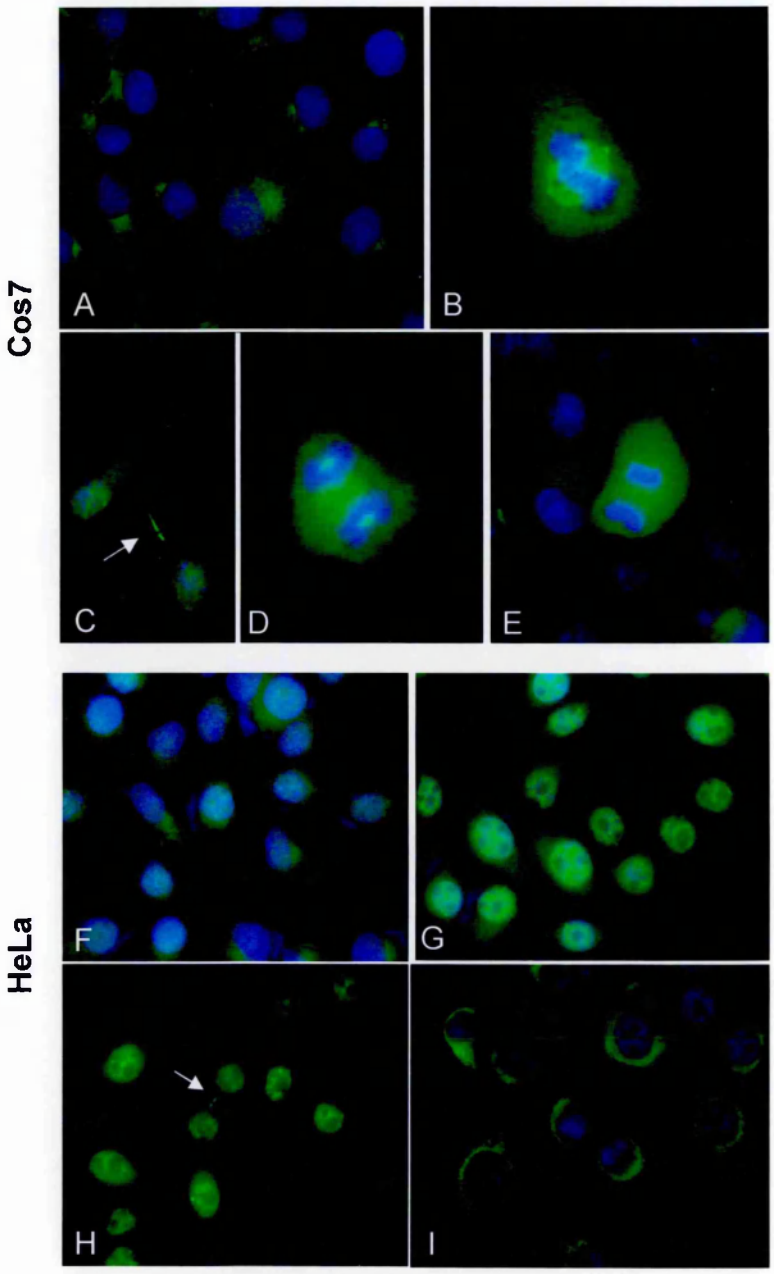

Figure 16. Immunofluorescence experiments on HeLa and Cos7 cells with SP-R74

Cos7 (A-E) and HeLa (F-I) cells were fixed in PFA 4% and stained with the specific spastin antibody SP-R74 or with the pre-immune sera as control. The specificity of the signal was confirmed by the staining with an antigen-antibody mix. The signals were detected using as secondary antibody an anti-rabbit FITC-conjugated. In A and F are shown the pre-immune serum staining, respectively in Cos7 and HeLa cells. In B, C and D are shown the IF on Cos7 cells, where the SP-R74 stains the spindle poles and the midbody. In HeLa cells, the SP-R74 has a diffuse nuclear staining (G,H) and marks the midbody (H). The signals detected by the SP-R74 in Cos7 and HeLa cells were specific as demonstrated by the competition with the antigen (E, I), where these signals disappeared.

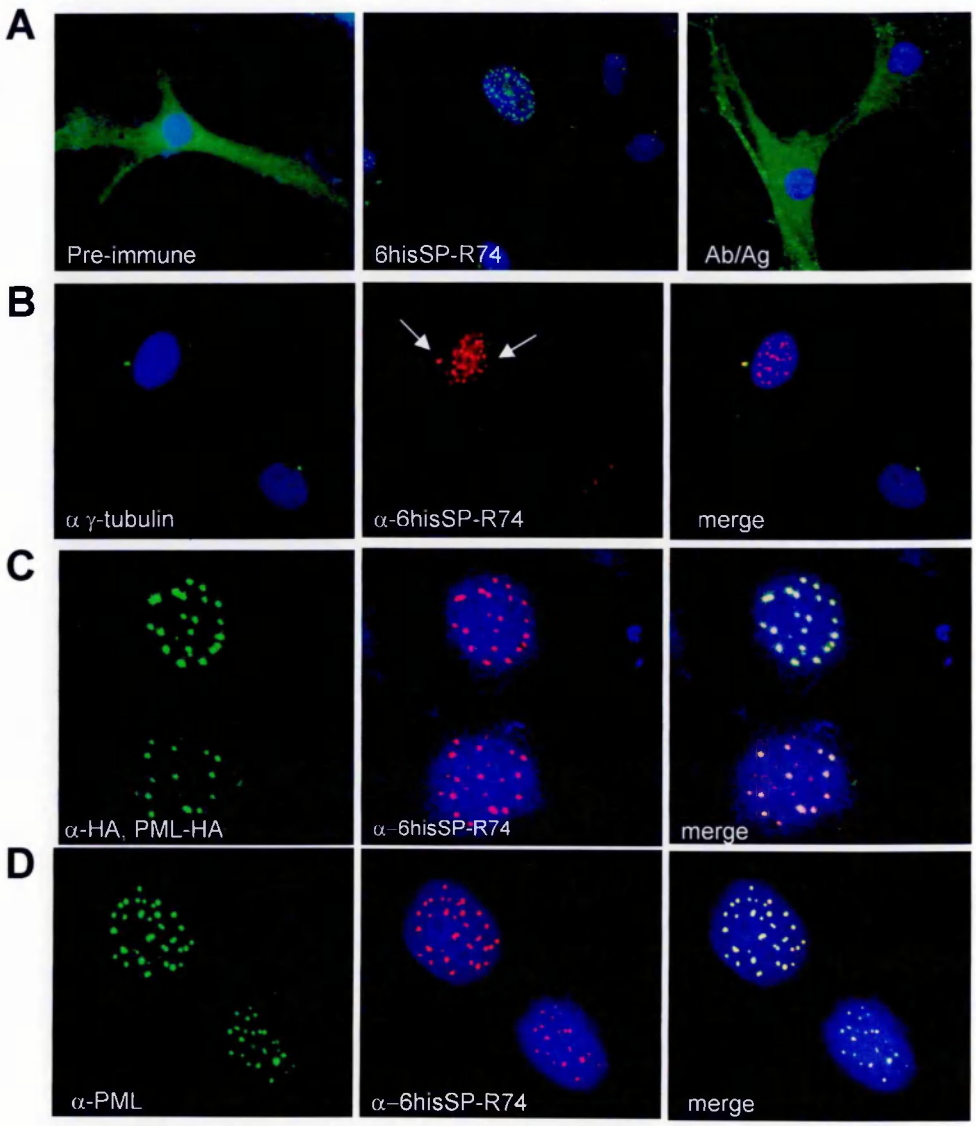

Figure 17. Immunofluorescence experiments on Human Fibroblasts with SP-R74.

(A) Fibroblasts were fixed in methanol and stained with pre-immuneserum, SP-R74 and an antigen-antibody mix. The SP-R74 revealed both a spotted nuclear signal and a discrete cytoplasmic signal (arrows). (B) A double IF experiments was performed using the SP-R74 to stain Spastin and a monoclonal antibody that recognizes the γ-tubulin. The co-localization is indicated by the yellow signal in the merge figure (third panel). (C) Human fibroblasts were transfected with a PML-HA construct. Double IF experiments using the SP-R74 to stain Spastin and a monoclonal antibody against the HA tag were performed. Co-localization between spastin and PML in the nuclear dots is indicated by the yellow signal in the merge figure. (D) Double IF experiments with the SP-R74 to stain Spastin and a monoclonal antibody that recognizes the endogenous PML. SP-R74 is revealed with a rabbit-secondary antibody FITC-conjugated in the single staining. In double IF experiments, SP-R74 was revealed with a rabbit-secondary antibody TRITC-conjugated; anti γ-tubulin, anti-HA and anti-PML were revealed with a mouse-secondary antibody FITC-conjugated. Nuclei were marked with DAPI (blue signal).

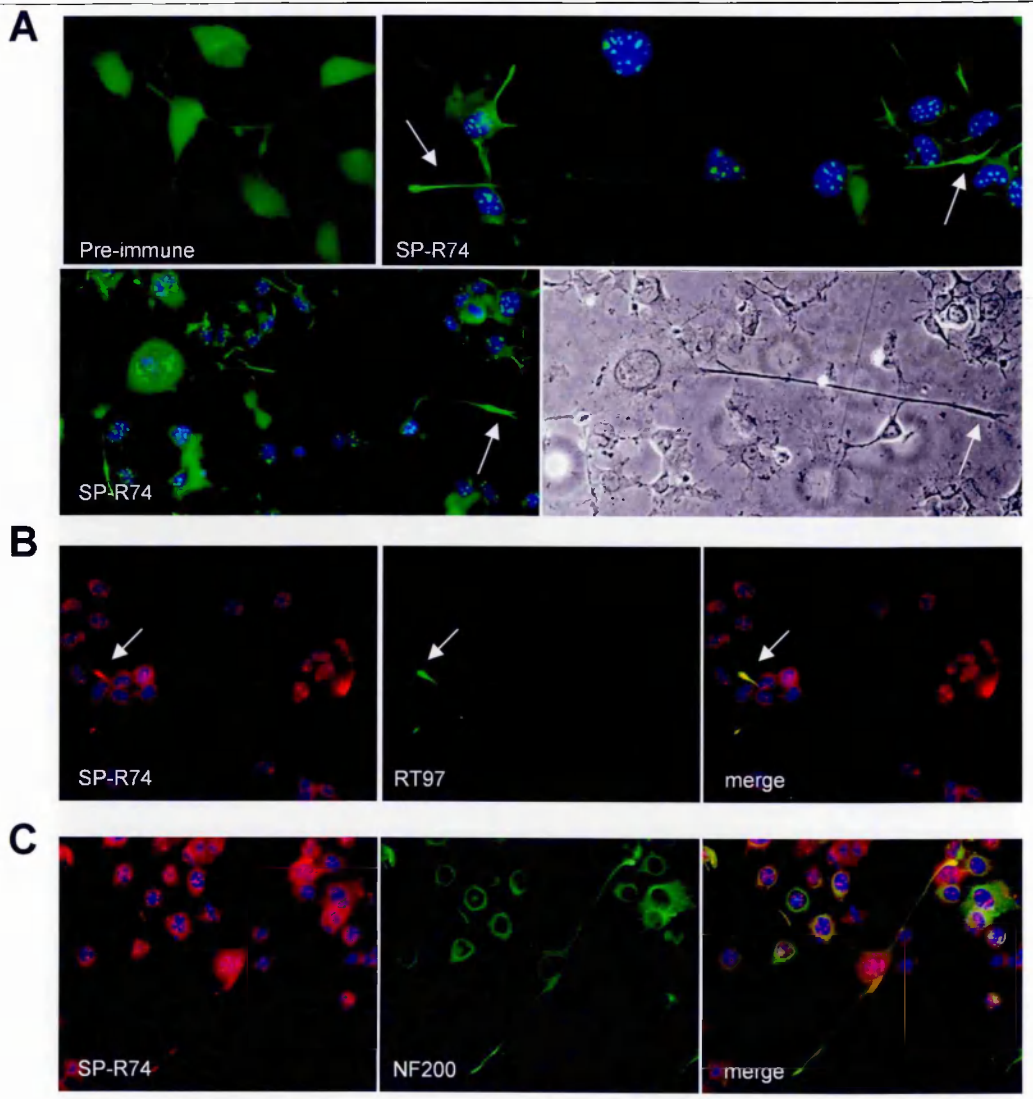

Figure 18. Immunofluorescence experiments on NSC34 with SP-R74.

(A) NSC34 were fixed in methanol and stained with pre-immune serum, SP-R74 and an antigen-antibody mix. The SP-R74 revealed a spotted nuclear signal and also a signal enriched in the terminal portion of the neuronal processes (arrows). (B) A double IF experiments was performed using SP-R74 to stain Spastin and a monoclonal antibody, RT97, that recognizes phosphorylated epitopes on neurofilaments protein. The co-localization is indicated by the yellow signal in the merge figure (third panel). (C) Double IF experiments with SP-R74 to stain Spastin and a monoclonal antibody, NF200, which marks the neurofilaments.
SP-R74 was revealed with a rabbit-secondary antibody FITC-conjugated in the single staining. In double IF experiments SP-R74 was revealed with a rabbit-secondary antibody TRITC-conjugated; anti NF200 and anti RT97 were revealed with a mouse-secondary antibody FITC-conjugated. Nuclei were marked with DAPI (blue signal).

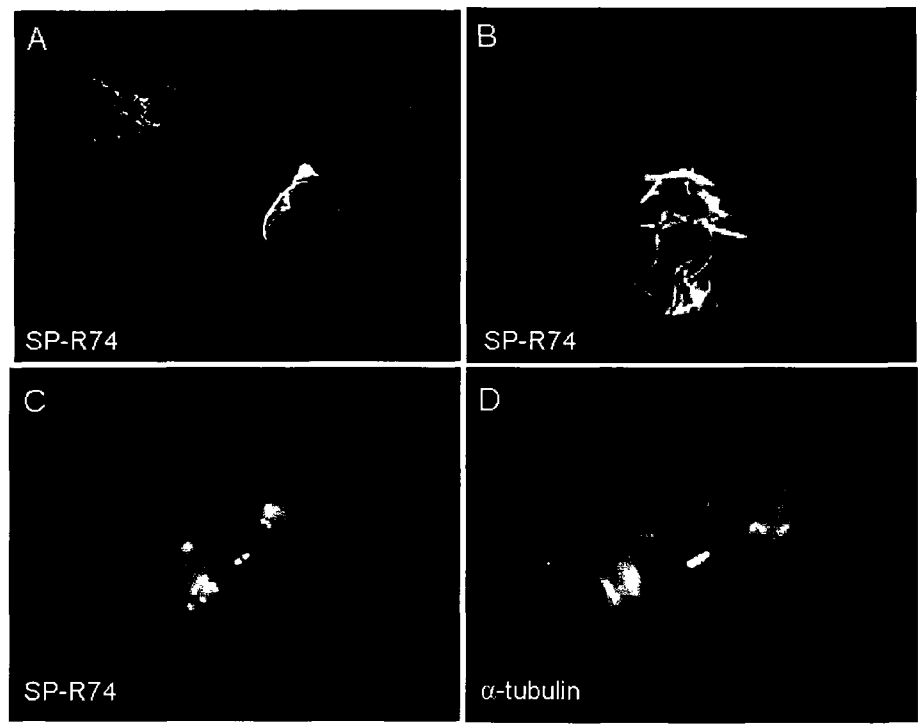

Figure 19. Immunofluorescence experiments on cycling NSC34 with SP-R74.
NSC34 were fixed in methanol and stained with pre-immune serum, SP-R74 and an antigen-antibody mix. When cells are going through cell cycle, as stated by the nucleus staining (blue), SP-R74 marks filaments which are surrounding the nucleus (A, B). SP-R74 revealed also a signal at the midbody during cytokinesis (C), as stated by the double IF experiments with SP-R74 and a monoclonal antibody, anti α-tubulin, that stains microtubules (D). SP-R74 was revealed with a rabbit-secondary antibody FITC-conjugated in the single staining. In double staining, SP-R74 was revealed with a rabbit secondary antibody TRITC-conjugated; anti a-tubulin was revealed with a mouse secondary antibody FITC-conjugated. Nuclei are marked with DAPI (blue signal).

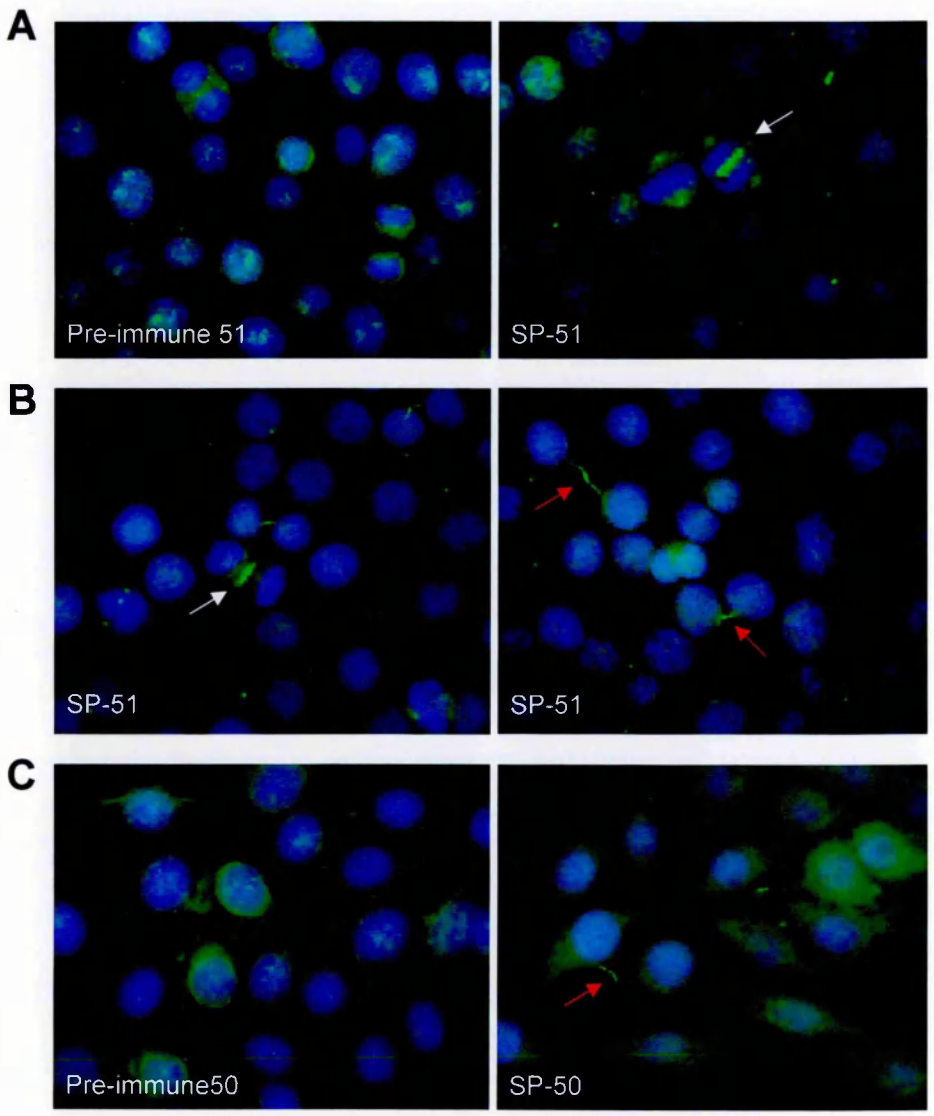

Figure 20. Immunofluorescence experiments on HeLa cells with SP-50 and SP-51.

(A, B) HeLa cells were fixed in PFA 4% and stained with pre-immune serum and SP-51. SP-51 revealed a spastin signal at the midbody (B, red arrow) and also a discrete signal in the region between the two nucleus that are going through cytokinesis (A, B, white arrow). (C) Immunofluorescence analysis on HeLa cells with the pre-immune serum and the SP-50 antibody confirmed the localization to the midbody (C, red arrow). SP-50 and SP-51 were revealed with a rabbit secondary antibody FITC-conjugated, nuclei were marked with DAPI (blue signal).

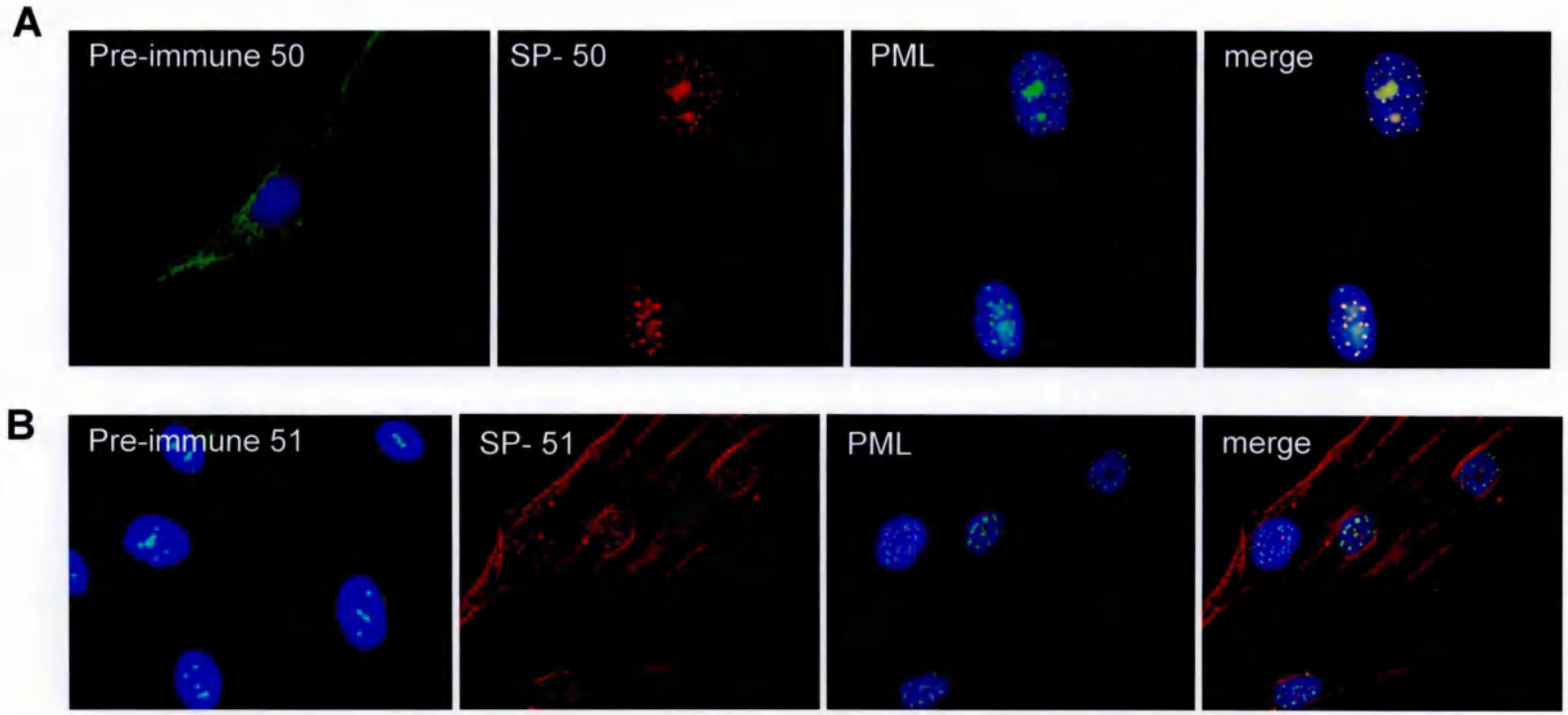

Figure 21. IF experiments on Human Fibroblasts with SP-50/51.
(A, B) Fibroblasts were fixed in PFA 4% and stained with pre-immune serum and SP-50/51 antibodies. The SP-50 revealed a spotted nuclear signal (A, panel 2). A double IF experiments using the SP-50 to stain Spastin and a monoclonal antibody that recognizes PML showed that spastin was partially co-localizing with the PML bodies (A, panel 2,3,4). The SP-51 revealed also a spotted nuclear signal (B), which corresponds to the PML bodies as assessed by the double IF experiments with the SP-51 and the anti-PML antibody. The partial co-localization between spastin and PML in the nuclear dots is indicated by the yellow signal in the merge figure (A, B panel 4). SP-50 and SP-51 were revealed with a rabbit secondary antibody TRITC-conjugated; anti-PML was revealed with a mouse-secondary antibody FITC-conjugated, while nuclei are marked with DAPI (blue signal).

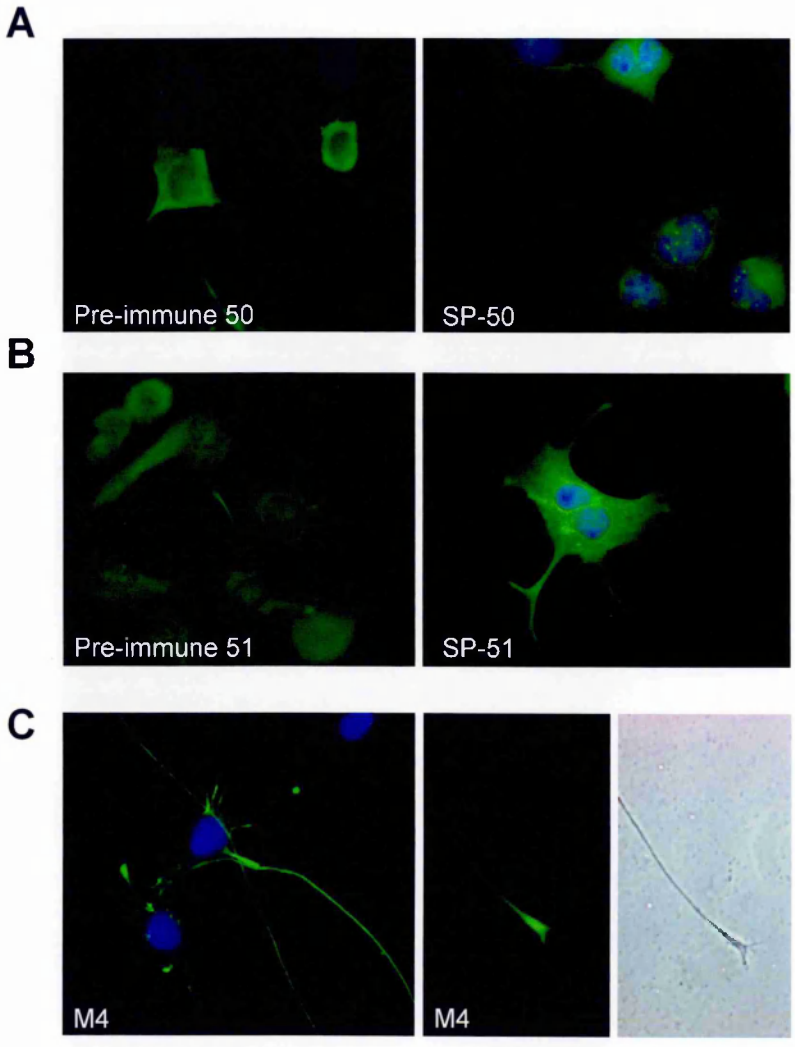

Figure 22. IF experiments on NSC34 with SP-50/51.

(A, B) NSC34 were fixed in methanol and stained with pre-immune sera (SP-50/51) or with the anti-spastin SP-50 and SP-51 antibodies. SP-50 revealed a spotted nuclear signal (A). Both antibodies revealed a diffuse staining in the cytoplasm (A, B). (C) NSC34 were fixed in methanol and stained with the M4 monoclonal antibody. The M4 revealed a staining in the terminal part of the neuronal processes (C), in particular the signal at the growth cone is shown (C, panel 2 and 3). SP-50 and SP-51 were revealed with a rabbit secondary antibody FITC-conjugated; M4 was revealed with a mouse secondary antibody FITC-conjugated, while nuclei are marked with DAPI (blue signal).

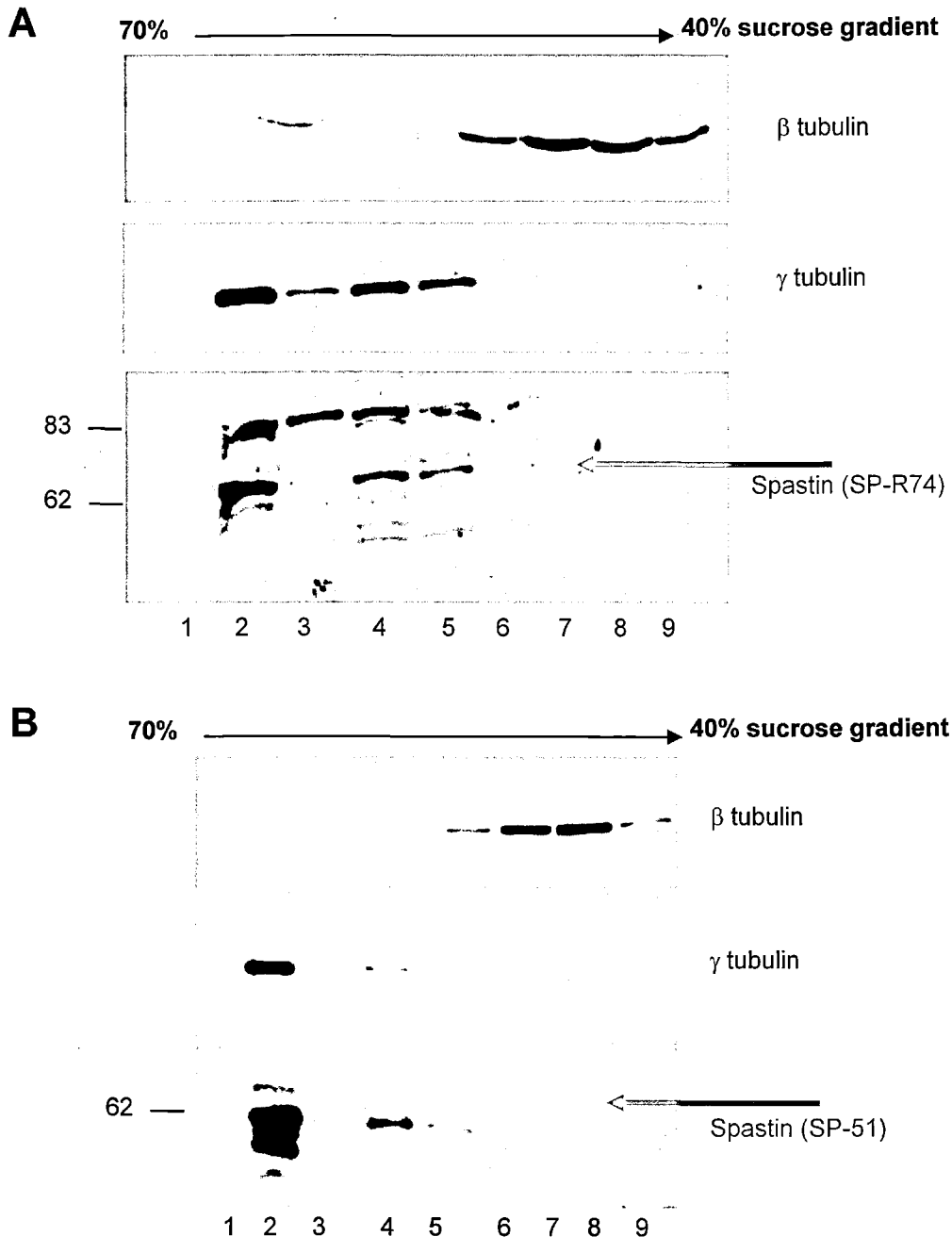

Figure 23. Spastin is enriched in a centrosome fraction.

HeLa cells were treated with 0.2μM Nocodazole and 1 μg/ml of cytochalasin D. Cells were collected by trypsinization, washed and resuspended in lysis buffer (see methods). Centrosomes were concentrated by centrifugation on a 60% sucrose cushion (w/v) and then purified on a discontinuous sucrose gradient (70% - 50%-40%). The fractions eluted from the gradient were loaded on a 10% SDS/PAGE, transferred to a PVDF membrane and analyzed by immunoblot using an anti b-tubulin, an anti γ-tubulin and a specific anti-spastin antibody. SP-R74 revealed the presence of spastin in the same fractions where the g-tubulin was eluted (fractions 2 to 5) (A), while the β-tubulin was present in fractions 6 to 9. The same experiment was performed and spastin was revealed with the SP-51 antibody (B). SP-51 detected also spastin in the fraction 2 to 5 together with the γ-tubulin, while β-tubulin was detected in fractions 6 to 9 (B).

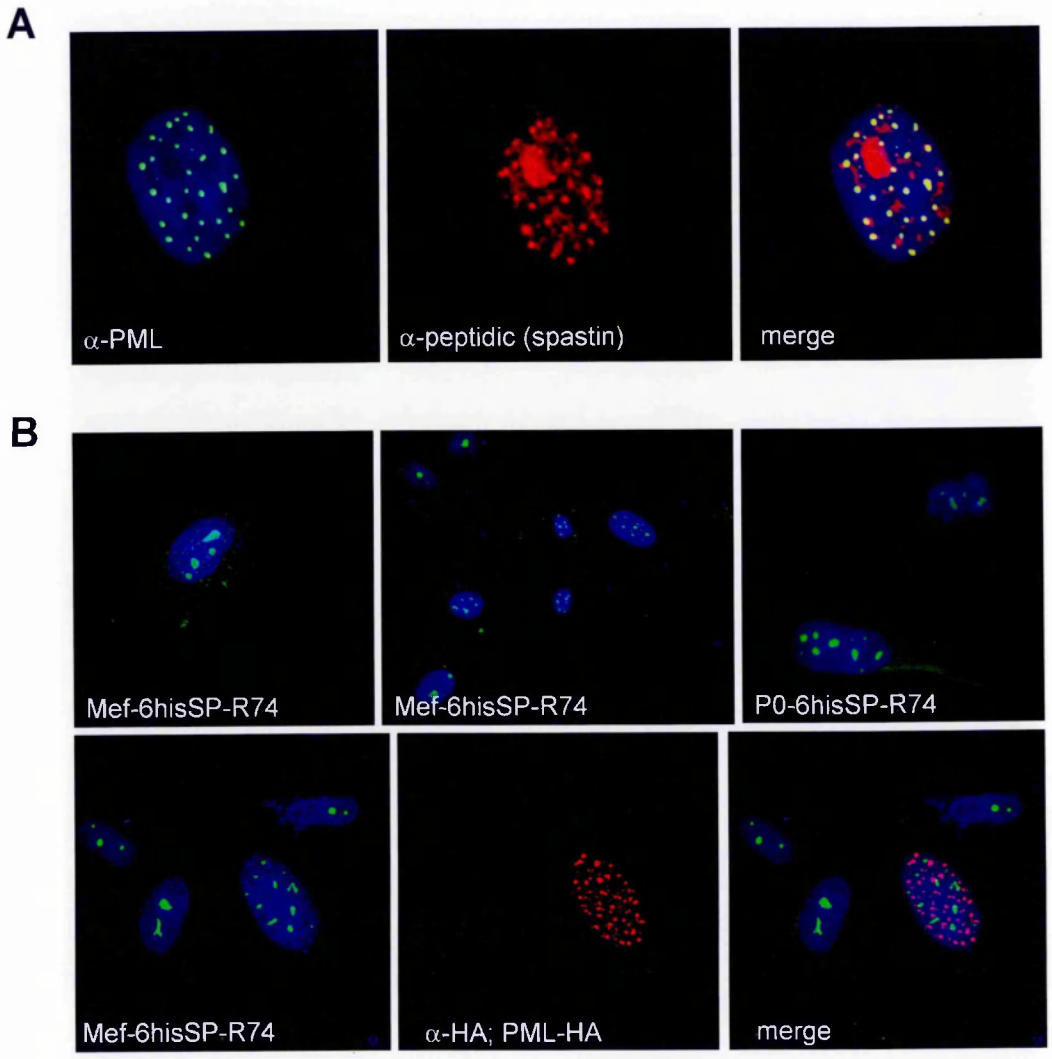

Figure 24. Spastin localizes to the PML bodies in human fibroblasts but not in mouse fibroblasts.

(A) Human fibroblasts were fixed in methanol. PML bodies were detected (green signal) using the monoclonal anti-PML antiboy. While spastin was detected using a specific polyclonal anti-peptidic antibody (red signal). Nuclei were stained with DAPI (blue signal). A partial colocalization is evident as shown in the merge figure by the yellow signal.

(B) Mouse embryonic fibroblasts (mef) or fibroblasts from a mouse at P0 were fixed in methanol and immunofluorescence experiments were performed with the SP-R74 antibody. The SP-R74 detected in both cell type a spotted nuclear signal, but these spots are larger then those observed in the human fibroblasts. Mef were transfected with the PML-HA construct. Double IF experiments were performed on mef transfected cells using the SP-R74 and the anti-HA antibody to recognize PML. It is evident that the nuclear domains recognized by SP-R74 in the murine cell lines are not PML bodies.

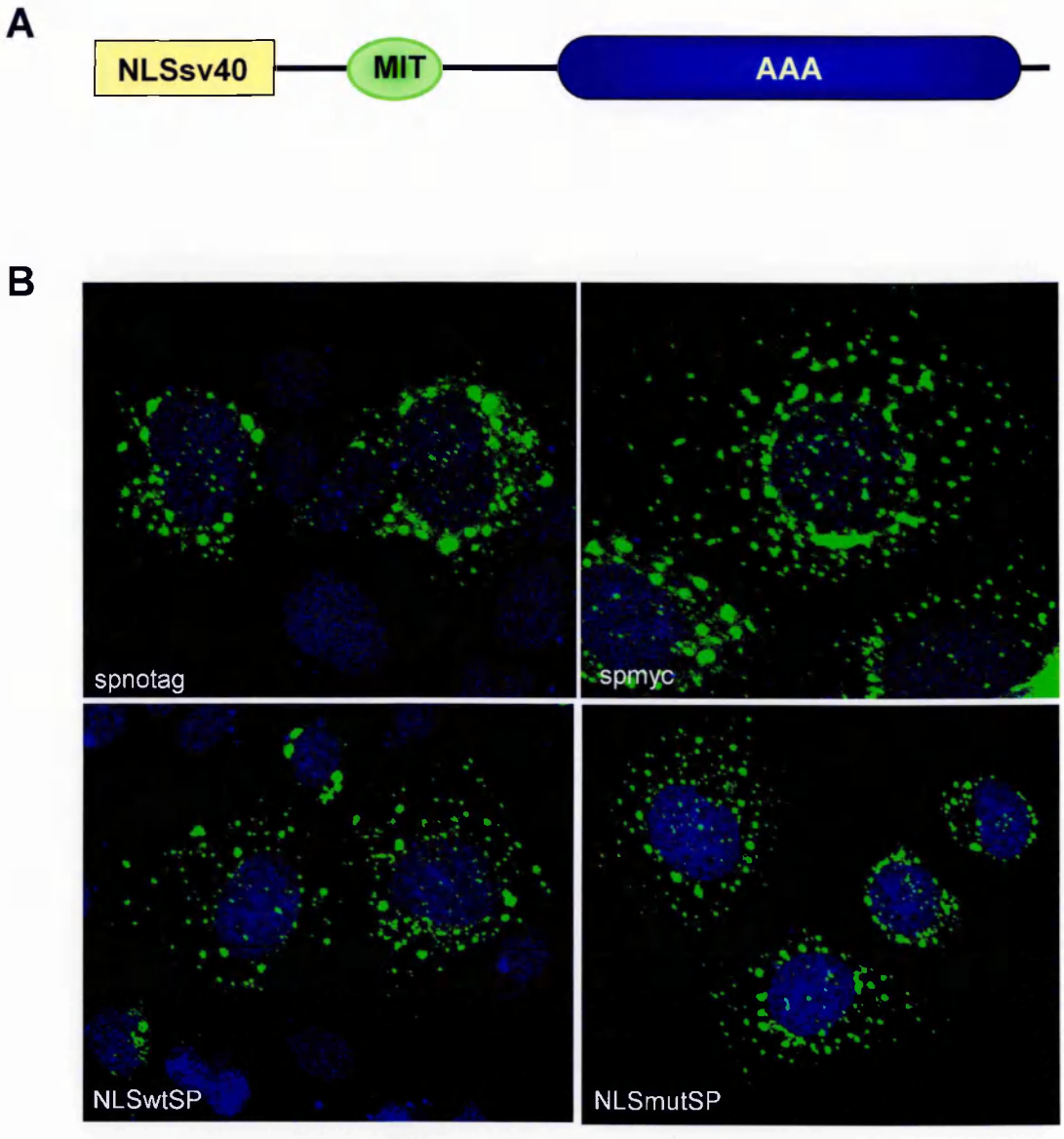

Figure 25. A NLS-spastin chimera does not localize to the nucleus

The SV40 NLS, wild type (*wt*) or mutated, was fused at the 5' of the spastin cDNA in the pcDNA$_3$-spastin construct (A). Cos7 cells were transfected with spastin (without tag), spastin-myc or with the two chimeric protein containing the *wt* or mutated NLS fused to spastin cDNA (B). Cells were fixed 24 hrs post-transfection in PFA 4% and analyzed by immunofluorescence at the confocal microscope. Both spastin constructs, without tag and with the myc tag, shown the typical cytoplasmic pattern, although few nuclear spots were detected. The NLS*wt*Spastin and NLSmutSpastin constructs did not show a different localization from the precedent constructs.

CHAPTER 4: Spastin and Microtubules

4.1 ATPase defective spastin localizes to microtubules

Other members of the AAA family, such as SKD1, p60 katanin, and NSF bind and release protein substrates in a nucleotide-dependent manner (Babst et al., 1998; Hartman and Vale, 1999; Whiteheart, 1994; Wilson et al., 1992). This may lead to transient association *in vivo* with their targets. However, this transient association can be revealed by expressing dominant-negative mutants unable to bind or hydrolyze ATP. To test whether this is true also for spastin, a spastin construct was prepared, expressing a well-characterized mutation (K388R), which falls into the Walker A motif or P loop of the AAA domain, and is known to abrogate ATP binding in other members of the family (Babst et al., 1998; Hartman and Vale, 1999; Whiteheart, 1994; Wilson et al., 1992). This mutant has been found in a patient with HSP and therefore represents also a pathogenic form of spastin (Fonknechten et al., 2000). The construct Spastin-mycGFP was subjected to site directed mutagenesis to introduce the missense mutation K388R. Cos7 cells were transfected with spastin^{K388R} and subcellular localization was analysed by immunofluorescence. The beginning of expression of the mutated spastin was seen in a single perinuclear domain, similarly to the wild-type protein (Fig. 26 A). However, with longer periods of expression, a filamentous pattern, reminiscent of association with the cytoskeleton, was detected (Fig. 26 B). In some transfected cells a combination of filaments and of cytoplasmic aggregates was also observed.

To assess the nature of the filaments, double immunofluorescence experiments were performed, using the antibody to recognise the transfected spastin and monoclonal antibodies against α-tubulin or vimentin, to detect microtubules and intermediate filaments, respectively. The filaments labelled in spastin^{K388R}-transfected cells co-localize with α-tubulin (Fig. 26 C, D), and not with vimentin (Fig. 26 E, F). To further confirm binding of spastin^{K388R} to microtubules, cells transfected with spastin^{K388R} were treated with nocodazole, a drug capable of inducing microtubule depolymerization by inhibiting addition of tubulin monomers. Treatment with 20□M nocodazole for 2,5 hours results in the disruption of the microtubules network with a consequent dispersion of mutant spastin and tubulin monomers within the cytoplasm in most cells (Fig. 26 G, H). Co-localization of spastin^{K388R} with microtubules shows peculiar features. First, although all filaments labelled by mutant spastin seem to co-localize with microtubules, not all the microtubules present in the cell are labelled by spastin (Fig. 26 C, D). This data suggests that the mutant may bind a subset of microtubules. Second, microtubule distribution in transfected cells seems to be altered, with the disappearance of the aster, typical of an interphase cell, and the formation of thick and long perinuclear bundles (Fig. 26 C, D). Consistent with a redistribution of microtubules, also dispersal of intermediate filaments appears affected in transfected cells (Fig. 26 E, F). Third, in some cases these bundles appear to be more resistant to nocodazole treatment, suggesting that spastin may protect them from depolymerization (Fig. 26 H).

4.2 Spastin associates with microtubules via its N-terminal region

The findings that spastin expression begins in the microtubule organizing center and that an ATPase-defective mutant associates with microtubules *in vivo* strongly suggest that also *wild type* (*wt)* spastin may associate with MTs. So, *in vitro* experiments were performed to investigate if *wt* spastin may bind taxol-stabilised microtubules. Cos7 cells were transfected with the Spastin-myc construct (Fig. 8 A). Extracts from spastin transfected cells were supplemented with taxol and GTP, and centrifuged on sucrose cushion to sediment microtubules and associated proteins. In these conditions, full-length spastin was enriched in the microtubule fraction (Fig. 27 A). As negative control lysates from transfected cells were not supplemented with taxol. In order to map a putative microtubule-binding domain, we produced two artificial mutants in which either the AAA domain (spastin$^{\Delta AAA}$) or the N-terminal part of spastin were deleted (spastin$^{\Delta N}$) in the pMT21-myc plasmid. Those deletion constructs were transfected into Cos-7 cells and used in the same assay. The spastin$^{\Delta AAA}$ retained the ability to co-sediment with polymerised microtubules in the *in vitro* binding assay, whereas spastin$^{\square N}$ lost it (Fig. 27A). These results were confirmed by immunofluorescence experiments on Cos7 cells previously transfected with either spastin$^{\Delta AAA}$ or spastin$^{\Delta N}$. In both cases a α-myc antibody was used to reveal spastin levels. The spastin$^{\Delta AAA}$ construct showed a filamentous pattern of expression, which was susceptible to nocodazole treatment (Fig. 27 B, C). Spastin$^{\Delta\text{-}N}$, instead, exhibited a diffuse cytoplasmic staining (Fig. 27 D). All together, these data indicate that spastin interacts with microtubules via its N-terminal region.

4.3 Mapping of the microtubules binding domain

To map more precisely a microtubule (MTs) binding domain, the N-terminal region of spastin was dissected by generating several constructs carrying different and progressive deletion of the N-terminal moiety (Δ50, Δ100, Δ190)(Fig.28). The analysis of spastin sequence revealed the presence of a MIT domain which seems to be present in microtubule interacting and endosomal trafficking molecules. Therefore, a spastin construct lacking the MIT domain was generated (□MIT), to understand if this domain could be involved in the MT binding. All the constructs were then subjected to site directed mutagenesis to introduce the missense mutation K388R in the AAA, in order to abrogate the ATPase activity of spastin and reveal, when present, the MTs interaction. All the constructs were myc-tagged. Then, *wt* and mutated constructs were transfected in Cos-7 cells and analysed by immunofluorescence. The ATPase defective mutants Δ50 and ΔMIT, retained the ability to stably associate with the MTs network, while the mutants Δ100 and Δ190 lost this ability. So, the MTs binding domain of spastin is located in its N-terminal region between amino acids 50 and 100; furthermore the MIT domain is not implicated in this association.

4.4 Overexpression of WT spastin leads to Microtubule disassembly

Spastin ability to bind microtubules in an ATP-dependent manner and to alter microtubule distribution and morphology suggest that it could be implicated in some aspects of microtubule dynamics. Another AAA protein of the same subfamily, p60 katanin, has been largely studied for its microtubule severing activity at the

centrosome (Hartman and Vale, 1999; McNally and Vale, 1993). To assess a putative microtubule severing activity of spastin *in vivo*, an assay previously used to measure *in vivo* microtubule severing of katanin and of its *C. elegans* homologue MEI-1 (McNally, 2000; Srayko et al., 2000) was employed. In this assay, the microtubule cytoskeleton is examined by anti-tubulin immunofluorescence in Cos-7 cells expressing spastin-GFP and compared to neighbouring untransfected cells. When wild-type spastin was expressed in Cos7 cells, a dramatic reduction in the intensity of tubulin immunofluorescence in approximately 50% of transfected cells (Table 3; Fig. 29 A, B, D, E) was observed. Reduced intensity of tubulin staining was never observed in cells transfected with the spastin^{K388R} mutant or with GFP alone. Overexposure of the spastin transfected cells showed that microtubules are broken, with the end of the filament recognizable in a few cases (Fig. 29 C, F). The remaining filaments are still emanating from the centrosome, but the dimension of the aster is greatly reduced (Fig. 29 C, F).

4.5 Functional characterisation of spastin missense mutation

All the spastin missense mutations found in HSP patients up to now are located into the AAA domain. The only exception is a serine to leucine substitution in position 44 that was reported to occur in the homozygous state (Lindsey et al., 2000). As already shown, the K388R mutant associates with microtubules. As a first step to investigate the functional role of all the missense mutations identified in HSP patients, their subcellular localization has been investigated. Several spastin missense mutations, found in HSP patients, have been introduced in appropriate

expression vectors, by site-directed mutagenesis (Table 4). Based on available knowledge on other members of the AAA family, missense mutations into the AAA domain are predicted to interfere either with ATP binding or hydrolysis.

When transfected in Cos7 cells, all the mutants showed a filamentous pattern, which corresponded to association with microtubules, as demonstrated after nocodazole treatment of the cells (Fig 30). Microtubule binding showed the same characteristics that were described above for the K388R mutation, i.e. formation of thick perinuclear bundles, disappearance of the aster, and, in some cases, increased resistance to nocodazole treatment. The only two exceptions were the S44L substitution, and the S362C mutation that behaved like the wild-type protein. The first mutation lies outside the AAA, while the second affects an amino acid just at the beginning of the domain.

4.6 *Wt* and mutated spastin form complexes in transfected cells

AAA proteins perform their functions in homo- or hetero-oligomeric complexes. In order to determine whether the spastin missense mutants could act as dominant-negative and interfere with expression of wild-type spastin, Cos7 cells were co-transfected with HA-spastin and respectively with spastin^{K388R}-GFP or spastin^{L426V}-GFP. Subcellular localization was analysed by immunofluorescence in double-transfected cells. In all cases of co-transfection, the wild-type and the mutant proteins always co-localize (Fig. 31). In some co-transfected cells the wild-type protein labelled microtubules (Fig. 31E). In other cases, both the mutant and wild-type spastin localized to the cytoplasmic spots (Fig. 31A, B). This different

behaviour may reflect different rates of expression of the mutants relative to the wild-type protein.

Moreover, the effect of "spastin complexes" on the microtubule network, in the double transfected cells, depends on the behaviour of the complexes. In fact, if the complexes form cytosolic aggregates, it is possible to observe a disrupted MTs network (Fig.31 G,H,I,L). Otherwise, if both proteins localise to the MTs, then the typical ATPase defective mutant phenotype is observed.

4.7 Summary

- ✓ Spastin associates dynamically with microtubules
- ✓ This association is mediated by the N-terminal region, and is regulated through the AAA domain.
- ✓ The MIT domain is not involved in microtubule binding, which is delimited to the region between amino acids 50 and 100.
- ✓ Expression of all the missense mutations suggests a role of spastin in microtubule dynamics
- ✓ Wild-type spastin promotes microtubule disassembly in transfected cells

Transfected plasmid	% GFP-positive cells with reduced microtubule staining	Cells counted/transfection	Number of transfection
pcDNA3-mycGFP	0.7 ± 1.1	100	3
Spastin-GFP	50.5 ± 3.4	100	4
SpastinK388R-GFP	2.4 ± 2.5	100	3

Table 3. Effects of overexpression of wild-type spastin on microtubule disassembly.

Spastin mutation	Subcellular localization	Sensitivity to nocodazole treatment
S44L	Cytosolic bodies	-
S362C	Cytosolic bodies	-
G370R	Filaments and cytosolic bodies	+
F381C	Filaments and cytosolic bodies	+
N386K	Filaments and few cytosolic bodies	+
N386S	Filaments and few cytosolic bodies	+
K388R	Filaments and few cytosolic bodies	+
L426V	Filaments and sporadic cytosolic bodies	+
C448Y	Filaments and few cytosolic bodies	+
R460L	Filaments and sporadic cytosolic bodies	+
R499C	Filaments and few cytosolic bodies	+
A556V	Filaments and few cytosolic bodies	+

Table 4. Subcellular localization of transiently expressed spastin missense mutations reported in HSP patients.

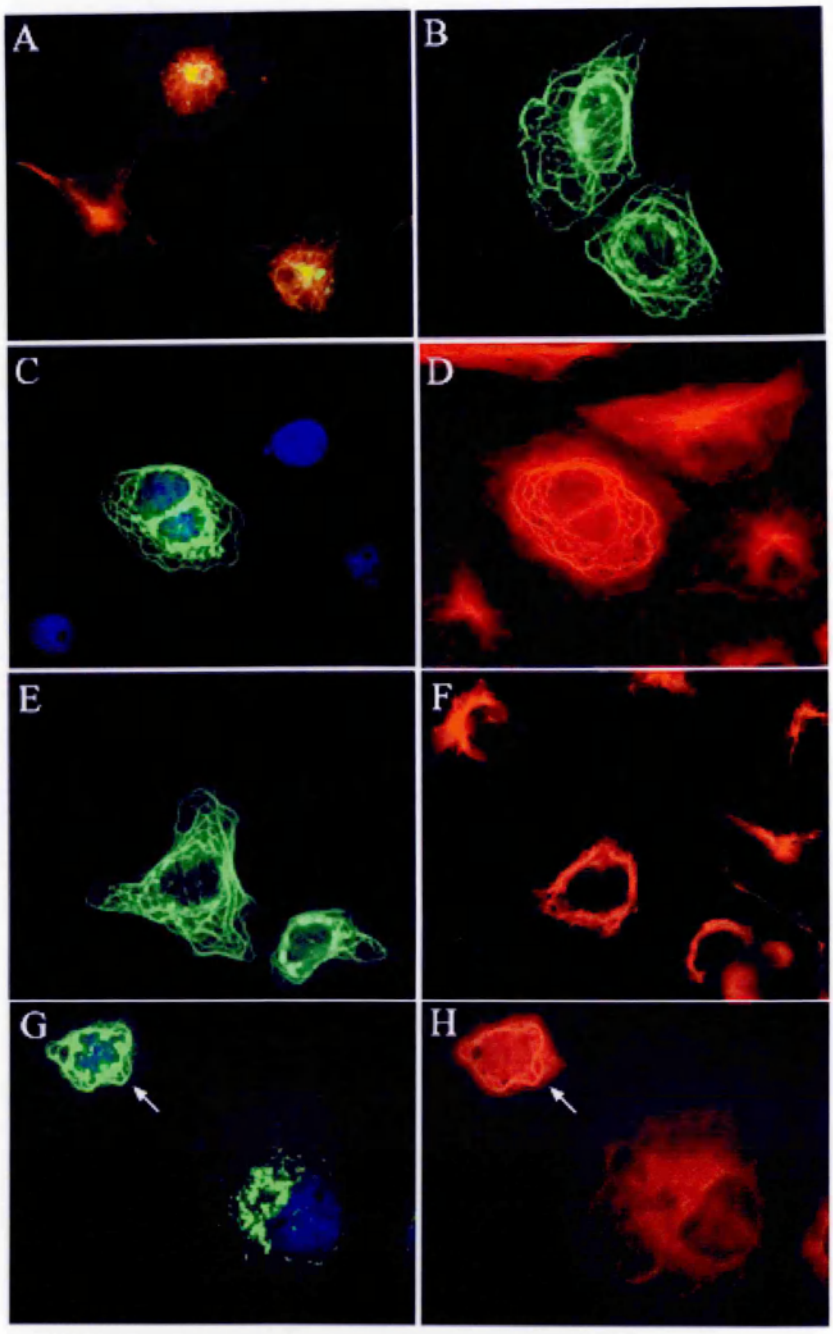

Figure 26. ATPase defective spastin localizes to microtubules.
In all cases spastin^{K388R} was expressed as GFP fusion in Cos7 cells and is visible as green signal, nuclei are stained with DAPI, blue signal; microtubules and intermediate filaments were revealed using monoclonal antibodies against α-tubulin and vimentin, respectively, red signal. Spastin^{K388R} expression begins in correspondence of the microtubule aster (A) and proceeds with the accumulation in filamentous structures (B). These filaments correspond to a subset of microtubules (C, D) and do not co-localize with vimentin (E, F). Microtubules association was confirmed by nocodazole treatment, which disrupts both the filamentous pattern of expression of spastin (G) and the microtubule network (H). In some cases, the spastin-labelled microtubule bundles were protected from nocodazole effect (arrows in G and H).

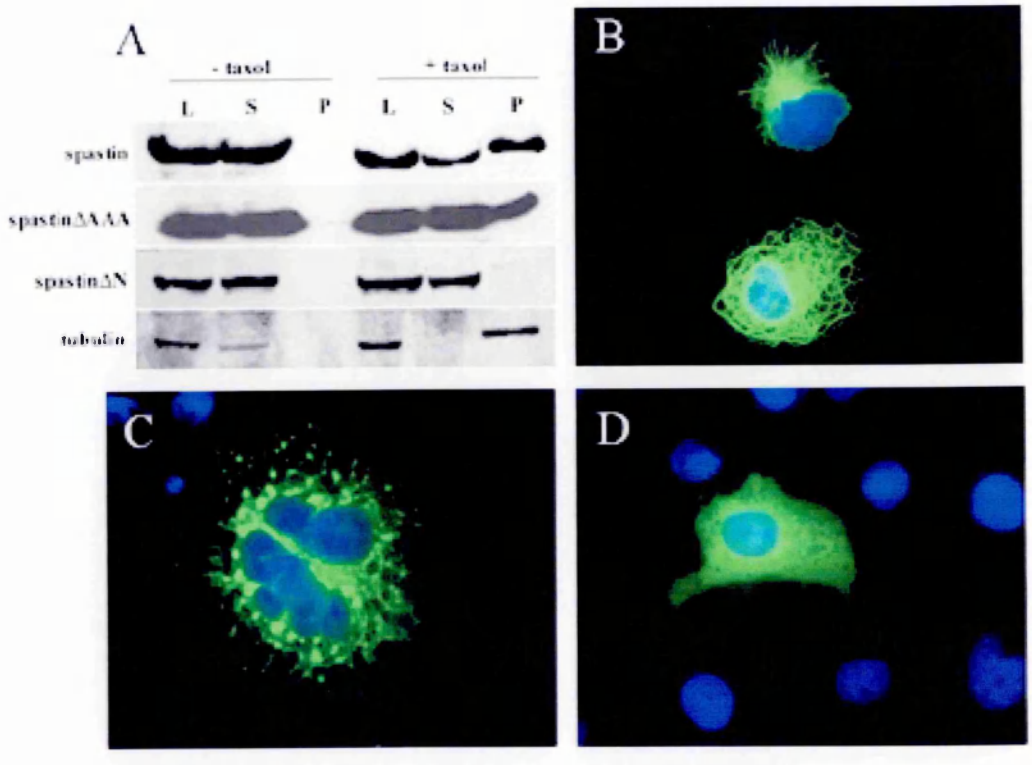

Figure 27. Spastin interacts with microtubules via its N-terminus.

(A) Microtubule binding assay. Cos-7 cells were transfected with spastin-myc, spastin$^{\Delta AAA}$ or spastin$^{\Delta N}$ constructs. Lysates (L) from transfected cells were either supplemented or not with 40 μM taxol. After sedimentation on sucrose cushion, supernatant (S) and pellet (P) fractions were assayed for spastin, spastin$^{\Delta AAA}$, spastin$^{\Delta N}$ and β-tubulin detection, using appropriate antibodies (anti-myc for spastin constructs and anti β-tubulin). When lysates are supplemented with taxol, in order to stabilize polymerized microtubules, both full-length spastin and spastin$^{\Delta AAA}$ proteins were detected in the pellet together with the polymerized microtubules, while spastin$^{\Delta N}$ remains in the supernatant. As control, when samples are not treated with taxol, all the proteins are detected in the supernatant fractions after the sedimentation. Immunofluorescence analysis of spastin$^{\Delta AAA}$ showed a filamentous pattern of expression (B), which is disrupted by nocodazole treatment (C). On the contrary, the spastin$^{\Delta N}$ construct showed a diffuse cytoplasmic localization (D), confirming that the spastin$^{\Delta N}$ construct is not able to bind microtubules both *in vivo* and *in vitro*.

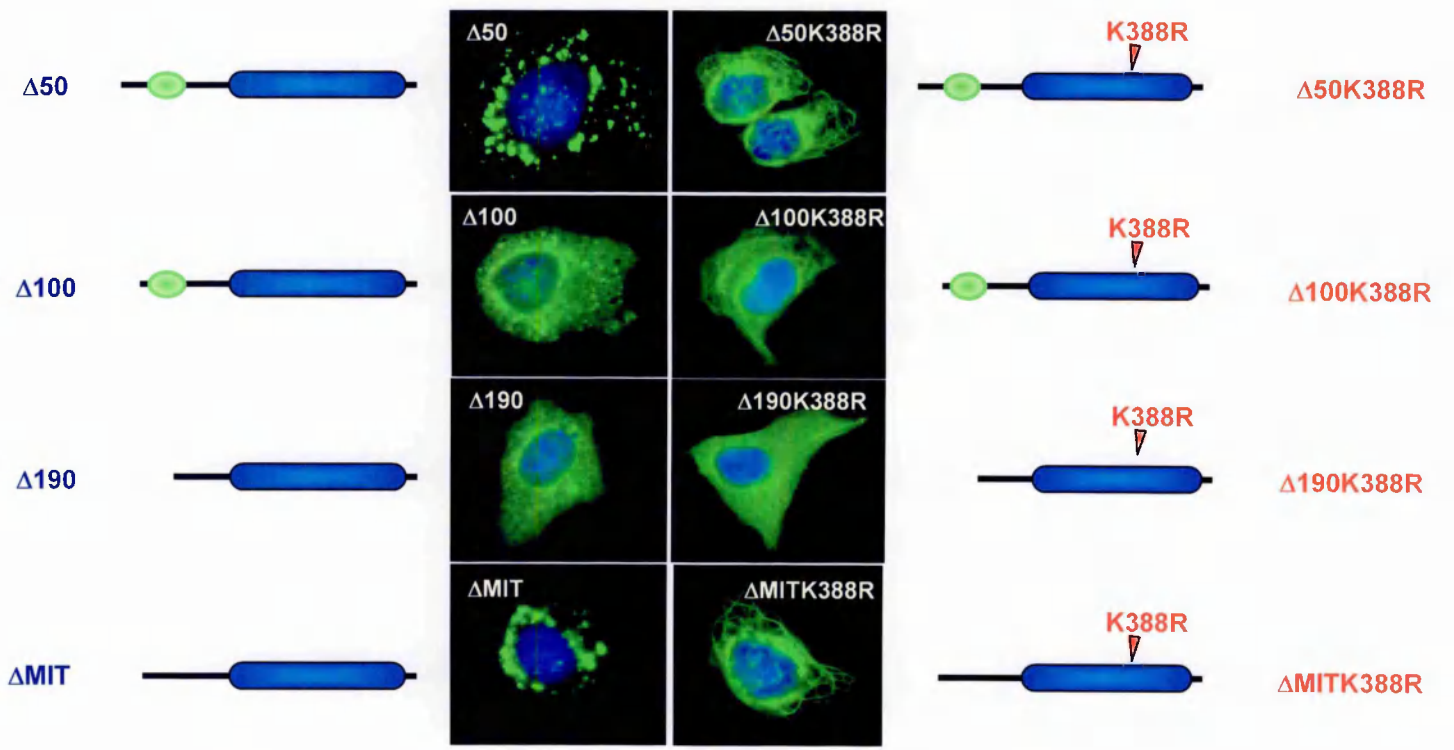

Figure 28. Spastin microtubule binding domain is between aa 50 and 100.
Several spastin deletion myc-tagged constructs (Δ50, Δ100, Δ190 and ΔMIT) have been produced both in the *wt* status and in the ATPase defective status (K388R). These constructs were transfected in Cos7 cells and immunofluorescence experiments were performed to investigate their subcellular localization. All the constructs were revealed using the anti-myc antibody (green signal) and nuclei were stained with DAPI (blue signal). Δ50 and ΔMIT had the same localization of the *wt* spastin and their ATPase defective mutants associate with microtubules. Δ100 and Δ190 had a different localization from the *wt* spastin, with a more diffuse cytoplasmic staining. Their ATPase defective mutants lost the ability to localize to filaments; therefore the region of spastin responsible for the association to microtubules was mapped between aa 50 and aa 100.

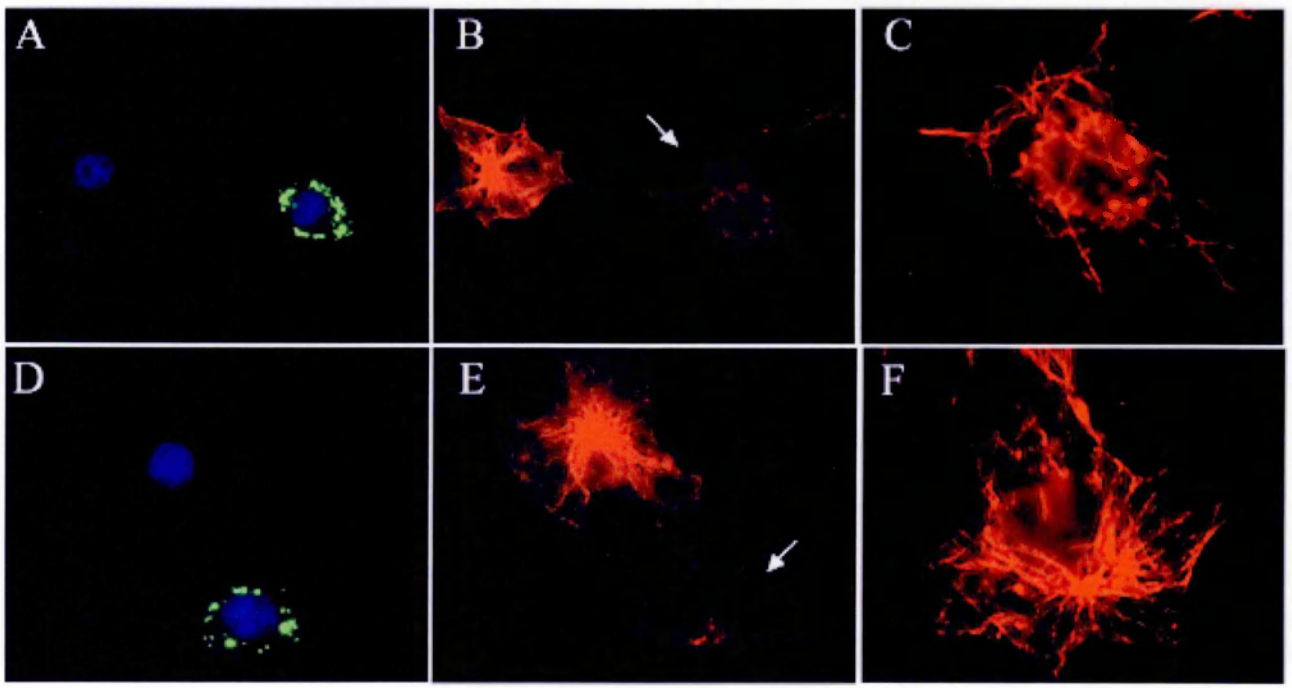

Figure 29. Overexpression of wt spastin promotes microtubules disassembly.
Spastin-mycGFP was expressed in Cos-7 cells. 24 hrs post-transfection cells were fixed and the microtubule network was analyzed in transfected cells by immunofluorescence. Spastin is revealed as green signal, microtubules were stained with the anti-α tubulin antibody, red signal; nuclei are stained with DAPI, blue signal. Cells overexpressing spastin (A, D) show a lower intensity of α–tubulin staining (B, E arrows) with respect to non-transfected cells. Moreover, overexposure of the transfected cells in B and E shows that microtubules are disassembled and appear fragmented (C, F, enlarged views).

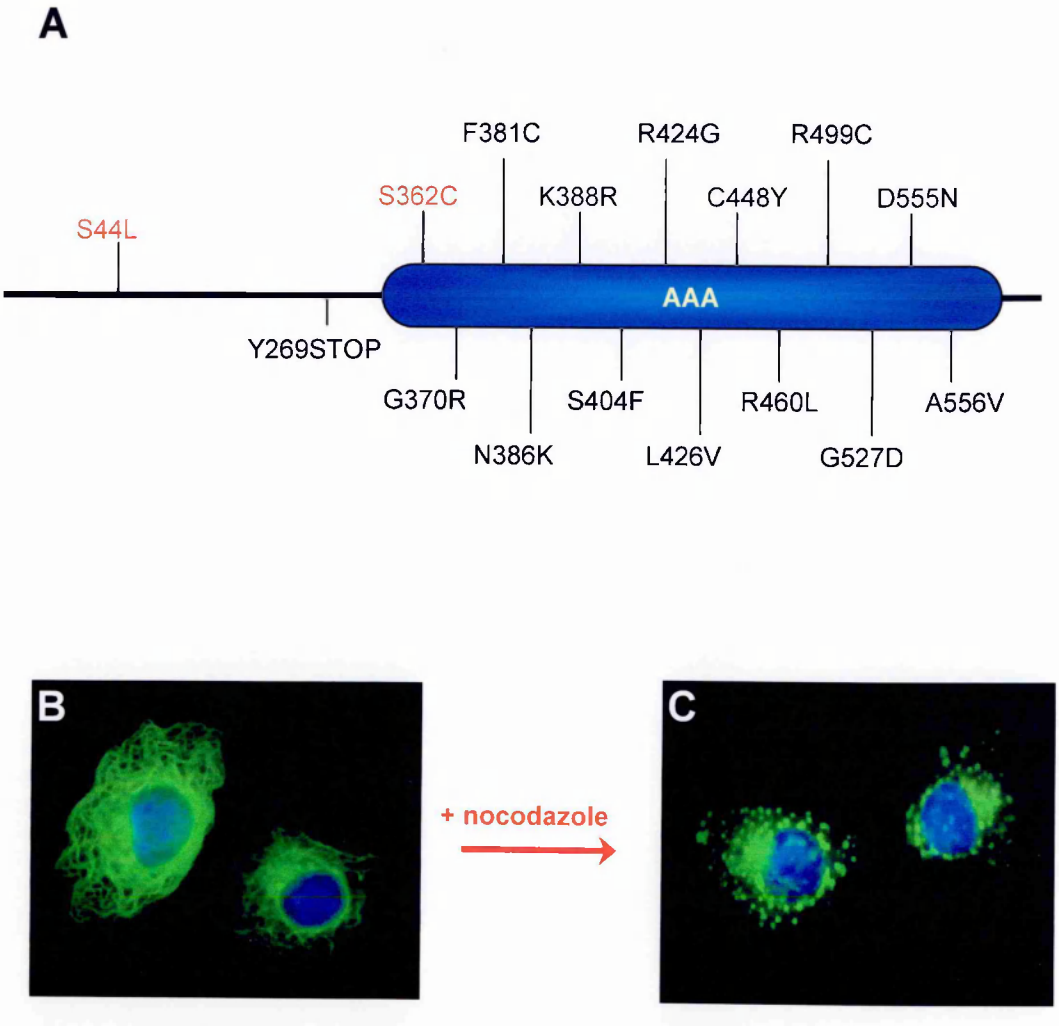

Figure 30. Almost all spastin missense mutations localize to microtubules.

All spastin missense mutations fall into the AAA cassette, with the only S44L exception (A). The subcellular localization of transiently expressed missense mutations was analyzed after transfection in Cos7 cells. All of them, with the exception of S44L and S362C, showed a filamentous pattern (B). These filaments were disrupted after nocodazole treatment (C). The S44L and S362C exhibit a subcellular localization similar to the *wt* protein (data not shown).

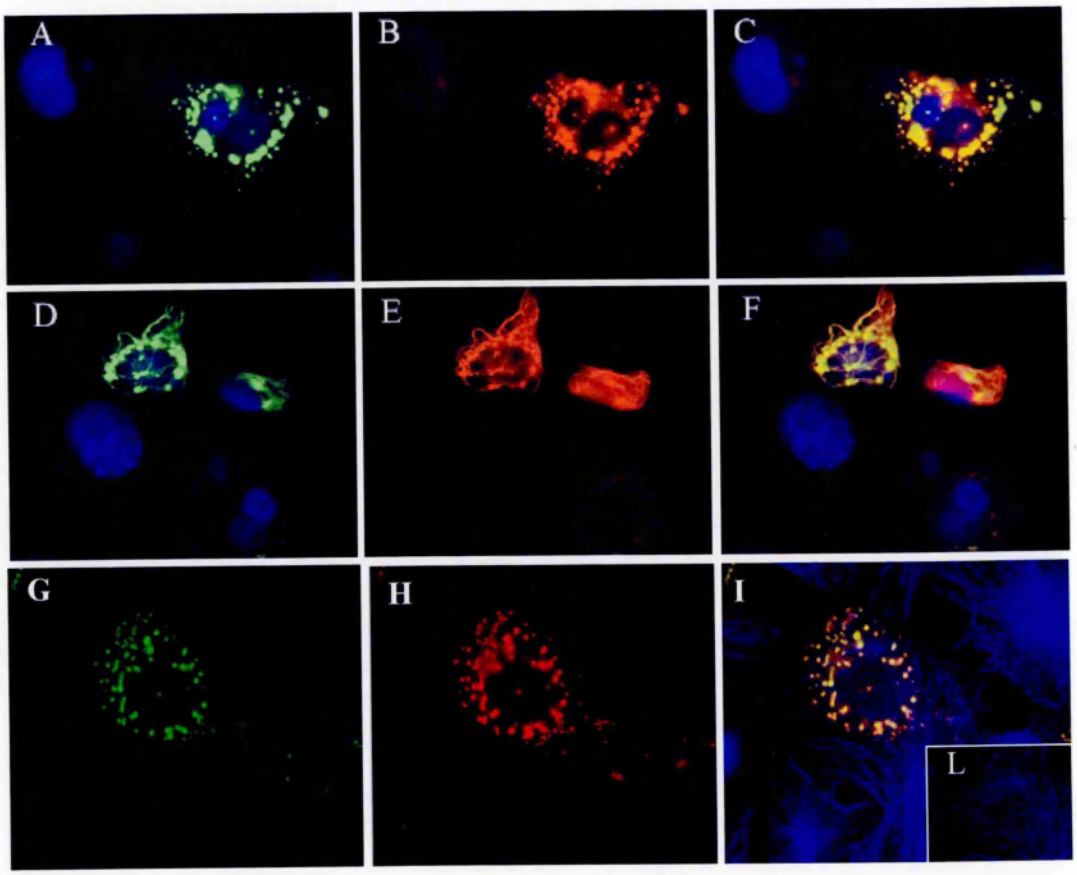

Figure 31. Wt and mutated spastin associates in transfected cells.
Either GFP-tagged spastin^{L426V} (A) or spastin^{K388R} (D, G) were co-transfected with *wt* spastin-HA in Cos7 cells. Both mutated proteins are visible as green signal; nuclei are stained with DAPI, blue signal; *wt* HA-spastin was revealed using a monoclonal anti-HA antibody, red signal (B, E, H). Co-localization is indicated by yellow signal in merged images (C, F, I). In some co-transfected cells, both mutant and *wt* spastin localize to the cytoplasmic spots (A-C, G-I). In other cases the *wt* spastin localizes to the filaments generated from the ATPase defective spastin mutant (D-F). We observed the microtubule network when both mutant and *wt* spastin localized to the cytoplasmic spots (G-L) using the anti α-tubulin marker. In this case, the microtubules appeared disassembled. α-tubulin marker was revealed with a mouse secondary antibody AMCA conjugated; HA-spastin was revealed using a polyclonal anti-HA and a rabbit secondary antibody TRITC-conjugated.

CHAPTER 5: Two Hybrid system and spastin interactors

5.1 Searching for spastin interactors: The Interaction Trap

The basis of the two hybrid system relies on the structure of some transcription factors that have two distinct functional domains: a DNA binding domain and a transcription activation domain. The DNA binding domain functions to target the transcription factor to specific promoter sequence, while the activation domain facilitates the assembly of the transcription complex allowing the initiation of the transcription. A functional transcription factor can be assembled through non-covalent interaction of two independent hybrid proteins carrying either a DNA binding domain or a transcription activation domain (Fields and Song, 1989). When those proteins are interacting, they bring a transcriptional activation domain into close proximity with a DNA binding site that regulates expression of an adjacent reporter gene (Fields and Sternglanz, 1994).

The interaction trap is a two hybrid system for identifying cDNAs encoding proteins that interact with a protein whose coding sequence is known. It can also be used to study interaction between known proteins. The interaction trap consists of three critical components. First, it uses a vector expressing a protein of interest fused to the DNA binding domain of the LexA, and this is referred as the bait of the system. Secondly it uses a yeast strain with two reporter genes: LEU reporter (which is integrated in the yeast chromosome and is downstream to the lexA operator) and the LacZ reporter (which is transformed into the yeast strain and provides a second assay for testing the interactions). Thirdly, it uses a library plasmid that directs the

conditional expression of cDNA-encoded proteins fused at their N-terminus to a moiety containing three domains: a nuclear localisation signal, a transcription activation domain and an epitope tag. The activation domain used in this system is B42, which is derived from bacteria and it is weaker than the activation domains of Gal4 or VP16.

The bait protein cloned into the pAR202 vector is constitutively expressed, it binds to the LexA operators upstream of the reporter genes, but it does not activate transcription by itself. The activation-tagged cDNAs (from the cDNAs library into the pJG4-5 vector) are conditionally expressed from the GAL1 promoter, so they are induced by galactose and repressed by glucose.

So, in glucose medium (Fig.32 A) the GAL1 promoter is repressed, the activation-tagged cDNA encoded protein is not expressed, and the yeast does not grow on a medium lacking leucine. In a galactose medium (Fig. 32 B,C), activation tagged cDNA encoded proteins are expressed. Those that interact with the bait will activate transcription of the two reporter genes, and the yeast will grow on medium lacking leucine (Leu^-) and will form blue colonies on galactose (Gal) Xgal plates. Other proteins from the library that do not interact with the bait, will not activate the transcription of the reporter genes, so the yeast will not grow on Leu^- and will form white colonies on Gal-Xgal plates.

To get clues on possible biological function of spastin, we used the interaction trap technique to search for molecular partners by screening a human fetal brain (HFB) library. Three different "bait" constructs have been prepared with different portions of spastin: the full length spastin cDNA, the N-terminal region of the protein ($spastin^{\Delta\text{-}AAA}$) and the C-terminal portion of the protein ($spastin^{\Delta\text{-}N}$). These constructs

were transformed in the yeast strain EGY48, together with the lacZ reporter (SH18.34), and tested for the transactivation of the system (see methods). The construct pAR202-LexA-spastin$^{\Delta\text{-}AAA}$ was discarded because it was transactivating the system by itself. In contrast, yeasts transformed with the other two constructs, pAR202-LexA-spastin and pAR202-LexA-spastin$^{\Delta\text{-}N}$, were processed to determine if the "bait proteins" were expressed in yeast cells. Western blot analysis, using an anti-LexA antibody, on lysates from yeast transformed either with the empty pAR202 vector or with the bait construct (pAR202-LexA-spastin and pAR202-LexA-spastin$^{\Delta\text{-}N}$), showed that the expected fusion proteins (respectively 88 kDa and 60 kDa) were produced (Fig 33).

5.1.1 Screening of HFB library with pAR202-LexA-spastin and pAR202-LexA-spastinΔ-N

When the full length spastin was used as bait for the two hybrid screening, 310 positive clones were obtained (out of 400 screened). All those clones were identical and corresponded to an ORF of 900bp. The DNA sequences of the clones were blasted against the non-redundant database and all of them identified a unique transcript, Na14 (NM 003731). The HFB library was also screened using as bait the construct lacking the N-terminal region of spastin (pAR202-LexA-spastin$^{\Delta\text{-}N}$). 20 positive clones, out of 200 screened, were isolated. The DNA of the positive clones were extracted by the yeast, subjected to sequence analysis and used in interaction mating assay to test the interaction with spastin. The DNA sequences of the clones were blasted against the non-redundant database and permitted to identify 9 independent transcripts (table 5).

Clones 6, 17, 36, 47, 80, 81, 111, 161 correspond to the Bromodomain containing protein 7 (NM 013263). These clones are different in the 5' region, in particular clones 6, 17, 36, 47, 80, 111 start at amino acid 276, clone 81 start at amino acid 453 and clone 161 start at amino acid 394, all the clones include the TGA stop codon. Analysis of the clones 93, 125, 150 identified the SUMO-1 cDNA (NM 003352); the clones were all identical and contained the full-length cDNA.

The third group of clones identified 34, 133 correspond to the cDNA sequence of Daxx (NM 001350). They are identical clones, start at amino acid 484 of Daxx protein and include the TGA of the gene.

The other two independent putative interactors were clone 97 and 176, corresponding respectively to the bromodomain PhD finger transcription (XM 166450) factor and to the sumo activating enzyme subunit 2 (NM 004634) (they both represent uncompleted cDNA).

5.1.2 Putative interactors were reconfirmed in yeast by interaction mating assay

The interaction mating assay takes advantage of the fact that haploid cells of the opposite mating type will fuse to form diploids when brought into contact with each other (Finley and Brent, 1994). This mating approach is complementary to the library screening procedure described above; it permits to test interaction between known proteins and is also a mean to confirm the data obtained from the interaction trap. Interaction mating assay was set up to confirm the interactors obtained by the screening of the HFB library with the two different spastin baits. All the confirmed clones are shown in figure 34. This assay was also used to test the interaction

between the clones identified and the bait not used for that screening. We showed that Na14 does not interact with the spastin$^{\Delta-N}$ construct. Furthermore, all the positive clones obtained from the screening with spastin$^{\Delta-N}$ truncated construct did not interact with the full length spastin bait (Figure 34)

5.2 Na14: spastin anchor to the centrosome and MT

Na14 is a small coiled coil protein that was first identified as a nuclear autoantigen from patients with an autoimmune disease, the Sjogren syndrome (Ramos-Morales et al., 1998). Immunofluorescence using the serum from patients with Sjogren syndrome showed a punctuate nuclear localisation, but recently a centrosomal localisation of this protein has been demonstrated (Pfannenschmid et al., 2003), and the protein was identified as a centrosome component by a proteomic approach (Andersen et al., 2003).

The region of spastin that is responsible for the interaction with Na14 was determined by using several deletion mutants of spastin in the interaction mating assay. The deletion mutants Δ50, Δ100,Δ190, ΔN were prepared in the pAR202 vector. Both the full length spastin and the deletion mutants were transformed in the yeast strain EGY42 together with the lacZ reporter. The Na14 cDNA, in the pJ4-5 vector, was transformed in the yeast strain EGY48. The yeasts are streaked on selective plates. The two strains are mated by applying them to the same replica velvet (one perpendicular to the other), replicated to an YPD plate and incubated at 30°C for 1-2 days. At the intersection of the YPD plate the diploids are formed. This plate is then replicated on the four selective plates for testing the activation of the

two reporter genes. Na14 is interacting with the full length spastin and with the □50 construct as assessed by the growth of the diploid yeast cells on the LEU selective plate and by the positivity of the LacZ-Xgal reaction on the Xgal plates (blue colonies), but this interaction is lost with the deletion mutants Δ100, Δ190 and ΔN (Figure 35 A). Therefore, the region of spastin able to bind Na14 is located between aa 50 and 100. This region was also defined as the minimal microtubule interaction region, so Na14, being a centrosomal protein, could represent the anchor for spastin microtubule binding.

The cDNA obtained from the library screening was incomplete, lacking the first 99bp (33 aa) at the 5' of the gene. To confirm that Na14 is a spastin interactor, the full length cDNA was obtained by RT-PCR using a HeLa cDNA as template and cloned both in the pGEX-3X vector and in the $pcDNA_3$ vector. pGEX-Na14 was used for the production of a GST-Na14 recombinant protein that was used for a pull down assay from whole cell lysates. Extracts from different cell lines (HeLa, NSC34, and a neuroblastoma cell line SKNBE) were prepared and the agarose-GSTNa14 beads were used for the pull down of the endogenous spastin from those lysates. Agarose-GST beads were used as control. The proteins bound to the GST or to the GST-Na14 beads were fractionated on an 8% SDS/PAGE, transferred to a PVDF membrane and analysed with a specific spastin polyclonal antibody SP-R74. The presence of a band of the expected size in the lane corresponding to the GST-Na14 pull down (Fig 35 B), which was absent in the pull down with GST alone, in all three cell lines is another evidence of the spastin-Na14 interaction.

5.3 Spastin is SUMO-1 conjugated in yeast

SUMO-1 is a small protein with high structural homology to Ubiquitin (Bayer et al., 1998), which modify target substrates via formation of a covalent isopeptide bond. The covalent modification of target proteins by SUMO-1 is very similar to that of ubiquitin, three kind of enzymatic activity are involved in this system: a SUMO-1 activating enzyme, SAE, which consists of two subunits, respectively SAE1 and SAE2; a SUMO-1 conjugating enzyme, UBC9; and a SUMO-1 ligase (Desterro et al., 1999; Desterro et al., 1997; Hochstrasser, 2001).

The two hybrid screening of a human fetal brain library, using as bait Spastin$^{\Delta N}$, permitted to isolate the sumo activating enzyme (subunit2, SAE2) and SUMO-1 as putative interactors of spastin. SAE2 is a component of the enzymatic machinery, which catalyses the addition of a molecule of SUMO-1 to a target protein. Since spastin seems to interact both with SAE2 and SUMO-1, interaction-mating experiments were performed to assess if spastin was able to associate also with the other component of the sumo machinery: UBC9. pAR202-LexA-spastin and pAR202-LexA-spastin$^{\Delta\text{-}N}$ were introduced into the EGY48 yeast strain, while pJ4-5 UBC9 and the lacZ reporter SH18.34 were introduced into the EGY42 yeast strain. The yeasts are streaked on selective plates. The two strains are mated, replicated to an YPD plate and incubated at 30°C for 1-2 days. At the intersection of the YPD plate the diploids are formed. This plate is then replicated on the four selective plates for testing the activation of the two reporter genes. Confirming the previous results, the full length spastin is not able to bind UBC9, instead the Spastin$^{\Delta N}$, which interact with SAE2 and SUMO-1, is also able to interact with UBC9.

Since spastin seems to be SUMO1 modified in the yeast two hybrid system, spastin amino acidic sequence was examined in order to determine the presence of possible sites for SUMO1 conjugation. SUMO-1 (small ubiquitin-related modifier) is a member of the ubiquitin and ubiquitin-like superfamily. Most SUMO-modified proteins contain the tetrapeptide motif Ψ-K-x-D/E where Ψ is a hydrophobic residue, K is the lysine conjugated to SUMO, x is any amino acid, D or E is an acidic residue. SUMOplot™ program (http://www.abgent.com/sumoplot.html) predicts the probability for the SUMO consensus sequence to be engaged in SUMO attachment. Analysis of the spastin primary structure indicates that four different lysine residues (Lys 279, Lys 340, Lys 462, Lys 565) (Fig. 36) conform to the consensus sequence (-ψKxD/E-) for this modification; all of them are in the C-terminal portion of the protein (the portion retained in the Spastin$^{\Delta N}$ construct). Lys 565 is conserved in human and mouse, but not in Drosophila spastin sequence. Lys340 and Lys462 appear to be conserved also in Drosophila and are therefore strong candidates to be targets of the SUMO1 modification. Lys 279 is not conserved in the mouse and Drosophila spastin sequences and therefore was not taken in account. We have therefore investigated which of these lysines K340, K462 and K565 may represent the target for SUMO-1 conjugation in the human spastin.

We have generated pAR202-LexA-spastin$^{\Delta N}$ carrying the mutations K340R, K462R, K565R and also the double mutant K462/K565R. These constructs were used in interaction mating experiments to determine if one of the mutations could abrogate the interaction with SUMO1 and other components of the SUMO machinery, or if any of the interactions found using the pAR202-LexA-spastin$^{\Delta N}$ construct was dependent on one of these residues. Spastin$^{\Delta NK340R}$ and spastin$^{\Delta NK462/565R}$ proteins are

not expressed in yeast (data not shown) and could not be used in our studies. Spastin$^{\Delta N}$, spastin$^{\Delta NK462R}$ and spastin$^{\Delta NK565R}$ interact with SUMO1, SAE2, UBC9 as revealed by the LacZ reporter in figure 37 A. Furthermore spastin$^{\Delta N}$, spastin$^{\Delta NK462R}$ and spastin$^{\Delta NK565R}$ interact with daxx and brd7 (Fig. 37 A). The interaction of spastin$^{\Delta NK462R}$ with SUMO1, SAE2, UBC9, daxx and brd7 is weaker, in terms of the colorimetric reaction, respect to spastin$^{\Delta N}$ and spastin$^{\Delta NK565R}$. When we checked that the fusion proteins relatives to the constructs we used in the interaction mating assay were made properly, we saw that the levels of expression of the LexA-spastin$^{\Delta NK462R}$ were lower respect to the other constructs (Fig. 37B). Therefore the weaker colorimetric reaction is probably due to a low level of the protein available for the interaction.

5.3.1 Spastin is SUMO-1 modified *in vitro*

To investigate if spastin is a new substrate for SUMO-1, we performed in collaboration with R.T. Hay and E. Jaffray (University of St. Andrews) an "*in vitro*" system for SUMO-1 modification (Desterro et al., 1998). ^{35}S-labelled *in vitro* translated Spastin was incubated with a source of SUMO-1 activating enzyme (SAE1/2) (Desterro et al., 1999) and SUMO-1 conjugating enzyme (Ubch9)(Desterro et al., 1997) in the presence of SUMO-1 and ATP. Under these conditions ^{35}S-labelled Spastin was converted to a more slowly migrating form that is consistent with SUMO-1 modification. To confirm that this species was indeed a SUMO-1 modified product, GST-SUMO-1 was substituted for SUMO-1 in the reaction, resulting in the detection of a modified species with altered electrophoretic mobility

(Fig. 38A). SUMO-1 modification was abolished if SUMO-1, SAE, Ubch9 or ATP was omitted from the reaction (Fig. 38B). Both constructs are mono-SUMO-1 modified. Constructs carrying the mutations K340R, K462R, K565R, K462/565R, K340/462/565R were tested in the in vitro conjugation assay. None of the mutations (single or multiple) resulted in the abrogation of the SUMO-1 conjugation (Fig. 39). The fact that mutating the putative target lysines there is no abrogation of SUMO-1 conjugation could suggest that when the target lysine is mutated, other lysine become reactive in the conjugation reaction.

5.3.2 Spastin is SUMO-1 modified *in vivo*

To test the hypothesis that spastin is a substrate for SUMO-1 modification in vivo, HeLa cells were transfected with a vector expressing a 6His tagged SUMO-1 protein and full length spastin-myc or spastin$^{\Delta N}$-myc. Cells were collected 48 hrs post transfection, lysed in 6M guanidine-HCl and the extracts were subjected to affinity purification with nickel-charged agarose beads to recover proteins covalently attached to 6His-SUMO1. Materials bound to the beads were then separated by SDS-PAGE and analysed by Western blotting with the anti-myc antibody (Fig. 40A). Unfortunately, both full length spastin-myc and spastin$^{\Delta N}$-myc bind not specifically to nickel beads also when 6His-SUMO1 has not been co-transfected in cells. Since spastin seems to bind non-specifically to the nickel beads, this system cannot be used to investigate whether spastin is SUMO1 modified also *in vivo*.

Since spastin localize to the PML bodies in human fibroblasts, we have performed immunofluorescence experiments to determine if spastin colocalizes with SUMO-1 in these structures. Human fibroblasts were transfected with a HA-SUMO-

1 construct. Double immunofluorescence experiments, using the anti-HA antibody to stain SUMO-1 and the spastin specific antibody SP-R74, revealed that spastin colocalize with SUMO-1 in those nuclear punctuate structures (Fig. 40B). This result does not imply a direct interaction between SUMO-1 and spastin, which could be mediated by a component of the PML bodies.

5.4 Brd7

Brd7 is a bromodomain containing protein. The bromodomain is a conserved sequence of approximately 110 amino acids (Jeanmougin et al., 1997). Brd7 function is not clear, although many of the bromodomain proteins seem to be involved in transcriptional regulation (Cuppen et al., 1999). To demonstrate that the interaction between spastin and brd7 occurs also in a mammalian environment, immunoprecipitation analysis of the two proteins from mammalian cell lysates was carried out.

We used the full length Brd7 cDNA cloned into the $pCDNA_3$-FLAG expression vector (from Dr. Julia Kzhyshkowska), which allows expression of Brd7 with an N-terminal FLAG epitope tag. Since spastin mis-localizes when overexpressed, we used the SP-51 antibody to work with the endogenous protein.

HeLa cells were transiently transfected with the Brd7-FLAG construct, and 48 hours post-transfection, cell lysates were prepared, quantified and pre-cleared by incubation with protein A. Immunoprecipitation was carried out using the anti-FLAG antibody, the SP-51 and an unrelated antibody (HA) as control. As negative control, untransfected HeLa cell extracts were subjected to the same experimental procedure

(see Material and methods). Following washing to remove non-specifically bound proteins, immunoprecipitated complexes were eluted in the disruption buffer and fractionated on a 7.5% SDS/PAGE. Western blot analysis of eluted proteins using the anti-Flag antibody (Fig. 41) resulted in the detection of the 85 kDa band corresponding to the Brd7-flag protein in the transfected lysates and also in the immunoprecipitate using the flag, SP-51 an HA antibodies. This band was not detected in any of the untransfected samples. In addition, western blot analysis with the SP-51 antibody showed the presence of the band corresponding to the endogenous spastin exclusively in the SP-51 immunoprecipitation samples. Unfortunately, these results indicate that the Brd7 protein is sticky to the protein A resin and it is in fact immunoprecipitated also by an unrelated antibody. Further experiments, changing the experimental conditions (such as different washing conditions), will be needed to confirm this interaction.

5.5 Daxx

Daxx has been implicated in several processes, but its exact role has to be still elucidated. Many reports have implicated Daxx in apoptosis, but whether it functions as a pro- or anti- apoptotic molecule has not yet been clarified (Michaelson, 2000).

Daxx was identified as a putative spastin interactor with the two hybrid technique. To confirm that this interaction occurs also in mammalian cells, immunoprecipitation analysis of the two proteins from mammalian cell lysates was performed.

The full length Daxx cDNA was cloned into the pMT21-myc expression vector, which allows expression of Daxx with a C-terminal MYC epitope tag. We want to demonstrate the interaction between the exogenous Daxx-myc and the endogenous spastin, using respectively an anti-myc antibody and the SP-51 anti-spastin antibody.

HeLa cells were transiently transfected with the Daxx-myc construct, and 48 hours post-transfection, cell lysates were prepared, quantified and pre-cleared by incubation with protein A. Immunoprecipitation was carried out using the anti-myc antibody, the SP-51 and, as control, the pre-immune serum from the rabbits that were injected with the SP-51 antigen for the antibody production. Untransfected HeLa cell extracts were subjected to the same experimental procedure (see Material and methods). Immunoprecipitated complexes were eluted in the disruption buffer and fractionated on a 7.5% SDS/PAGE. Western blot analysis using the anti-myc antibody resulted in the detection of the 95 KDa band corresponding to the Daxx-myc protein in the transfected lysates (Fig. 42, lane 5). Daxx was immunoprecipitated by the anti-myc antibody as expected (Fig. 42, lane 6) and it was also possible to detect a fainter band in the immunoprecipitate with the SP-51 antibody (Fig. 41, lane 7). This band was not detected either in the untransfected samples (Fig. 42, lane 1-4) or in the immunoprecipitate with the pre-immune serum (Fig. 42, lane 8). Furthermore, the SP-51 antibody detected the presence of the band corresponding to the endogenous spastin in the samples immunoprecipitated both with the SP-51 (Fig. 42, lane 7) and the myc (Fig. 42, lane 6) antibodies. Spastin band was not detected in none of the controls (Fig. 42, lane 1-4, 8). This result confirmed the physical interaction between spastin and daxx.

Interestingly, in the co-immunoprecipitation experiments of spastin and daxx, we have noticed that the levels of the endogenous spastin were different between untransfected and transfected cells. The endogenous spastin was never detected in the 50 µg of total lysates of untransfected cells. However spastin was clearly detected when 25 µg of the Daxx-myc transfected lysates were loaded on the SDS/PAGE and analysed by immunoblot. This striking increase in the amount of the band corresponding to the full length spastin was also noticed in the immunoprecipitated samples (Fig. 42). Moreover, a slower migrating band, which is immunoprecipitated both by the SP-51 and by the myc antibodies, was detected at higher levels (see arrow). A hypothesis could be that the slow migrating form is the SUMO-1 modified spastin.

5.5.1 The level of spastin transcript are increased upon Daxx overexpression

To investigate if the increased level of spastin in HeLa cells transiently transfected with Daxx was due to an increase in the level of spastin transcription or to a stabilization of spastin protein, we perform real-time reverse transcriptase PCR on untransfected HeLa cells, cells transfected with Daxx-myc and cells transfected with a n other construct which did not show the same effect (Na14-ha).

The real-time PCR system is based on the detection and quantification of a fluorescent reporter. This signal increases in direct proportion to the amount of PCR product in a reaction. By recording the amount of fluorescence emission at each cycle, it is possible to monitor the PCR reaction during the exponential phase where the first significant increase in the amount of PCR product correlates to the initial amount of template. The SYBR^{TM} Green dye was utilized for fluorescent detection of

cDNA. SYBR Green is a non-sequence specific fluorescent DNA intercalating agent and it binds exclusively to double-strand DNA. We used an endogenous gene as normalizer, GAPDH (Glyceraldehyde-3-phosphate dehydrogenase), which is more abundant and remains constant, in proportion to total mRNA, among the samples.

We extracted the total RNA from HeLa cells untransfected or transfected with Daxx-myc or with Na14 (as control) and we performed real-time quantitative PCR measurements on total RNA. For each sample, three distinct amplifications were carried out, in parallel, to amplify spastin, β-actin and GAPDH mRNA as a reference gene. β-actin was used as control to ensure that Daxx-myc overexpression was not affecting the transcriptional level of every gene.

We demonstrate that spastin transcription levels are higher in cells overexpressing Daxx of 3.5-4.6 fold respect to the untransfected cells or to the cells transfected with an unrelated protein (Fig. 43). The fold of increase is probably related to how efficient is the transfection of Daxx and therefore on how much Daxx we are expressing. As control, the levels of β-actin are constant in the different samples.

5.6 Summary

- ✓ Spastin interacts with Na14, a small coiled-coil centrosomal protein, and this interaction is mediated by the N-terminal portion of spastin (aa 50 and 100)
- ✓ Na14 and Microtubules share the same region of interaction on spastin, therefore Na14 could represent the anchor for spastin to the microtubules
- ✓ Spastin is sumoylated *in vitro*
- ✓ Spastin interacts specifically with Daxx via its C-terminal portion
- ✓ Daxx overexpression in HeLa cells cause an increase in the level of transcription of spastin gene

Positive clones	Interaction mating (+ confirmed interaction)	gene
6	+	Brd7
17	+	Brd7
36	+	Brd7
47	+	Brd7
80	+	Brd7
81	+	Brd7
111	+	Brd7
161	+	Brd7
93	+	SUMO-1
125	+	SUMO-1
150	+	SUMO-1
34	+	Daxx
133	+	Daxx
12	-	HDAC-1
29	-	HDAC-1
97	+	Bromodomain PhD finger transcription factor
140	-	S100 calcium binding protein
151	-	Site specific recombinase FLP yeast
176	+	Sumo-1 activating enzyme (subunit 2)
184	-	Thioredoxin related protein

Table 5. Positive clones from the two hybrid screening of HFB library with pAR202-LexA-spastin□N. The positive clones have been subjected to sequence analysis and retested by interaction mating.

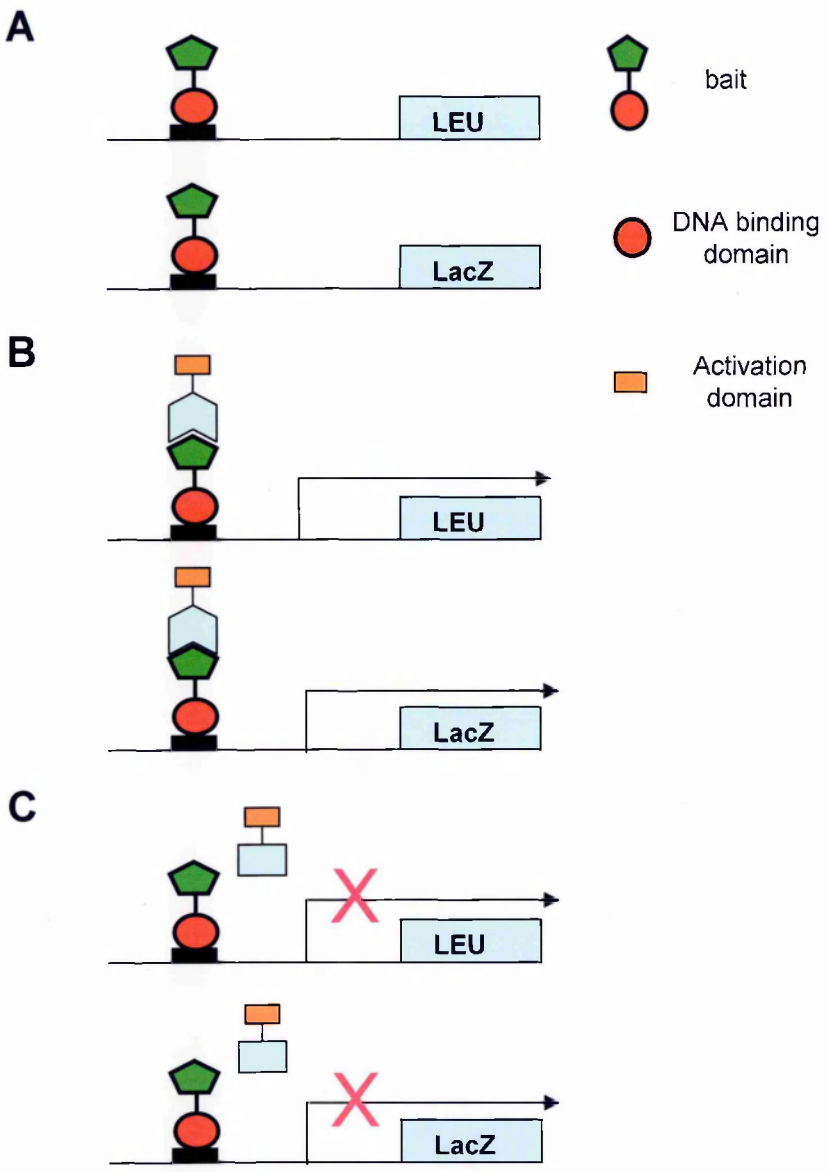

Figure 32. The interaction trap.

(A) Glucose medium. The LexA fusion protein (bait) is made and binds to LexA operators (black box) upstream of the two reporter genes, LEU and LacZ. The bait does not activate the transcription of the reporters because it lacks an activation domain. The activation domain-tagged cDNAs are not expressed because the GAL1 promoter is repressed in presence of glucose. Yeast cells do not grow in medium lacking leucine and forms white colonies on an X-Gal plate. (B) Galactose medium: interaction. Galactose induces expression of the activated tagged cDNA library. A protein encoded from the library interacts with the bait; the activation domain activates the transcription of LEU and LacZ. Yeast cells will grow on a medium lacking leucine and form blue colonies on an X-gal plate. (C) Galactose medium: no interaction. Galactose induces the expression of the proteins encoded from the activation-tagged cDNA library. A protein encoded from the library does not interact with the bait; the activation domain cannot activate the transcription of LEU and LacZ. Yeast cells will not grow on a medium lacking leucine and form white colonies on an X-gal plate.

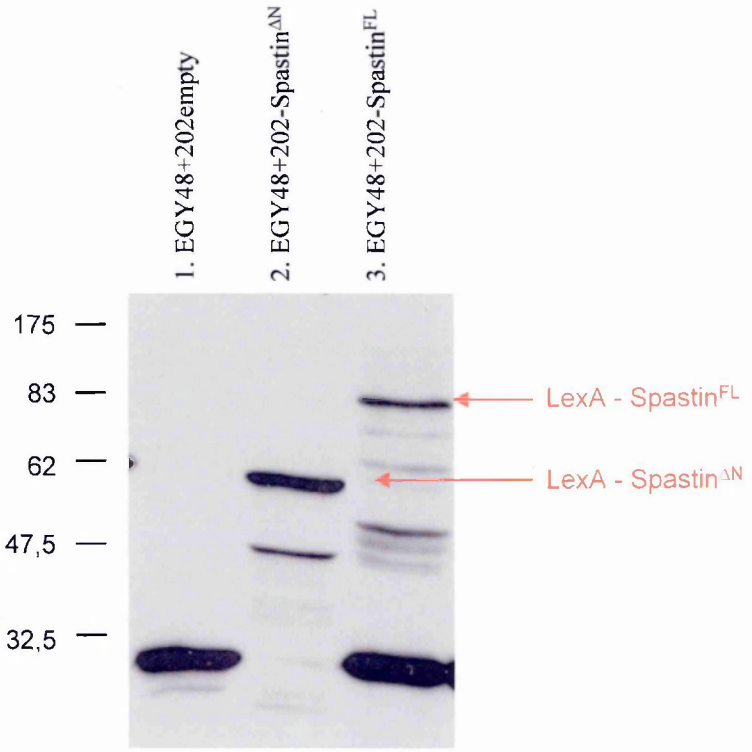

Figure 33. Expression of the LexA fusion proteins.

pAR202-Spastin^{FL} and pAR202-Spastin$^{\Delta N}$ were transformed in EGY48 yeast strain and yeast cells were lysed to check that a fusion protein was made. As control, yeasts transformed with the empty pAR202 vector have been used. Cell extracts were prepared from over night culture and samples were fractionated on a 10% SDS/PAGE. Immunoblot analysis was performed with the monoclonal anti-LexA antibody. The constructs, pAR202-Spastin^{FL} and pAR202-Spastin$^{\Delta N}$, express fusion proteins of the expected size as indicated by the arrows.

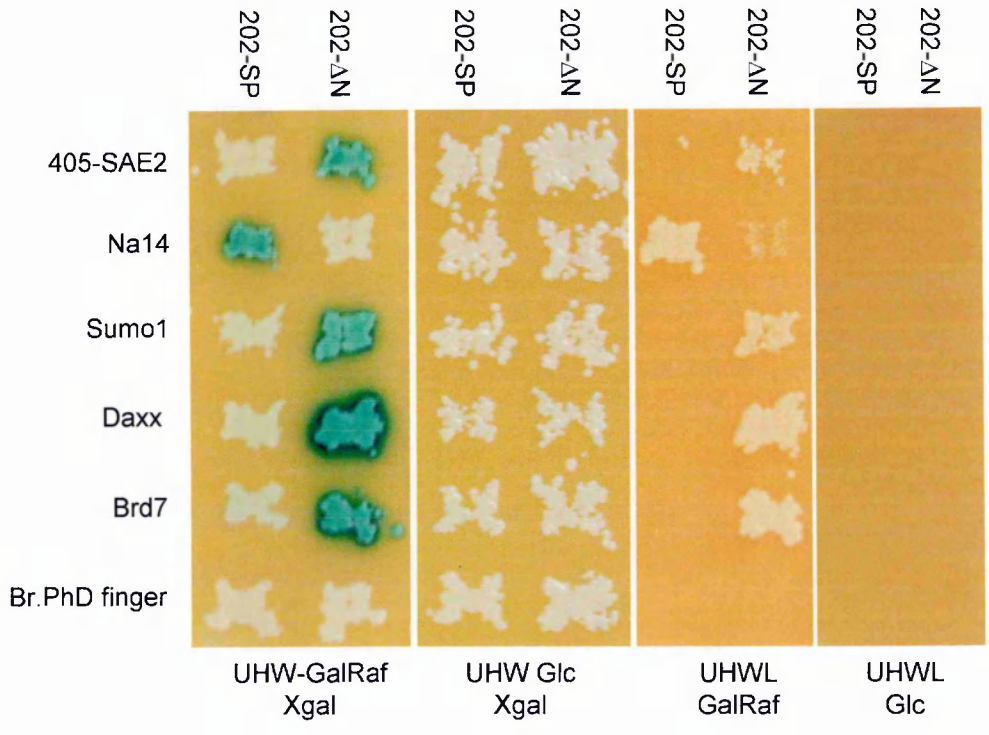

Figure 34. Interaction mating assay to confirm spastin putative interactors.

The pAR-202 constructs (pAR202-Spastin^{FL} and pAR202-Spastin$^{\Delta N}$) and the LacZ reporter (SH18.34) were transformed in the yeast strain EGY42 (mate type a). The clones identified with the interaction trap are in the pJ4-5 vector and were transformed into the EGY48 yeast strain (mate type α). The yeasts were streaked on selective plates. The two strains are mated on an YPD (rich medium) plate and incubated at 30°C for 1-2 days. At the intersection of the YPD plate the diploids are formed. This plate is then replicated on the four selective plates for testing the activation of the two reporter genes. Each bait has been crossed with the putative interacting clones identified in both screenings. Na14 interacts exclusively with the spastin^{FL}; the PhD finger protein was not confirmed by interaction mating. The other clones, SAE2, SUMO-1, Daxx and Brd7, interact specifically with the Spastin$^{\Delta N}$ protein and not with Spastin^{FL}.

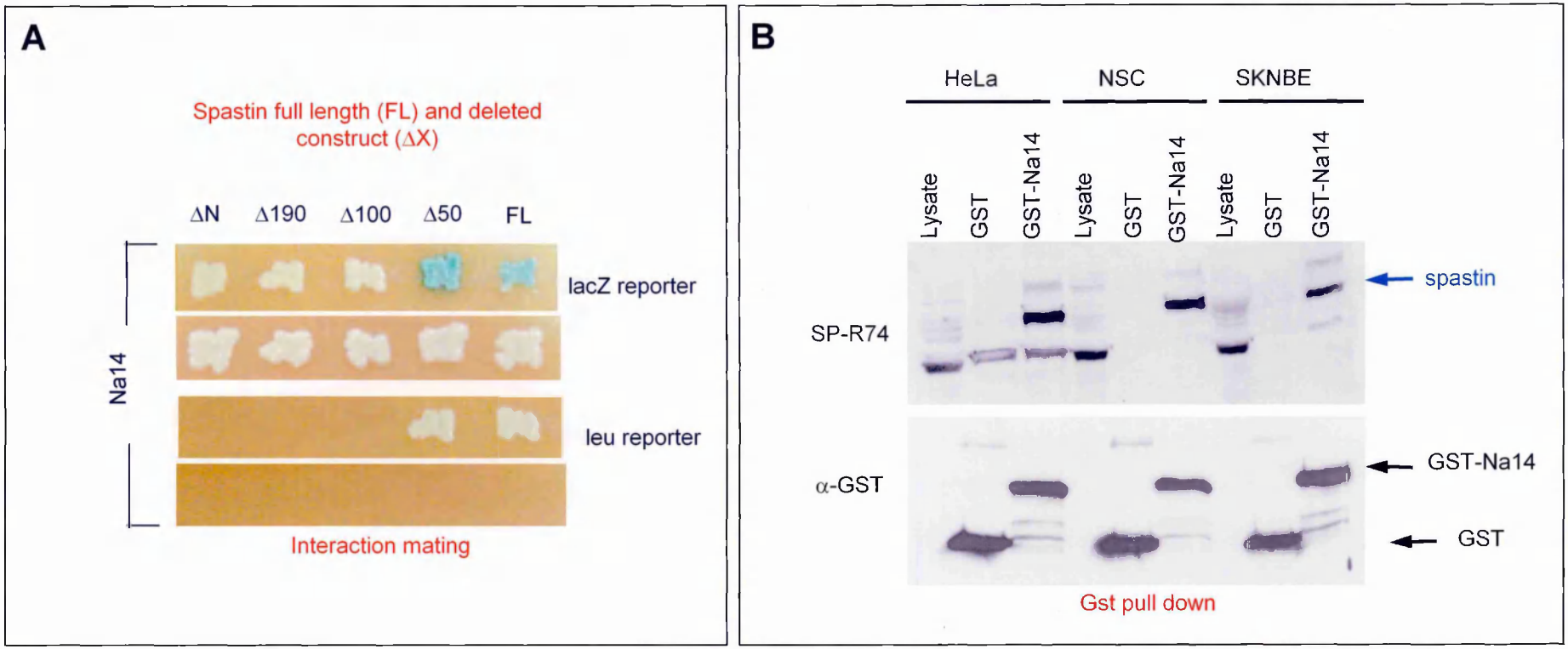

Figure 35. Spastin and Na14.

(A) Several deletion constructs from spastin N-ter were cloned in the pAR202 vector: Δ50, Δ100, Δ190. These constructs and the Spastin$^{\Delta N}$ bait, were transformed in the EGY42 yeast strain together with the lacZ reporter. All of them were crossed with EGY48 yeast strain transformed with Na14 and replicated on the selective plates. Na14 interacts with Spastin^{FL} and Δ50, but not with Δ100, Δ190 and Spastin$^{\Delta N}$. Therefore the region of spastin responsible for the interaction with Na14 is between aa 50 and 100. (B) Total lysates were prepared from HeLa, SKNBE and NSC34 cells. Lysates were supplemented with agarose beads either bound with GST or GST-Na14 recombinant protein. Samples were incubated at RT for 3 hrs. Beads were washed for three times and proteins interacting with GST or GST-Na14 were eluted in disruption buffer. Samples were fractionated on 10% SDS/PAGE and analysed by immunoblot using the SP-R74 or the anti-GST antibodies. SP-R74 detected a band of the apparent molecular weight of spastin in the GST-Na14 lane and not in lysates treated with GST alone.

```
  1   MNSPGGRGKK KGSGGASNPV PPRPPPPCLA PAPPAAGPAP PPESPHKRNL
 51   YYFSYPLFVG FALLRLVAFH LGLLFVWLCQ RFSRALMAAK RSSGAAPAPA
101   SASAPAPVPG GEAERVRVFH KQAFEYISIA LRIDEDEKAG QKEQAVEWYK
151   KGIEELEKGI AVIVTGQGEQ CERARRLQAK MMTNLVMAKD RLQLLEKMQP
201   VLPFSKSQTD VYNDSTNLAC RNGHLQSESG AVPKRKDPLT HTSNSLPRSK
251   TVMKTGSAGL SGHHRAPSYS GLSMVSGVKQ GSGPAPTTHK GTPKTNRTNK
301   PSTPTTATRK KKDLKNFRNV DSNLANLIMN EIVDNGTAVK FDDIAGQDLA
351   KQALQEIVIL PSLRPELFTG LRAPARGLLL FGPPGNGKTM LAKAVAAESN
401   ATFFNISAAS LTSKYVGEGE KLVRALFAVA RELQPSIIFI DEVDSLLCER
451   REGEHDASRR LKTEFLIEFD GVQSAGDDRV LVMGATNRPQ ELDEAVLRRF
501   IKRVYVSLPN EETRLLLLKN LLCKQGSPLT QKELAQLARM TDGYSGSDLT
551   ALAKDAALGP IRELKPEQVK NMSASEMRNI RLSDFTESLK KIKRSVSPQT
601   LEAYIRWNKD FGDTTV
```

Figure 36 . Searching for SUMO-1 consensus sequence yKxE

Spastin (human and drosophila) sequence was analysed with the SUMO-plot program (http://www.abgent.com/sumoplot.html) in order to identify lysine that could be substrates for SUMO1 conjugation. Sequences in red correspond to lysine with a high probability to be SUMO1 modified, while sequences in blue correspond to lysine with low probability to undergo SUMO1 modification. The underlined sequences are conserved in Human, Mouse and Drosophila spastin.

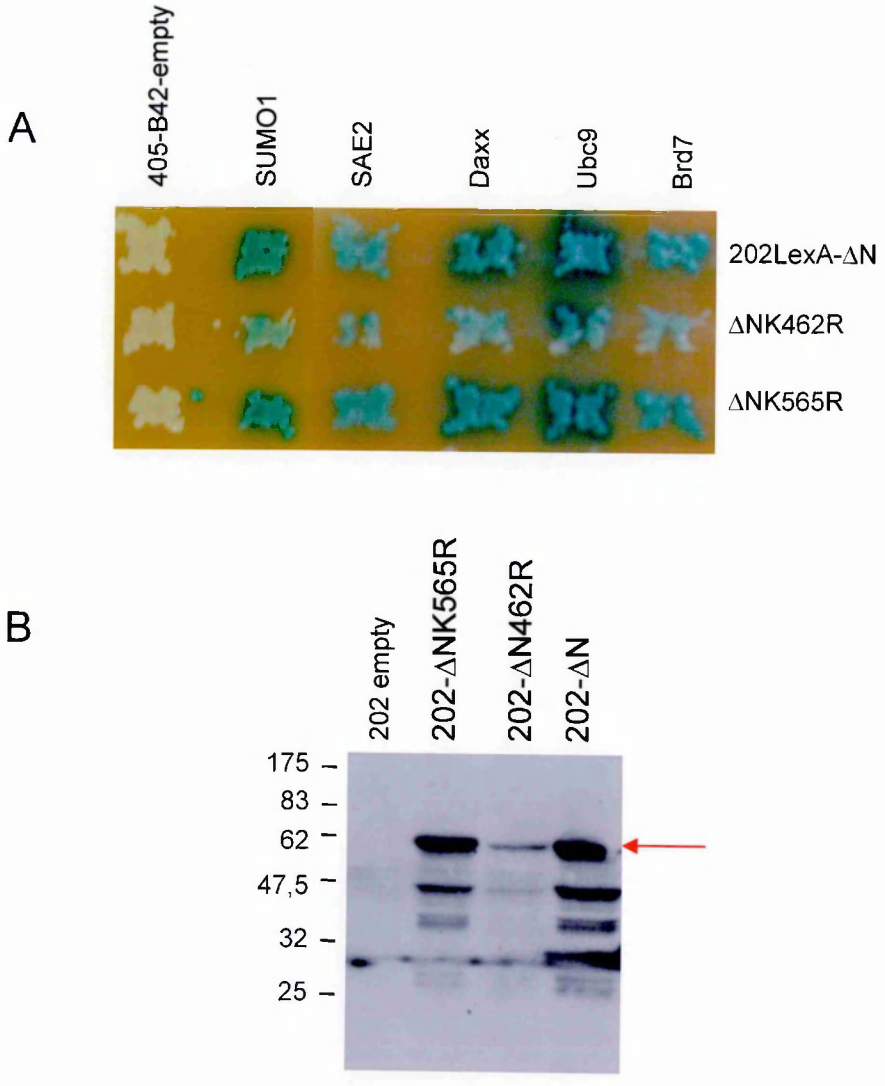

Figure 37. Spastin is SUMO-1 conjugated in yeast.

SUMO1 and SAE2 were identified as putative interactor of spastin. pAR202-Spastin$^{\Delta N}$ construct mutated in the putative target lysines for SUMO-1 conjugation were generated: ΔNK462R and ΔNK565R. (A) SpastinΔN, ΔNK462R and ΔNK565R were transformed in EGY42 yeast strain together with the LacZ reporter. SUMO-1, SAE2, Daxx, UBC9 and Brd7 (cloned in the pJ4-5 vector) were transformed in the EGY48 yeast strain and an interaction mating assay was performed. As control, we transformed also the pJ4-5 empty vector in the EGY48. Spastin$^{\Delta N}$ interacts with SUMO-1, SAE2, Daxx, Brd7 and also UBC9. ΔNK462R interacts with all the constructs although a weaker colorimetric reaction was observed. ΔNK565R interacts with all the constructs. (B) Spastin$^{\Delta N}$, ΔNK462R and ΔNK565R were transformed in EGY42 yeast strain together with the LacZ reporter for the interaction mating assay. Yeast cells were lysed to check that a fusion protein was made. As control, yeasts transformed with the empty pAR202 vector were used. Cell extracts were prepared and samples were fractionated on a 10% SDS/PAGE. Immunoblot analysis was performed with the monoclonal anti-LexA antibody. All the constructs express fusion proteins of the expected size as indicated by the arrow, although the LexA-ΔNK462R protein is expressed at a lower level.

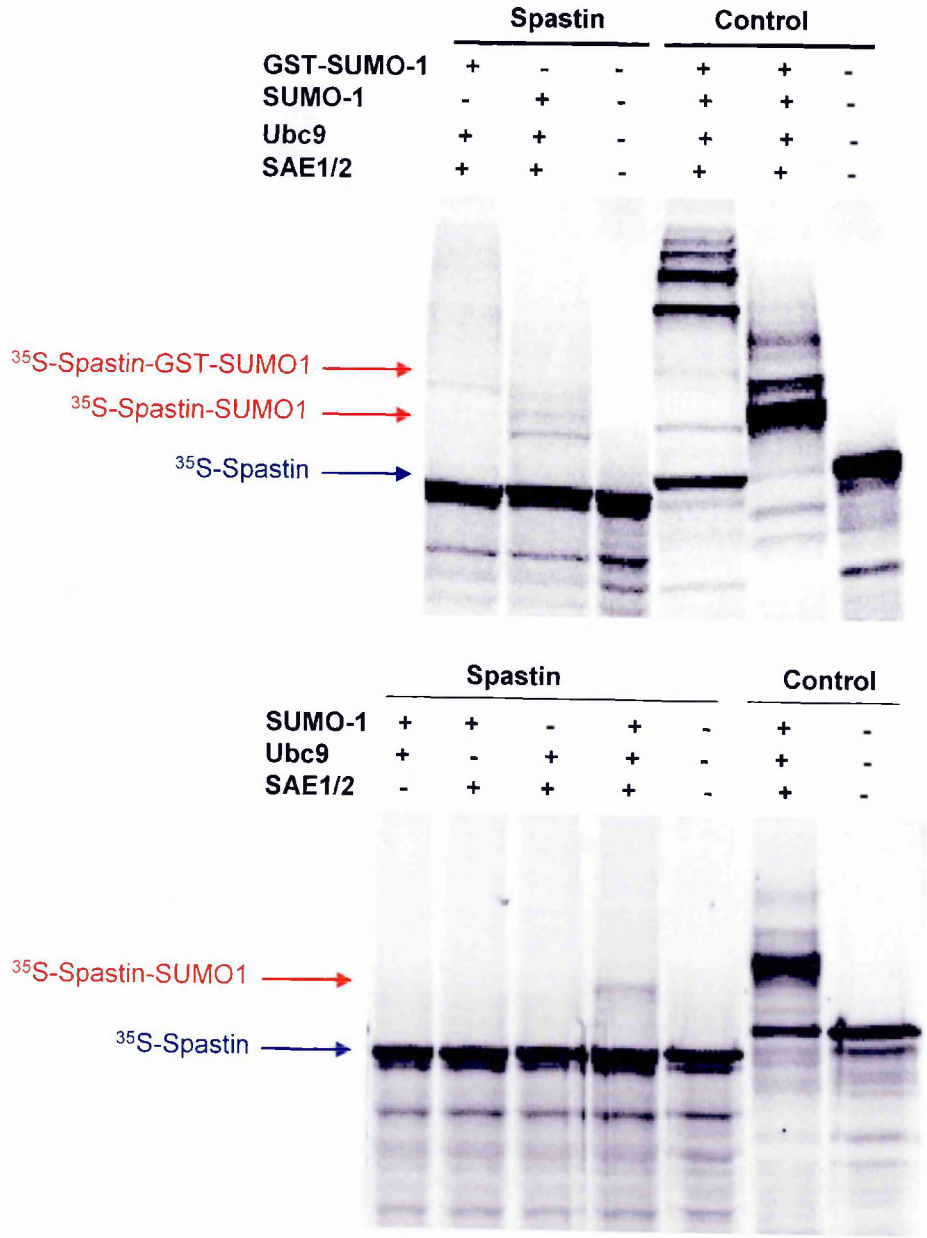

Figure 38. In vitro conjugation of SUMO-1 to Spastin.

(A) In vitro expressed and ^{35}S labelled Spastin or a control protein were incubated with ATP, recombinant SUMO-1 or GST-SUMO-1, UBC9 and SAE (1/2) as indicated. Reactions products were fractionated by SDS/PAGE, and the dried gel was analyzed by phopshorimaging. The bands corresponding to spastin, SUMO-1 conjugated spastin and the GST-SUMO1 conjugated spastin are indicated by the arrows. (B) ^{35}S labelled Spastin or a control protein were incubated with ATP, recombinant SUMO-1, UBC9 and SAE (1/2) as indicated. The SUMO-1 conjugation of spastin is abolished if either SUMO-1, SAE or UBC9 was omitted from the reaction.

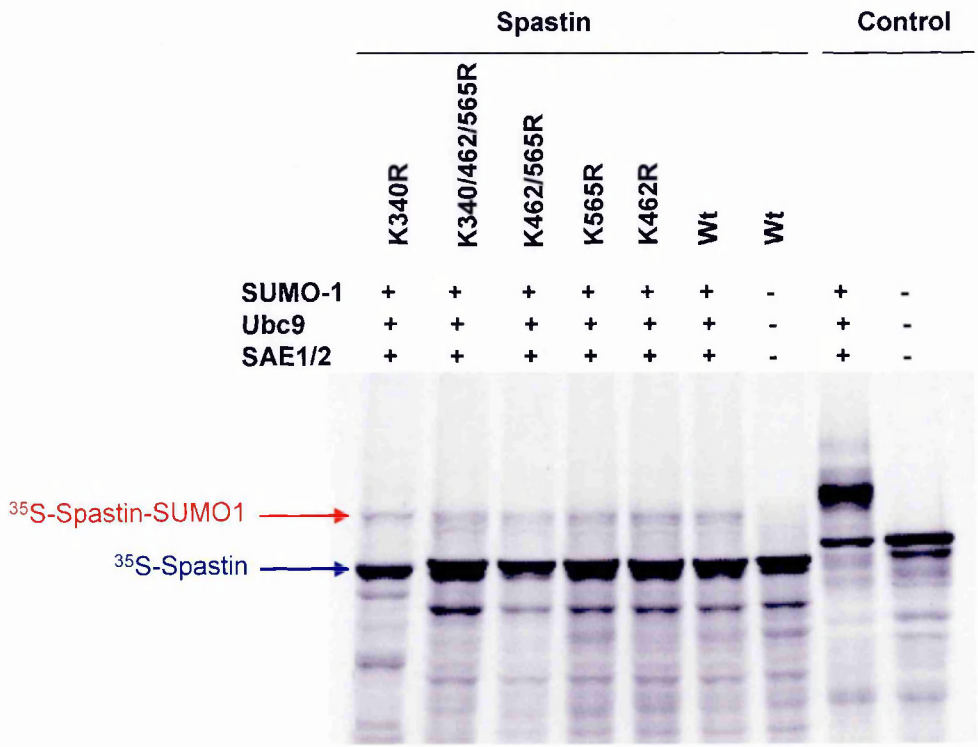

Figure 39. In vitro conjugation of SUMO-1 to several spastin mutants.

In vitro expressed and ^{35}S labelled Spastin (*wt*, K340R, K462R, K565R, K462/565R or K340/462/565R) or a control protein were incubated with ATP, recombinant SUMO-1 or GST-SUMO-1, UBC9 and SAE (1/2) as indicated. Reactions products were fractionated by SDS/PAGE, and the dried gel was analyzed by phopshorimaging. The bands corresponding to spastin and SUMO-1 conjugated spastin are indicated by the arrows. None of the mutations abrogate the SUMO-1 modification of spastin.

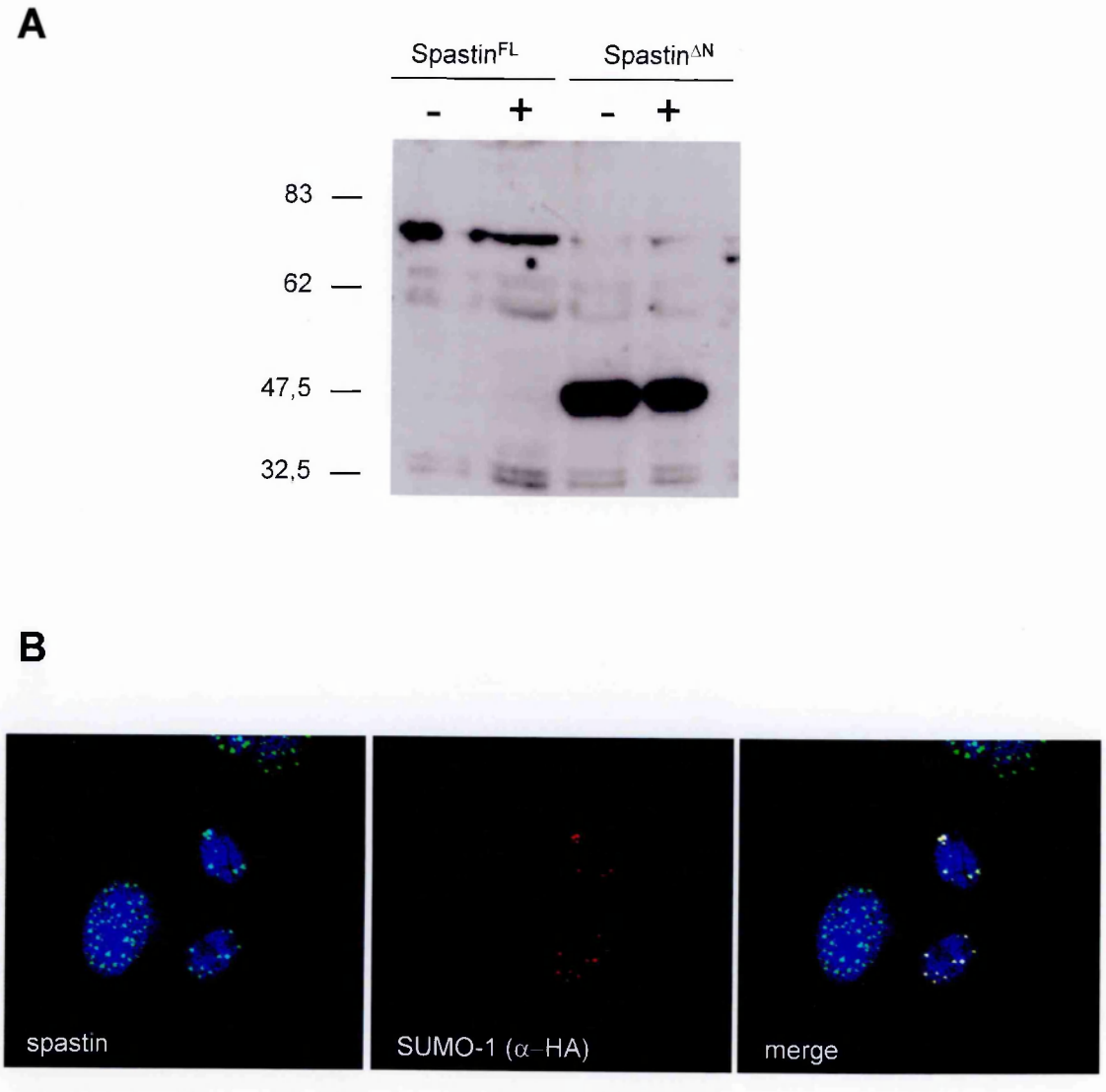

Figure 40 . SUMO-1 modification of spastin in vivo.

(A) HeLa cells were co-transfected with 6His tagged SUMO1 and spastin-myc or spastin$^{\Delta N}$ myc. Cells were lysed in guanidine-HCl buffer, and proteins linked to 6His tagged SUMO were purified using Ni-agarose beads and, after extensive washing, eluted with 200 mM imidazole. Eluted proteins were fractionated on a 10% SDS/PAGE, transferred to a PVDF membrane and analyzed by Western blot using the anti-myc monoclonal antibody. Molecular weight markers are shown on the left. (B) Human fibroblasts were transfected with Ha tagged SUMO-1. 24 hrs post-transfection cells were fixed in methanol. SUMO-1 was detected (red signal) using the monoclonal anti-HA antibody. While spastin was detected using a specific polyclonal SP-R74 antibody (green signal). Nuclei were stained with DAPI (blue signal). A co-localization is evident as shown in the merge figure by the yellow signal.

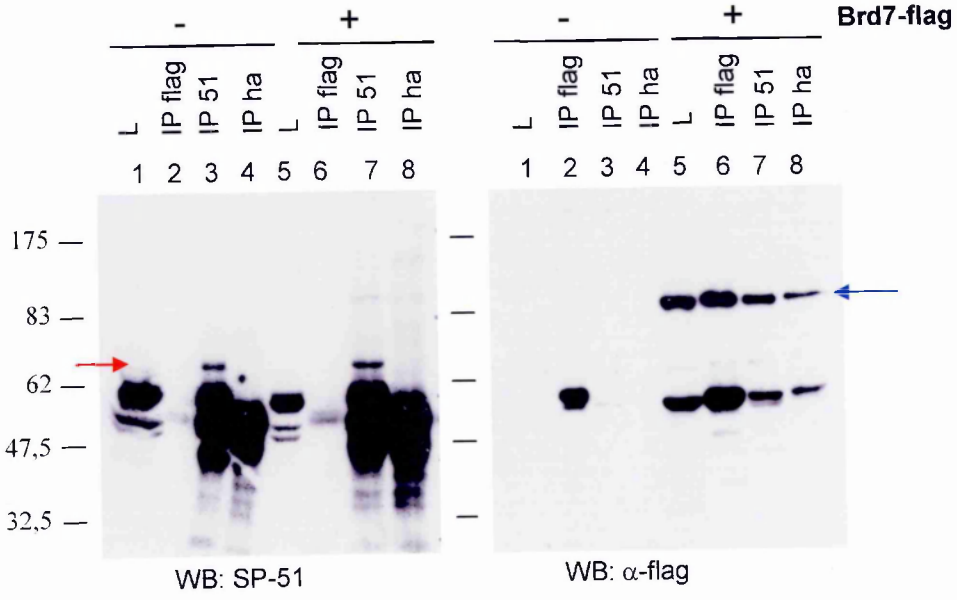

Figure 41. Spastin molecular partner: Brd7

HeLa cells were transfected with the Brd7-flag construct. Extracts from untransfected (lane 1-4) or transfected (lane 5-8) cells were immunoprecipitated with the anti-flag, the SP-51 or the anti-ha (as control) antibodies. Samples were fractionated on a 7.5% SDS/PAGE and analysed by western blot using the anti-flag or the SP-51 antibodies. Brd7-flag was immunoprecipitated by the anti-flag antibody (WB flag, lane 6, blue arrow), by the SP-51 (WB flag, lane 7), but also by the unrelated anti-HA antibody (WB flag, lane 8), suggesting that Brd7 binds non specifically the resin. On the contrary, spastin was immunoprecipitated only by the SP-51 antibody (WB SP-51, lane 3, 7 red arrow).

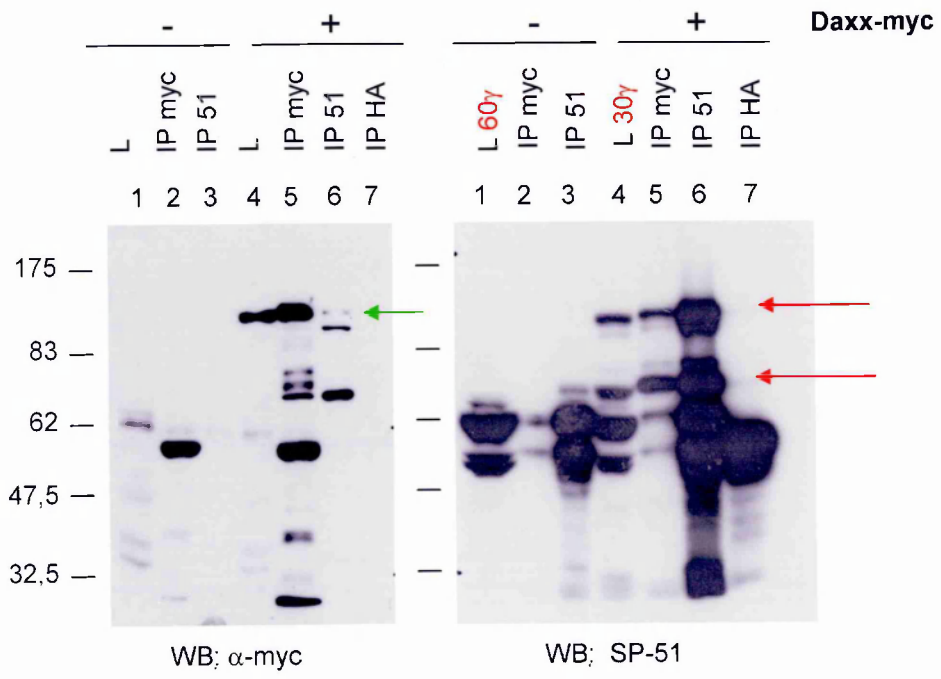

Figure 42. Spastin interacts physically with Daxx.

HeLa cells were transfected with the Daxx-myc construct. Lysates from untransfected (lanes 1-3) or transfected (lanes 4-8) cells were immunoprecipitated with the anti-myc, the SP-51 or the anti-ha (as control) antibodies. Samples were fractionated on a 7.5% SDS/PAGE and analysed by immunoblot using the a-myc or the SP-51 antibodies. Daxx-myc was immunoprecipitated by the a-myc antibody and by the SP-51 antibody, but not by the unrelated anti-HA antibody (WB a-myc, lane 5,6,7). Consistently, spastin was immunoprecipitated by the SP-51 and by the a-myc antibodies, but not by the anti-HA (WB SP-51, lane 5,6,7). Both the SP-51 and the a-myc immunoprecipitated the 68kDa form and a slower migrating form of 90 kDa (red arrows). When cells were transfected with daxx, it is possible to detect a higher level of spastin, both in the total lysate (WB SP-51, lane 4) and in the immunoprecipitate samples (WB SP-51, lane 5,6), respect to the untransfected cell (WB SP-51, lane 1,2,3).

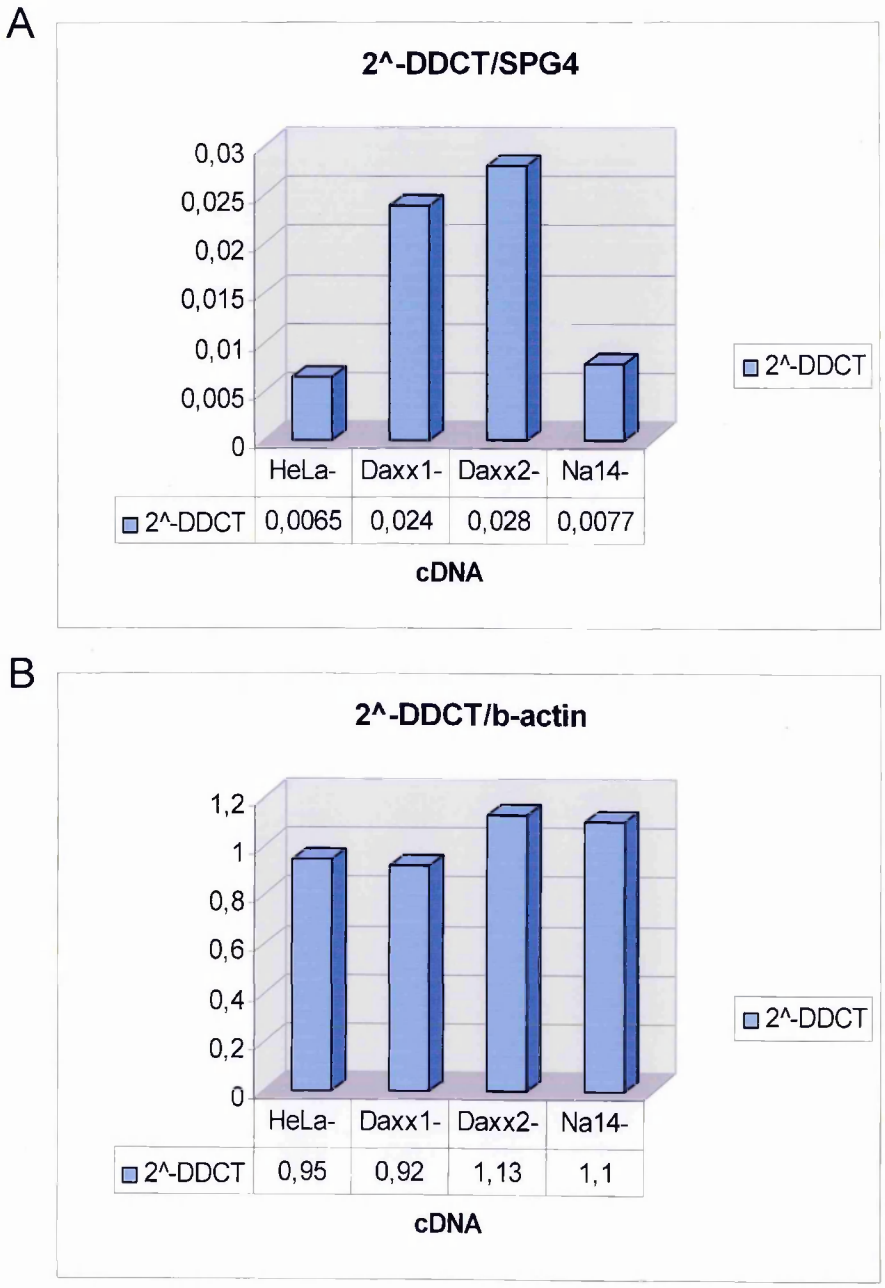

Figure 43. Real-time quantitative PCR

Total RNA was extracted from untransfected HeLa cells or cells transfected with Daxx-myc or Na14. cDNA was transcribed from 3 μg of RNA and 1:20 dilution was used as template for the real-time PCR. Daxx1 and Daxx2 represent two independent transfections. GAPDH was used as reference; spastin (A) and b-actin (B) transcription level were evaluated in the different samples. Spastin transcription levels are 3.5 to 4.6 fold higher in Daxx transfected cells respect to untransfected cells, while b-actin levels are constant in the different samples.

CHAPTER 6: A structural model for spastin

6.1 Spastin sequence analysis

The linear polypeptidic chain contains all the information necessary for the acquisition of the correct and functional three-dimensional fold, as well as information regarding the subcellular compartment where the protein is localized.

Spastin primary sequence has been analyzed with Pfam (this program scans a sequence against the Pfam protein families database http://www.sanger.ac.uk/Software/Pfam/search.shtml/) and SMART (Simple Modular Architecture Research Tool; http://smart.embl-heidelberg.de/) programs searching for domain architecture. Both programs identified two main domains: the AAA domain between amino acid 374 and 562; the MIT domain between amino acids 116 and 194. Furthermore, a small transmembrane domain is recognized between residues 57 and 79. A nuclear localization signal (NLS) between amino acids 7 and 11 was originally identified in spastin sequence (Hazan et al., 1999). Analysis of spastin protein sequence with PSORT, a program for the prediction of a protein subcellular localization, lead to the identification of three NLS: PKRKDPL at aa 233; RKKK at aa 309; PGGRGKK at aa 4. By computer analysis the protein has therefore a strong probability to be nuclear.

6.2 Spastin 3D structure prediction

The biological function of a protein is directly determined by its three-dimensional structure. When structural data are not available for the construction of a three-dimensional model, some information can be retrieved by using 3D structure prediction programs. The 3D-PSSM program (http://www.sbg.bio.ic.ac.uk/~3dpssm/) analyzes a protein sequence of interest and attempts to predict its 3-dimensional structure. It is based on a library constructed with known protein structures onto each of which the input sequence is "threaded" and scored for compatibility. Protein fold recognition is achieved using 1D and 3D sequence profiles coupled with secondary structure information (Foldfit). Spastin amino acidic sequence was analysed via the 3D-PSSM program. Unfortunately the full length protein could not be used because no structural homology for the N-terminal portion was detected by the program. A sequence corresponding to the C-terminal portion of the protein (aa 250-616), mainly containing the AAA cassette, was therefore used for a 3D structure prediction. The resulting atomic coordinates for spastin model were superposed on the crystal structure obtained from the AAA of p97 using the "least square fitting" program (local program, Imperial College of London) (PDB code: 1E32) (Zhang et al., 2000). Because the two set of atomic coordinates were almost perfectly overlapping, we could use the structure of p97 AAA as a base for generating our model of Spastin AAA. The program used for the model generation and for all the calculation shown is the PREPI (Dr. S. Islam, Imperial college of London). The resulting model for spastin has some gaps due to the absence of few amino acids that were instead present in p97 and *vice versa*. In this way we could generate a model for the spastin AAA domain. In this model

Spastin AAA domain comprises, as for p97, an N-terminal subdomain which has a □/□ fold, a nucleotide binding pocket (ADP in red) and a smaller C-terminal □-helical subdomain (Fig. 44). p97 forms a symmetric homo-hexamer. Because of the high degree of similarity between the AAA domain of p97 and spastin, we have constructed also a hexameric model for spastin AAA (Fig. 45).

6.2.1 Mapping of missense mutations to the model

All the missense mutations found in SPG4-HSP patients fall in the AAA domain of spastin. They are predicted to interfere with ATP binding and/or hydrolysis and therefore interfere with ATPase activity of the domain.

In order to understand the effect of the missense mutations, we have investigated the localization of these mutated residues on our model. All the mutated residues are represented on the model in purple and in the ball and stick format, both on the monomer (Fig. 44) and on the hexamer (Fig. 45).

Based on our model, we have estimated the amino acids that constitute the active site and are therefore responsible for ATP-binding. Considering that the radius of the Carbon atom (C) is 1.6 Å and that of the Oxygen (O) atom is 1.4 Å, the maximum distance that accounts for the interaction between atoms is given by the sum of C and O radius (3 Å) plus an error correction of 0.5 Å. Two atoms interact if they are at a distance equal or inferior to 3.5 Å. In this way we have identified which are the atoms and therefore the residues involved in the interaction with the ADP molecule (table 6, figure 46).

Some of the residues of the active site have been found mutated in patients with HSP. Clearly for these residues, the mutation interferes with the ATP binding. In particular, the K388 is the lysine predicted to bind the ATP.

In figure 43, it is evident that some missense mutations fall in structural element of the AAA module, for example R424 and L426 are in the middle of a α-helix, while F404 is on a β-sheet. Some mutations, therefore, altering structural elements, could generate changes in the structure which compromise the AAA function.

Another important observation has been to evaluate which is the surface of the protein which is exposed to the solvent and therefore involved in possible interactions with other molecules. The concept of solvent accessible area was originally introduced by Lee and Richards (Lee and Richards, 1971) and it describes the area over which contact between protein and solvent can occur. With the PREPI program we have calculated which is the solvent accessible area (Lee & Richardson algorithm) (Lee and Richards, 1971) of each residue and we have generated a surface model as shown in figure 47. All the missense mutations are in purple, while the ADP is in red. If a residue, localized on the surface, is mutated, this can disturb the eventual interaction with other molecules and therefore interfere with the protein's function.

Since we have generated also a hexameric model for spastin AAA, we have calculated which are the residues localized at the interface between two subunits. We have determined which residues lost solvent accessible area comparing the monomer calculation with the hexamer one. These will be the residues at the interface. If we suppose that spastin, as the other members of the AAA family (p97 or Katanin), acts

as an hexamer, mutations in the sites at the interface between two subunits of the oligomer can interfere with the assembling of the hexamer and therefore with its function.

On this basis, it is clear that mutations of a residue in the AAA, which is involved in the active site formation, exposed on the protein surface, localized in structural elements or at the interface between subunits in the hexameric models (table 7), can interfere with the AAA module activity, via different mechanism and cause a defect in spastin function leading to HSP.

6.2.2 SUMO-1 consensus lysine and spastin structure

The analysis of spastin primary structure and the sequence homology between the Drosophila, mouse and human protein permit us to identify three candidate lysines for the SUMO-1 conjugation: K340, K462, and K565.

To be SUMO-1 modified the lysine residue has to be exposed on the surface of the protein. Therefore we observed where these lysines were localized on our AAA model (fig 47, yellow residues). The K565 is the residue which is not conserved in the Drosophila spastin and on our model it is hidden in the structure. The K340 and K462 are conserved in these three species. They are both exposed on the surface of the spastin AAA. The side chain of the K462 is laying on the structure, while the side chain of the K340 is exposed toward the solvent. The K340 residue has indeed a higher solvent accessible area. Since we are discussing on a model which has no experimental support, we can not tell which residues between K340 and K462 is most probably SUMO modified. But they are both, in terms of consensus and of surface accessibility, good candidates for this modification.

6.3 Summary

- ✓ Missense mutations of the spastin gene interfere with the AAA module function, by altering structural elements, disrupting the ATP binding site, or modifying residues important for molecular interactions.
- ✓ K340 and K462 are the most probable lysines for SUMO-1 conjugation, because they match the consensus and are exposed on the protein surface.

Residues in the active site	Mutation in HSP-SPG4 patients
D343	
I344	I344K
A345	
Q347	Q347K
G385	
N386	N386K/S
G387	
K388	K388R
T389	
M390	
L517	
S547	
T550	

Table 6. Amino acidic residues of Spastin active site.

Missense mutation	Active site	Surface	Interface	Structural motif H: Helix S: □-strand	Residues with a lower "solvent accessibility area" in the hexameric model
S44L			Not present in	the model	
I344K	+				
Q347K	+	+			
S362C		+		+ (H)	
G370R		+		+ (H)	+
F381C				+ (S)	
N386K	+				
N386S	+				
K388R	+				
F404S		+		+ (S)	
R424G		+		+ (H)	
L426V		+		+ (H)	
C448Y				loop	
R460L		+	+	+ (H)	+
T486I				+ (S)	
R499C		+	+	+ (S)	
R504L		+		+ (S)	
E512D					
G526D				loop	
L534P				+ (H)	
D555N		+	+	+ (H)	+
A556V				+ (H)	
R562G			+		+
D584H					

Table 7. SPG4 missense mutation and their location on the three-dimensional model of spastin AAA domain.

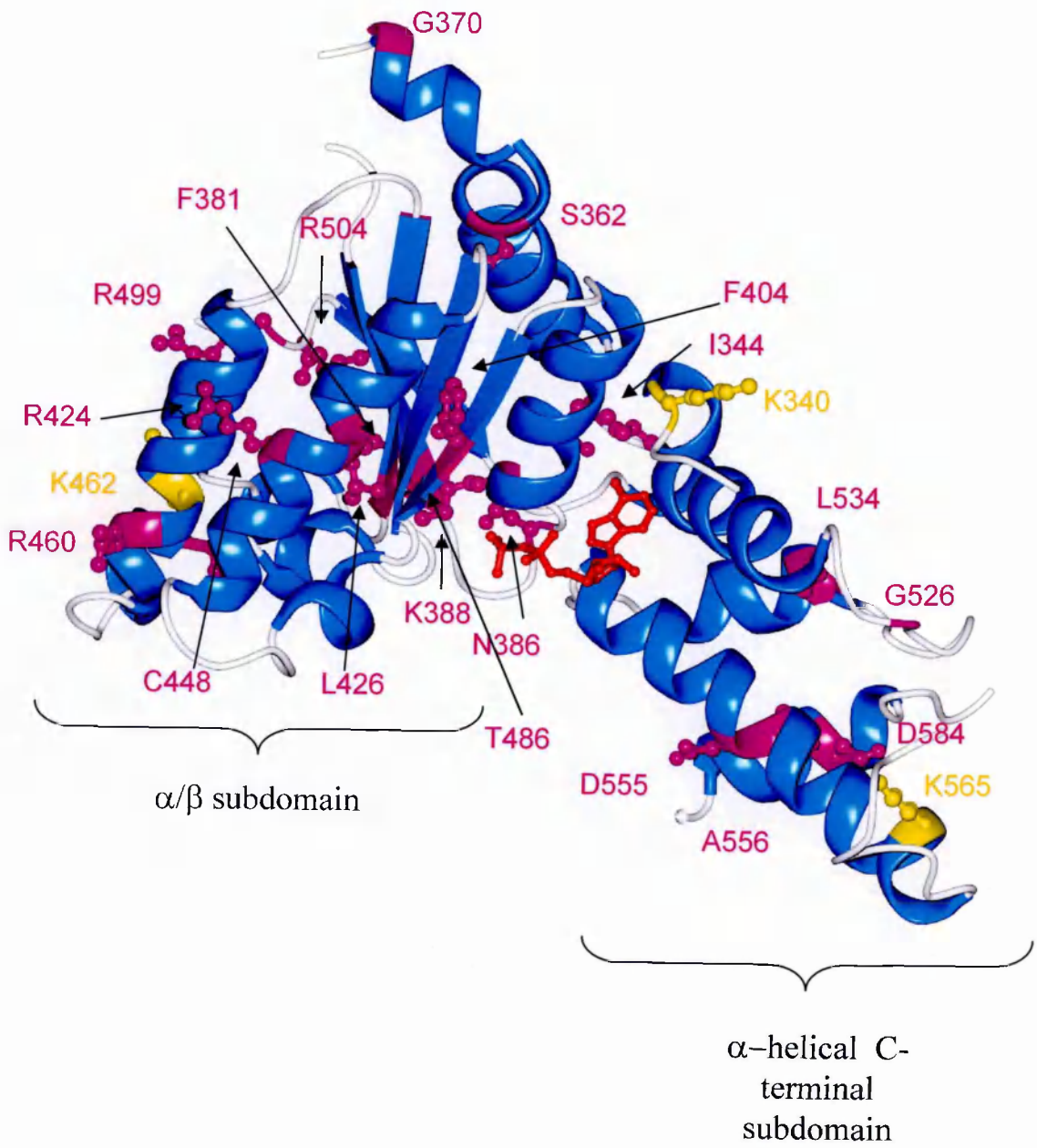

Figure 44. Secondary structure model of spastin AAA.

A model of the AAA domain of spastin has been realized with the PREPI program on the basis of the homology with p97. The model consists of an N-terminal α/β fold subdomain, a nucleotide binding pocket and a C-terminal α-helical subdomain. Missense mutations are represented in purple and in the ball and stick format. Lysines candidate for SUMO-1 conjugation are in yellow and in the ball and stick format. The ADP is in red.

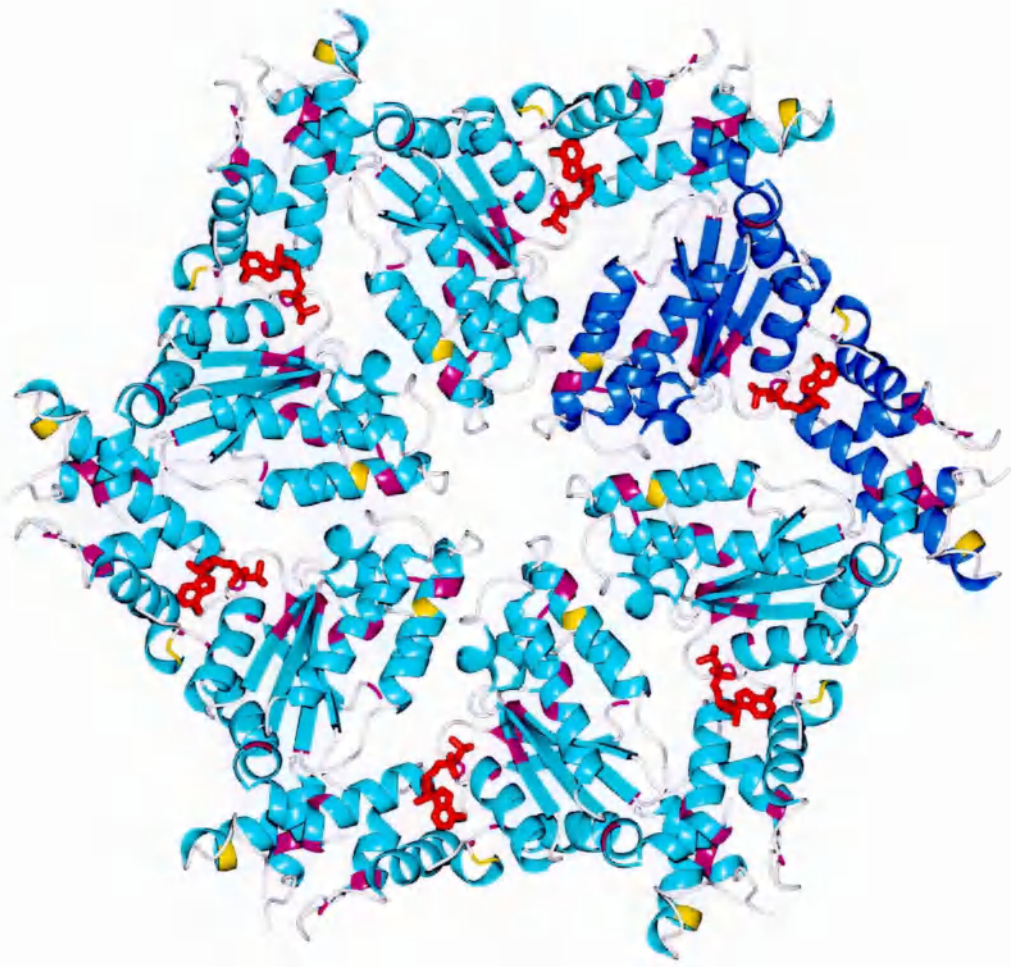

Figure 45. Hexameric model of spastin AAA.

On the basis of the p97 hexameric model, we have generated a hexameric model of the spastin AAA. In blue is evidenced one monomeric subunit. In purple are the missense mutations, in yellow the lysines candidates for SUMO-1 conjugation, while in red is the ADP.

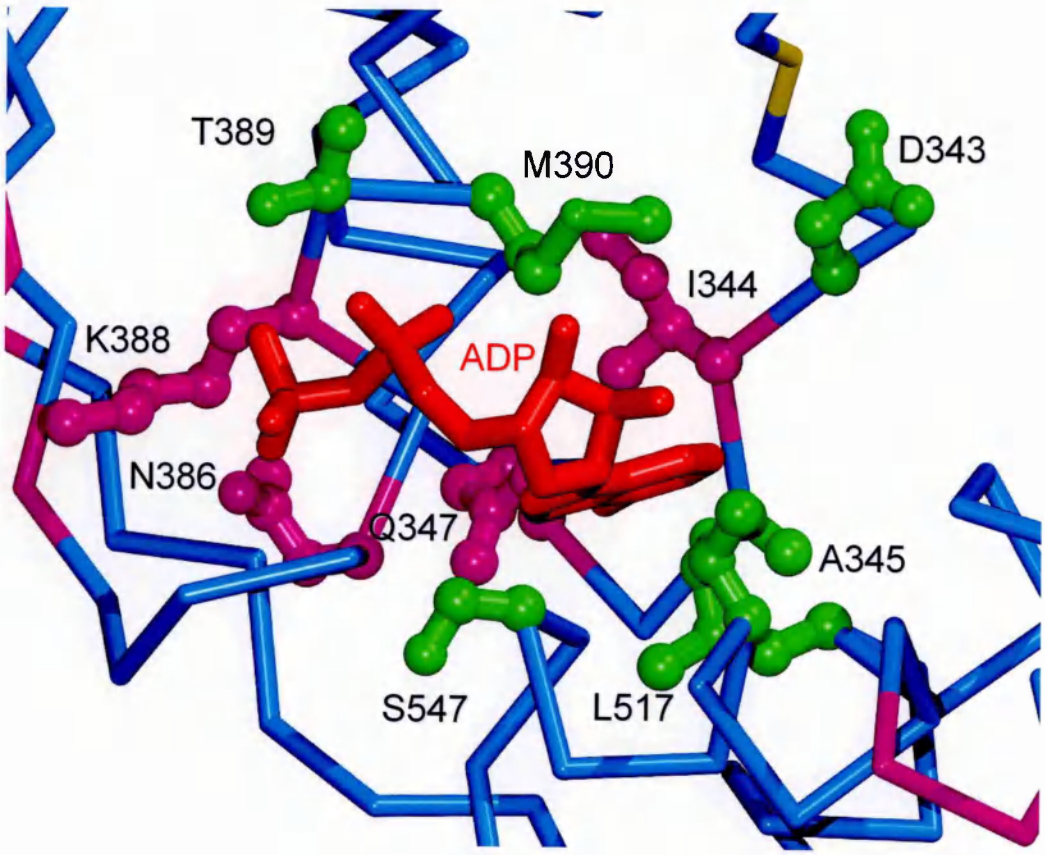

Figure 46. Active site of spastin AAA.

This is a schematic representation of the active site of the spastin AAA. In cyan is the Cα skeleton of the AAA structure. In ball and stick are the amino acids that constitute the active sites. In purple are the missense mutations. In green are the other amino acids of the active site. In red is the ADP.

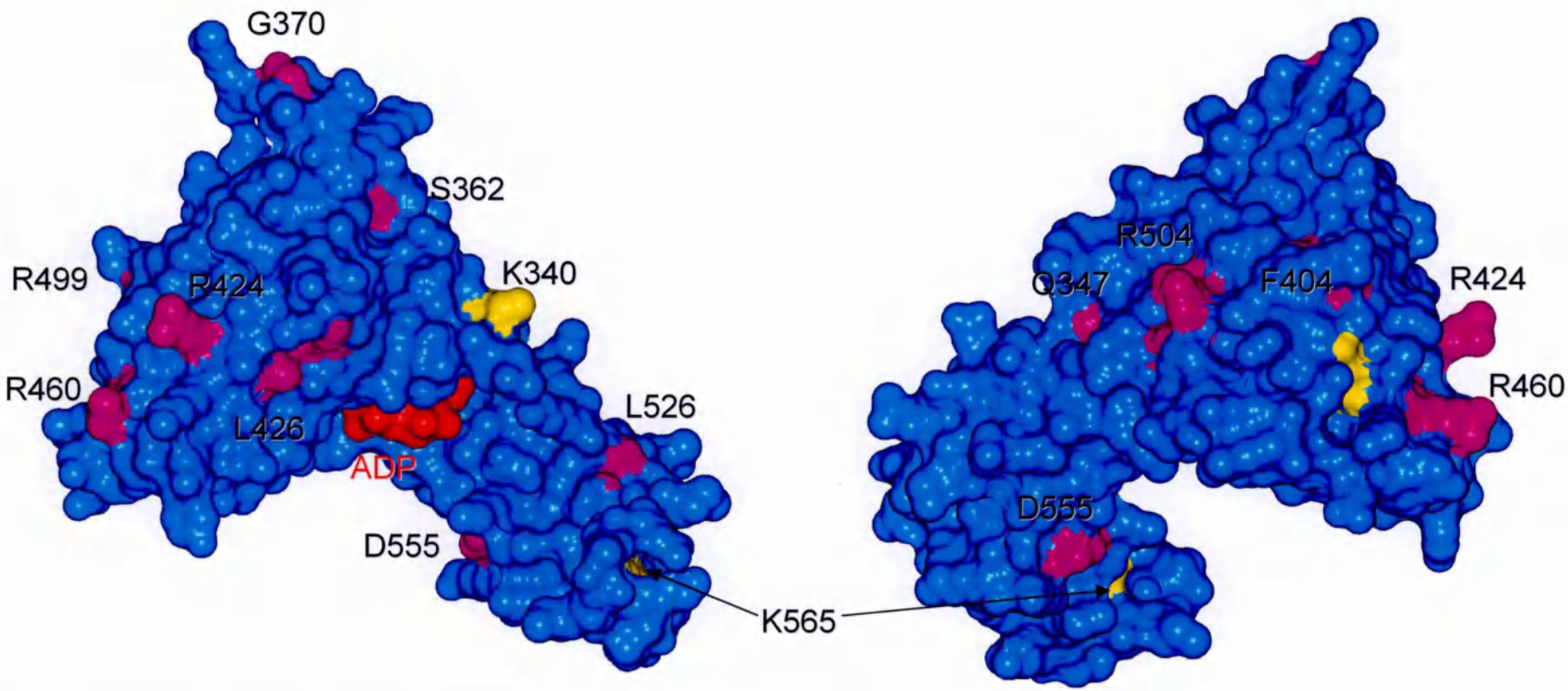

Figure 47. Surface model of the spastin AAA.
The solvent accessibility of each residues has been calculated with the PREPI program and a surface model has been generated. (A) and (B) represent a front and a back view of the model. In red is the ADP. In purple are the missense mutations which are exposed on the surface of the AAA structure. In yellow are the lysine candidates for SUMO-1 conjugation, K340 and K462 are quite exposed on this model, while K565 seems to be hidden in the structure.

CHAPTER 7: DISCUSSION

Hereditary spastic paraplegia (HSP) is a clinically and genetically heterogeneous group of neurodegenerative disorders. So far, 21 HSP loci have been mapped and 10 genes have been identified. All the genes involved in the different forms of HSPs are ubiquitously expressed and they are involved in many different cellular processes. An important issue in studying HSP is to understand how it is possible that mutations in ubiquitous proteins involved in different pathways can all lead to a very specific cellular phenotype, which is the retrograde and progressive degeneration of the longest axons of human body.

The most common form of HSP is due to mutations in the SPG4 gene. Therefore we have studied the protein product of the SPG4 gene, spastin, as a mean to understand the pathogenesis of this group of diseases.

7.1 Spastin has a complex subcellular localization

A first step, in investigating spastin function, was to determine its subcellular localization. We have investigated the localization of both the endogenous and the exogenous protein. When spastin is transfected into cells, it starts to be expressed at the microtubule organizing center and then, with longer period of expression, it

accumulates in cytoplasmic spots. This predominantly cytoplasmic localization is in contrast with the presence of three NLS in spastin amino acidic sequence. Moreover, a recent report indicate that spastin is an abundant neuronal protein which localizes to the nucleus (Charvin et al., 2003).

We have produced specific spastin antibodies and we have found that spastin has a complex subcellular localization, both nuclear and cytosolic, which depends on the cell type analyzed.

In Cos-7 cells a specific spastin signal was detected at the spindle poles in different phases of the cell cycle and at the midbody. The presence of a spastin signal at the midbody was detected also in other cell lines, such as HeLa and the immortalized motoneuronal cell line NSC34, and was confirmed by the three polyclonal antibodies we have analyzed: SP-R74, SP-50 and SP-51. In human fibroblasts and in NSC34, spastin had both a nuclear and cytoplasmic localization. Indeed, in fibroblasts spastin was present at the centrosome and also in discrete nuclear structures, which were the PML bodies. In NSC34, spastin was localized to nuclear dots that were bigger in size in respect to those revealed in fibroblasts. More interestingly, an enrichment of spastin signal was detected in the terminal portion of the neuronal processes, in correspondence of the growth cone of the axon. A diffuse nuclear staining was also observed in HeLa and Cos7 cells, but the signal is faint and is very difficult to distinguish it from background staining. It is possible that the cellular levels of spastin are low, rendering very hard to detect spastin if it is not concentrated in defined structures (like nuclear dots or midbody).

There is clearly a discrepancy between the localization observed with the antibodies that recognize the endogenous protein, in respect to the localization

observed when spastin is transfected into the cell. Indeed, the exogenous spastin has a predominantly cytoplasmic localization with the formation of cytosolic aggregates. A hypothesis could be that low levels of spastin are normally present in a cell. The high levels of expression achieved upon transfection are not tolerated by the cell; therefore spastin is mis-localized into cytoplasmic aggregates. When we performed transfection experiments to achieve low level of expression, we could detect a signal at the centrosome. Many centrosomal proteins mis-localize when overexpressed. Indeed, the centrosomal localization can be appreciated at low levels of expression, while a diffuse staining throughout the cytoplasm or the formation of cytoplasmic aggregates can be observed at higher levels of expression (Andersen et al., 2003). Moreover, also studies on the p60 katanin, a centrosomal component belonging to the AAA family and homologous to spastin in the AAA domain, have shown that overexpression leads to the formation of aggregates which do not localize with the centrosome, suggesting that once the centrosome binding-sites are saturated, the additional protein expressed aggregates into the cytoplasm (Hartman et al., 1998).

A confocal analysis of cells overexpressing spastin showed that, although the major part of the protein is present in the cytoplasmic compartment, there is a small fraction of spastin that localizes to the nucleus. We have also forced spastin to enter the nucleus by generating a chimeric construct where the strong NLS of the SV40 was fused at the 5' of spastin cDNA. When this chimeric protein was transfected into the cells, we observed the same localization of the exogenous *wt* spastin. This suggests that the levels of spastin tolerated in the nucleus may be low and that there might be a threshold level. When spastin expression reaches levels higher than this threshold, the cell activates probably a mechanism to export spastin which will be

otherwise toxic for the nucleus. Alternatively, spastin translocation into the nucleus may depend on the association with a "carrier" protein or on a post-translational modification of the protein. Further experiments are needed to understand the mechanisms of spastin nuclear localization and also to determine if spastin may shuttle between the nucleus and cytoplasm upon certain stimuli.

Recent findings validate our data concerning a complex localization of spastin protein (Wharton et al., 2003). Indeed, immunohistochemistry experiments, with the use of specific antibodies on human tissue, demonstrated that spastin is a neuronal protein predominantly expressed in the cytoplasm, with staining also along the axons. Interestingly, spastin expression was present throughout the brain and the spinal cord and not confined to the motor system. In motor cortex, pyramidal neurons, Betz cells and a portion of small neurons demonstrated cytoplasmic expression with staining in the proximal neurites. A diffuse synaptic staining was observed in the neuropil. Moreover, a nuclear signal was also reported in a portion of cells. This staining was generally diffuse, but sometimes a punctuate pattern was observed (Wharton et al., 2003). A similar pattern of expression was revealed in the hippocampus, with strong expression in the pyramidal cells and dentate granule neurons. In the cerebellum, a cytoplasmic staining was detected in dentate neurons and Purkinje neurons. There was also a nuclear staining in the cerebellar molecular layer, with more than 50% of granule layer neurons exhibiting a nuclear punctuate pattern. In the grey matter of the spinal cord, a strong staining of neurites was observed in large neurons. Furthermore, anterior horn motorneurons showed exclusively a cytoplasmic staining with no nuclear expression (Wharton et al., 2003).

All these data suggest that spastin has both a nuclear and cytosolic localization. This localization depends on the cell type analyzed and it is probably also dependent on the animal species studied.

7.2 The role of spastin on the microtubules cytoskeleton

Microtubules provide architectural support to eukaryotic cells, organize membranous organelles and act as railways along which cytoplasmic molecules are transported. Microtubules are highly dynamic structures that switch continuously between growing and shrinking phases. Several proteins have been identified which are responsible for the changes of the microtubule cytoskeleton in vivo (Hunter and Wordeman, 2000; Quarmby, 2000; Schroer, 2001; Srayko et al., 2000). The work reported in this thesis suggests that spastin may be involved in microtubule dynamics.

We find that spastin associates with microtubules *in vitro* and that this interaction is mediated by the N-terminal portion of the protein. *In vivo*, microtubules association can be detected only by expressing mutants lacking the entire AAA cassette or defective in ATP binding or hydrolysis. This suggests that the binding to microtubules is transient and is regulated through the nucleotide-binding state of the AAA domain. This is not completely unexpected, indeed other members of the AAA family, such as SKD1 and p60 Katanin, show a transient and nucleotide dependent association with their substrate. These proteins bind and release continuously from their substrate in a nucleotide dependent manner, and only the expression of ATPase

defective mutant has permitted the identification of their targets *in vivo* (McNally et al., 2000; Yoshimori et al., 2000). Taking advantage of the fact that ATPase defective spastin binds constitutively microtubules, we have generated several ATPase defective deletion constructs in the N-terminal region of spastin in order to map more precisely the region of spastin responsible for the microtubule association. Studying the localization of these ATPase defective deletion mutants, we have shown that the region of spastin responsible for the association with microtubules is located between amino acid 50 and 100. Notably, the MIT domain is not responsible for the spastin association to microtubules. The MIT domain was initially reported as "ESP" domain because it was originally identified in only three molecules: End13/Vps4p, SNX15 (sorting nexin 15) and PalB (Phillips et al., 2001). Because of the limited information available at the time, no functional implication was suggested for the domain. Recently, a multiple alignment study showed that the domain is present in a larger group of proteins (Ciccarelli et al., 2003). Since the domain was identified in a microtubule binding protein, Spastin, and in other molecules mainly involved in intracellular transport, such as SNX15, Calpain7 or SKD1 (Fig.3), a more descriptive term was adopted for this domain. It was named MIT, which stands for a domain contained in "microtubule interacting and trafficking molecules". Moreover, this domain is present in the N-terminal portion of two proteins mutated in different forms of HSP: Spastin and Spartin (Ciccarelli et al., 2003; Patel et al., 2002). This fact together with the fact that the N-terminal portion of spastin was involved in the microtubule association lead to the hypothesis that also Spartin may associate with microtubules and that this association may be mediated by the MIT domain (Patel et al., 2002). Since we have now demonstrated that this domain is not

involved in microtubule association, further experiments have to be performed to investigate the function of the MIT domain and its relevance to hereditary spastic paraplegia.

The association to microtubules was confirmed by the data on the subcellular localization of the endogenous spastin. Although we could never detect endogenous spastin on the microtubule array in interphase cells, we found that spastin was enriched in structures rich of microtubules during the cell cycle. Spastin specific antibodies detected, in fact, a signal at the centrosome and at the midbody. Furthermore, it is possible to detect an enrichment of spastin signal in the region between two cells that are undergoing cytokinesis (Fig.20). This is the region where the midbody will originate from and is therefore rich in microtubules.

We found that a spastin ATPase-defective mutant constitutively binds microtubules. This association showed some peculiar features. Indeed, the overexpression of ATPase defective spastin alters the microtubule network distribution, leading to the disappearance of the aster (typical of an interphase cell) and to the formation of thick perinuclear bundles. Moreover, the overexpression of wild type spastin promotes microtubules disassembly in transfected cells. These findings together with the fact that spastin is highly homologous, within the AAA domain, to p60 katanin, a microtubule severing protein, suggest that spastin may play a role in microtubule dynamics.

Katanin is a heterodimer consisting of the AAA-ATPase catalytic subunit (p60) and an accessory subunit (p80), which targets the heterodimer to the centrosome. Katanin seems to be responsible for the release of microtubules from the centrosome (McNally, 2000; McNally et al., 2000). Although the N-terminal regions

of spastin and p60 katanin are not highly conserved, both of them harbour a microtubule binding domain. Furthermore, the N-terminal regions of other members of the AAA family, such as the well studied NSF, seem to be involved in protein targeting to the substrate (Nagiec et al., 1995).

Katanin, as many other AAA proteins, acts as a hexamer. The accepted model is that the substrate (in this case MTs) acts as a scaffold upon which the enzyme can oligomerizes. At this point the presence of the substrate stimulates the ATPase activity of the AAA domain and the ATP is hydrolysed. For katanin, the ATP hydrolysis and the consequent phosphate release generate the driving force for the destabilization of the tubulin-tubulin contacts, leading to the severing of microtubules (Fig.7)(McNally, 2000; Quarmby, 2000). We do not have direct proof of spastin oligomerization. However, studying the structural model we have generated for the spastin AAA domain, we have observed that the regions of the AAA domain important for the oligomerization are conserved in spastin AAA sequence and indeed we were able to generate a hexameric model. Furthermore, we have shown that in co-transfected cells, the *wt* protein and the ATPase defective mutant, which have different subcellular localization, co-localize, either in the localization of the *wt* protein or in the localization of the mutated protein. This can depend on which construct is expressed first in the cell, but can also depend on the wt/mutant ratio in the hexamer, if we accept the formation of the oligomer as model for spastin function. All these observations suggest that spastin may also function as hexamer, although further experiments are needed to confirm this hypothesis.

Although spastin may share functional properties with the known microtubule-severing proteins, several issues are still unresolved. The use of spastin specific

antibodies indicated that spastin localizes to the centrosome and also to other structure, such as the midbody, which are rich in tubulin. This suggests that spastin binds microtubules also outside the centrosome; this association is restricted to a subset of microtubules and is probably related to a remodelling of the cytoskeleton. In this context, it is very interesting the localization of spastin in the growth cones of axons in the NSC34 cell line. Local changes in microtubule organization and distribution are required for the axon to grow. The growth cone of an axon contains a dense array of microtubules that are tightly coalesced into bundles (Dent et al., 1999). During growth of the axon, the microtubule array within the growth cone reorganizes and reorients toward the future direction of axon outgrowth. The presence of short microtubules is essential for the dynamicity of the growth cone. It is known that microtubules fragment to generate short microtubules during the transition from the quiescent to growth states (Dent et al., 1999). The current hypothesis is that microtubule fragmentation may be regulated by factors that locally activate katanin (Ahmad et al., 1999a; Dent et al., 1999; McNally and Thomas, 1998). The finding that spastin localizes at the growth cone may suggest that it can also be involved, together with katanin perhaps, in the cytoskeleton reorganization of the axon. Therefore, spastin may act as a microtubule severing protein not only at the centrosome, but also in different locations, where probably there is a higher requirement of cytoskeleton reorganization. This aspect would be very important because of the specific cellular phenotype of the disease. Moreover, the current model is that most of the cellular mechanisms that regulate the microtubule arrays of the postmitotic neuron are variations of mechanisms that organize microtubules in mitotic cells (Baas, 1999). In this context, we can speculate that spastin may act

during cell cycle in non neuronal cells because of its localization at the centrosome and at the midbody, and that spastin function is then used by postmitotic neurons for cytoskeleton remodelling in the regulation of important processes such as axonal growth and axonal transport.

It is still unclear if the association of spastin with microtubules is direct or mediated by other proteins. We have isolated a centrosomal protein, Na14 as a putative spastin interactor. Notably, Na14 is a nuclear autoantigen found in patients with an autoimmune disease, the Sjogren syndrome (Ramos-Morales et al., 1998). Na14 is the homologous of the *Chlamydomonas reinhardtii* DIP13 protein (deflagellation inducible protein 13). DIP13 and Na14 are described as a new class of proteins associated to microtubules, they indeed localize to the basal bodies and flagella in *Chlamydomonas*, as well as centrosomes in HeLa cells and basal bodies and flagella of human sperm cells (Pfannenschmid et al., 2003). RNA interference experiments have showed that the reduction the levels of DIP13 causes defects in cell division with the formation of multiflagellate and multinucleate *Chlamydomonas* cells, suggesting a role for this protein in proper cell division. Based on the cellular localization and on the fact that they both contain the KREE motif similar to the microtubule binding sites found in MAP1B (Noble et al., 1989), it is believed that both Na14 and DIP13 bind microtubules directly (Pfanneschmid, 2003).

We have mapped the region of spastin responsible for the binding to Na14 in the N-terminal moiety of spastin, more precisely between amino acid 50 and 100. This is the same region we have identified as necessary for the microtubules association. An intriguing possibility would be that Na14 represents the anchor for spastin to the centrosome and to the microtubules, although further experiments have

to be performed to confirm this possibility. This hypothesis would draw another line of homology with p60 katanin, which is targeted to the centrosome by the p80 subunit.

7.3 The pathogenic role of spastin missense mutations

Almost all spastin missense mutations fall into the AAA cassette, and they are predicted to interfere with spastin function by altering the AAA domain ability to bind and/or hydrolyze ATP. We have shown that almost all these mutations when transfected into the cells behave as the ATPase defective mutant (table 4) and therefore they constitutively bind to microtubules. An exception is the S362C mutant; in fact its subcellular localization is undistinguishable from the *wt*. In order to understand the effect of the missense mutations, we have generated a structural model for the AAA cassette of spastin and we have analyzed the localization of the mutated residues on the model. The features of each mutation with respect to the structural model are summarized in table 7. Some mutations occur in residues involved in the active site formation, some other are exposed on the protein surface, localized in structural elements or at the interface between subunits in the hexameric models. On these bases, it is clear that each mutation, depending on its location on the structural model, can interfere with the AAA module activity via a different mechanism, and cause a defect in spastin function leading to HSP. For example, the S362C mutant, which has the same subcellular localization of the *wt*, is localized in a □-helix and it is exposed on the protein surface. The substitution from a serine to a

cysteine residue is not dramatic from the point of view of the amino acid characteristics, they both have a polar side chain and the only difference is the presence of the SH group in the cysteine respect to the OH group in the serine. This could explain why we do not see an alteration of the subcellular localization of the S362C mutant. However, since the S362 residue is on the surface of the protein on the AAA spastin model, a substitution in this position can interfere with protein interactions altering spastin function and leading to HSP. An important point would be to investigate if this mutant can promote microtubule disassembly when transfected in cells.

Previous studies of genotype-phenotype correlation showed that there is no difference in the severity of spastic paraplegia between patients with missense mutations and those with mutations that lead to a premature protein termination (Fonknechten et al., 2000). Whenever the level of spastin mRNA has been tested in tissues from patients with this last kind of mutations, it has been found that the mRNA was greatly reduced. These findings are consistent with mRNA instability and have suggested that haploinsufficiency is the molecular cause of the disease (Burger et al., 2000). However, our data on the possible association between *wt* and mutated protein open up the possibility that a dominant negative pathogenic mechanism could be involved in patients with spastin missense mutations. We cannot exclude that the stable association to microtubules of the mutants is an effect of the overexpression and we don't know yet if the mutated protein in SPG4 patients carrying a missense mutation localize to microtubules, therefore the dominant negative hypothesis has to be considered carefully.

Interestingly, in some SPG4 patients a subtle cognitive impairment, primarily affecting executive function, was detected. Disease progression and cognitive impairment appeared to be more severe in carriers with missense mutations than in those with truncating mutations. Moreover the cognitive dysfunction seems to be more frequent in patients with missense mutations (Tallaksen et al., 2003). These findings may validate the hypothesis that a different mechanism from haploinsufficiency may be responsible for the disease in the case of missense mutations.

7.4 Spastin is SUMO-1 modified

Post-translational modifications generally modulate protein function by altering its activity, subcellular localisation and, at least, the ability to interact with other proteins. They thus represent an extremely selective and valid means for the cell to modulate protein function, to trigger cellular response and to control a crucial equilibrium that ensures the survival of the cell.

Specific amino-acid residues of target proteins are chemically modified by molecules, such as phosphate, acetate, lipids or sugar, thus modulating protein function. A unique case in post-translational modification is the covalent attachment of proteins to other proteins. With respect to small molecule modifiers, protein modifiers have larger and more chemically varied surfaces, and they represent a tool for altering protein conformation and protein-protein interactions. The first and

probably better characterised example of a protein acting as a modifier is Ubiquitin. Ubiquitination is a post-translational modification in which the C-terminus of the small protein ubiquitin is covalently attached to lysine side chains of target proteins; this process is an important step in earmarking a protein for proteasomal degradation.

In recent years many proteins related to ubiquitin have been identified. SUMO-1 is a small protein of 11.5 KDa with high structural homology to Ubiquitin (Bayer et al., 1998). Like Ubiquitin, SUMO-1 is synthesised as a prepolypeptide that is cotranslationally processed to expose the mature glycine dipeptide conserved in ubiquitin and responsible for conjugation. The similarity in the three-dimensional structure reflects a similar function, and both proteins modify target substrates via formation of a covalent isopeptide bond. SUMO is covalently conjugated to target proteins, in a similar multistep process to ubiquitination (Fig. 48).

SUMO-1 is activated by formation of a thioester bond between the carboxyterminal glycine and a cysteine of the SUMO-activating E1 enzyme. The SUMO-activating is a heterodimeric complex of two subunits, respectively of 38 (SAE1) and 72 (SAE2) kDa (Desterro et al., 1999). Once activated, SUMO-1 is transferred to a conjugating E2 enzyme (Ubc9) (Desterro et al., 1997; Johnson and Blobel, 1997; Saitoh, 1997; Schwarz et al., 1998) and finally passed to the ε amino group of specific lysine residues on target proteins. In some cases, at least, this last step is regulated by SUMO-specific ligases (E3s).

In fact, recently, members of the Siz/PIAS (protein inhibitor of activated STAT) protein family (Johnson and Gupta, 2001; Kahyo et al., 2001; Schmidt and Muller, 2002; Takahashi et al., 2001) have been found to function as E3 ligase for SUMO. They have, in fact, the capability to interact with both UBC9 and the target protein

and to increase the rate and the efficiency of the modification reaction. The Siz/PIAS proteins are structurally characterized by the presence of a central RING finger-like domain (Hochstrasser, 2001), which is necessary for ligase activity. However different kinds of SUMO ligases, like RanBP2 (Ran binding protein 2) (Kirsh et al., 2002; Miyauchi et al., 2002; Pichler et al., 2002) and the polycomb protein Pc2 (Kagey et al., 2003), have also been identified.

In the yeast two hybrid system we found that spastin interacts with SAE2, UBC9 and SUMO-1. In particular the bait that permitted us to identify the interactions with the SUMO1 machinery is the spastin$^{\Delta N}$ (the construct lacking the first 263 amino acid). When the spastin^{FL} construct (spastin full length) was used in the interaction mating assay, we could not confirm the interaction with SAE2, UBC9 and SUMO1. Spastin^{FL} did not interact with the other proteins isolated from the screening with spastin$^{\Delta N}$ bait, Daxx and Brd7. We have then used different deletion constructs (designed to generate a fusion protein between the DNA binding domain of the LexA and spastin deleted of the first 50, 100 or 190 amino acids) and found that SAE2, UBC9, SUMO1, Daxx and Brd7 were interacting with Δ190 spastin and Δ100 spastin constructs but not with the Δ50 construct. Therefore, we hypothesized that in the full length and in the Δ50 construct the presence of the portion of spastin protein between amino acids 1-50 leads LexA-spastin to acquire a fold which inhibits the interaction with the described molecules. An alternative explanation is that the region 1-50 contains sites responsible for a negative regulation of SUMO1 conjugation and also of the interaction with Daxx and Brd7.

To confirm that spastin is SUMO-1 modified, we have used the in vitro conjugation assay. In this assay, full length spastin is SUMO-1 conjugated. The size of the sumoylated spastin suggests that spastin is mono-SUMO-1 conjugated.

The lysine which is sumoylated on a target protein belongs, usually, to a consensus sequence Ψ-K-x-D/E, where Ψ is a hydrophobic residue, K is the lysine conjugated to SUMO, x is any amino acid, D or E is an acidic residue.

We have identified three lysines in spastin primary structures, which are good candidate for SUMO-1 conjugation: K340, K462 and K565. The analysis of the location of these lysines on our structural model showed that K340 and K462 are exposed on the protein surface, while K565 is quite hidden in the structure. This leads us to identify K340 and K462 as the strongest candidates for SUMO-1 conjugation. Notably, these lysines are conserved in human, mouse and Drosophila. Unfortunately, we were not able to identify the residue responsible for the SUMO-1 conjugation, neither in the yeast nor in the in vitro system. Using single or double mutants of the candidate lysines in the *in vitro* assay, we could not abrogate the spastin SUMO-1 modification. It is possible that even if we are knocking out the real target lysine (or lysines), other lysines become reactive in the *in vitro* assay. We can not exclude at this point that both K340 and K462 are modified.

Future experiments to confirm that spastin is SUMO-1 modified *in vivo* will be performed. We will investigated if overexpressing SUMO-1 and UBC9 into cells, we can promote the sumoylation of spastin and see the presence of a slower migrating spastin form by immunoblot analysis. Because the levels of spastin in total cell extracts are low, we will try to co-immunoprecipitate spastin and SUMO-1 both in untransfected cells and in cells transfected with SUMO-1 and UBC9. An interesting

observation is that when we overexpress Daxx in cells, we detect an additional band with respect to the endogenous spastin. This band has a higher molecular weight and we hypothesized that this slower migrating form represents the sumoylated spastin.

SUMO-1 is a versatile modifier for a large number of proteins in many different pathways. SUMO-1 conjugation (sumoylation) is highly regulated in all eukaryotes and participates in several processes, such as nuclear transport, transcriptional regulation, chromosome segregation and cell cycle control (Scheuring et al., 2001)(Table 8). SUMO-1 is responsible for the post-translational modification of many target proteins such as RanGAP1, PML, Sp100, p53 and IkBα (Desterro et al., 1998; Kamitani et al., 1997; Matunis et al., 1996; Rodriguez et al., 1999; Saitoh, 1997). For example, SUMO-1 conjugation of RanGAP1 seems to be necessary for its translocation to the nuclear envelope, where it binds RanBP2, a cytoplasmic component of the nuclear pore complex (NPC) (Mahajan et al., 1998). RanBP2 is a GTPase required for the transport of proteins across the NPC, and its GTP/GDP cycle is regulated by RanGAP1. Interestingly a necessary requirement for the functional interaction of RanGAP1 with RanBP2 is the SUMO-1 modification of RanGAP1 (Mahajan et al., 1998). Moreover, recent data showed that sumoylation is also required for targeting RanGAP1 to mitotic spindle and kinetochores in dividing cells (Joseph et al., 2002). Thus sumoylation seems to be involved both in regulating protein-protein interaction and in targeting of substrate proteins to specific cellular compartment upon modification (Seeler and Dejean, 2003). Another important function for SUMO-1-modification consists in modulation of transcription. A number of transcription factors are sumoylated. Among them are p53, the androgen receptor, LEF1, C/EBPs, Sp3 and many more (Verger et al., 2003). SUMO-1

modification can either activate or, more frequently, repress their transactivating function. In particular, sumoylation is regulating the transcription factor Sp3, by leading to a repression of its transcriptional targets in association with a relocalization of Sp3 from a diffuse subnuclear distribution to nuclear speckles (Ross et al., 2002; Sapetschnig et al., 2002). Besides, a number of transcriptional co-factors, such as HDAC1 (Colombo et al., 2002; David et al., 2002)or p300 (Girdwood et al., 2003), are sumoylated. This modification is important for optimal protein function as co-activator or co-repressor. In fact, p300-sumoylation seems to be necessary for the repressing activity of p300 by enabling the recruitment of the histone deacetylase HDAC6.

All these examples show that there is a wide spectrum of physiological processes affected by sumoylation, highlighting the importance of this modification. Sumoylation is a highly dynamic and fully reversible modification. A family of cysteine proteases specifically hydrolyze SUMO isopeptide bonds; therefore substrates are continuously conjugated and deconjugated, depending on the cellular requests.

Unfortunately, the SUMO-1 conjugation has been involved in so many different processes that it is very difficult to predict the role that the modification would have on a target protein. We have strong indications that spastin is SUMO-1 modified, but which is the effect of this modification on spastin function is unknown. Because we observe different subcellular localization of spastin, one hypothesis could be that SUMO-1 conjugation is important for acquiring one of these subcellular localizations. In particular we have revealed a co-localization of spastin with the PML bodies in human fibroblasts.

The PML protein was first identified as part of a fusion product with the retinoic acid receptor alpha, resulting from the t(15;17) chromosomal translocation associated with acute promyelocytic leukemia (Grimwade and Solomon, 1997). PML is tightly bound to the nuclear matrix and is concentrated in defined subnuclear structures (NB, nuclear bodies or PML bodies or ND10) that are disorganised in certain human disease, such as leukemia, neurodegenerative disorder and viral infections. PML is the scaffold for the NB formation and it can recruit to the NB several other proteins. PML undergoes SUMO-1 conjugation and this modification seems to be a pre-requisite for the formation of these structures (Zhong et al., 2000). It is interestingly to observe that various proteins that transiently associate with NB, such as p53 (Kwek et al., 2001; Muller et al., 2000), Daxx (Jang et al., 2002), Lef-1 (Sachdev et al., 2001) are also sumoylated. But in these cases it is not clear if the sumoylation is a pre-requisite for NB localisation or if NB might be a site for SUMO-conjugation. In the case of Sp100, its sumoylation is not necessary for its NB localisation and in fact in absence of PML SUMO1-Sp100 is not able to acquire a NB localisation (Sternsdorf et al., 1999; Zhong et al., 2000).

The function of PML bodies is still unclear; the variety of their components suggests a wide range of possible functions, such as tumor and growth suppression and transcription regulation. An interesting hypothesis is that PML bodies act as storage sites, modulating concentrations of nuclear proteins by sequestering them until required and that they may be sites of post-translational modification of PML body components (Maul et al., 2000; Negorev and Maul, 2001).

In this context, we can hypothesize that spastin is either sumoylated in order to be translocated to the PML bodies or that it is recruited to the PML bodies where it could be SUMO-1 modified.

It is interestingly to note that recent studies implicate a role for the SUMO-1 modification in neurodegenerative disease (Lieberman, 2004). Neurons in affected regions of the brain of patients with polyglutamine disease, such as Huntington's disease, spinocerebellar ataxia type 1, Machado Joseph disease, and dentate-rubro-pallido-luysian atrophy (DRPLA) are strongly immunoreactive to SUMO-1 (Ueda et al., 2002). SUMO-1 modified proteins accumulate in the intranuclear aggregates of neuronal intranuclear inclusion disease (Poutney, 2004). Furthermore, an increase of sumoylation has been observed in brain tissues from patients with spinocerebellar ataxia type 3 (SCA3) and DRPLA (Terashima, 2002), and SUMO-1 aggregates were identified in neurons from patients with SCA3 (Pountney et al., 2003). An additional link between neurodegeneration and the SUMO pathway was found in Drosophila studies. A Drosophila model of polyglutamine disease was used to show that the disruption of the SUMO pathway may increase polyglutamine toxicity (Chan et al., 2002). A recent study showed that a pathogenic fragment of Huntingtin, the protein responsible for the Huntington disease, can be modified either by ubiquitin or by SUMO-1 on identical lysine residues. The SUMO-1 modification of this fragment seems to stabilize the protein, reduce its ability to aggregate and to increase the repression effect of Huntingtin on transcription (Steffan et al., 2004). Moreover, in a Drosophila model of Huntington disease, the expression of the pathogenic fragment of Huntingtin causes the lost of photoreceptor neurons and the disruption of the eye (Steffan et al., 2001). It has been demonstrated in this model that sumoylation of the

fragment worsens the neurodegeneration phenotype (Steffan et al., 2004). Therefore SUMO-1 pathway may contribute to the pathogenesis of certain neurodegenerative diseases, although further studies will be needed to understand the role of SUMO in these disorders. Further investigation will probably answer the question on which is the role for SUMO-1 modification with respect to spastin function and to hereditary spastic paraplegia.

7.5 Spastin and Daxx: a nuclear role for Spastin

We have shown that, at least in human fibroblasts, spastin localizes to the PML bodies. It is unclear why this localization is not conserved in all cell type, but it was confirmed using different spastin specific antibodies raised against different antigens. More interestingly this nuclear localization is validated by the isolation of nuclear partners for spastin. In particular we have isolated Daxx and SUMO-1 which are clearly related to the PML bodies. We have already discussed about the possibility that spastin is recruited to the PML bodies in order to be SUMO-1 modified and an additional corollary could be that this modification is a prerequisite for the interaction with nuclear bodies components, such as Daxx. Alternatively, SUMO-1 conjugation would translocate spastin to the nucleus where it can interact with its nuclear partners. Even if the PML bodies localization seems to be extremely cellular specific, a nuclear localization of spastin is underlined in all the cell type analysed. Therefore, spastin seems to have a complex subcellular localization, which is confirmed by the isolation of different classes of molecular interactors, suggesting that spastin may absolve different functions depending on its localization and its "partner". This concept is not unusual in the field of the AAA proteins. Indeed, an AAA protein represents an enzymatic activity, a source of chemical energy that can be used to different purposes depending on the molecule to which is coupled. A well studied example is p97. Several adaptor proteins have been identified for p97, which is involved in different cellular processes, such as ubiquitin-dependent processes and membrane fusion, depending on the co-factor to which is complexed (Cao et al., 2003; Meyer et al., 2000; Wojcik et al., 2004; Yamada et al., 2000).

One of the molecular interactor of spastin isolated by the two hybrid screening is Brd7, a bromodomain containing protein. The bromodomain is an evolutionary highly conserved domain in human, *Drosophila* and yeast proteins (Hirose and Manley, 2000) of approximately 110 aa that is found in over 40 proteins (Conrad et al., 2000). Many of these proteins are involved in transcriptional control. The conserved bromodomain is responsible for the interaction with transcriptionally active chromatin, and, in particular, for binding to acetylated lysine in histone tails (Dhalluin et al., 1999; Dyson et al., 2001; Jacobson et al., 2000; Owen et al., 2000). Bromodomains may thus be important determinants for targeting proteins or protein complexes to specific chromosomal sites by binding to acetylated histones and thereby regulating transcriptional activity (Kzhyshkowska et al., 2003). Further experiments are needed to understand if Brd7 is a real interactor of spastin.

We have demonstrated that full length spastin interacts physically with Daxx and that the cellular overexpression of daxx causes an upregulation of spastin transcript. Daxx is a multi-functional protein that modulates both apoptosis and transcription (Tang et al., 2004). Daxx seems to have alternative roles shuttling between the nucleus and the cytoplasm (Charette et al., 2000; Ko et al., 2001). However, it is predominantly nuclear (Kiriakidou et al., 1997; Pluta et al., 1998) and has been shown to associate with PML and to localize within PML nuclear Bodies (Ishov et al., 1999; Li et al., 2000a; Torii et al., 1999). Daxx is also SUMO-1 modified, but the sumoylation status of Daxx doesn't affect its localization in the PML bodies (Jang et al., 2002). Daxx recruitment to PML bodies has been reported to be essential for its pro-apoptotic effect and also to relieve its transcriptional repressive activity (Ishov et al., 1999; Li et al., 2000a; Zhong et al., 2000).

The ability of Daxx to interact with multiple cellular factors has resulted in its involvement in several putative functions, but its exact role still awaits elucidation (Michaelson, 2000). Many reports have suggested a role for Daxx in apoptosis, but whether it functions as a pro- or anti-apoptotic molecule is still poorly understood. In fact, Daxx was initially isolated as a pro-apoptotic molecule that binds the intracellular domain of Fas and enhances Fas-mediated apoptosis through the induction of the Jun amino-terminal kinase (JNK)(Yang et al., 1997). Daxx associates with and activates the Apoptosis Signal-regulating Kinase 1 (ASK1), a kinase of the JNK pathway (Chang et al., 1998). Moreover, hDaxx has been involved also in TGFß-induced (Perlman et al., 2001) as well as in nuclear, PML-dependent apoptotic pathways (Torii et al., 1999; Zhong et al., 2000). Depletion of hDaxx by antisense RNA showed a protective effect toward TGFß-induced apoptosis (Perlman et al., 2001).

In contrast with these observations, Daxx knock-out embryos showed early embryonic lethality and studies with Daxx-null murine embryonic stem cells revealed an anti-apoptotic role of this protein (Michaelson et al., 1999). Recently it has been shown that ablation of Daxx expression by RNA interference can cause increase in apoptosis in different cell types and that this effect is rescued by Bcl-2 overexpression (Michaelson and Leder, 2003). The pro-apoptotic function of Daxx within the nucleus has been linked with its ability to function as a transcriptional repressor (Hollenbach et al., 1999; Li et al., 2000b).

Daxx has indeed a role as a transcription regulator. It associates with several transcription factors, such as Pax3, Pax5, ETS1 and it seems to act as a repressor of the transcription (Emelyanov et al., 2002; Hollenbach et al., 1999; Li et al., 2000a; Li

et al., 2000b; Lin et al., 2003). Even though Daxx was shown to repress transcription in most of the cases, it has been shown that, in the case of Pax5, interaction with Daxx may result either in transcriptional repression or activation, depending on the cell type (Emelyanov et al., 2002). Daxx activity in a particular promoter context may be differentially regulated by association with transcription factors and additional co-repressors or co-activators. In fact, in the case of Pax5, Daxx was also found in complex with the transcriptional co-activator CBP (Emelyanov et al., 2002).

Daxx localizes to the PML bodies and more data strengthen the idea that the nuclear bodies can be a critical compartment for the regulation of transcription. PML has been implicated in transcriptional regulation and has been shown to modulate responses on different promoters via interaction and sequestration of co-activators or co-repressors to the PML bodies (Borden, 2002; Negorev and Maul, 2001). The PML bodies can, therefore, regulate transcriptional activity by limiting the access of regulatory proteins to their target genes or they can contribute to the assembly of transcriptional complex by bringing the complex components next to each other (Tang et al., 2004). A recent report indicates that PML bodies form in nuclear compartments of high transcriptional activity, but they do not directly regulate transcription of genes in these compartments (Wang et al., 2004).

In our study, we have found that spastin associates with Daxx, but we don't know if the interaction between these two proteins may be dependent on their localization to the PML bodies. We have detected spastin to the PML bodies only in human fibroblasts, while we have confirmed the interaction between Daxx and Spastin in HeLa cells. An important point would be to demonstrate the interaction between these two proteins also in human fibroblasts, performing co-

immunoprecipitation experiments with both endogenous proteins. Since we have indications that both proteins are probably SUMO-1 modified, an important factor in the formation of the complex spastin/daxx may be the SUMO-1 modification.

We have transfected Daxx into HeLa cells and we have performed co-immunoprecipitation experiments to demonstrate that the endogenous spastin interact with the exogenous Daxx. From immunoprecipitation experiments it is evident that Daxx is able to immunoprecipitate two bands, a band with an apparent molecular weight of 68 kDa, which corresponded to the endogenous spastin and a band that correspond to a higher molecular weight specie of about 90 kDa. The idea that the slow migrating band around 90 kDa may represent a sumoylated spastin is extremely fascinating. One can hypothesize that SUMO-1 modification of spastin is required for the interaction of spastin with its nuclear partner and therefore it's important for the nuclear function of the protein.

The other experimental evidence is that the overexpression of Daxx in HeLa cells causes an increase in the transcriptional levels of spastin. Daxx may regulate the levels of transcription of the spastin gene, but we have also shown that Daxx and spastin physically interact. A hypothesis could be that spastin and Daxx are part of a transcriptional complex and that one of the target genes of this complex is spastin itself. Interestingly, studies on muscle from SPG4 patients (both with missense mutations and nonsense mutations) showed that there are dramatic and disease-specific alterations in the transcriptome, with the down-regulation of genes associated with microtubule, protein and vesicle trafficking pathways (Molon et al., 2004). Muscle biopsies showed no signs of pathology; therefore these data suggest that many or most cells of the body have similar disruption of microtubule pathways

as a consequence of SPG4 mutations, but they seem able to survive with little or no evidence of cell dysfunction. Motor neurons are known to have particularly stringent requirements for efficient transport of vesicles and proteins through their long axons and processes (LaMonte et al., 2002) and therefore they are particularly sensitive to microtubule defects. This would explain why a defect in a ubiquitous protein leads to a specific cellular phenotype. The same study demonstrates that another important group of down regulated genes includes genes associated with transcriptional and translational machinery (Molon et al., 2004), suggesting a possible role of spastin in the nucleus as a transcription factor (Charvin et al., 2003). These data cannot exclude that the effect on the down regulation of the transcription of the implicated gene is indirect. However an attractive possibility is that spastin and daxx form a transcriptional complex, which probably includes other molecules, and that this complex functions activating the transcription of several genes, including the SPG4.

CONCLUSIONS

Spastin is the protein mutated in the most common form of hereditary spastic paraplegia. We have found that spastin has a complex subcellular localization, both nuclear and cytosolic, and that the protein has multiple functions, probably depending on its compartmentalization into the cell.

We have demonstrated that spastin localizes to the centrosomes and to regions rich in microtubules during cell cycle. We have also seen that in motoneuronal cells, spastin signal is enriched in the growth cone. We have indication that spastin associates dynamically with microtubules, this association is mediated by the N-terminal portion of spastin and is regulated through the nucleotide binding state of the AAA domain. We have seen that ATPase-defective spastin localizes constitutively to microtubules. The association of the ATPase-defective spastin to microtubules provokes a reorganization of the microtubule cytoskeleton with the formation of thick perinuclear bundles. Moreover the overexpression of wt spastin promotes microtubule disassembly in transfected cells. All these data, together with the homology with katanin, suggest that spastin may act as a microtubule severing protein.

The localization of endogenous spastin to regions where a highly dynamic reorganization of the cytoskeleton is required, such as the midbody, the centrosome or the growth cone of axons, well fit with the hypothesis of a role for spastin in microtubule dynamic. Moreover, we have isolated a centrosomal protein, Na14, as spastin molecular interactor. We have shown that the region of spastin responsible for the binding to Na14 is the same region involved in the microtubule association.

We have therefore hypothesized that Na14 is responsible for the association of spastin to the centrosome and to microtubules.

In neurons all the protein necessary for axonal surviving and growth are produced in the cell body and then transported along the axon. Microtubules play a very important role in this process and they have to be maintained sufficiently short to be efficiently transported along the axon. So microtubules are nucleated at the centrosome (Fig. 49A) and then actively transported along axons and dendrites. In this context, microtubule severing activities, as katanin and perhaps spastin, have a crucial role in generating short microtubules that will guarantee the transport of mitochondria, endosomes and of all the molecules that the axon will need for its growth and function.

We have also shown that spastin may have a different function in the nucleus. We have seen, in fact, that spastin localizes also to the nucleus and we have isolated several nuclear interactors. In particular, we have demonstrated that spastin interacts with Daxx and that Daxx overexpression positively regulates SPG4 transcription. These data and the recent findings that the downregulation of genes involved in the organization of microtubule cytoskeleton is observed in muscles of SPG4 patients (Molon et al., 2004) lead us to hypothesize that spastin can be part of a transcriptional complex and be involved in the regulation of genes important for the organization of microtubule cytoskeleton. In this case spastin defects will still affect axonal transport although via a different mechanism.

We have also evidence that spastin is subjected to a post-translational modification: SUMO-1 conjugation. Which is the role of this modification is still

unknown, although several hypotheses can be done regarding the importance of the SUMO-1 modification for the nuclear localization of spastin and its nuclear function.

Therefore, we propose that the impairment of the fine regulation of the microtubule cytoskeleton in long axons may underlie pathogenesis of HSP due to spastin mutations.

Interestingly, mice deficient for stathmin, a microtubule-destabilizing factor, develop an age-dependent axonopathy with the dysmyelination and the degeneration of axons of the central and peripheral nervous systems (Liedtke et al., 2002).

This idea fits well with the putative functions of other genes involved in HSP. In fact, the genes identified as responsible for the different forms of HSP include endosomal, mitochondrial and microtubule motor proteins, supporting the hypothesis that any defect of normal trafficking processes and therefore of the axonal transport, may lead to axonal degeneration.

In the model described above (Fig. 49B) it is clear how a defect in a severing activity (spastin) or in a kinesin protein (KIF5a), or in mitochondrial proteins (Paraplegin and Hsp60) or in endosomal protein (Spartin and Atlastin) can affect the efficiency of the axonal transport. An additional point of view comes from a possible role for spastin in reorganizing the microtubule network of the growth cone of axons, a fundamental process for the growth of the axon. A defect in the cytoskeleton reorganization of the axon would compromise axonal growth leading to the degeneration of the axon.

The long axons composing the corticospinal tracts and the fasciculus gracilis would be preferential pathological target for this defect. Therefore, the impairment of

the axonal transport seems to be the common cause of a group of hereditary spastic paraplegia (Crosby and Proukakis, 2002; Fink, 2003; Reid, 2003).

Protein	Function	Role of Sumoylation	References
Mammalian			
RanGAP1	Nuclear import	Mediates interaction with RanBP2	(Mahajan et al., 1998) (Matunis et al., 1996)
PML	Tumor suppressor	Allows formation of NBs and recruitment of other molecules to the NBs	(Duprez et al., 1999; Muller et al., 1998) (Sternsdorf et al., 1997)
Sp100	Chromatin remodelling (?)	Mediates interaction with HP1	(Jang et al., 2002; Seeler et al., 2001; Seeler et al., 1998; Sternsdorf et al., 1999)
Daxx	Transcriptional repression		(Jang et al., 2002)
p53	Tumor suppressor	Activate p53 transactivation and apoptosis	(Gostissa et al., 1999; Rodriguez et al., 1999)
p73	P53 homologue	Unknown	(Minty et al., 2000)
HIPK2	Transcriptional corepression	Mediates the localisation of HIPK2 to nuclear dots	(Kim et al., 1999)
TEL	Transcriptional repression	Mediates the localisation of TEL to nuclear dots	(Chakrabarti and Nucifora, 1999; Chakrabarti et al., 2000)
c-Jun	Trascriptional activation	Sligthly reduces transcriptional activity of c-Jun	(Muller et al., 2000)
Androgen receptor	Trascriptional activation	Reduces transcriptional activity of androgen receptor	(Poukka et al., 2000)
I□B□	Signal trunsduction, NF-□B inhibition	Inhibits ubiquitination of IκBα̃ Blocks NF-κB activity	(Desterro et al., 1998)
Mdm2	E3 ubiquitin ligase for p53	Inhibits ubiquitination of Mdm2, activates the E3 function of Mdm2	(Buschmann et al., 2000)
Topoisomerase I	DNA replication/ repair	Unknown	(Mao et al., 2000b)
Topoisomerase II	DNA replication/ repair	Unknown	(Mao et al., 2000a)

WRN	DNA helicase Req family	Unknown	(Kawabe et al., 2000)
RanBP2	Component of nuclear pore complex	Unknown	(Saitoh et al., 1998)
GLUT1	Glucose transport	Unknown, GLUT1 protein levels are downregulated by UBC9	(Giorgino et al., 2000)
GLUT4	Glucose transport	Unknown, GLUT4 protein levels are upregulated by UBC9	(Giorgino et al., 2000)
TIF1□	chromatin-associated factor	Unknown	(Seeler and Dejean, 2001)
Yeast			
Septins (Cdc33p,Cdc11p,Sep7p)	Bud-neck formation	Regulates dynamics of the neck ring	(Johnson and Blobel, 1999; Takahashi et al., 1999)
Drosophila			
Tramtrack 69	Trancrptional repression	Unknown	(Lehembre et al., 2000)
Dorsal	Signal transduction	Activates nuclear import of dorsal	(Bhaskar et al., 2000)
CaMK	Calcium/calmodulin-dependent kinase	Unknown	(Long and Griffith, 2000)
Viral proteins			
CMV-IE1	Cytomegalovirus-immediate early regulator	Unknwon. Correlates with the loss of PML sumoylation	(Muller and Dejean, 1999)
CMV-IE2	Cytomegalovirus-immediate early regulator	Decrease trasactivation potential of IE2	(Hofmann et al., 2000)
Ad-E1B	Adenovirus-early protein 1B	nuclear import of E1B protein	(Endter et al., 2001)
HPV/BPV-E1	Human and bovine papilloma virus DNA helicase (initiates viral replication)	Regulates nuclear import of E1	(Rangasamy et al., 2000)
EBV-BZLF1	Epstein Barr virus-immediate early regulator	Unknwon. Correlates with the loss of PML sumoylation	(Adamson et al., 2000)

Table 8. Known substrates for SUMO-1 (Muller et al., 2001).

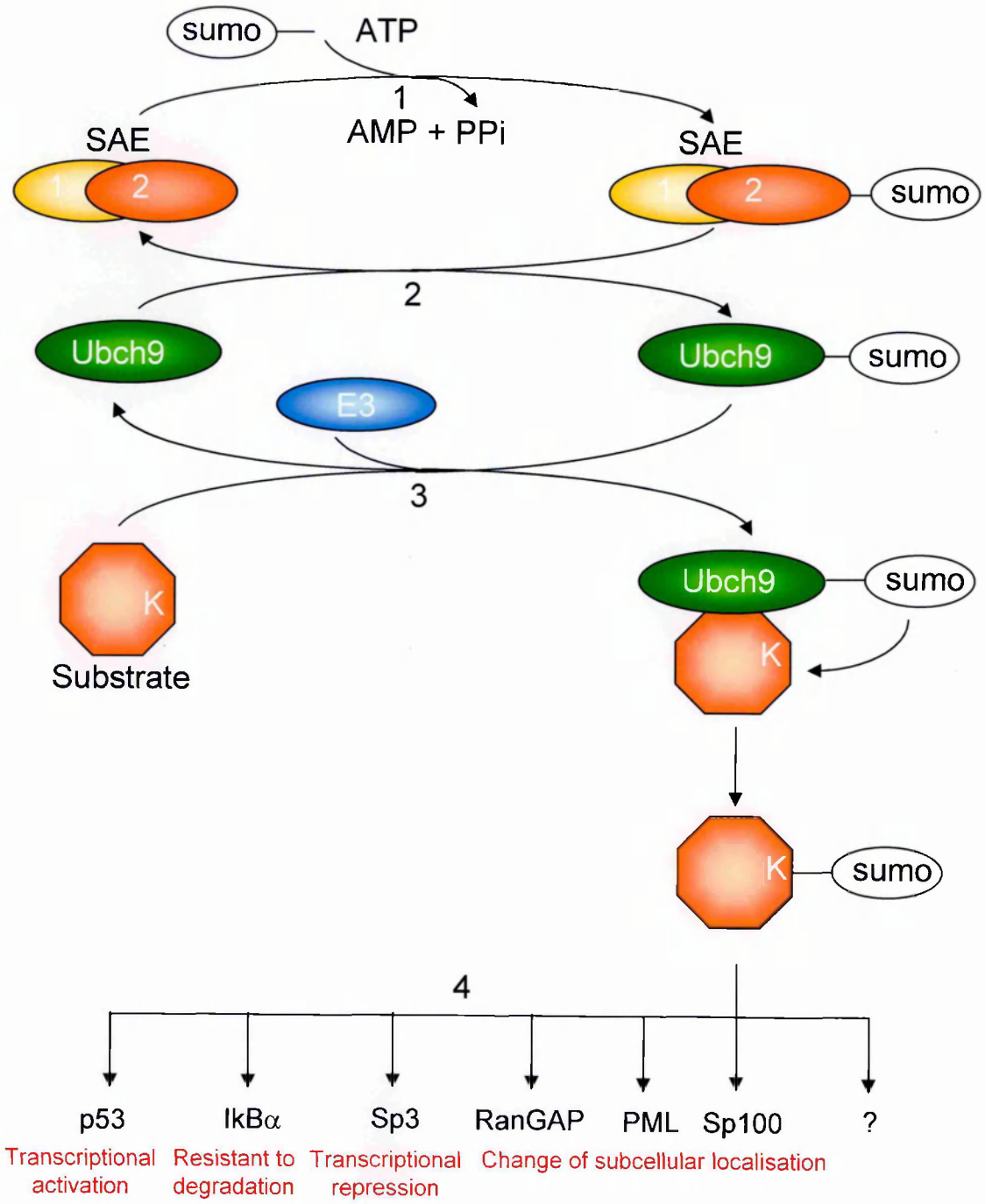

Figure 48. SUMO-1 conjugation pathway.

(1) In the first step of the SUMO-1 conjugation pathway, the SUMO-1 activating enzyme (SAE1/2) catalyses the ATP dependent activation of SUMO-1 protein. (2) Then SAE1/2 catalyzes the transfer of SUMO-1 to the active cysteine residue of the SUMO conjugating enzyme, UBC9. (3) Finally an isopeptide bond is formed between the C-terminal glycine in the SUMO and the e-amino group of a lysine in the target protein. This can occur in the absence of an additional factor or might require an E3 ligase. (4) SUMO-1 modified protein and effect of SUMO-1 conjugation.

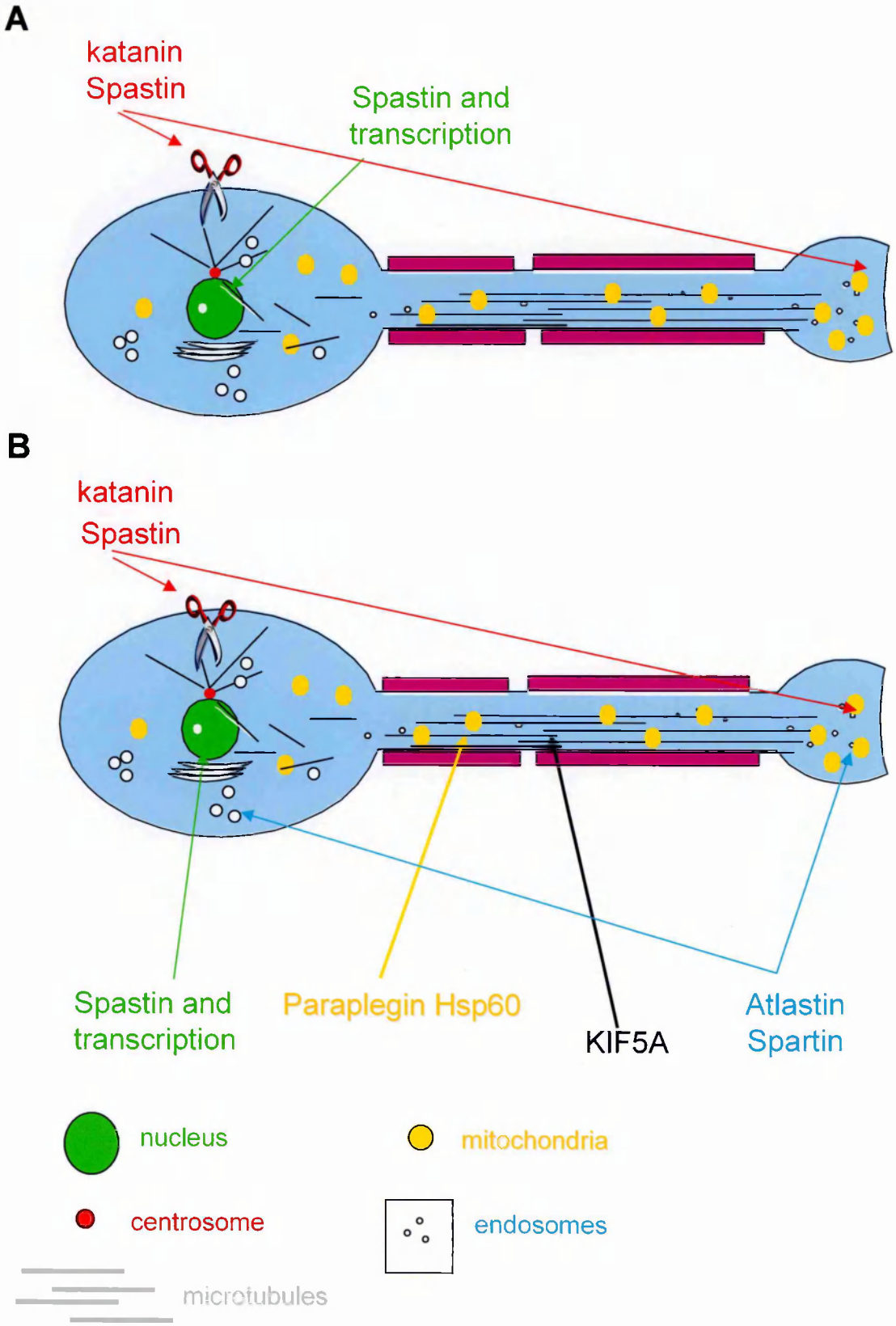

Figure 49. A model for hereditary spastic paraplegia.

In this model it is illustrated how the impairment of the axonal transport can be a common basis for a group of HSPs.

CHAPTER 8: REFERENCES

Acharya, U., Jacobs, R., Peters, J. M., Watson, N., Farquhar, M. G., and Malhotra, V. (1995). The formation of Golgi stacks from vesiculated Golgi membranes requires two distinct fusion events. Cell *82*, 895-904.

Adamson, A. L., Darr, D., Holley-Guthrie, E., Johnson, R. A., Mauser, A., Swenson, J., and Kenney, S. (2000). Epstein-Barr virus immediate-early proteins BZLF1 and BRLF1 activate the ATF2 transcription factor by increasing the levels of phosphorylated p38 and c-Jun N-terminal kinases. J Virol *74*, 1224-1233.

Aderem, A., and Underhill, D. M. (1999). Mechanisms of phagocytosis in macrophages. Annu Rev Immunol *17*, 593-623.

Ahmad, F. J., Yu, W., McNally, F. J., and Baas, P. W. (1999a). An essential role for katanin in severing microtubules in the neuron. J Cell Biol *145*, 305-315.

Ahmad, F. J., Yu, W., McNally, F. J., and Baas, P. W. (1999b). An essential role for katanin in severing microtubules in the neuron. J Cell Biol *145*, 305-315.

Almenar-Queralt, A., and Goldstein, L. S. (2001). Linkers, packages and pathways: new concepts in axonal transport. Curr Opin Neurobiol *11*, 550-557.

Amann, E., Brosius, J., and Ptashne, M. (1983). Vectors bearing a hybrid trp-lac promoter useful for regulated expression of cloned genes in Escherichia coli. Gene *25*, 167-178.

Andersen, J. S., Wilkinson, C. J., Mayor, T., Mortensen, P., Nigg, E. A., and Mann, M. (2003). Proteomic characterization of the human centrosome by protein correlation profiling. Nature *426*, 570-574.

Anderson, R. G. (1998). The caveolae membrane system. Annu Rev Biochem *67*, 199-225.

Anderson, R. G., and Jacobson, K. (2002). A role for lipid shells in targeting proteins to caveolae, rafts, and other lipid domains. Science *296*, 1821-1825.

Anderton, B. H., Breinburg, D., Downes, M. J., Green, P. J., Tomlinson, B. E., Ulrich, J., Wood, J. N., and Kahn, J. (1982). Monoclonal antibodies show that neurofibrillary tangles and neurofilaments share antigenic determinants. Nature *298*, 84-86.

Apodaca, G. (2001). Endocytic traffic in polarized epithelial cells: role of the actin and microtubule cytoskeleton. Traffic *2*, 149-159.

Atorino, L., Silvestri, L., Koppen, M., Cassina, L., Ballabio, A., Marconi, R., Langer, T., and Casari, G. (2003). Loss of m-AAA protease in mitochondria causes complex I deficiency and increased sensitivity to oxidative stress in hereditary spastic paraplegia. J Cell Biol *163*, 777-787.

Azzouz, M., Leclerc, N., Gurney, M., Warter, J. M., Poindron, P., and Borg, J. (1997). Progressive motor neuron impairment in an animal model of familial amyotrophic lateral sclerosis. Muscle Nerve *20*, 45-51.

Baas, P. W. (1998). The role of motor proteins in establishing the microtubule arrays of axons and dendrites. J Chem Neuroanat *14*, 175-180.

Baas, P. W. (1999). Microtubules and neuronal polarity: lessons from mitosis. Neuron *22*, 23-31.

Baas, P. W., and Joshi, H. C. (1992). Gamma-tubulin distribution in the neuron: implications for the origins of neuritic microtubules. J Cell Biol *119*, 171-178.

Babst, M., Sato, T. K., Banta, L. M., and Emr, S. D. (1997). Endosomal transport function in yeast requires a novel AAA-type ATPase, Vps4p. Embo J *16*, 1820-1831.

Babst, M., Wendland, B., Estepa, E. J., and Emr, S. D. (1998). The Vps4p AAA ATPase regulates membrane association of a Vps protein complex required for normal endosome function. Embo J *17*, 2982-2993.

Barr, V. A., Phillips, S. A., Taylor, S. I., and Haft, C. R. (2000). Overexpression of a novel sorting nexin, SNX15, affects endosome morphology and protein trafficking. Traffic *1*, 904-916.

Bayer, P., Arndt, A., Metzger, S., Mahajan, R., Melchior, F., Jaenicke, R., and Becker, J. (1998). Structure determination of the small ubiquitin-related modifier SUMO-1. J Mol Biol *280*, 275-286.

Beattie, E. C., Carroll, R. C., Yu, X., Morishita, W., Yasuda, H., von Zastrow, M., and Malenka, R. C. (2000). Regulation of AMPA receptor endocytosis by a signaling mechanism shared with LTD. Nat Neurosci *3*, 1291-1300.

Behan, M., Appell, P. P., and Graper, M. J. (1988). Ultrastructural study of large efferent neurons in the superior colliculus of the cat after retrograde labeling with horseradish peroxidase. J Comp Neurol *270*, 171-184.

Behan, W. M., and Maia, M. (1974). Strumpell's familial spastic paraplegia: genetics and neuropathology. J Neurol Neurosurg Psychiatry *37*, 8-20.

Beyer, A. (1997). Sequence analysis of the AAA protein family. Protein Sci *6*, 2043-2058.

Bhaskar, V., Valentine, S. A., and Courey, A. J. (2000). A functional interaction between dorsal and components of the Smt3 conjugation machinery. J Biol Chem *275*, 4033-4040.

Bishop, N. a. W., P. (2000). ATP-ase defective mammalian VPS4 localizes to aberrant endosomes and impairs cholesterol trafficking. Mol Biol Cell *11*, 227-239.

Blatch, G. L., and Lassle, M. (1999). The tetratricopeptide repeat: a structural motif mediating protein-protein interactions. Bioessays *21*, 932-939.

Bochtler, M., Hartmann, C., Song, H. K., Bourenkov, G. P., Bartunik, H. D., and Huber, R. (2000). The structures of HsIU and the ATP-dependent protease HsIU-HsIV. Nature *403*, 800-805.

Borden, K. L. (2002). Pondering the promyelocytic leukemia protein (PML) puzzle: possible functions for PML nuclear bodies. Mol Cell Biol *22*, 5259-5269.

Bradford, M. M. (1976). A rapid and sensitive method for the quantitation of microgram quantities of protein utilizing the principle of protein-dye binding. Anal Biochem *72*, 248-254.

Burger, J., Fonknechten, N., Hoeltzenbein, M., Neumann, L., Bratanoff, E., Hazan, J., and Reis, A. (2000). Hereditary spastic paraplegia caused by mutations in the SPG4 gene. Eur J Hum Genet *8*, 771-776.

Buschmann, T., Fuchs, S. Y., Lee, C. G., Pan, Z. Q., and Ronai, Z. (2000). SUMO-1 modification of Mdm2 prevents its self-ubiquitination and increases Mdm2 ability to ubiquitinate p53. Cell *101*, 753-762.

Cao, K., Nakajima, R., Meyer, H. H., and Zheng, Y. (2003). The AAA-ATPase Cdc48/p97 regulates spindle disassembly at the end of mitosis. Cell *115*, 355-367.

Cardoso, C., Leventer, R. J., Dowling, J. J., Ward, H. L., Chung, J., Petras, K. S., Roseberry, J. A., Weiss, A. M., Das, S., Martin, C. L., *et al.* (2002). Clinical and molecular basis of classical lissencephaly: Mutations in the LIS1 gene (PAFAH1B1). Hum Mutat *19*, 4-15.

Casari, G., De Fusco, M., Ciarmatori, S., Zeviani, M., Mora, M., Fernandez, P., De Michele, G., Filla, A., Cocozza, S., Marconi, R., *et al.* (1998). Spastic paraplegia and OXPHOS impairment caused by mutations in paraplegin, a nuclear-encoded mitochondrial metalloprotease. Cell *93*, 973-983.

Casari, G., and Rugarli, E. (2001). Molecular basis of inherited spastic paraplegias. Curr Opin Genet Dev *11*, 336-342.

Cavanagh, J. B. (1964). The significance of the "dying back" process in experimental and human neurological disease. Int Rev Exp Pathol *3*, 219-267.

Chakrabarti, S. R., and Nucifora, G. (1999). The leukemia-associated gene TEL encodes a transcription repressor which associates with SMRT and mSin3A. Biochem Biophys Res Commun *264*, 871-877.

Chakrabarti, S. R., Sood, R., Nandi, S., and Nucifora, G. (2000). Posttranslational modification of TEL and TEL/AML1 by SUMO-1 and cell-cycle-dependent assembly into nuclear bodies. Proc Natl Acad Sci U S A *97*, 13281-13285.

Chan, H. Y., Warrick, J. M., Andriola, I., Merry, D., and Bonini, N. M. (2002). Genetic modulation of polyglutamine toxicity by protein conjugation pathways in Drosophila. Hum Mol Genet *11*, 2895-2904.

Chang, H. Y., Nishitoh, H., Yang, X., Ichijo, H., and Baltimore, D. (1998). Activation of apoptosis signal-regulating kinase 1 (ASK1) by the adapter protein Daxx. Science *281*, 1860-1863.

Charette, S. J., Lavoie, J. N., Lambert, H., and Landry, J. (2000). Inhibition of Daxx-mediated apoptosis by heat shock protein 27. Mol Cell Biol *20*, 7602-7612.

Charvin, D., Cifuentes-Diaz, C., Fonknechten, N., Joshi, V., Hazan, J., Melki, J., and Betuing, S. (2003). Mutations of SPG4 are responsible for a loss of function of

spastin, an abundant neuronal protein localized in the nucleus. Hum Mol Genet *12*, 71-78.

Chimini, G., and Chavrier, P. (2000). Function of Rho family proteins in actin dynamics during phagocytosis and engulfment. Nat Cell Biol *2*, E191-196.

Ciccarelli, F. D., Proukakis, C., Patel, H., Cross, H., Azam, S., Patton, M. A., Bork, P., and Crosby, A. H. (2003). The identification of a conserved domain in both spartin and spastin, mutated in hereditary spastic paraplegia. Genomics *81*, 437-441.

Cifuentes-Diaz, C., Frugier, T., and Melki, J. (2002). Spinal muscular atrophy. Semin Pediatr Neurol *9*, 145-150.

Coleman, M. P., Conforti, L., Buckmaster, E. A., Tarlton, A., Ewing, R. M., Brown, M. C., Lyon, M. F., and Perry, V. H. (1998). An 85-kb tandem triplication in the slow Wallerian degeneration (Wlds) mouse. Proc Natl Acad Sci U S A *95*, 9985-9990.

Coleman, M. P., and Perry, V. H. (2002). Axon pathology in neurological disease: a neglected therapeutic target. Trends Neurosci *25*, 532-537.

Colombo, R., Boggio, R., Seiser, C., Draetta, G. F., and Chiocca, S. (2002). The adenovirus protein Gam1 interferes with sumoylation of histone deacetylase 1. EMBO Rep *3*, 1062-1068.

Confalonieri, F., and Duguet, M. (1995). A 200-amino acid ATPase module in search of a basic function. Bioessays *17*, 639-650.

Conforti, L., Tarlton, A., Mack, T. G., Mi, W., Buckmaster, E. A., Wagner, D., Perry, V. H., and Coleman, M. P. (2000). A Ufd2/D4Cole1e chimeric protein and overexpression of Rbp7 in the slow Wallerian degeneration (WldS) mouse. Proc Natl Acad Sci U S A *97*, 11377-11382.

Conner, S. D., and Schmid, S. L. (2003). Regulated portals of entry into the cell. Nature *422*, 37-44.

Conrad, N. K., Wilson, S. M., Steinmetz, E. J., Patturajan, M., Brow, D. A., Swanson, M. S., and Corden, J. L. (2000). A yeast heterogeneous nuclear ribonucleoprotein complex associated with RNA polymerase II. Genetics *154*, 557-571.

Cox, G. A., Mahaffey, C. L., Nystuen, A., Letts, V. A., and Frankel, W. N. (2000). The mouse fidgetin gene defines a new role for AAA family proteins in mammalian development. Nat Genet *26*, 198-202.

Crosby, A. H., and Proukakis, C. (2002). Is the transportation highway the right road for hereditary spastic paraplegia? Am J Hum Genet *71*, 1009-1016.

Cross, H. E., and McKusick, V. A. (1967). The Troyer syndrome. A recessive form of spastic paraplegia with distal muscle wasting. Arch Neurol *16*, 473-485.

Cuppen, E., van Ham, M., Pepers, B., Wieringa, B., and Hendriks, W. (1999). Identification and molecular characterization of BP75, a novel bromodomain-containing protein. FEBS Lett *459*, 291-298.

David, G., Neptune, M. A., and DePinho, R. A. (2002). SUMO-1 modification of histone deacetylase 1 (HDAC1) modulates its biological activities. J Biol Chem *277*, 23658-23663.

De Camilli, P., and Takei, K. (1996). Molecular mechanisms in synaptic vesicle endocytosis and recycling. Neuron *16*, 481-486.

Dent, E. W., Callaway, J. L., Szebenyi, G., Baas, P. W., and Kalil, K. (1999). Reorganization and movement of microtubules in axonal growth cones and developing interstitial branches. J Neurosci *19*, 8894-8908.

Desterro, J. M., Rodriguez, M. S., and Hay, R. T. (1998). SUMO-1 modification of IkappaBalpha inhibits NF-kappaB activation. Mol Cell *2*, 233-239.

Desterro, J. M., Rodriguez, M. S., Kemp, G. D., and Hay, R. T. (1999). Identification of the enzyme required for activation of the small ubiquitin-like protein SUMO-1. J Biol Chem *274*, 10618-10624.

Desterro, J. M., Thomson, J., and Hay, R. T. (1997). Ubch9 conjugates SUMO but not ubiquitin. FEBS Lett *417*, 297-300.

Dhalluin, C., Carlson, J. E., Zeng, L., He, C., Aggarwal, A. K., and Zhou, M. M. (1999). Structure and ligand of a histone acetyltransferase bromodomain. Nature *399*, 491-496.

Dickson, D. W. (1998). Pick's disease: a modern approach. Brain Pathol *8*, 339-354.

Dow, M. R., and Mains, P. E. (1998). Genetic and molecular characterization of the caenorhabditis elegans gene, mel-26, a postmeiotic negative regulator of mei-1, a meiotic-specific spindle component. Genetics *150*, 119-128.

Downing, K. H., and Nogales, E. (1998). Tubulin and microtubule structure. Curr Opin Cell Biol *10*, 16-22.

Dubois-Dauphin, M., Frankowski, H., Tsujimoto, Y., Huarte, J., and Martinou, J. C. (1994). Neonatal motoneurons overexpressing the bcl-2 protooncogene in transgenic mice are protected from axotomy-induced cell death. Proc Natl Acad Sci U S A *91*, 3309-3313.

Duprez, E., Saurin, A. J., Desterro, J. M., Lallemand-Breitenbach, V., Howe, K., Boddy, M. N., Solomon, E., de The, H., Hay, R. T., and Freemont, P. S. (1999). SUMO-1 modification of the acute promyelocytic leukaemia protein PML: implications for nuclear localisation. J Cell Sci *112*, 381-393.

Dyson, M. H., Rose, S., and Mahadevan, L. C. (2001). Acetyllysine-binding and function of bromodomain-containing proteins in chromatin. Front Biosci *6*, D853-865.

Emelyanov, A. V., Kovac, C. R., Sepulveda, M. A., and Birshtein, B. K. (2002). The interaction of Pax5 (BSAP) with Daxx can result in transcriptional activation in B cells. J Biol Chem *277*, 11156-11164.

Endter, C., Kzhyshkowska, J., Stauber, R., and Dobner, T. (2001). SUMO-1 modification required for transformation by adenovirus type 5 early region 1B 55-kDa oncoprotein. Proc Natl Acad Sci U S A *98*, 11312-11317.

Evan, G. I., Lewis, G. K., Ramsay, G., and Bishop, J. M. (1985). Isolation of monoclonal antibodies specific for human c-myc proto-oncogene product. Mol Cell Biol *5*, 3610-3616.

Fadok, V. A., and Chimini, G. (2001). The phagocytosis of apoptotic cells. Semin Immunol *13*, 365-372.

Feany, M. B., and La Spada, A. R. (2003). Polyglutamines stop traffic: axonal transport as a common target in neurodegenerative diseases. Neuron *40*, 1-2.

Ferreirinha, F., Quattrini, A., Pirozzi, M., Valsecchi, V., Dina, G., Broccoli, V., Auricchio, A., Piemonte, F., Tozzi, G., Gaeta, L., *et al.* (2004). Axonal degeneration in paraplegin-deficient mice is associated with abnormal mitochondria and impairment of axonal transport. J Clin Invest *113*, 231-242.

Fields, S., and Song, O. (1989). A novel genetic system to detect protein-protein interactions. Nature *340*, 245-246.

Fields, S., and Sternglanz, R. (1994). The two-hybrid system: an assay for protein-protein interactions. Trends Genet *10*, 286-292.

Fink, J. K. (1997). Advances in hereditary spastic paraplegia. Curr Opin Neurol *10*, 313-318.

Fink, J. K. (2003). The hereditary spastic paraplegias: nine genes and counting. Arch Neurol *60*, 1045-1049.

Finley, R. L., Jr., and Brent, R. (1994). Interaction mating reveals binary and ternary connections between Drosophila cell cycle regulators. Proc Natl Acad Sci U S A *91*, 12980-12984.

Fonknechten, N., Mavel, D., Byrne, P., Davoine, C. S., Cruaud, C., Boentsch, D., Samson, D., Coutinho, P., Hutchinson, M., McMonagle, P., *et al.* (2000). Spectrum of SPG4 mutations in autosomal dominant spastic paraplegia. Hum Mol Genet *9*, 637-644.

Fransen, E., Lemmon, V., Van Camp, G., Vits, L., Coucke, P., and Willems, P. J. (1995). CRASH syndrome: clinical spectrum of corpus callosum hypoplasia, retardation, adducted thumbs, spastic paraparesis and hydrocephalus due to mutations in one single gene, L1. Eur J Hum Genet *3*, 273-284.

George, E. B., Glass, J. D., and Griffin, J. W. (1995). Axotomy-induced axonal degeneration is mediated by calcium influx through ion-specific channels. J Neurosci *15*, 6445-6452.

Ghosh, R. N., Mallet, W. G., Soe, T. T., McGraw, T. E., and Maxfield, F. R. (1998). An endocytosed TGN38 chimeric protein is delivered to the TGN after trafficking through the endocytic recycling compartment in CHO cells. J Cell Biol *142*, 923-936.

Giorgino, F., de Robertis, O., Laviola, L., Montrone, C., Perrini, S., McCowen, K. C., and Smith, R. J. (2000). The sentrin-conjugating enzyme mUbc9 interacts with

GLUT4 and GLUT1 glucose transporters and regulates transporter levels in skeletal muscle cells. Proc Natl Acad Sci U S A *97*, 1125-1130.

Girdwood, D., Bumpass, D., Vaughan, O. A., Thain, A., Anderson, L. A., Snowden, A. W., Garcia-Wilson, E., Perkins, N. D., and Hay, R. T. (2003). P300 transcriptional repression is mediated by SUMO modification. Mol Cell *11*, 1043-1054.

Goldstein, L. S. (2001). Kinesin molecular motors: transport pathways, receptors, and human disease. Proc Natl Acad Sci U S A *98*, 6999-7003.

Goldstein, L. S., and Yang, Z. (2000). Microtubule-based transport systems in neurons: the roles of kinesins and dyneins. Annu Rev Neurosci *23*, 39-71.

Gostissa, M., Hengstermann, A., Fogal, V., Sandy, P., Schwarz, S. E., Scheffner, M., and Del Sal, G. (1999). Activation of p53 by conjugation to the ubiquitin-like protein SUMO-1. Embo J *18*, 6462-6471.

Grant, P., Tseng, D., Gould, R. M., Gainer, H., and Pant, H. C. (1995). Expression of neurofilament proteins during development of the nervous system in the squid Loligo pealei. J Comp Neurol *356*, 311-326.

Griffin, J. W., George, E. B., and Chaudhry, V. (1996). Wallerian degeneration in peripheral nerve disease. Baillieres Clin Neurol *5*, 65-75.

Griffiths, I., Klugmann, M., Anderson, T., Yool, D., Thomson, C., Schwab, M. H., Schneider, A., Zimmermann, F., McCulloch, M., Nadon, N., and Nave, K. A. (1998). Axonal swellings and degeneration in mice lacking the major proteolipid of myelin. Science *280*, 1610-1613.

Grimwade, D., and Solomon, E. (1997). Characterisation of the PML/RAR alpha rearrangement associated with t(15;17) acute promyelocytic leukaemia. Curr Top Microbiol Immunol *220*, 81-112.

Guelin, E., Rep, M., and Grivell, L. A. (1994). Sequence of the AFG3 gene encoding a new member of the FtsH/Yme1/Tma subfamily of the AAA-protein family. Yeast *10*, 1389-1394.

Guenther, B., Onrust, R., Sali, A., O'Donnell, M., and Kuriyan, J. (1997). Crystal structure of the delta' subunit of the clamp-loader complex of E. coli DNA polymerase III. Cell *91*, 335-345.

Gunawardena, S., Her, L. S., Brusch, R. G., Laymon, R. A., Niesman, I. R., Gordesky-Gold, B., Sintasath, L., Bonini, N. M., and Goldstein, L. S. (2003). Disruption of axonal transport by loss of huntingtin or expression of pathogenic polyQ proteins in Drosophila. Neuron *40*, 25-40.

Hall, A., and Nobes, C. D. (2000). Rho GTPases: molecular switches that control the organization and dynamics of the actin cytoskeleton. Philos Trans R Soc Lond B Biol Sci *355*, 965-970.

Hansen, J. J., Durr, A., Cournu-Rebeix, I., Georgopoulos, C., Ang, D., Nielsen, M. N., Davoine, C. S., Brice, A., Fontaine, B., Gregersen, N., and Bross, P. (2002). Hereditary spastic paraplegia SPG13 is associated with a mutation in the gene encoding the mitochondrial chaperonin Hsp60. Am J Hum Genet *70*, 1328-1332.

Harding, A. E. (1983). Classification of the hereditary ataxias and paraplegias. Lancet *1*, 1151-1155.

Harding, A. E. (1993). Hereditary spastic paraplegias. Semin Neurol *13*, 333-336.

Hartman, J. J., Mahr, J., McNally, K., Okawa, K., Iwamatsu, A., Thomas, S., Cheesman, S., Heuser, J., Vale, R. D., and McNally, F. J. (1998). Katanin, a microtubule-severing protein, is a novel AAA ATPase that targets to the centrosome using a WD40-containing subunit. Cell *93*, 277-287.

Hartman, J. J., and Vale, R. D. (1999). Microtubule disassembly by ATP-dependent oligomerization of the AAA enzyme katanin. Science *286*, 782-785.

Hayashi, S., Okada, T., Igarashi, N., Fujita, T., Jahangeer, S., and Nakamura, S. (2002). Identification and characterization of RPK118, a novel sphingosine kinase-1-binding protein. J Biol Chem *277*, 33319-33324.

Hazan, J., Fonknechten, N., Mavel, D., Paternotte, C., Samson, D., Artiguenave, F., Davoine, C. S., Cruaud, C., Durr, A., Wincker, P., *et al.* (1999). Spastin, a new AAA protein, is altered in the most frequent form of autosomal dominant spastic paraplegia. Nat Genet *23*, 296-303.

Hazan, J., Fontaine, B., Bruyn, R. P., Lamy, C., van Deutekom, J. C., Rime, C. S., Durr, A., Melki, J., Lyon-Caen, O., Agid, Y., and et al. (1994). Linkage of a new locus for autosomal dominant familial spastic paraplegia to chromosome 2p. Hum Mol Genet *3*, 1569-1573.

Heald, R., and Nogales, E. (2002). Microtubule dynamics. J Cell Sci *115*, 3-4.

Hentati, A., Deng, H. X., Zhai, H., Chen, W., Yang, Y., Hung, W. Y., Azim, A. C., Bohlega, S., Tandan, R., Warner, C., *et al.* (2000). Novel mutations in spastin gene and absence of correlation with age at onset of symptoms. Neurology *55*, 1388-1390.

Hentati, A., Pericak-Vance, M. A., Lennon, F., Wasserman, B., Hentati, F., Juneja, T., Angrist, M. H., Hung, W. Y., Boustany, R. M., Bohlega, S., and et al. (1994). Linkage of a locus for autosomal dominant familial spastic paraplegia to chromosome 2p markers. Hum Mol Genet *3*, 1867-1871.

Hirokawa, N. (1998). Kinesin and dynein superfamily proteins and the mechanism of organelle transport. Science *279*, 519-526.

Hirokawa, N., and Takemura, R. (2003). Biochemical and molecular characterization of diseases linked to motor proteins. Trends Biochem Sci *28*, 558-565.

Hirose, Y., and Manley, J. L. (2000). RNA polymerase II and the integration of nuclear events. Genes Dev *14*, 1415-1429.

Hochstrasser, M. (2001). SP-RING for SUMO: new functions bloom for a ubiquitin-like protein. Cell *107*, 5-8.

Hofmann, H., Floss, S., and Stamminger, T. (2000). Covalent modification of the transactivator protein IE2-p86 of human cytomegalovirus by conjugation to the ubiquitin-homologous proteins SUMO-1 and hSMT3b. J Virol *74*, 2510-2524.

Hollenbach, A. D., Sublett, J. E., McPherson, C. J., and Grosveld, G. (1999). The Pax3-FKHR oncoprotein is unresponsive to the Pax3-associated repressor hDaxx. Embo J *18*, 3702-3711.

Hoyt, M. A., He, L., Totis, L., and Saunders, W. S. (1993). Loss of function of Saccharomyces cerevisiae kinesin-related CIN8 and KIP1 is suppressed by KAR3 motor domain mutations. Genetics *135*, 35-44.

Hunter, A. W., and Wordeman, L. (2000). How motor proteins influence microtubule polymerization dynamics. J Cell Sci *113 Pt 24*, 4379-4389.

Iseki, E., Kato, M., Marui, W., Ueda, K., and Kosaka, K. (2001). A neuropathological study of the disturbance of the nigro-amygdaloid connections in brains from patients with dementia with Lewy bodies. J Neurol Sci *185*, 129-134.

Ishov, A. M., Sotnikov, A. G., Negorev, D., Vladimirova, O. V., Neff, N., Kamitani, T., Yeh, E. T., Strauss, J. F., 3rd, and Maul, G. G. (1999). PML is critical for ND10 formation and recruits the PML-interacting protein daxx to this nuclear structure when modified by SUMO-1. J Cell Biol *147*, 221-234.

Jacobson, R. H., Ladurner, A. G., King, D. S., and Tjian, R. (2000). Structure and function of a human TAFII250 double bromodomain module. Science *288*, 1422-1425.

Jang, M. S., Ryu, S. W., and Kim, E. (2002). Modification of Daxx by small ubiquitin-related modifier-1. Biochem Biophys Res Commun *295*, 495-500.

Jeanmougin, F., Wurtz, J. M., Le Douarin, B., Chambon, P., and Losson, R. (1997). The bromodomain revisited. Trends Biochem Sci *22*, 151-153.

Johnson, E. S., and Blobel, G. (1997). Ubc9p is the conjugating enzyme for the ubiquitin-like protein Smt3p. J Biol Chem *272*, 26799-26802.

Johnson, E. S., and Blobel, G. (1999). Cell cycle-regulated attachment of the ubiquitin-related protein SUMO to the yeast septins. J Cell Biol *147*, 981-994.

Johnson, E. S., and Gupta, A. A. (2001). An E3-like factor that promotes SUMO conjugation to the yeast septins. Cell *106*, 735-744.

Johnstone, M., Goold, R. G., Fischer, I., and Gordon-Weeks, P. R. (1997). The neurofilament antibody RT97 recognises a developmentally regulated phosphorylation epitope on microtubule-associated protein 1B. J Anat *191 (Pt 2)*, 229-244.

Jones, A. T., and Wessling-Resnick, M. (1998). Inhibition of in vitro endosomal vesicle fusion activity by aminoglycoside antibiotics. J Biol Chem *273*, 25301-25309.

Joseph, J., Tan, S. H., Karpova, T. S., McNally, J. G., and Dasso, M. (2002). SUMO-1 targets RanGAP1 to kinetochores and mitotic spindles. J Cell Biol *156*, 595-602.

Jouet, M., Rosenthal, A., Armstrong, G., MacFarlane, J., Stevenson, R., Paterson, J., Metzenberg, A., Ionasescu, V., Temple, K., and Kenwrick, S. (1994). X-linked spastic paraplegia (SPG1), MASA syndrome and X-linked hydrocephalus result from mutations in the L1 gene. Nat Genet *7*, 402-407.

Kagey, M. H., Melhuish, T. A., and Wotton, D. (2003). The polycomb protein Pc2 is a SUMO E3. Cell *113*, 127-137.

Kahyo, T., Nishida, T., and Yasuda, H. (2001). Involvement of PIAS1 in the sumoylation of tumor suppressor p53. Mol Cell *8*, 713-718.

Kamal, A., Almenar-Queralt, A., LeBlanc, J. F., Roberts, E. A., and Goldstein, L. S. (2001). Kinesin-mediated axonal transport of a membrane compartment containing beta-secretase and presenilin-1 requires APP. Nature *414*, 643-648.

Kamal, A., Stokin, G. B., Yang, Z., Xia, C. H., and Goldstein, L. S. (2000). Axonal transport of amyloid precursor protein is mediated by direct binding to the kinesin light chain subunit of kinesin-I. Neuron *28*, 449-459.

Kamitani, T., Nguyen, H. P., and Yeh, E. T. (1997). Preferential modification of nuclear proteins by a novel ubiquitin-like molecule. J Biol Chem *272*, 14001-14004.

Kawabe, Y., Seki, M., Seki, T., Wang, W. S., Imamura, O., Furuichi, Y., Saitoh, H., and Enomoto, T. (2000). Covalent modification of the Werner's syndrome gene product with the ubiquitin-related protein, SUMO-1. J Biol Chem *275*, 20963-20966.

Keating, T. J., Peloquin, J. G., Rodionov, V. I., Momcilovic, D., and Borisy, G. G. (1997). Microtubule release from the centrosome. Proc Natl Acad Sci U S A *94*, 5078-5083.

Kent, C., and Clarke, P. J. (1991). The immunolocalisation of the neuroendocrine specific protein PGP9.5 during neurogenesis in the rat. Brain Res Dev Brain Res *58*, 147-150.

Ki, C. S., Lee, W. Y., Han do, H., Sung, D. H., Lee, K. B., Lee, K. A., Cho, S. S., Cho, S., Hwang, H., Sohn, K. M., *et al.* (2002). A novel missense mutation (I344K) in the SPG4gene in a Korean family with autosomal-dominant hereditary spastic paraplegia. J Hum Genet *47*, 473-477.

Kim, Y. H., Choi, C. Y., and Kim, Y. (1999). Covalent modification of the homeodomain-interacting protein kinase 2 (HIPK2) by the ubiquitin-like protein SUMO-1. Proc Natl Acad Sci U S A *96*, 12350-12355.

Kiriakidou, M., Driscoll, D. A., Lopez-Guisa, J. M., and Strauss, J. F., 3rd (1997). Cloning and expression of primate Daxx cDNAs and mapping of the human gene to chromosome 6p21.3 in the MHC region. DNA Cell Biol *16*, 1289-1298.

Kirsh, O., Seeler, J. S., Pichler, A., Gast, A., Muller, S., Miska, E., Mathieu, M., Harel-Bellan, A., Kouzarides, T., Melchior, F., and Dejean, A. (2002). The SUMO E3 ligase RanBP2 promotes modification of the HDAC4 deacetylase. Embo J *21*, 2682-2691.

Ko, Y. G., Kang, Y. S., Park, H., Seol, W., Kim, J., Kim, T., Park, H. S., Choi, E. J., and Kim, S. (2001). Apoptosis signal-regulating kinase 1 controls the proapoptotic function of death-associated protein (Daxx) in the cytoplasm. J Biol Chem *276*, 39103-39106.

Kruyt, F. A., Waisfisz, Q., Dijkmans, L. M., Hermsen, M. A., Youssoufian, H., Arwert, F., and Joenje, H. (1997). Cytoplasmic localization of a functionally active Fanconi anemia group A-green fluorescent protein chimera in human 293 cells. Blood *90*, 3288-3295.

Kwek, S. S., Derry, J., Tyner, A. L., Shen, Z., and Gudkov, A. V. (2001). Functional analysis and intracellular localization of p53 modified by SUMO-1. Oncogene *20*, 2587-2599.

Kzhyshkowska, J., Rusch, A., Wolf, H., and Dobner, T. (2003). Regulation of transcription by the heterogeneous nuclear ribonucleoprotein E1B-AP5 is mediated by complex formation with the novel bromodomain-containing protein BRD7. Biochem J *371*, 385-393.

Lamaze, C., Dujeancourt, A., Baba, T., Lo, C. G., Benmerah, A., and Dautry-Varsat, A. (2001). Interleukin 2 receptors and detergent-resistant membrane domains define a clathrin-independent endocytic pathway. Mol Cell *7*, 661-671.

LaMonte, B. H., Wallace, K. E., Holloway, B. A., Shelly, S. S., Ascano, J., Tokito, M., Van Winkle, T., Howland, D. S., and Holzbaur, E. L. (2002). Disruption of dynein/dynactin inhibits axonal transport in motor neurons causing late-onset progressive degeneration. Neuron *34*, 715-727.

Langer, T., Kaser, M., Klanner, C., and Leonhard, K. (2001). AAA proteases of mitochondria: quality control of membrane proteins and regulatory functions during mitochondrial biogenesis. Biochem Soc Trans *29*, 431-436.

Latterich, M., Frohlich, K. U., and Schekman, R. (1995). Membrane fusion and the cell cycle: Cdc48p participates in the fusion of ER membranes. Cell *82*, 885-893.

Layfield, R., Cavey, J. R., and Lowe, J. (2003). Role of ubiquitin-mediated proteolysis in the pathogenesis of neurodegenerative disorders. Ageing Res Rev *2*, 343-356.

Lee, B., and Richards, F. (1971). The interpretation of protein structures: estimation of static accessibility. J Mol Biol *55*, 379-400.

Lehembre, F., Badenhorst, P., Muller, S., Travers, A., Schweisguth, F., and Dejean, A. (2000). Covalent modification of the transcriptional repressor tramtrack by the ubiquitin-related protein Smt3 in Drosophila flies. Mol Cell Biol *20*, 1072-1082.

Lenzen, C. U., Steinmann, D., Whiteheart, S. W., and Weis, W. I. (1998). Crystal structure of the hexamerization domain of N-ethylmaleimide-sensitive fusion protein. Cell *94*, 525-536.

Li, H., Leo, C., Zhu, J., Wu, X., O'Neil, J., Park, E. J., and Chen, J. D. (2000a). Sequestration and inhibition of Daxx-mediated transcriptional repression by PML. Mol Cell Biol *20*, 1784-1796.

Li, R., Pei, H., Watson, D. K., and Papas, T. S. (2000b). EAP1/Daxx interacts with ETS1 and represses transcriptional activation of ETS1 target genes. Oncogene *19*, 745-753.

Liberzon, A., Shpungin, S., Bangio, H., Yona, E., and Katcoff, D. J. (1996). Association of yeast SAP1, a novel member of the 'AAA' ATPase family of proteins, with the chromatin protein SIN1. FEBS Lett *388*, 5-10.

Lieberman, A. P. (2004). SUMO, a ubiquitin-like modifier implicated in neurodegeneration. Exp Neurol *185*, 204-207.

Liedtke, W., Leman, E. E., Fyffe, R. E., Raine, C. S., and Schubart, U. K. (2002). Stathmin-deficient mice develop an age-dependent axonopathy of the central and peripheral nervous systems. Am J Pathol *160*, 469-480.

Lin, D. Y., Lai, M. Z., Ann, D. K., and Shih, H. M. (2003). Promyelocytic leukemia protein (PML) functions as a glucocorticoid receptor co-activator by sequestering Daxx to the PML oncogenic domains (PODs) to enhance its transactivation potential. J Biol Chem *278*, 15958-15965.

Lindsey, J. C., Lusher, M. E., McDermott, C. J., White, K. D., Reid, E., Rubinsztein, D. C., Bashir, R., Hazan, J., Shaw, P. J., and Bushby, K. M. (2000). Mutation analysis of the spastin gene (SPG4) in patients with hereditary spastic paraparesis. J Med Genet *37*, 759-765.

Lohret, T. A., Zhao, L., and Quarmby, L. M. (1999). Cloning of Chlamydomonas p60 katanin and localization to the site of outer doublet severing during deflagellation. Cell Motil Cytoskeleton *43*, 221-231.

Long, X., and Griffith, L. C. (2000). Identification and characterization of a SUMO-1 conjugation system that modifies neuronal calcium/calmodulin-dependent protein kinase II in Drosophila melanogaster. J Biol Chem *275*, 40765-40776.

Lowe, J., Mayer, R. J., and Landon, M. (1993). Ubiquitin in neurodegenerative diseases. Brain Pathol *3*, 55-65.

Lunn, E. R., Perry, V. H., Brown, M. C., Rosen, H., and Gordon, S. (1989). Absence of Wallerian Degeneration does not Hinder Regeneration in Peripheral Nerve. Eur J Neurosci *1*, 27-33.

Lupas, A. N., and Martin, J. (2002). AAA proteins. Curr Opin Struct Biol *12*, 746-753.

Lyon, M. F., Ogunkolade, B. W., Brown, M. C., Atherton, D. J., and Perry, V. H. (1993). A gene affecting Wallerian nerve degeneration maps distally on mouse chromosome 4. Proc Natl Acad Sci U S A *90*, 9717-9720.

Mahajan, R., Gerace, L., and Melchior, F. (1998). Molecular characterization of the SUMO-1 modification of RanGAP1 and its role in nuclear envelope association. J Cell Biol *140*, 259-270.

Mallet, W. G., and Maxfield, F. R. (1999). Chimeric forms of furin and TGN38 are transported with the plasma membrane in the trans-Golgi network via distinct endosomal pathways. J Cell Biol *146*, 345-359.

Mao, Y., Desai, S. D., and Liu, L. F. (2000a). SUMO-1 conjugation to human DNA topoisomerase II isozymes. J Biol Chem *275*, 26066-26073.

Mao, Y., Sun, M., Desai, S. D., and Liu, L. F. (2000b). SUMO-1 conjugation to topoisomerase I: A possible repair response to topoisomerase-mediated DNA damage. Proc Natl Acad Sci U S A *97*, 4046-4051.

Matunis, M. J., Coutavas, E., and Blobel, G. (1996). A novel ubiquitin-like modification modulates the partitioning of the Ran-GTPase-activating protein RanGAP1 between the cytosol and the nuclear pore complex. J Cell Biol *135*, 1457-1470.

Maul, G. G., Negorev, D., Bell, P., and Ishov, A. M. (2000). Review: properties and assembly mechanisms of ND10, PML bodies, or PODs. J Struct Biol *129*, 278-287.

McNally, F. (2000). Capturing a ring of samurai. Nat Cell Biol *2*, E4-7.

McNally, F. J., and Thomas, S. (1998). Katanin is responsible for the M-phase microtubule-severing activity in Xenopus eggs. Mol Biol Cell *9*, 1847-1861.

McNally, F. J., and Vale, R. D. (1993). Identification of katanin, an ATPase that severs and disassembles stable microtubules. Cell *75*, 419-429.

McNally, K. P., Bazirgan, O. A., and McNally, F. J. (2000). Two domains of p80 katanin regulate microtubule severing and spindle pole targeting by p60 katanin. J Cell Sci *113*, 1623-1633.

McNiven, M. A., Kim, L., Krueger, E. W., Orth, J. D., Cao, H., and Wong, T. W. (2000). Regulated interactions between dynamin and the actin-binding protein cortactin modulate cell shape. J Cell Biol *151*, 187-198.

Meyer, H. H., Shorter, J. G., Seemann, J., Pappin, D., and Warren, G. (2000). A complex of mammalian ufd1 and npl4 links the AAA-ATPase, p97, to ubiquitin and nuclear transport pathways. Embo J *19*, 2181-2192.

Michaelson, J. S. (2000). The Daxx enigma. Apoptosis *5*, 217-220.

Michaelson, J. S., Bader, D., Kuo, F., Kozak, C., and Leder, P. (1999). Loss of Daxx, a promiscuously interacting protein, results in extensive apoptosis in early mouse development. Genes Dev *13*, 1918-1923.

Michaelson, J. S., and Leder, P. (2003). RNAi reveals anti-apoptotic and transcriptionally repressive activities of DAXX. J Cell Sci *116*, 345-352.

Minty, A., Dumont, X., Kaghad, M., and Caput, D. (2000). Covalent modification of p73alpha by SUMO-1. Two-hybrid screening with p73 identifies novel SUMO-1-interacting proteins and a SUMO-1 interaction motif. J Biol Chem *275*, 36316-36323.

Miyauchi, Y., Yogosawa, S., Honda, R., Nishida, T., and Yasuda, H. (2002). Sumoylation of Mdm2 by protein inhibitor of activated STAT (PIAS) and RanBP2 enzymes. J Biol Chem *277*, 50131-50136.

Molon, A., Di Giovanni, S., Chen, Y. W., Clarkson, P. M., Angelini, C., Pegoraro, E., and Hoffman, E. P. (2004). Large-scale disruption of microtubule pathways in morphologically normal human spastin muscle. Neurology.

Molon, A., Montagna, P., Angelini, C., and Pegoraro, E. (2003). Novel spastin mutations and their expression analysis in two Italian families. Eur J Hum Genet *11*, 710-713.

Moudjou, M., and Bornens, M. (1998). Method of centrosome isolation from cultured animal cells. In Cell Biology: A laboratoty handbook Academic press, Inc New York, 111-119.

Muglia, M., Magariello, A., Nicoletti, G., Patitucci, A., Gabriele, A. L., Conforti, F. L., Mazzei, R., Caracciolo, M., Ardito, B., Lastilla, M., *et al.* (2002). Further evidence that SPG3A gene mutations cause autosomal dominant hereditary spastic paraplegia. Ann Neurol *51*, 794-795.

Mukoyama, M., Yamazaki, K., Kikuchi, T., and Tomita, T. (1989). Neuropathology of gracile axonal dystrophy (GAD) mouse. An animal model of central distal axonopathy in primary sensory neurons. Acta Neuropathol (Berl) *79*, 294-299.

Muller, S., Berger, M., Lehembre, F., Seeler, J. S., Haupt, Y., and Dejean, A. (2000). c-Jun and p53 activity is modulated by SUMO-1 modification. J Biol Chem *275*, 13321-13329.

Muller, S., and Dejean, A. (1999). Viral immediate-early proteins abrogate the modification by SUMO-1 of PML and Sp100 proteins, correlating with nuclear body disruption. J Virol *73*, 5137-5143.

Muller, S., Hoege, C., Pyrowolakis, G., and Jentsch, S. (2001). SUMO, ubiquitin's mysterious cousin. Nat Rev Mol Cell Biol *2*, 202-210.

Muller, S., Matunis, M. J., and Dejean, A. (1998). Conjugation with the ubiquitin-related modifier SUMO-1 regulates the partitioning of PML within the nucleus. Embo J *17*, 61-70.

Nagiec, E. E., Bernstein, A., and Whiteheart, S. W. (1995). Each domain of the N-ethylmaleimide-sensitive fusion protein contributes to its transport activity. J Biol Chem *270*, 29182-29188.

Namekawa, M., Takiyama, Y., Sakoe, K., Nagaki, H., Shimazaki, H., Yoshimura, M., Ikeguchi, K., Nakano, I., and Nishizawa, M. (2002). A Japanese SPG4 family with a novel missense mutation of the SPG4 gene: intrafamilial variability in age at onset and clinical severity. Acta Neurol Scand *106*, 387-391.

Namekawa, M., Takiyama, Y., Sakoe, K., Shimazaki, H., Amaike, M., Niijima, K., Nakano, I., and Nishizawa, M. (2001). A large Japanese SPG4 family with a novel insertion mutation of the SPG4 gene: a clinical and genetic study. J Neurol Sci *185*, 63-68.

Nara, A., Mizushima, N., Yamamoto, A., Kabeya, Y., Ohsumi, Y., and Yoshimori, T. (2002). SKD1 AAA ATPase-dependent endosomal transport is involved in autolysosome formation. Cell Struct Funct *27*, 29-37.

Negorev, D., and Maul, G. G. (2001). Cellular proteins localized at and interacting within ND10/PML nuclear bodies/PODs suggest functions of a nuclear depot. Oncogene *20*, 7234-7242.

Neuwald, A. F., Aravind, L., Spouge, J. L., and Koonin, E. V. (1999). AAA+: A class of chaperone-like ATPases associated with the assembly, operation, and disassembly of protein complexes. Genome Res *9*, 27-43.

Nicoziani, P., Vilhardt, F., Llorente, A., Hilout, L., Courtoy, P. J., Sandvig, K., and van Deurs, B. (2000). Role for dynamin in late endosome dynamics and trafficking of the cation-independent mannose 6-phosphate receptor. Mol Biol Cell *11*, 481-495.

Noble, M., Lewis, S. A., and Cowan, N. J. (1989). The microtubule binding domain of microtubule-associated protein MAP1B contains a repeated sequence motif unrelated to that of MAP2 and tau. J Cell Biol *109*, 3367-3376.

Ochoa, G. C., Slepnev, V. I., Neff, L., Ringstad, N., Takei, K., Daniell, L., Kim, W., Cao, H., McNiven, M., Baron, R., and De Camilli, P. (2000). A functional link between dynamin and the actin cytoskeleton at podosomes. J Cell Biol *150*, 377-389.

Odde, D. J., Ma, L., Briggs, A. H., DeMarco, A., and Kirschner, M. W. (1999). Microtubule bending and breaking in living fibroblast cells. J Cell Sci *112 (Pt 19)*, 3283-3288.

Ogura, T., and Wilkinson, A. J. (2001). AAA+ superfamily ATPases: common structure--diverse function. Genes Cells *6*, 575-597.

O'Leary, D. D., and Koester, S. E. (1993). Development of projection neuron types, axon pathways, and patterned connections of the mammalian cortex. Neuron *10*, 991-1006.

Omran, H., Haffner, K., Volkel, A., Kuehr, J., Ketelsen, U. P., Ross, U. H., Konietzko, N., Wienker, T., Brandis, M., and Hildebrandt, F. (2000). Homozygosity mapping of a gene locus for primary ciliary dyskinesia on chromosome 5p and identification of the heavy dynein chain DNAH5 as a candidate gene. Am J Respir Cell Mol Biol *23*, 696-702.

Orlacchio, A., Kawarai, T., Totaro, A., Errico, A., St george Hyslop, P., Rugarli, E. I., and Bernardi, G. (2004). Hereditary spastic paraplegia: clinical and genetic study of 15 families. Arch Neurol.

Owen, D. J., Ornaghi, P., Yang, J. C., Lowe, N., Evans, P. R., Ballario, P., Neuhaus, D., Filetici, P., and Travers, A. A. (2000). The structural basis for the recognition of

acetylated histone H4 by the bromodomain of histone acetyltransferase gcn5p. Embo J *19*, 6141-6149.

Ozelius, L. J., Hewett, J. W., Page, C. E., Bressman, S. B., Kramer, P. L., Shalish, C., de Leon, D., Brin, M. F., Raymond, D., Corey, D. P., *et al.* (1997). The early-onset torsion dystonia gene (DYT1) encodes an ATP-binding protein. Nat Genet *17*, 40-48.

Pant, H. C., Veeranna, and Grant, P. (2000). Regulation of axonal neurofilament phosphorylation. Curr Top Cell Regul *36*, 133-150.

Patel, H., Cross, H., Proukakis, C., Hershberger, R., Bork, P., Ciccarelli, F. D., Patton, M. A., McKusick, V. A., and Crosby, A. H. (2002). SPG20 is mutated in Troyer syndrome, an hereditary spastic paraplegia. Nat Genet *31*, 347-348.

Patel, S., and Latterich, M. (1998). The AAA team: related ATPases with diverse functions. Trends Cell Biol *8*, 65-71.

Patrono, C., Casali, C., Tessa, A., Cricchi, F., Fortini, D., Carrozzo, R., Siciliano, G., Bertini, E., and Santorelli, F. M. (2002). Missense and splice site mutations in SPG4 suggest loss-of-function in dominant spastic paraplegia. J Neurol *249*, 200-205.

Paul, M. F., and Tzagoloff, A. (1995). Mutations in RCA1 and AFG3 inhibit F1-ATPase assembly in Saccharomyces cerevisiae. FEBS Lett *373*, 66-70.

Perlman, R., Schiemann, W. P., Brooks, M. W., Lodish, H. F., and Weinberg, R. A. (2001). TGF-beta-induced apoptosis is mediated by the adapter protein Daxx that facilitates JNK activation. Nat Cell Biol *3*, 708-714.

Pfannenschmid, F., Wimmer, V. C., Rios, R. M., Geimer, S., Krockel, U., Leiherer, A., Haller, K., Nemcova, Y., and Mages, W. (2003). Chlamydomonas DIP13 and human NA14: a new class of proteins associated with microtubule structures is involved in cell division. J Cell Sci *116*, 1449-1462.

Phillips, S. A., Barr, V. A., Haft, D. H., Taylor, S. I., and Haft, C. R. (2001). Identification and characterization of SNX15, a novel sorting nexin involved in protein trafficking. J Biol Chem *276*, 5074-5084.

Pichler, A., Gast, A., Seeler, J. S., Dejean, A., and Melchior, F. (2002). The nucleoporin RanBP2 has SUMO1 E3 ligase activity. Cell *108*, 109-120.

Piel, M., Nordberg, J., Euteneuer, U., and Bornens, M. (2001). Centrosome-dependent exit of cytokinesis in animal cells. Science *291*, 1550-1553.

Pitts, K. R., Yoon, Y., Krueger, E. W., and McNiven, M. A. (1999). The dynamin-like protein DLP1 is essential for normal distribution and morphology of the endoplasmic reticulum and mitochondria in mammalian cells. Mol Biol Cell *10*, 4403-4417.

Pluta, A. F., Earnshaw, W. C., and Goldberg, I. G. (1998). Interphase-specific association of intrinsic centromere protein CENP-C with HDaxx, a death domain-binding protein implicated in Fas-mediated cell death. J Cell Sci *111 (Pt 14)*, 2029-2041.

Poukka, H., Karvonen, U., Janne, O. A., and Palvimo, J. J. (2000). Covalent modification of the androgen receptor by small ubiquitin-like modifier 1 (SUMO-1). Proc Natl Acad Sci U S A *97*, 14145-14150.

Pountney, D. L., Huang, Y., Burns, R. J., Haan, E., Thompson, P. D., Blumbergs, P. C., and Gai, W. P. (2003). SUMO-1 marks the nuclear inclusions in familial neuronal intranuclear inclusion disease. Exp Neurol *184*, 436-446.

Proukakis, C., Auer-Grumbach, M., Wagner, K., Wilkinson, P. A., Reid, E., Patton, M. A., Warner, T. T., and Crosby, A. H. (2003). Screening of patients with hereditary spastic paraplegia reveals seven novel mutations in the SPG4 (Spastin) gene. Hum Mutat *21*, 170.

Proukakis, C., Hart, P. E., Cornish, A., Warner, T. T., and Crosby, A. H. (2002). Three novel spastin (SPG4) mutations in families with autosomal dominant hereditary spastic paraplegia. J Neurol Sci *201*, 65-69.

Puls, I., Jonnakuty, C., LaMonte, B. H., Holzbaur, E. L., Tokito, M., Mann, E., Floeter, M. K., Bidus, K., Drayna, D., Oh, S. J., *et al.* (2003). Mutant dynactin in motor neuron disease. Nat Genet *33*, 455-456.

Quarmby, L. (2000). Cellular Samurai: katanin and the severing of microtubules. J Cell Sci *113 (Pt 16)*, 2821-2827.

Rabouille, C., Levine, T. P., Peters, J. M., and Warren, G. (1995). An NSF-like ATPase, p97, and NSF mediate cisternal regrowth from mitotic Golgi fragments. Cell *82*, 905-914.

Raff, M. C., Whitmore, A. V., and Finn, J. T. (2002). Axonal self-destruction and neurodegeneration. Science *296*, 868-871.

Ramos-Morales, F., Infante, C., Fedriani, C., Bornens, M., and Rios, R. M. (1998). NA14 is a novel nuclear autoantigen with a coiled-coil domain. J Biol Chem *273*, 1634-1639.

Rangasamy, D., Woytek, K., Khan, S. A., and Wilson, V. G. (2000). SUMO-1 modification of bovine papillomavirus E1 protein is required for intranuclear accumulation. J Biol Chem *275*, 37999-38004.

Reid, E. (2003). Science in motion: common molecular pathological themes emerge in the hereditary spastic paraplegias. J Med Genet *40*, 81-86.

Reid, E., Kloos, M., Ashley-Koch, A., Hughes, L., Bevan, S., Svenson, I. K., Graham, F. L., Gaskell, P. C., Dearlove, A., Pericak-Vance, M. A., *et al.* (2002). A

Kinesin Heavy Chain (KIF5A) Mutation in Hereditary Spastic Paraplegia (SPG10). Am J Hum Genet *71*, 1189-1194.

Reiner, O., Carrozzo, R., Shen, Y., Wehnert, M., Faustinella, F., Dobyns, W. B., Caskey, C. T., and Ledbetter, D. H. (1993). Isolation of a Miller-Dieker lissencephaly gene containing G protein beta-subunit-like repeats. Nature *364*, 717-721.

Reuber, B. E., Germain-Lee, E., Collins, C. S., Morrell, J. C., Ameritunga, R., Moser, H. W., Valle, D., and Gould, S. J. (1997). Mutations in PEX1 are the most common cause of peroxisome biogenesis disorders. Nat Genet *17*, 445-448.

Rodriguez, M. S., Desterro, J. M., Lain, S., Midgley, C. A., Lane, D. P., and Hay, R. T. (1999). SUMO-1 modification activates the transcriptional response of p53. Embo J *18*, 6455-6461.

Ross, C. A. (2002). Polyglutamine pathogenesis: emergence of unifying mechanisms for Huntington's disease and related disorders. Neuron *35*, 819-822.

Ross, S., Best, J. L., Zon, L. I., and Gill, G. (2002). SUMO-1 modification represses Sp3 transcriptional activation and modulates its subnuclear localization. Mol Cell *10*, 831-842.

Sachdev, S., Bruhn, L., Sieber, H., Pichler, A., Melchior, F., and Grosschedl, R. (2001). PIASy, a nuclear matrix-associated SUMO E3 ligase, represses LEF1 activity by sequestration into nuclear bodies. Genes Dev *15*, 3088-3103.

Sagot, Y., Dubois-Dauphin, M., Tan, S. A., de Bilbao, F., Aebischer, P., Martinou, J. C., and Kato, A. C. (1995). Bcl-2 overexpression prevents motoneuron cell body loss but not axonal degeneration in a mouse model of a neurodegenerative disease. J Neurosci *15*, 7727-7733.

Saigoh, K., Wang, Y. L., Suh, J. G., Yamanishi, T., Sakai, Y., Kiyosawa, H., Harada, T., Ichihara, N., Wakana, S., Kikuchi, T., and Wada, K. (1999). Intragenic deletion in the gene encoding ubiquitin carboxy-terminal hydrolase in gad mice. Nat Genet *23*, 47-51.

Saitoh, H., Pu,R.T., and Dasso,M. (1997). SUMO-1: wrestling with a new ubiquitin-related modifier. Trends In Biochemical Sciences *22*, 374-376.

Saitoh, H., Sparrow, D. B., Shiomi, T., Pu, R. T., Nishimoto, T., Mohun, T. J., and Dasso, M. (1998). Ubc9p and the conjugation of SUMO-1 to RanGAP1 and RanBP2. Curr Biol *8*, 121-124.

Sambrook J, Fritsch EF, and T., M. (1989). Molecular Cloning: A Laboratory Manual. Second edition (Cold Spring Harbor, NY: Cold Spring Harbor Laboratory Press).

Sapetschnig, A., Rischitor, G., Braun, H., Doll, A., Schergaut, M., Melchior, F., and Suske, G. (2002). Transcription factor Sp3 is silenced through SUMO modification by PIAS1. Embo J *21*, 5206-5215.

Saugier-Veber, P., Munnich, A., Bonneau, D., Rozet, J. M., Le Merrer, M., Gil, R., and Boespflug-Tanguy, O. (1994). X-linked spastic paraplegia and Pelizaeus-Merzbacher disease are allelic disorders at the proteolipid protein locus. Nat Genet *6*, 257-262.

Schaumburg, H. H., Wisniewski, H. M., and Spencer, P. S. (1974). Ultrastructural studies of the dying-back process. I. Peripheral nerve terminal and axon degeneration in systemic acrylamide intoxication. J Neuropathol Exp Neurol *33*, 260-284.

Scheuring, S., Rohricht, R. A., Schoning-Burkhardt, B., Beyer, A., Muller, S., Abts, H. F., and Kohrer, K. (2001). Mammalian cells express two VPS4 proteins both of which are involved in intracellular protein trafficking. J Mol Biol *312*, 469-480.

Schmalbruch, H., Jensen, H. J., Bjaerg, M., Kamieniecka, Z., and Kurland, L. (1991). A new mouse mutant with progressive motor neuronopathy. J Neuropathol Exp Neurol *50*, 192-204.

Schmidt, D., and Muller, S. (2002). Members of the PIAS family act as SUMO ligases for c-Jun and p53 and repress p53 activity. Proc Natl Acad Sci U S A *99*, 2872-2877.

Schroer, T. A. (2001). Microtubules don and doff their caps: dynamic attachments at plus and minus ends. Curr Opin Cell Biol *13*, 92-96.

Schwarz, G. A., and Liu, C. N. (1956). Hereditary (familial) spastic paraplegia; further clinical and pathologic observations. AMA Arch Neurol Psychiatry *75*, 144-162.

Schwarz, S. E., Matuschewski, K., Liakopoulos, D., Scheffner, M., and Jentsch, S. (1998). The ubiquitin-like proteins SMT3 and SUMO-1 are conjugated by the UBC9 E2 enzyme. Proc Natl Acad Sci U S A *95*, 560-564.

Seeler, J. S., and Dejean, A. (2001). SUMO: of branched proteins and nuclear bodies. Oncogene *20*, 7243-7249.

Seeler, J. S., and Dejean, A. (2003). Nuclear and unclear functions of SUMO. Nat Rev Mol Cell Biol *4*, 690-699.

Seeler, J. S., Marchio, A., Losson, R., Desterro, J. M., Hay, R. T., Chambon, P., and Dejean, A. (2001). Common properties of nuclear body protein SP100 and TIF1alpha chromatin factor: role of SUMO modification. Mol Cell Biol *21*, 3314-3324.

Seeler, J. S., Marchio, A., Sitterlin, D., Transy, C., and Dejean, A. (1998). Interaction of SP100 with HP1 proteins: a link between the promyelocytic leukemia-associated

nuclear bodies and the chromatin compartment. Proc Natl Acad Sci U S A *95*, 7316-7321.

Seto, E. S., Bellen, H. J., and Lloyd, T. E. (2002). When cell biology meets development: endocytic regulation of signaling pathways. Genes Dev *16*, 1314-1336.

Shimura, H., Hattori, N., Kubo, S., Mizuno, Y., Asakawa, S., Minoshima, S., Shimizu, N., Iwai, K., Chiba, T., Tanaka, K., and Suzuki, T. (2000). Familial Parkinson disease gene product, parkin, is a ubiquitin-protein ligase. Nat Genet *25*, 302-305.

Simpson, M. A., Cross, H., Proukakis, C., Pryde, A., Hershberger, R., Chatonnet, A., Patton, M. A., and Crosby, A. H. (2003). Maspardin is mutated in mast syndrome, a complicated form of hereditary spastic paraplegia associated with dementia. Am J Hum Genet *73*, 1147-1156.

Smith, D. B., and Johnson, K. S. (1988). Single-step purification of polypeptides expressed in Escherichia coli as fusions with glutathione S-transferase. Gene *67*, 31-40.

Smith, D. S., Niethammer, M., Ayala, R., Zhou, Y., Gambello, M. J., Wynshaw-Boris, A., and Tsai, L. H. (2000). Regulation of cytoplasmic dynein behaviour and microtubule organization by mammalian Lis1. Nat Cell Biol *2*, 767-775.

Soltys, B. J., and Borisy, G. G. (1985). Polymerization of tubulin in vivo: direct evidence for assembly onto microtubule ends and from centrosomes. J Cell Biol *100*, 1682-1689.

Spector, D. L. (2001). Nuclear domains. J Cell Sci *114*, 2891-2893.

Spillantini, M. G., and Goedert, M. (1998). Tau protein pathology in neurodegenerative diseases. Trends Neurosci *21*, 428-433.

Srayko, M., Buster, D. W., Bazirgan, O. A., McNally, F. J., and Mains, P. E. (2000). MEI-1/MEI-2 katanin-like microtubule severing activity is required for Caenorhabditis elegans meiosis. Genes Dev *14*, 1072-1084.

Steffan, J. S., Agrawal, N., Pallos, J., Rockabrand, E., Trotman, L. C., Slepko, N., Illes, K., Lukacsovich, T., Zhu, Y. Z., Cattaneo, E., *et al.* (2004). SUMO modification of Huntingtin and Huntington's disease pathology. Science *304*, 100-104.

Steffan, J. S., Bodai, L., Pallos, J., Poelman, M., McCampbell, A., Apostol, B. L., Kazantsev, A., Schmidt, E., Zhu, Y. Z., Greenwald, M., *et al.* (2001). Histone deacetylase inhibitors arrest polyglutamine-dependent neurodegeneration in Drosophila. Nature *413*, 739-743.

Sternsdorf, T., Jensen, K., Reich, B., and Will, H. (1999). The nuclear dot protein sp100, characterization of domains necessary for dimerization, subcellular localization, and modification by small ubiquitin-like modifiers. J Biol Chem *274*, 12555-12566.

Sternsdorf, T., Jensen, K., and Will, H. (1997). Evidence for covalent modification of the nuclear dot-associated proteins PML and Sp100 by PIC1/SUMO-1. J Cell Biol *139*, 1621-1634.

Svenson, I. K., Ashley-Koch, A. E., Gaskell, P. C., Riney, T. J., Cumming, W. J., Kingston, H. M., Hogan, E. L., Boustany, R. M., Vance, J. M., Nance, M. A., *et al.* (2001). Identification and expression analysis of spastin gene mutations in hereditary spastic paraplegia. Am J Hum Genet *68*, 1077-1085.

Swaffield, J. C., and Purugganan, M. D. (1997). The evolution of the conserved ATPase domain (CAD): reconstructing the history of an ancient protein module. J Mol Evol *45*, 549-563.

Szebenyi, G., Morfini, G. A., Babcock, A., Gould, M., Selkoe, K., Stenoien, D. L., Young, M., Faber, P. W., MacDonald, M. E., McPhaul, M. J., and Brady, S. T. (2003). Neuropathogenic forms of huntingtin and androgen receptor inhibit fast axonal transport. Neuron *40*, 41-52.

Tai, C. Y., Dujardin, D. L., Faulkner, N. E., and Vallee, R. B. (2002). Role of dynein, dynactin, and CLIP-170 interactions in LIS1 kinetochore function. J Cell Biol *156*, 959-968.

Takahashi, Y., Iwase, M., Konishi, M., Tanaka, M., Toh-e, A., and Kikuchi, Y. (1999). Smt3, a SUMO-1 homolog, is conjugated to Cdc3, a component of septin rings at the mother-bud neck in budding yeast. Biochem Biophys Res Commun *259*, 582-587.

Takahashi, Y., Kahyo, T., Toh, E. A., Yasuda, H., and Kikuchi, Y. (2001). Yeast Ull1/Siz1 is a novel SUMO1/Smt3 ligase for septin components and functions as an adaptor between conjugating enzyme and substrates. J Biol Chem *276*, 48973-48977.

Tallaksen, C. M., Guichart-Gomez, E., Verpillat, P., Hahn-Barma, V., Ruberg, M., Fontaine, B., Brice, A., Dubois, B., and Durr, A. (2003). Subtle cognitive impairment but no dementia in patients with spastin mutations. Arch Neurol *60*, 1113-1118.

Tanaka, Y., and Hirokawa, N. (2002). Mouse models of Charcot-Marie-Tooth disease. Trends Genet *18*, S39-44.

Tang, J., Wu, S., Liu, H., Stratt, R., Barak, O. G., Shiekhattar, R., Picketts, D. J., and Yang, X. (2004). A novel transcription regulatory complex containing Daxx and the ATR-X syndrome protein. J Biol Chem.

Tang, Q., and Edidin, M. (2001). Vesicle trafficking and cell surface membrane patchiness. Biophys J *81*, 196-203.

Tauer, R., Mannhaupt, G., Schnall, R., Pajic, A., Langer, T., and Feldmann, H. (1994). Yta10p, a member of a novel ATPase family in yeast, is essential for mitochondrial function. FEBS Lett *353*, 197-200.

Thelen, K., Kedar, V., Panicker, A. K., Schmid, R. S., Midkiff, B. R., and Maness, P. F. (2002). The neural cell adhesion molecule L1 potentiates integrin-dependent cell migration to extracellular matrix proteins. J Neurosci *22*, 4918-4931.

Torii, S., Egan, D. A., Evans, R. A., and Reed, J. C. (1999). Human Daxx regulates Fas-induced apoptosis from nuclear PML oncogenic domains (PODs). Embo J *18*, 6037-6049.

Treier, M., Staszewski, L. M., and Bohmann, D. (1994). Ubiquitin-dependent c-Jun degradation in vivo is mediated by the delta domain. Cell *78*, 787-798.

Tzagoloff, A., Yue, J., Jang, J., and Paul, M. F. (1994). A new member of a family of ATPases is essential for assembly of mitochondrial respiratory chain and ATP synthetase complexes in Saccharomyces cerevisiae. J Biol Chem *269*, 26144-26151.

Ueda, H., Goto, J., Hashida, H., Lin, X., Oyanagi, K., Kawano, H., Zoghbi, H. Y., Kanazawa, I., and Okazawa, H. (2002). Enhanced SUMOylation in polyglutamine diseases. Biochem Biophys Res Commun *293*, 307-313.

Vale, R. D. (1991). Severing of stable microtubules by a mitotically activated protein in Xenopus egg extracts. Cell *64*, 827-839.

Vale, R. D. (2000). AAA proteins. Lords of the ring. J Cell Biol *150*, F13-19.

Vallee, R. B., Tai, C., and Faulkner, N. E. (2001). LIS1: cellular function of a disease-causing gene. Trends Cell Biol *11*, 155-160.

Verger, A., Perdomo, J., and Crossley, M. (2003). Modification with SUMO. A role in transcriptional regulation. EMBO Rep *4*, 137-142.

Wagner, O. I., Lifshitz, J., Janmey, P. A., Linden, M., McIntosh, T. K., and Leterrier, J. F. (2003). Mechanisms of mitochondria-neurofilament interactions. J Neurosci *23*, 9046-9058.

Walker, J. E., Saraste, M., Runswick, M. J., and Gay, N. J. (1982). Distantly related sequences in the alpha- and beta-subunits of ATP synthase, myosin, kinases and other ATP-requiring enzymes and a common nucleotide binding fold. EMBO J *1*, 945-951.

Waller, A. (1850). Experiments on the section of glossopharyngeal and hypoglossal nerves of the frog and observations of the alternatives produced thereby in the structure of their primitive fibers. Philos Trans R Soc Lond B Biol Sci *140*, 423-429.

Walz, J., Erdmann, A., Kania, M., Typke, D., Koster, A. J., and Baumeister, W. (1998). 26S proteasome structure revealed by three-dimensional electron microscopy. J Struct Biol *121*, 19-29.

Wang, J., Shiels, C., Sasieni, P., Wu, P. J., Islam, S. A., Freemont, P. S., and Sheer, D. (2004). Promyelocytic leukemia nuclear bodies associate with transcriptionally active genomic regions. J Cell Biol *164*, 515-526.

Weber-Ban, E. U., Reid, B. G., Miranker, A. D., and Horwich, A. L. (1999). Global unfolding of a substrate protein by the Hsp100 chaperone ClpA. Nature *401*, 90-93.

Wharton, S. B., McDermott, C. J., Grierson, A. J., Wood, J. D., Gelsthorpe, C., Ince, P. G., and Shaw, P. J. (2003). The cellular and molecular pathology of the motor system in hereditary spastic paraparesis due to mutation of the spastin gene. J Neuropathol Exp Neurol *62*, 1166-1177.

White, K. D., Ince, P. G., Lusher, M., Lindsey, J., Cookson, M., Bashir, R., Shaw, P. J., and Bushby, K. M. (2000). Clinical and pathologic findings in hereditary spastic paraparesis with spastin mutation. Neurology *55*, 89-94.

Whiteheart, S. W., Rossnagel, K.,Buhrow, S.A., Brunner,M., Jaenicke,R. and Rothman,J.E. (1994). N-ethylmaleimide-sensitive fusion protein: a trimeric ATPase whose hydrolysis of ATP is required for membrane fusion. J Cell Biol *126*, 945-954.

Wilson, D. W., Whiteheart, S. W., Wiedmann, M., Brunner, M., and Rothman, J. E. (1992). A multisubunit particle implicated in membrane fusion. J Cell Biol *117*, 531-538.

Wojcik, C., Yano, M., and DeMartino, G. N. (2004). RNA interference of valosin-containing protein (VCP/p97) reveals multiple cellular roles linked to ubiquitin/proteasome-dependent proteolysis. J Cell Sci *117*, 281-292.

Wood, J. N., and Anderton, B. H. (1981). Monoclonal antibodies to mammalian neurofilaments. Biosci Rep *1*, 263-268.

Worby, C. A., and Dixon, J. E. (2002). Sorting out the cellular functions of sorting nexins. Nat Rev Mol Cell Biol *3*, 919-931.

Wynshaw-Boris, A., and Gambello, M. J. (2001). LIS1 and dynein motor function in neuronal migration and development. Genes Dev *15*, 639-651.

Xia, C., Rahman, A., Yang, Z., and Goldstein, L. S. (1998). Chromosomal localization reveals three kinesin heavy chain genes in mouse. Genomics *52*, 209-213.

Xu, Z., Cork, L. C., Griffin, J. W., and Cleveland, D. W. (1993). Involvement of neurofilaments in motor neuron disease. J Cell Sci Suppl *17*, 101-108.

Yabe, I., Sasaki, H., Tashiro, K., Matsuura, T., Takegami, T., and Satoh, T. (2002). Spastin gene mutation in Japanese with hereditary spastic paraplegia. J Med Genet *39*, e46.

Yamada, T., Okuhara, K., Iwamatsu, A., Seo, H., Ohta, K., Shibata, T., and Murofushi, H. (2000). p97 ATPase, an ATPase involved in membrane fusion, interacts with DNA unwinding factor (DUF) that functions in DNA replication. FEBS Lett *466*, 287-291.

Yang, X., Khosravi-Far, R., Chang, H. Y., and Baltimore, D. (1997). Daxx, a novel Fas-binding protein that activates JNK and apoptosis. Cell *89*, 1067-1076.

Yoshimori, T., Yamagata, F., Yamamoto, A., Mizushima, N., Kabeya, Y., Nara, A., Miwako, I., Ohashi, M., Ohsumi, M., and Ohsumi, Y. (2000). The mouse SKD1, a homologue of yeast Vps4p, is required for normal endosomal trafficking and morphology in mammalian cells. Mol Biol Cell *11*, 747-763.

Yu, R. C., Hanson, P. I., Jahn, R., and Brunger, A. T. (1998). Structure of the ATP-dependent oligomerization domain of N-ethylmaleimide sensitive factor complexed with ATP. Nat Struct Biol *5*, 803-811.

Zhang, H., Saitoh, H., and Matunis, M. J. (2002). Enzymes of the SUMO modification pathway localize to filaments of the nuclear pore complex. Mol Cell Biol *22*, 6498-6508.

Zhang, X., Shaw, A., Bates, P. A., Newman, R. H., Gowen, B., Orlova, E., Gorman, M. A., Kondo, H., Dokurno, P., Lally, J., *et al.* (2000). Structure of the AAA ATPase p97. Mol Cell *6*, 1473-1484.

Zhao, C., Takita, J., Tanaka, Y., Setou, M., Nakagawa, T., Takeda, S., Yang, H. W., Terada, S., Nakata, T., Takei, Y., *et al.* (2001a). Charcot-Marie-Tooth disease type 2A caused by mutation in a microtubule motor KIF1Bbeta. Cell *105*, 587-597.

Zhao, X., Alvarado, D., Rainier, S., Lemons, R., Hedera, P., Weber, C. H., Tukel, T., Apak, M., Heiman-Patterson, T., Ming, L., *et al.* (2001b). Mutations in a newly identified GTPase gene cause autosomal dominant hereditary spastic paraplegia. Nat Genet *29*, 326-331.

Zhong, S., Muller, S., Ronchetti, S., Freemont, P. S., Dejean, A., and Pandolfi, P. P. (2000). Role of SUMO-1-modified PML in nuclear body formation. Blood *95*, 2748-2752.

Publications from this thesis

Errico A., Ballabio A. and Rugarli E.I. Spastin, the protein mutated in autosomal dominant hereditary spastic paraplegia, is involved in microtubules dynamics. Human molecular genetics, 2002. Vol.11(2),153-163.

Orlacchio, A., Kawarai, T., Totaro, A., **Errico, A.,** St george Hyslop, P., Rugarli, E. I., and Bernardi, G. (2004). Hereditary spastic paraplegia: clinical and genetic study of 15 families. Arch Neurol.(*in press*)

APPENDIX 1: PRIMERS USED IN THIS THESIS

SP1	CTGATATCATGAATTCTCCGGGTGGACG
SP2	CAGTCGACCAGTGGTATCTCCAAAGTC
SP3	GAGTCGACACAGTGGTATCTCCAAAGTC
SP4	GAGGATCCATGAATTCTCCGGGTGGACGAG
SP5	CAGCGGCCGCATTTGTCACCACAGAGG
SP6	CAGTCGACCACTAGGTGCTCTATGGTG
SP7	CAGCGGCCGCATTCACTAGGTGCTCTATG
SP8	CAGGATCCTCATGGCAGCCAAGAGGAGC
SP9	CAGAATTCTGCTTGTTTTGCCAAGTCTTG
NLS-Up	AATTCTCCACCTTTCTCTTTTTCTTCGGCGGCATG
NLS-Dw	GATCCATGCCGCCGAAGAAAAAGAGAAAGGTGGAG
mNLS-Up	GATCCATGCCGCCGAAGACAAAGAGAAAGGTGGAG
mNLS-Dw	AATTCTCCACCTTTCTCTTTGTCTTCGGCGGCATG
SP10	CAGAATTCATGCTGTACTATTTCTCTTACCCGC
SP11	CAGAATTCATGGGCGAGGCCGAGCGCGTCC
SP12	CAGAATTCATGGAGAAGATGCAACCAGTTTTG
SP13	CAGAATTCTCCGGGTGGACGAGGGAAG
SP14	CATCTAGACGCTCGGCCTCGCCGC
SP15	CAGGATCCCTGTACTATTTCTCCTACCCG
SP16	CAGGATCCGAGGCCGAGCGCGTCCGAGTC
SP17	CAGGATCCGAGAAGATGCAACCAGTTTTG
BCO1	CCAGCCTCTTGCTGAGTGGAGATG
BCO2	GACAAGCCGACAACCTTGATTGCAG
NA14-1	CATGAATTCATGACCCAGCAGGGCGCGGC
NA14-2	CATCTCGAGTCAGCTGTCCCTGCCGCCGC
NA14-3	CAGGATCCTAATGACCCAGCAGGGCGCG

NA14-4	CAGAATTCTCAGCTGTCCCTGCCGCCGC
DAXX1	CAGAATTCATGGTCACCGCTAACAGCATC
DAXX2	CAGTCGACCATCAGAGTCTGAGAGCACG
S44L	GCCCCTCCGCCCGAGTTGCCGCATAAGCGGAAC
S362C	GTTATTCTTCCTTGTCTGAGGCCTGAG
G370R	CCTGAGTTGTTCACAAGGCTTAGAGCTCCTG
F381C	GGCTGTTACTCTGTGGTCCACCTGG
N386K	GTCCACCTGGGAAGGGGAAGACAATGC
N386S	GTCCACCTGGGACTGGGAAGACAATGC
K388R	CTGGGAATGGGAGGACAATGCTGGC
L426V	GAAATTGGTGAGGGCTGTTTTTGCTGTGGCTCG
C448Y	GTTGATAGCCTTTTGTATGAAAGAAGAGAAGGG
R460L	GCACGATGCTAGTAGACTCCTAAAAACTGAATTTC
R499C	GGCTGTTCTCAGGTGTTTCATCAAACG
A556V	GCTTTGGCAAAAGATGTAGCACTGGGTCCTATC
K340R	AATGGAACAGCTGTTAGATTTGATGATATAGCT
K462R	GCTAGTAGACGCCTAAGAAGTGAATTTCTAATAG
K565R	CCTATCCGAGAACTAAGACCAGAACAGGTGAAG
B-actin.up	5'-TCACCCACACTGTGCCCATCTACGA-3'
B-actin.dw	5'-CAGCGGAACCGCTCATTGCCAATGG-3'
GAPDH.up	5'-GAAGGTGAAGGTCGGAGTC-3'
GAPDH.dw	5'-GAAGATGGTGATGGGATTTC-3'
Spastin.up	5'-TCGAGTACATCTCCATTGCCC-3'
Spastin.dw	5'-TTCCACAGCTTGCTCCTTCTG-3'

APPENDIX 2: PLASMID MAPS

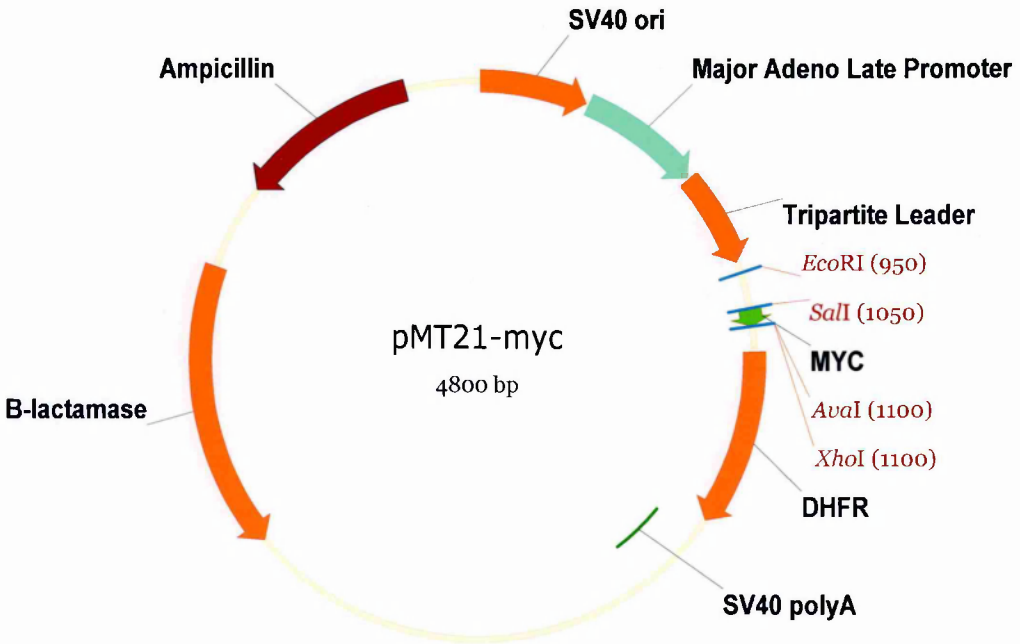
SV40 ori
Ampicillin
Major Adeno Late Promoter
Tripartite Leader
EcoRI (950)
SalI (1050)
MYC
AvaI (1100)
XhoI (1100)
DHFR
SV40 polyA
B-lactamase
pMT21-myc
4800 bp

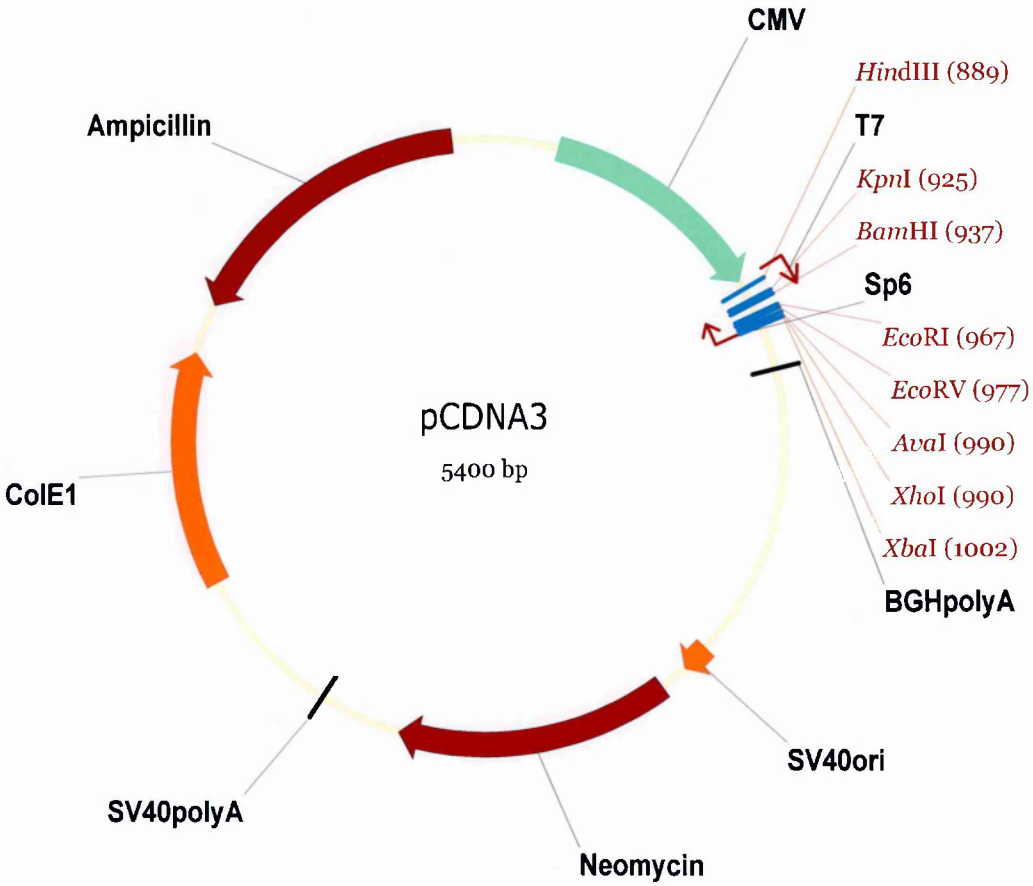
CMV
HindIII (889)
T7
KpnI (925)
BamHI (937)
Sp6
EcoRI (967)
EcoRV (977)
AvaI (990)
XhoI (990)
XbaI (1002)
BGHpolyA
Ampicillin
pCDNA3
5400 bp
ColE1
SV40polyA
Neomycin
SV40ori

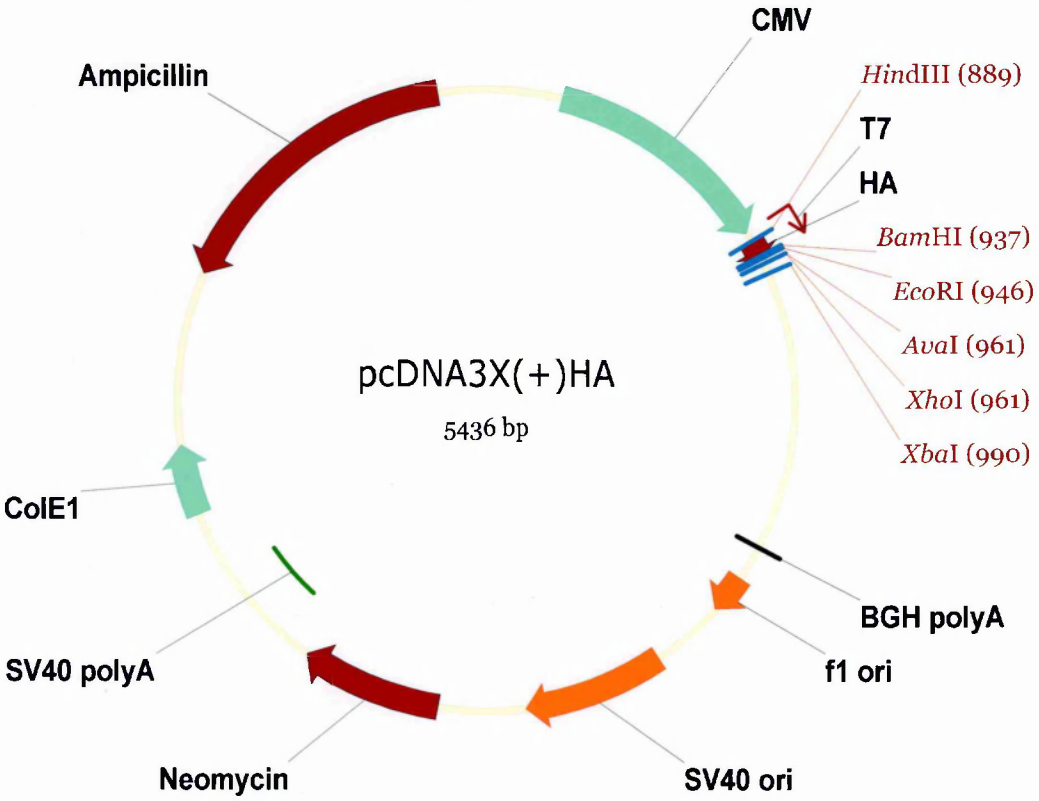
CMV
Ampicillin
HindIII (889)
T7
HA
BamHI (937)
EcoRI (946)
AvaI (961)
XhoI (961)
XbaI (990)
pcDNA3X(+)HA
5436 bp
ColE1
BGH polyA
f1 ori
SV40 polyA
Neomycin
SV40 ori

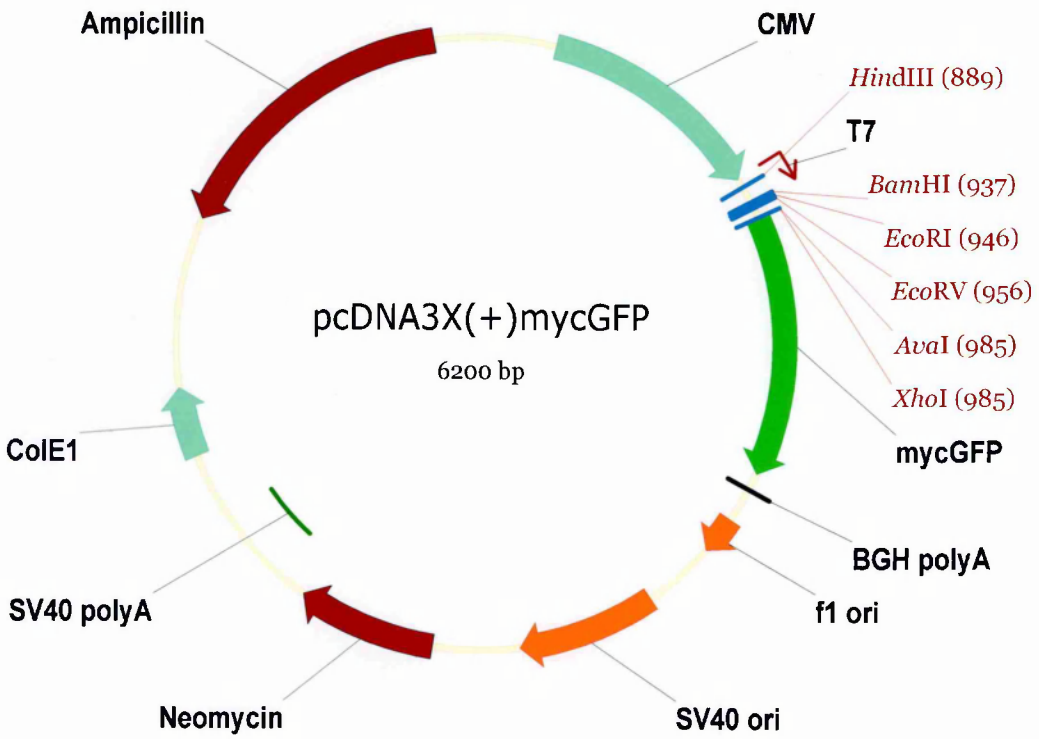
Ampicillin
CMV
HindIII (889)
T7
BamHI (937)
EcoRI (946)
EcoRV (956)
AvaI (985)
XhoI (985)
pcDNA3X(+)mycGFP
6200 bp
ColE1
mycGFP
BGH polyA
f1 ori
SV40 polyA
SV40 ori
Neomycin

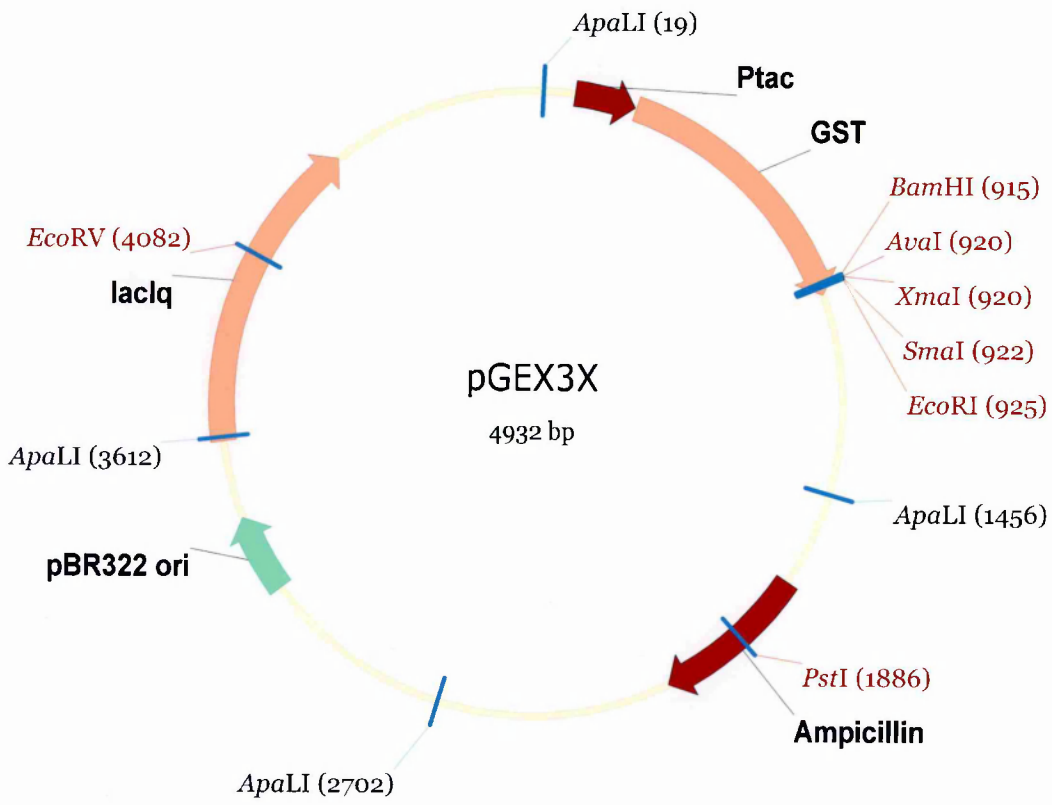
ApaLI (19)
Ptac
GST
BamHI (915)
AvaI (920)
XmaI (920)
SmaI (922)
EcoRI (925)
ApaLI (1456)
PstI (1886)
Ampicillin
ApaLI (2702)
pBR322 ori
ApaLI (3612)
laclq
EcoRV (4082)
pGEX3X
4932 bp

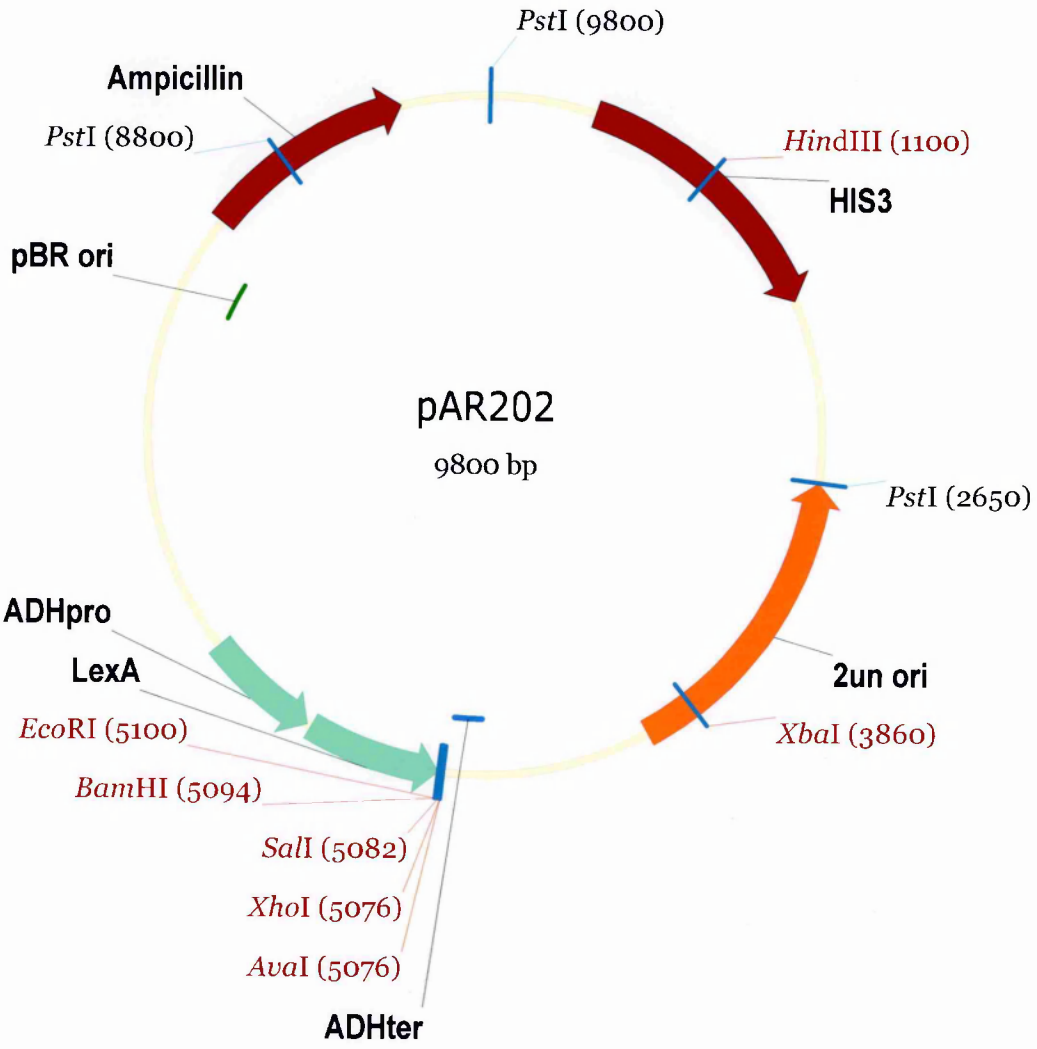
PstI (9800)
Ampicillin
PstI (8800)
HindIII (1100)
HIS3
pBR ori
pAR202
9800 bp
PstI (2650)
ADHpro
LexA
2un ori
EcoRI (5100)
XbaI (3860)
BamHI (5094)
SalI (5082)
XhoI (5076)
AvaI (5076)
ADHter